NASA TECHNICAL TRANSLATION

NASA TT F-603

NASA TT F-603

c. 1

SYSTEMS FOR DEFLECTION OF THE JET STREAMS OF TURBO-JET ENGINES

by A. A. Svyatogorov, K. N. Popov, and N. I. Khvostov

"Mashinostroyeniye" Press
Moscow, 1968

NATIONAL AERONAUTICS AND SPACE ADMINISTRATION • WASHINGTON, D. C. • MARCH 1970

SYSTEMS FOR DEFLECTION OF THE JET STREAMS OF TURBO-JET ENGINES

By A. A. Svyatogorov, K. N. Popov,
and N. I. Khvostov

Translation of "Ustroystva dlya Otkloneniya Reaktivnoy Strui Turboreaktivnykh Dvigateley," "Mashinostroyeniye" Press, Moscow, 1968

NATIONAL AERONAUTICS AND SPACE ADMINISTRATION

For sale by the Clearinghouse for Federal Scientific and Technical Information
Springfield, Virginia 22151 – Price $3.00

TABLE OF CONTENTS

FOREWORD

At present reversers intended to produce a reverse thrust of turbojet engines in aircraft landings are widely used in passenger and transport jet aircraft. We know of foreign publications in which data are given on particular reversers; several studies dealing with calculation and theory have been published in the Soviet Union. Still, works generalizing research on reversers that can serve as a basis for new developments have not been published either in the domestic or in the foreign literature. Textbooks evidently merely provide a definition of reversers.

In recent years aircraft with shortened and vertical takeoff and landing have made considerable advances; the power plants of these aircraft are equipped with devices for deflecting turbojet exhaust downward. The literature contains almost no account of the results of experimental research on turbojet deflectors.

This monograph written by a collective of authors on the initiative of K. N. Popov, is the first attempt to fill this gap. It sets forth the results of calculations-theoretical and experimental investigations on models of reverser and deflecting devices for turbojet engines. The greater part of the book deals with reversers.

For the first time, basic information on a variety of reverser layouts is set forth in a systematic way (Chapter I). Many constructed designs of reversers and deflectors are also considered.

The divisions of the book in which the results of experimental research on reverser and deflecting devices obtained from models (Chapters IV, V and VIII) and information on the propagation of the reverse stream in the external flow (Chapter VI) are of vital importance. Systematized and generalized data from model and full-scale tests of reversers are recommended for use in conducting evaluational calculations. Of interest are the results of experimental research, conducted on models, of different schemes of deflector devices for main and lift turbojet engines (Chapter VIII). These results can be used in practical developments.

Bearing in mind that building experimental forced-measurement facilities for research on reverser and deflecting devices encounters certain difficulties, the author deemed it worthwhile to take up a number of methodological problems involved in using such facilities and also, in particular, in using a facility equipped with forced-measuring elements fitted with wire resistance transducers (Chapter III). These questions are thus far not touched on in the literature.

K. N. Popov wrote §2 and 4 in Chapter III, §3 in Chapter IV, §3 and 5 in Chapters 7 and Chapter 8; N. I. Khvostov-- §2 in Chapter I, §2 in Chapter II,

§4 in Chapter IV, §1, 2 and 3 in Chapter VI and §2 in Chapter VII; A. A. Svyatogorov--§1, the first part of §4 and 5 in Chapter I, §1 and 3 in Chapter III, §1, 2, 5 and 6 in Chapter IV, §4 in Chapter VI and §1 in Chapter VII; A. A. Svyatogorov wrote together with K. N. Popov-- §3 and the second part of §4 in Chapter I, §1 in Chapter II, Chapter V, and §4 in Chapter VII; A. A. Svyatogorov wrote the Introduction together with N. I. Khvostov.

The authors are deeply indebted to V. M. Akimov and L. A. Sorkin for their assistance in conducting the studies that served as the basis for the monograph.

In carrying out the graphic work and putting together the manuscript, the authors were greatly helped by L. I. Savichev and L. A. Sabushkin, to whom the authors express their gratitude.

Comments and recommendations about the book should be sent to Mashinostroyeniye Publishing House,(Moscow, K-51, Petrovka, 24).

SYSTEMS FOR DEFLECTION OF THE JET STREAMS OF TURBO-JET ENGINES

A. A. Svyatogorov, K. N. Popov and N. I. Khvostov

ABSTRACT: Turbojet engine thrust reversers and devices for deflecting the jet exhaust are examined in this book. The present status of research and development of reversers and deflecting devices is described and domestic priorities in building reversers is underscored. The efficiency of thrust reversal in braking aircraft upon landing and in flight is indicated, as well as efficiency in deflecting the jet exhaust downward to shorten the takeoff and landing distance. A classification is given and principles laid down for building reverser and deflecting devices and examples of the construction of a variety of devices are cited. The fundamentals of gas-dynamic calculation of reverser and deflection devices are given. The method of calculation is illustrated by an example of the development of a reverser design from data of experimental research.

Methods of research and experimental facilities for testing models of reverser and deflecting devices are examined. The results of studies made by the authors on models of these devices using facilities equipped with force-measurement instruments are set forth. In the investigations gas-dynamic measurements were also made with the aim of studying the physical flow pattern. Systematized and generalized data rooted in experimental investigations of models and full-scale reversers is recommended for use in calculations: full pressure recovery coefficients in deflecting devices of reversers and information on the effect on the reverse coefficient of by-passing part of the exhaust gases through the nozzle in the straight-flow direction. The results of measuring the exit angle of the flow from deflecting screens and connecting pipes of the reversers and the results of research on the diffusion of the reverse stream into the external flow bear scientific interest as well as practical worth.

The book is intended for engineering-technical personnel in the aviation industry. It can also be used by instructors and students in senior courses at aviation technical colleges.

Introduction

The steady increase in flight speed and weight of modern aircraft with turbojet engines has lead to an appreciable deterioration of their takeoff /5*

* Numbers in the margin indicate pagination in the foreign text.

and landing capabilities. The takeoff and landing speeds of aircraft have risen sharply, in spite of an increase in the lift coefficient through mechanization of the wing, suction or blowing of the boundary layer. The increase of takeoff and landing velocities leads to an intensive increase in the takeoff run and in the landing run, since these quantities are proportional to the square of the liftoff and landing velocities. The increase in takeoff and landing distances leads to a rise in the extent and cost of airports and reduces the operating potentialities of aircraft.

The reduction in the takeoff run distance is attained by increasing the thrust-to-weight ratio of an aircraft, that is, the thrust produced per unit aircraft weight. In addition, takeoff boosters can be used.

More complex is the problem of reducing the landing run distance, depending as it does on the landing velocity and on the braking devices used. An aircraft can be started at the beginning of the runway, however, the touchdown point will always be at some distance from the start of the runway.

The landing run distance can be reduced by effective slowing up of the aircraft.

Until recently, the principal devices used in braking aircraft with turbojet engines included wheel brakes, brake flaps, and brake parachutes. An increase in the frictional force of wheel brakes leads to larger brake sizes and the need to increase the wear resistance of tire treads. An increase in the aerodynamic resistance of brake flaps and parachutes is attained by a sizeable expansion of their area, and consequently, of their weight. In addition, parachutes are unsuitable when there are sidewinds and inconvenient for repeated use. Brake parachutes in passenger and transport avaiation at the present time find use only in emergency situations, when landing on wet /6
or iced runways.

In braking aircraft, use can also be made of engine thrust reversal, affording a reduction in landing run distance. Producing negative thrust is attained by deflecting the turbojet engine gases in the opposite direction in so-called reversers (thrust reversers). The landing run distance of aircraft equipped with reversers becomes considerably less than when braked only with wheel brakes.

Thrust reversal proves to be an especially effective means of braking at low coefficients of friction of wheel treads on runways, for example, when landing on wet or iced runways. In these cases wheel braking is not only ineffective, but also hazardous, therefore reversing turbojet engine thrust proves to be the only way of slowing down the aircraft (excluding fixed retarding devices). Thus, under severe meteorological conditions safety is also increased when the plane lands after touchdown.

The reverser can be used under any engine performance condition--from low to maximum throttle. Inclusion of the reverser when climbing an aircraft affords a more precise landing approach and increases by 3-4 times the glide

angle compared with the usual value. It is possible to brake an aircract with a reverser also in the hold pattern when landing. All this makes it feasible to achieve further shortening of the landing distance of the aircraft. In the event of improper landing approach it becomes possible to bring the aircraft in on the second turn around from the glide section.

Engines without reversers operate upon landing at low rpm, and the pick-up capability of jet engines not being high enough does not afford a sufficiently large increase in thrust to the level needed for the climb. In contrast, the time required to change from reverse to positive thrust of turbojet engines fitted with reversers is 1-2 seconds. The reverser can be used in braking aircraft also in the event it is necessary to abort the takeoff run.

Reversers can be used in braking aircraft also in mid-flight, for example, in approaching zones with unfavorable meteorological conditions or in accident situations. Thus, reversers of turbojet engines are a universal braking device. In addition, when braking with reversers wear on the tread of aircraft landing gear is considerably reduced.

Reversers increase the weight and cost of an aircraft, complicate its /7
construction and piloting, but these disadvantages are slight compared to the indisputable benefits from using these devices. A convincing demonstration of this is the wide use of reversers in braking when landing passenger and transport jet aircraft for which questions of safety (in particular, in landing) are of paramount importance.

The first part of the book deals with reversers.

Another avenue to reducing the landing run distance and also a device to reduce takeoff distance is the use of turbojet engines to produce a lift on aircraft capable of short and vertical takeoff and landings (VTOL). These aircraft solve the problem of airportless basing and increase the mobility of modern aviation, finding considerable acceptance in recent years. Aircraft capable of landing on small, unequipped areas and taking off from these sites can deliver passengers and cargo to locations that are hard to get to otherwise. The importance of aircraft with vertical takeoff and landing in military application is especially great owing to the high vulnerability of todays airports during wartime. VTOL power plants are equipped with deflecting devices that afford diversion of exhaust gases of turbojet engines downward and also their deflection forward. Thus, the deflecting devices can be used in takeoff, landing, and in horizontal flight of aircraft. Turbojet engines with deflecting devices are also called lift-main (lift-sustainer) engines.

Vertical takeoff and landing of aircraft are also made possible by using special, so-called lift, engines located vertically on the aircraft. In contrast to lift engines intended only for horizontal aircraft flight, these are called main (sustainer) engines. To use the thrust of lift engines in shortened takeoff and landings and to accelerate aircraft these engines are also equipped with devices for deflecting the jet exhaust. Such lift engines are sometimes called lift-booster types. Deflecting devices on lift engines may

not in principle differ from those used for lift-main engines, however, in lift engines a smaller jet exhaust rotation angle is required.

Increasing the flight ceiling of aircraft leads to aerodynamic control surfaces becoming of low efficiency. The reason for this is the drop in the air density and, as a consequence, the reduction of aerodynamic forces applied to the control surfaces. At low flight velocities the efficiency of aerodynamic control surfaces is also lowered. We know that some modern fighters /8
become hard to control at velocities approaching the landing speed. The controlability of vertical takeoff aircraft at zero or near to zero flight velocities is a serious problem. In addition to exhaust control surfaces, deflecting devices of turbotude engines can also be used to control aircraft under conditions when aerodynamic forces operating on control surfaces are small.

Deflecting devices of lift-main and lift-turbojet engines are examined in the second part of the book.

CHAPTER I

TURBOJET ENGINE THRUST REVERSERS

§1. Present Status of Research and Development of Reversers /9

The first turbojet engine reverser was built in the Soviet Union.

In 1948 S. V. Vorozhbiyev and others under the leadership of V. Ya. Klimov built a reverser for the RD-45 engine. Two shutters of the reverser were located aft of the exit section of the jet nozzle (Figure 1.1). When they were rotated the gases were expelled in two directions. In the non-operative position the shutters were satisfactorily encompassed within the dimensions of the tail end of the aircraft. The device was designed to brake an aircraft upon landing and also as a device to increase engine acceleration affording a rapid change in thrust level. Stand and flight tests of the engine conducted in 1949 showed the possibility of achieving reverse coefficients of 0.35-0.40[1]. Opening up of the shutters into the working position took 1-1.5 seconds.

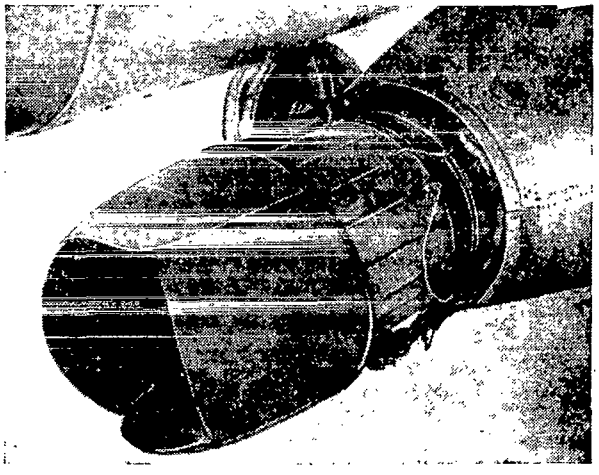

Figure 1.1. Reverser on the RD-45 Engine at the Flight Laboratory.

In 1948 V. Ye. Medov and G. P. Anan'yev ran stand tests on the RD-10 engine of a device fitted aft of the turbine and mounted to a pipe of rectilinear cross-section with two controllable shutters deflecting exhaust gases forward (Figure 1.2). This device was viewed as a means of increasing engine acceleration and also affording a change of engine thrust to the reverse setting, that is, serving the function of a reverser. The transition from full positive to maximum negative thrust took about 1 second, and from negative to positive thrust, even shorter--0.7 sec. A reverse coefficient of 0.24 was achieved. However, in experiments involving rotating shutters into the working position an increase in temperature and pressure /10

1 Below we will call the ratio of the negative thrust produced at the nozzle to the positive thrust for the same engine rpm levels and the same degree of pressure reduction in the jet nozzle the reverse coefficient (degree) and label it $\overline{R}_{rev}$.

of the gases at the jet nozzle and the reduction of engine rpm level were observed. As a consequence of gas leaks caused by design and production shortcomings, losses in direct thrust produced by the engine amounted to 4.5%.

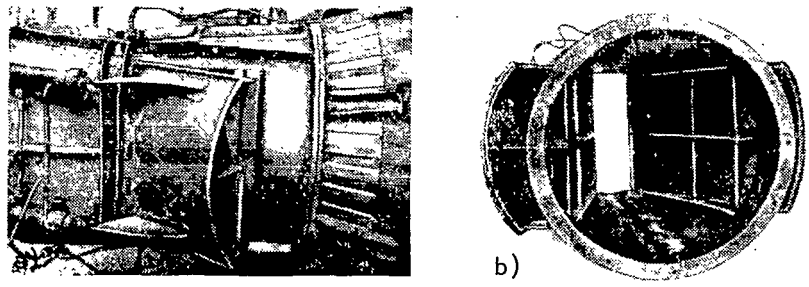

Figure 1.2. Reverser Investigated on the RD-10 Engine: a, Side View; b, View from Jet Tailpipe.

In 1949 A. V. Chesalov, A. I. Prut and S. S. Filler developed two schemes of reversers and conducted stand tests on RD-10 engines fitted with reversers (Figure 1.3).

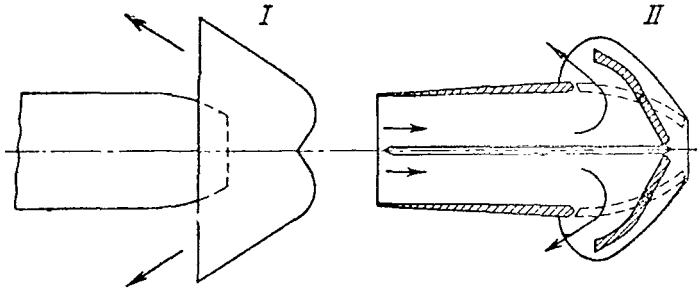

Figure 1.3. Reversers Investigated on the RD-10 Engine with Rectangular Cross-Section Nozzles: I, With a reflector ($\bar{R}_{rev}$ = 0.67); II,With Tilting Shutters ($\bar{R}_{rev}$ = 0.57).

A number of reversers were studied on turbojet engines by A. I.Prut (Fig. 1.4). Flight tests of scheme III conducted at the flight laboratory showed that at rpm levels close to the nominal value the engine performance conditions when the thrust was reversed remained unchanged, while at lower rpm levels an increase in gas temperatures in the nozzle and decrease in engine rpm were observed. The possibilities of using reversers in braking aircraft in landing and in flight were also examined and the principal requirements placed on reversers were formulated. /11

Thus, even in early domestic studies the possibility of reaching high reverse coefficient values was demonstrated. However, increase in pressure and temperature of gases in the jet nozzle when certain reversers were incorporated into the aircraft layout, associated with inadequate flow through sections, made it impossible to use these developments in a practical way. This was also

promoted by the unsatisfactory design execution of most of the layouts studied. Later, interest in work on reversers lagged and no new studies were carried out,

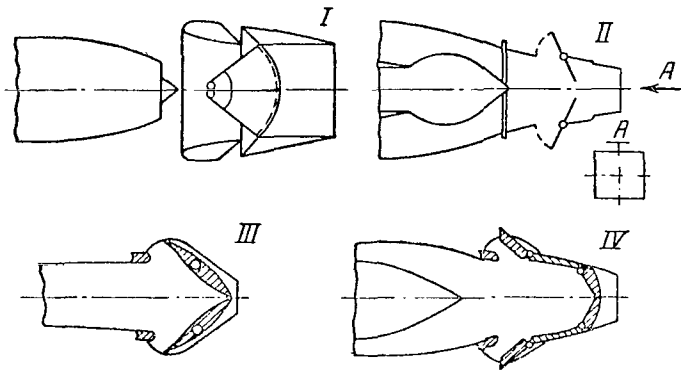

Figure 1.4. Reversers Investigated on the RD-10 Engine: I, With Spherical Shutters in the Ejector ($\overline{R}_{rev}$ = 0.30); II, With Tilting Shutters on the Constricting Nozzle ($\overline{R}_{rev}$ = 0.12); III, With Tilting Shutters at the Diffuser Section of the Exhaust Passage ($\overline{R}_{rev}$ = 0.65); IV, With Tilting Shutters of the Reverser and Jet Nozzle ($\overline{R}_{rev}$ = 0.57).

Since approximately 1954 work on reversers conducted in the United States, France, Great Britain, and Switzerland by many firms over a period of several years began to be known from the foreign periodic literature.

Several schemes of reversers were proposed that provided high reverse coefficient values and an applicable design execution of the reversers in engines. Designs were developed for reversers of a variety of schemes intended for turbojet engines and bypass engines installed on jet airliners. At present airliners of the United States (Boeing 707, Douglas DC-8 and DC-9, Convair 990 and others), Great Britain (Comet) and France (Caravelle), and several transport aircraft have reversers used in braking aircraft during landing runs after touchdown.

A distinctive feature of many foreign reports is their advertising slant. For example, sometimes only test data is given in the form of reverse coefficients obtained. /12 We will limit ourselves here to recounting only the fullest studies. The study [26] examines general considerations on the possibilities of using reversers, on their construction principles, on weight and requirements for reliability and reverser control systems. General questions associated with selection and design of reversers, problems cropping up in their use on aircraft are the subject of the articles [25-37].

A description of specific designs of reversers can be found in the following studies [20, 22, 25, 28, 32, 40, 44, 46]. Experience in final adjustment, operation, and testing of reversers on aircraft is highlighted in the studies [22, 28, 33, and 45]. Noteworthy is article [30] in which the problem of using a parachute for braking when landing heavy jet airliners is taken up. Based on calculation estimates, it is shown in the article that the main advantage of the brake parachute compared with the reverser is the substantial weight reduction, and under certain conditions operating outlays as well.

Not one of the studies we cited contained data that could serve as the basis for developing reversers even of the types described. The study [38] in which results are given of studies of reversers of different types built on models also lacks such information.

In 1955 research on reversers was resumed in the USSR. Studies began to be conducted on models. In several engine experimental-design bureaus designs were worked up for a variety of reverser schemes applied to specific engines. Reversers were built under the supervision of S. K. Tumanskiy for turbojet engines and under the supervision of N. D. Kuznetsov for bypass engines. /13

In recent years several studies have appeared in domestic literature, mainly of the calculation-theoretical kind, on turbojet engine reversers [2, 8, 9, 10, 11, 12, 16, 17 and 18].

We must note that initially reversers were developed for military aircraft (fighters). Flight tests were made of fighters with reversers. Thus, for example, one of the reverser designs of the SNECMA firm (France) was used as air brakes at M = 0.9 and had a substantial effect. One of the first public demonstrations of the operation of a reverser was held in 1953. At the LeBourget airport (Paris) the De-Havilland Vampire aircraft with a Goblin engine traversed the airport facing backwards [34].

The question of the value of using reversers for turbojet engines on military aircraft at present is under discussion. The fact that reversers have not found use in military aircraft is accounted for in our view by the possibility of insuring braking when landing military aircraft by using wheel brakes, /14 wheel parachutes, and other devices. In fact, problems of safety in landing for military aircraft are of less importance than for civilian. In addition, the relative increase in the weight of the aircraft is of substantial importance, which for a given reverser weight is considerably greater for several types of military aircraft than for civilian.

Development of power plants for military aircraft is proceeding, moreover, along the line of building lift-main engines with devices deflecting exhaust gases in different directions and used both in takeoff and landing, as well as in horizontal flight.

§2. Effectiveness of Thrust Reversal When Braking Aircraft in Landing and Flight

Thrust Reversal upon Landing

In order to estimate the effectiveness of thrust reversal of a turbojet engine, let us look at the possibility of reducing the landing distance of the aircraft under a variety of conditions.

Let us denote the amount of negative thrust produced by the turbojet engine nozzle, neglecting the input momentum of the air passing through it, R_{rev}, and the value of the direct thrust in the nozzle--R_{nozzle}.

We will define the thrust reversal coefficient to be the ratio

$$\overline{R}_{rev} = R_{rev}/R_{nozzle}$$

for the same engine rpm and for the same extent of pressure reduction π^*_{nozzle}.

We can express the negative thrust of the engine P_{rev} via the reverse coefficient, input momentum, and direct thrust of the nozzle:

$$P_{rev} = \overline{R}_{rev} R_{nozzle} + G/g \cdot V,$$

where G/g is the mass air expenditure through the engine;

V is air speed of aircraft.

Substituting the nozzle thrust for the thrust of the engine P and the input momentum, we get

$$P_{rev} = \left(P + \frac{G}{g} V\right)\overline{R}_{rev} + \frac{G}{g} V. \qquad (1.1)$$

In calculations we will assume that the reversal coefficient $\overline{R}_{rev}$ when V varies from landing speed to halting of aircraft will not depend on the aircraft flight velocity and will equal the reversal coefficient when V = 0 and for the corresponding engine rpm. /15

Let us denote the ratio of the engine thrust in the landing run P to the thrust when running in a fixed position P_0 by $f_1 = P/P_0$, and air expenditure

through the engine close to the earth as the function of the M number in the landing run will be represented with the aid of the function $f_2 = G/G_0$, where G_0 = expenditure of air through the engine when running in place.

Substituting the corresponding expressions into equation (1.1), we finally obtain for the negative thrust of the engine

$$R_{rev} = \left(P_0 f_1 + \frac{G_0}{g} f_2 V\right) \overline{R}_{rev} + \frac{G_0}{g} f_2 V, \tag{1.2}$$

where the right-hand member depends only on the landing velocity of the aircraft.

In addition, the force of aerodynamic resistance will operate on the aircraft in the landing run

$$X = \frac{c_x \rho V^2}{2} S$$

and the force of friction

$$F = \mu \left(Q - \frac{c_y \rho V^2}{2} S\right),$$

where c_x, c_y = aerodynamic coefficients of resistance and lift;

ρ = density of air;

S = wing span area of the aircraft;

Q = weight of aircraft upon landing;

μ = coefficient of friction.

We will write the equation of the motion of the aircraft upon landing in the following form:

$$\frac{Q}{g} \frac{dV}{dt} = X + F + P_{rev} \quad . \tag{1.3}$$

After substituting expressions for X, F and P_{rev} into equation (1.3) and several transformations, we get the acceleration $\ddot{x}$ of the aircraft as a function of its flight velocity

$$\ddot{x}=\overline{P}_0 g\left[f_1\bar{R}_{\text{rev}}+\frac{f_2 V(\bar{R}_{\text{rev}}+1)}{P_{0\,\text{spec}}\,g}\right]+c_y\frac{\varrho V^2}{2\overline{Q}}\,g\left(\frac{1}{K}-\mu\right)+\mu g,$$

where $K = c_y/c_x$ = aerodynamic characteristic of aircraft in landing run;

$\overline{P} = P_0/Q$ = thrust-to-weight ratio of aircraft, that is, the ratio of the engine thrust to aircraft weight;

$P_{0_{\text{specific}}} = P_0/G_0$ = specific thrust of engine, that is, the thrust of the engine related to the air passing through the engine; /16

$\overline{Q} = Q/S$ = specific wing loading.

The landing run distance for the aircraft upon landing at a velocity V_{landing} up to complete stop

$$L=\int_0^{V_{\text{landing}}}\frac{V\,dV}{\ddot{x}}. \tag{1.4}$$

Knowing the characteristics of the engine and the aircraft in landing it is easy to determine the landing run distance by numerically integrating equation (1.4). If functions f_1 and f_2 vary slightly with change in velocity from V_{landing} to zero and if they can be substituted by average values for the landing run, then equation (1.4) can be integrated analytically

$$L=\frac{1}{2gA}\left[\ln\left(1+\frac{AV_H^2+BV_H}{C}\right)+\frac{2B}{\sqrt{B^2-4AC}}\operatorname{Arth}\frac{V_H\sqrt{B^2-4AC}}{-(2C+BV_H)}\right], \tag{1.5}$$

where for brevity, it is denoted:

$$A=\frac{c_y\varrho}{2Q}\left(\frac{1}{K}-\mu\right);\quad B=\frac{\overline{P}_0 f_{2\text{average}}}{P_{0\text{specific}}\,g}(\overline{R}_{\text{rev}}+1);$$
$$C=\overline{P}_0 f_{1\text{average}}\,\overline{R}_{\text{rev}}+\mu,$$

V_H = velocity of aircraft at the moment that the reverser and brakes are switched on.

Expanding in the series $\operatorname{Arth}\frac{V_H\sqrt{B^2-4AC}}{-(2C+BV_H)}$ and retaining only the first member of the series, we arrive at an approximational formula for

calculating the aircraft landing run distance:

$$L=\frac{1}{2gA}\left[\ln\left(1+\frac{AV_H^2+BV_H}{C}\right)-\frac{2BV_H}{2C+BV_H}\right]. \tag{1.6}$$

If the brakes and reverser are switched on not at the moment of landing at $V_{landing}$, but after the aircraft has slowed down to some velocity or the devices are not switched on simultaneously, the interval in which equation (1.4) is integrated must be divided up into the appropriate subintervals

$$L=\int_{V_1}^{V_2}\frac{VdV}{\ddot{x}_1}+\int_{0}^{V_1}\frac{VdV}{\ddot{x}_2}, \tag{1.7}$$

where, for example, V_2 = velocity at which the reverser is switched on; V_1 = /17
= velocity at which the brakes are connected; $\ddot{x}_1$, $\ddot{x}_2$ = slowing down of the aircraft over the appropriate landing run sections.

Substituting mean values for the expressions f_1, f_2, μ, and K in each integration interval and integrating by subintervals, we can obtain an approximational expression for calculating the landing distance run with high precision. Thus, in the case of two integration subintervals we obtain the following approximational expression for calculating the length of the aircraft landing run:

$$L=\frac{1}{2gA_1}\left[\ln\frac{C_1+B_1V_2+A_1V_2^2}{C_1+B_1V_1+A_1V_1^2}-\frac{2B_1(V_2-V_1)}{2C_1+2A_1V_2V_1+B(V_2+V_1)}+\right.$$
$$\left.+\frac{1}{2gA_2}\left[\ln\left(1+\frac{B_2V_1+A_2V_1^2}{C_2}\right)-\frac{2B_2V_1}{2C_2+B_2V_1}\right]\right. \tag{1.8}$$

The results of calculation by the approximational formulas (1.6) and (1.8) agree well with the results of calculation by the graphical method using equations (1.4) and (1.7).

The results of the calculations of the aircraft landing run length by the graphical method for equation (1.4) for values of specific wing loading $\overline{Q}$ = = 300 and 600 kg/m^2 are given in Figure 1.5 for different thrust-to-weight ratios.

The values of the function f_1 were taken from the study [6] for the compressor compression exponent $\pi^*_{compressor}$ = 8 and the temperature ahead of the turbine 1,200°K. The function f_2 in the velocity range from $V_{landing}$ to zero can be written, to the first approximation as $f_2 = (1 + 0.2M^2)^{2.5}$.

The lift coefficient c_y is taken as equal to unity. The landing run distance does not include the section of the aircraft landing run from the touchdown point ($V_{landing}$) to the moment the reverser and brakes are switched on (V_H), which for modern aircraft can amount to 200-300 m.

It is clear from Figure 1.5 that thrust reversal will lead to a sharp reduction in landing run distance, and from 60-80% of this reduction compared to the landing run distance when braking solely with wheel brakes will be attained for a reverse coefficient equal to about 0.6.

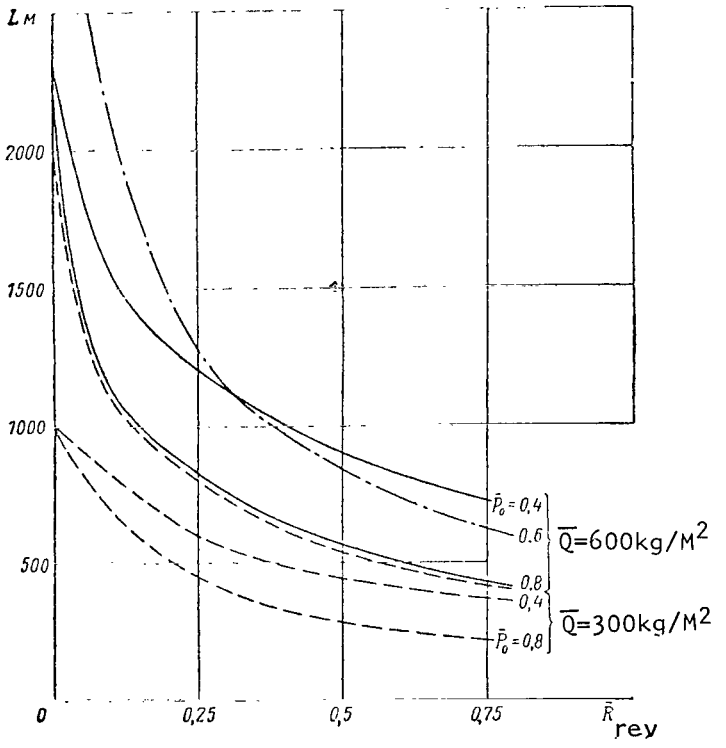

Figure 1.5. Aircraft Landing Run Distance as a Function of Reverse Coefficient for Specific Wing Loading $\bar{Q}$ = 300 and 600 kg/m^2 and for Different Thrust-to-Weight Ratios $\bar{P}_0$: ———, Aircraft Characteristic K = 7, Friction Coefficient μ = 0.2; ------, K = 5, μ = 0.2; — · — · — , K_1 = 7, μ = 0.02.

The greatest effect on the efficiency in turbojet engine thrust reversing in the landing run is exerted by the thrust-to-weight ratio of the aircraft, an increase in the latter resulting in greater reverse efficiency. For a reversal coefficient $\bar{R}_{reverse}$ = = 0.6, $\bar{Q}$ = 300 kg/m^2, and $\bar{P}_0$ = 0.4, the landing run distance owing to thrust reversal will be reduced by 58%, and for $\bar{P}_0$ = 0.8, by 75% compared with the landing run distance when only wheel brakes are used. Variation in the aerodynamic characteristics of the aircraft has but a slight effect on landing run distance.

From the foregoing example /18 of calculating the landing run distance of an aircraft in the event of landing on an iced-over airport, landing on ice, or malfunctioning of wheel brakes (μ = 0.02) it is also clear that thrust reversal is a highly effective means of braking. Even for a reversal coefficient $\bar{R}_{rev}$ = 0.1, landing run distance is

not greater than when the aircraft is braked under normal conditions just with wheel brakes, that is, when $\overline{R}_{rev} = 0$.

Thrust Reversal in Flight

Thrust reversal of an engine can also prove to be an effective means of braking an aircraft in flight, thus facilitating maneuvering of the aircraft at high velocities, and reducing the time required for braking the aircraft down to landing speed. /19

At the present time brake flaps are used in braking an aircraft in flight when maneuvering. However, design-wise it is an involved problem to locate flaps with an area of more than 5-7% of wing area on an aircraft. Therefore, the overload they produce $n_{flap} = X_{flap}/Q$, that is, the ratio of the force acting on the flaps to the aircraft weight, can with increasing thrust-to-weight ratio of the aircraft prove to be less than the overload that can be produced by using engine thrust reversal.

The expression for the negative thrust produced by an engine in flight differs from the corresponding expression for the landing run by the fact that the former takes into account thrust and air consumption as a function of altitude and flight velocity:

$$P_{rev} = P_0 \overline{R}_{rev} f_1 f_3 + \frac{G_0 \sigma}{g}_{inlet} - f_2 f_4 (\overline{R}_{rev} + 1) Ma,$$

where f_3 = engine thrust as a function of altitude;

f_4 = air consumption as a function of altitude;

M = flight Mach number;

a = velocity of sound at the given altitude;

σ_{inlet} = coefficient of pressure recovery at engine inlet.

The function f_4 at constant engine rpm [6] is approximately equal to the ratio of the density ρ at the given altitude to the density ρ_0 at sea level $f_4 = \Delta = \rho/\rho_0$. For simplicity, we can assume to the first approximation that $f_3 = f_4$ (actually up to the altitude H = 11 km engine thrust is reduced somewhat more slowly than air consumption).

When taking into account thrust as a function of altitude, the overload produced by engine equipped with thrust reversers

$$n_{rev} = \overline{P}_0 \left[f_1 \overline{R}_{rev} + \frac{Ma\sigma_{inlet}}{P_{0specific}\, g} (\overline{R}_{rev} + 1) f_2 \right] \Delta. \qquad (1.9)$$

The overload produced by means of flaps as a function of altitude and flight velocity can be represented by the following formula

$$n_{flap} = \frac{c_x k M^2}{2Q} \overline{S}_{flap}\ p_0 \Delta \frac{T}{T_0}, \qquad (1.10)$$

where p_0 and T_0 = pressure and temperature at sea level;

S_{flap} = ratio of flap area to wing area;

$k = C_p/C_v$ = ratio of specific heat capacities.

Equating expressions (1.9) and (1.10), we can find the value of the thrust-to-weight ratio $\overline{P}_{0_*}$, at which the equality $n_{reverse} = n_{flap}$ is satisfied as a function of M number and specific load $\overline{Q}$: /20

$$\overline{P}_{0_*} = \frac{c_x k p_0 M^2 \bar{S}_{flap} \frac{T}{T_0}}{2Q \left[f_1 \overline{R}_{rev} + \frac{Ma (\overline{R}_{rev} + 1) \sigma_{inlet} f_2}{P_{0specific}\, g} \right]}. \qquad (1.11)$$

When $\overline{P}_0 > \overline{P}_{0_*}$, turbojet engine thrust reversal is a more effective means of braking than brake flaps. For $\overline{P}_0 < \overline{P}_{0_*}$ brake flaps are more effective. If we consider that the coefficient of pressure recovery in the air intake for $M > 1$ depends on the M number approximately as $1/\sqrt{M}$, then from analysis of expression (1.11) it follows that when $M \to 0$ and $M \to \infty$ the value $\overline{P}_{0_*} \to 0$, that is, $\overline{P}_{0_*} = f(M)$ has a maximum. Consequently, when $\overline{P}_0 < \overline{P}_{0_{*max}}$ brake flaps have the edge only in a certain range of M numbers.

This is graphically shown in Figure 1.6 where the results of calculating $\overline{P}_{0_*}$ as a function of M number are presented by way of example. An increase in the specific wing loading and in the flight altitude leads to a reduction in the thrust-to-weight ratio beginning with which thrust reversal becomes a more effective means of braking then brake flaps. The values of the functions f_1 and $P_{specific}$ have been borrowed from data in the study [6] when $\pi^*_{compressor} = 8$ and the temperature forward of the turbine is 1,200°K.

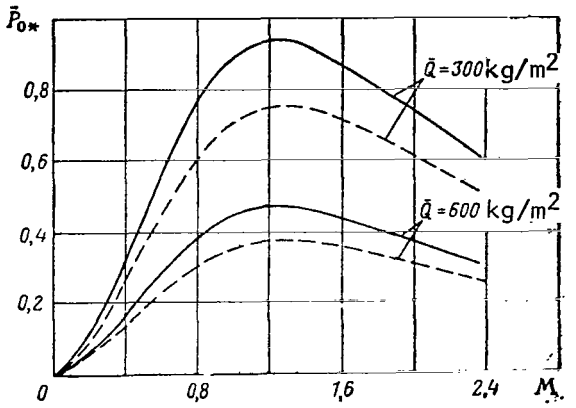

Figure 1.6. Thrust-to-Weight Ratio, Beginning with its Value for which Thrust Reversal is More Effective than use of Braking Flaps, as a Function of Flight M Number $\bar{R}_{rev} = 0.6$, $\bar{S}_{flap} = 0.07$ m^2 (The Solid Curves Represent Values Close to the Ground Level, the Dashed Lines Represent Those at an Altitude of 11 km.)

Thus, turbojet engine thrust reversal can substantially reduce the landing run distance of an aircraft after landing and improve its maneuvering characteristics in flight.

§3. Requirements Placed on Reversers

The first requirement placed on a reverser is that it ensure the desired reverse coefficient, which is the main parameter. The required value of the thrust reversal coefficient can be determined by starting from the necessary reduction in landing run distance for the aircraft when landing. We can take as the minimum value of the reverse coefficient the value at which the landing run distance upon landing under unfavorable winter conditions (iced-over runways, landing on ice) using a reverser is reduced to the landing run distance under favorable summer conditions (dry runway) when the aircraft is braked with wheel brakes (without using the reverser).

§2 of this chapter, in analyzing calculated functions of aircraft landing run length for landing, it was shown that when reversers are used the sizeable reduction in landing run distance is attained already for reverse coefficients equal to about 0.6. At larger values of $\bar{R}_{rev}$ the landing run distance decreases less appreciably. On the other hand, attaining higher values of the reverse coefficient encounters certain difficulties. In actual practice reversers with a reverse coefficient greater than 0.5 are not used (See Table 1).

The reverser, generally speaking, must not have an effect on the normal functioning of the turbo compressor group of the engine when switching on a reverser the pressure and temperature of gases aft of the turbine must remain unchanged. This requirement is satisfied by choosing the minimum passageway sections of the deflecting elements of the reverser to be of such dimensions that when the over-all consumption of gases through them and through the jet nozzle (when there is an overloading of part of the gases in the straight flow direction) for π^*_{nozzle} = const will be equal to the consumption for the straight thrust regime, that is, the consumption coefficient $\bar{G}_{rev} = G_{rev}/$

/G_{nozzle} (where G_{rev} is the consumption in reverse regime and G_{nozzle} is the consumption in straight thrust regime) must be equal to unity.

TABLE 1. BASIC DATA ON REVERSERS /22

Type and Model of Engine	Company, Country	Takeoff Thrust, kg	$\overline{R}_{rev}$	Relative Weight
With throttling shutters and deflecting screens located ahead of the exit section of the jet nozzle				
Avon RA-29 Turbojet Engine	Rolls Royce, Great Britain	4,760	0.50	0.11
Conway Bypass Engine RCo. 12	as above	7,945-8,165	0.50	0.14*
RCo. 42	as above	9,240	0.45	--
RCo. 43	as above	10,200	0.50	0.10
JT3C-6** Turbojet Engine	Pratt-Whitney, United States	5,080	0.40	--
CJ805-3 Turbojet Engine	General Electric, United States	5,285	0.50	0.14*
With shutters located at the exit cross-section of the jet nozzle				
CJ805-23 Bypass Engine	General Electric, United States	7,300	0.5	0.14
TF33-P-7 Bypass Engine	Pratt-Whitney, United States	9,525	0.45	--
JT3C-6*** Turbojet Engine	as above	5,080	0.43	--

* with noise-suppressor
** the Boeing 707-120 Aircraft
*** the Douglas DC-8.
Tr. Note: Commas indicate decimal points.

In actual practice, for design considerations it does not always appear possible to satisfy the requirement $\overline{G}_{rev} = 1$ when $\pi^*_{nozzle} = const$ for the nominal engine operating regime. However, usually there is the possibility of switching on the reverser with a slight change in engine operating conditions. Thus, we know that some reversers are switched on not at the rated engine rpm setting, but at 95% of this value.

In reversers located ahead of the exit cross-section of the jet nozzle, at the locations of contact of throttling members (for example, shutters) with

the jet pipe gas losses through the gaps between them are inevitable, leading to a loss in engine direct thrust. Sizeable loss of engine direct thrust can also stem from the presence in the gas channel of the engine or parts of the reverser. In several such schemes these losses can rise to 5%.

In reversers direct thrust losses must be at a minimum. From analyzing experience of building reversers located ahead of the exit cross-section of the jet nozzle it follows that direct thrust losses can be brought to 1%. In /23 rational schemes of reversers located aft of the exit cross-section of the jet nozzle, as a rule there is no loss in direct thrust.

The following characteristics of the reverser must be satisfied as specific requirements: reverse coefficients and consumption coefficients as functions of the extent of pressure reduction and of the parameter determining the position of the parts throttling the gas channel of the engine. The characteristics of reversers must be smooth, without abrupt changes in direction both in the transition from direct thrust to negative thrust, as well as vice versa. A jump-like transition from direct to negative thrust with rotation of vanes which serve to accomplish thrust reversal is noted in scheme VII (cf. Figure 1.9), described in §4 of this chapter.

Choice of the scheme of the reverser and its construction are governed by the conditions of its arrangement in the engine, and to a greater extent by the conditions of engine placement on the aircraft.

Operation of reversers shows that gases from the reverser on reaching the runway are reflected from it and enter the engine inlet, boosting the temperature of the inlet flow and, as a consequence, compressor stalling. It follows from experience that it is very difficult to altogether exclude ingestion of heated gases at the engine inlet, and in part impossible. Incursion of gases at the engine inlet limits the operating time of the reverser. Therefore, an important condition for reliability of engine performance when the engine is fitted with the reverser is to organize the flow at the exit from the deflecting elements of the reverser in such a way as would cut down to a minimum ingestion of heated gases at engine inlet.

Failure to satisfy this requirement can place the engine in hazard of an accident. Thus, for example, in operation by the aircraft company TCA (United States) of the Douglas DC-8 passenger airliners with four Conway Bypass engines, upon landing with thrust reversal fractures were observed in the sixth stage of the high pressure compressor of the external engines. These fractures were caused by stalling, when gases from the reverser of the inner engines entered the outer engine[1]

---

[1] *Flight*, 1961, No. 2737, p. 273. To avoid burdening the literature list with a large number of notes containing individual items of information, the references to these are given in the form of single line footnotes.

The stream escaping from the reverser produces erosion on the surface of the engine nacelle (under the stream), as a consequence of which its front part sticks to the streamlining (cf. Chapter V). To prevent the aircraft surfaces from being singed and contaminated when thrust reversal is in effect the designs of the deflecting parts of the reversers are made so as to avoid deflecting the front part of the stream (§5, Chapter 1). Heated gases from the reverser must also not strike the chassis, wings, ailerons, and other parts of the aircraft design. Experience shows that from the viewpoint of effect on design members of the aircraft thrust reversal does not represent insurmountable difficulties. /24

The reverser must have minimum dimensions in weight. Ensuring minimum weight of the reverser involves major design difficulties, since elements of reverser design for modern turbojet engines undergo very heavy loads. The dimensions of a reverser depend naturally on the magnitude of the necessary reverse coefficient. As the angle of flow exit is reduced, the reverse coefficient is increased, however, here the minimum cross-sectional area of the deflecting elements, (connecting pipes, screens) is also reduced. Therefore, to obtain the required passage sections the length and weight of the reverser are increased. Some optimal angles for exit of stream from the reverser at which the length of the deflecting screen will prove to be at a minimum[1] corresponds to a specific reverse coefficient.

The relative weight of the reversers operating in foreign aviation is approximately 12% of the engine weight, and together with the noise-suppressor nozzle--approximately 14% (See Table 1). In designing reversers these figures can be useful for orientation.

It is desirable to have high coefficients σ_2 of full pressure recovery in deflecting elements of reversers. An increase in σ_2 in deflecting elements makes it possible for given gas consumption through the reverser to attain high reverse coefficients and, vice versa for given reverse coefficient to be limited to a lesser consumption of gas deflected in the reverse direction. The latter fact simplifies efforts to control ingestion of heated gases at the engine inlet. Increasing σ_2 also means reducing the dimensions in weight of the reverser by reducing the dimensions both of the deflecting as well as of the throttling parts of the reversers.

On the other hand, the requirement of compactness of reversers complicates execution of the structures in which there would be no separation of flow and no substantial losses in total pressure. Nonetheless, the present level of σ_2 (6, Chapter IV) makes it possible to attain practically the needed reverse coefficient values in reversers of different types. /25

[1] This problem is taken up in greater detail in §2 of Chapter II.

Taking into account the high aircraft velocity in landing, in order to boost the effectiveness of braking and to insure the possibility of the aircraft's approach in the event of an unsuccessful landing in the second circling, the time required to attain maximum negative thrust from complete direct thrust, and vice versa, must be at a minimum. For present-day reversers the switching time is not more than 1-2 sec. (5, Chapter I).

Investigations have shown that reducing the time from the moment the aircraft touches down to obtaining full reverse thrust by 1 sec. is equivalent to increasing the reverse coefficient by about 30% [46].

The reverser must not noticeably increase the lateral resistance of the aircraft and must not have an effect on the stability of the aircraft in normal flight. Present-day reversers satisfy this requirement. Reversers located behind the exit cross-section of the jet nozzle have deflecting (screens) or throttling and deflecting (shutters) elements housed in the engine nacelle or the fuselage of the aircraft. Sometimes shutters of this type of reverser are part of the structure of the engine nacelle or the fuselage of the aircraft. In reversers with deflecting screens located ahead of the exit cross-section of the jet nozzle, the screens sometimes are covered from the outside by shutters placed flush with the cowling. However, for aircraft with moderate flight velocity there is no particular need to cover the screens from without, since with open-spaced screens, owing to the slight increase in external resistance of the aircraft, there is no practical change in the flight velocity of a heavy transport aircraft [45].

When one or several engines with reversers are installed on an aircraft, in reverse regimes no asymmetrical thrust must be developed as the result of which a pitching or yawing moment could be produced.

The reverser must ensure maximum safety and reliability in operation and have adequate safety margin. Necessary protective attachments preventing accidental pilot switching on of the reversers are provided for in the control drives of reversers. In fact the margin of safety of reversers must not be less and in sometimes greater than the safety margin of the engine on which they are installed.

When the reverser is turned on for landing in a glide regime, it is necessary to partially reverse thrust. Therefore the reversers of engines installed on passenger and transport aircraft must have at least a three-position device for elements regulating the size of direct and reverse thrust: the first position corresponds to full direct thrust regime; the second to the full damping of direct thrust or leaving it at a small value corresponding to low throttle thrust; the third corresponds to maximum negative thrust regime. The pilot switches from second to third regime at the moment of aircraft touchdown (or in 2-3 seconds). For reversers switched on after aircraft landing, a two-position control drive can prove adequate. /26

In all known designs of reversers exhaust of gases occurs always from two sides of the engine (sometimes not wholly symmetrical), but throttling of

the gas duct of the engine is carried out by two separate elements. If the control drives for these throttling elements are made independent, then when a different amount of gas is deflected in the reverse direction it will appear possible to use the reverser also to control the aircraft from single engine, for example, during landing on a slippery or ice-covered runway. In this case the gas exhaust must follow a horizontal plane, that is, along the sides of the aircraft, which can be easily done if the engine is placed in the fuselage. When several engines are installed in the aircraft, the control forces can be obtained by varying the engine operating regime.

Thus, when using a reverser to control an aircraft or to boost its maneuverability (if the reverser is installed on a fighter engine) the control drive must provide continuous, stepless regulation of negative thrust.

Thus, the following requirements are placed on reversers for turbojet engines:

1. Attainment of the desired reverse coefficient.

2. Absence of any effect on normal functioning of the turbo compressor group of the engine. Pressure and temperature of gases aft of the turbine must remain unchanged. Losses in direct thrust of the engine when the reverser is switched off must not be greater than 1%.

3. The handling characteristics must be smooth, without jumplike variation in thrust and gas consumption.

4. Minimum ingestion of heated gases into engine inlet and onto structural elements of the aircraft.

5. Minimum dimensions and weight.

6. The time required for converting from full positive thrust to full negative must not be greater than 1-2 seconds.

7. Minimum increase in lateral resistance of the aircraft; there must be no effect on aircraft stability in normal flight. /27

8. When one or several engines are installed on the aircraft, upon switching reversers on, no asymmetrical thrust must be induced.

9. Insurance of maximum in safety and reliability in operation.

§4. Classification and Principles of Constructing Reversers and their General Characteristics

Classification and Principles of Building Reversers

The first, most general classifying feature is the position of the reverser relative to the exit cross-section of the jet nozzle. The position of

the reverser determines not only the scheme and design implementation of the reverser, but to a considerable extent its gas dynamics perfection. Reversers placed forward of the exit cross-section of the gas nozzle will be called in this book Type I reversers, and those placed aft of it Type II.

Any reverser scheme has two types of structural elements: throttling elements whose purpose is covering the gas duct and partial rotation of the exhaust, and deflecting elements decisively rotating the exhaust in the reverse direction at a given angle at the exhaust outlet. Sometimes throttling and deflecting functions are fulfilled by the same structural elements.

Deflecting and throttling elements are located usually in direct proximity to each other. However, we know of schemes (XIII, Figure 1.7; III, Figure 1.9), in which the throttling and deflective elements are found on different sides of the exit cross-section of the jet nozzle. Therefore, we must take Type I reversers to include those in which the deflecting elements are located forward of the exhaust cross-section of the jet nozzle.

The second and third classifying features are, respectively, the method used in throttling the gas duct and the method of deflecting the duct in the reverse direction.

Distinguishing features of most reversers of Types I and II that are feasible in practice is the fact that in them throttling of the gas duct and deflection of the stream is carried out by different structural elements. Such /28 schemes differ in rational structural forms at fairly high gas dynamic perfection.

Investigations have been made of schemes of reversers including elements simultaneously serving throttling and deflecting functions (Schemes VII, VIII, Figure 1.7;I, III, Figure 1.8), but they have not won wide acceptance. Such schemes are usually less satisfactory designwise and exhibit poor gas dynamic properties.

Mechanical methods of throttling the gas duct are usually used in reversers of Types I and II: shutters in the form of semicylindrical surfaces of different types--with location of the axis of rotation on or near the axis of the jet pipe (Scheme I, Figure 1.7; I, Figure 1.8) or near the rear channels of the deflecting screens located forward of the exhaust cross-section of the jet nozzle (Scheme II, Figure 1.7), shutters in the form of separate flaps-baffles that do not become coupled (Scheme IV, Figure 1.7). These shutters in Type I reversers are installed in the direct thrust regime flush with the jet pipe of the engine and do not introduce considerable losses in direct thrust (Schemes I, II, III, IV and VIII, Figure 1.7). In Type II reversers throttling shutters located over the jet tube or over the nozzle do not result in direct thrust losses (for example, Schemes I, II, and IV, Figure 1.8). Throttling of the gas duct of the engine with the Type I reverser can also be performed by a regulated jet nozzle (Scheme XII, Figure 1.7) or by a cluster of shutters of the reverse regulated nozzle type (Scheme III, Figure 1.7).

Thus, when the mechanical method of throttling the gas ducts is used, the throttling elements are located to the rear of the deflecting elements.

Other methods of throttling the gas duct can also be used in reversers. Under the aerodynamic method of throttling the gas duct through slits in a streamlined strut installed in the jet pipe, the release of compressed air bled from aft of the compressor (Scheme I, Figure 1.9) is carried out perpendicular to the stream. This method, however, has not won acceptance owing to the considerably high air consumption required for substantial sweeping of the gas duct, low values of the reverse coefficient, and also because the strut causes losses in direct thrust.

Intermediate between these methods is throttling of the gas duct by using tilting vanes with symmetrical aerodynamic profile (Scheme X, Figure 1.7; III, Figure 1.9). Located in the direct thrust regime along the stream, these shutters in inverted position partially partition the gas ducts themselves, but more profound throttling is attained by their deflection of the stream in /29
two directions and by thus reducing the effective passage cross-section of the jet nozzle. This method can include throttling of the gas duct by shutters of different types partitioning only partially in the gas duct reverse regime (Schemes II and IV, Figure 1.9).

A possible method of throttling the gas duct is deflecting the stream under the action of centrifugal forces by rotating the stream using tilting vanes with symmetrical aerodynamic profile installed in the jet pipe. However, this original method (Scheme VI, Figure 1.9) owing to unsatisfactory reverser characteristics has not found practical application.

Thus, in non-mechanical methods of throttling the gas duct the throttling elements are located forward of the deflecting elements.

Profiled screens located directly in the engine jet pipe (for example, Scheme I, Figure 1.7) or over it (for example, Scheme II, Figure 1.9) have won acceptance as deflecting elements in reversers of both types. We also know of Type I reversers in which the deflection of the stream is carried out by separate connecting pipes (Scheme IV, Figure 1.7).

Under certain conditions of arrangement of an engine fitted with a Type I reverser on an aircraft, a gas diverting channel can be placed between the jet pipe of the engine with its installed deflecting screen and streamlining of the fuselage (motor nacelle). An example of this design is described in §5 of Chapter I (cf. Figure 1.12).

In reversers of type II, the role of the deflecting element is often played by flaps (Scheme II, Figure 1.8).

In reversers of Types I and II, the above listed throttling and deflecting elements can be rationally combined in various combinations. However, schemes with wholly specific combinations of throttling and deflecting elements

have found practical application in reversers. Brief characterization of known schemes is given in the next division of this section.

We must state that dividing structural elements of reversers into throttling and deflecting sometimes is arbitrary, since the stream is deflected in the reverse direction in some channels whose walls are formed by the throttling and deflecting elements.

The reversers of Type I can be divided also, in the fourth characteristic, by the method by which the deflecting screens or connecting sleeves are closed in the direct thrust regime. They are usually covered over by the throttling elements. /30 However, under certain arrangement conditions, for example, when the throttling elements are located far from the deflecting elements, it is necessary to provide for closing over of the deflecting elements using special parts. By way of an example, we can cite the variants of Schemes X, XI and XII cited below, and also the referred-to Scheme XIII, Figure 1.7, and several schemes of reversers of the nozzle with a central body, examined in §2, Chapter IV. These reversers will inevitably prove to be more complex in design and heavier in weight.

General Characteristics of Reversers

Below we consider schemes of reversers used in modern turbojet engines in conjunction with a necked jet nozzle.

Reversers installed forward of the exhaust cross-section of the jet nozzle (Figure 1.7)

Scheme I with two deflecting screens and cylindrical shutters has been developed by the Rolls-Royce Company (Great Britain). When the reverser is switched on, shutters cover the jet pipe and direct the thrust to the deflecting screens. When the reverser is switched off, the shutters covering the screen are positioned flush with the walls of the jet pipe and do not exert resistance to the straightforward exiting of the stream. One characteristic of this scheme is the fact that the resulting force of gas pressure on the shutters passes along the axis of rotation of the shutters lying along the jet pipe axis. Therefore, the moment required to rotate the shutters is considerably less than in Scheme II. The scheme has been realized on engines produced by Rolls-Royce, Pratt-Whitney, and General Electric (United States). The main parameters are as follows: reverse coefficient $\bar{R}_{rev} \approx 0.45\text{-}0.56$[1], and direct thrust losses when the reverser is switched off $\Delta\bar{R} < 0.01$. A description of the design features of certain reversers of this scheme has been given below, in §5 of this chapter. The sources are also indicated there. Some experimental data on a similar scheme has been presented in §2 of Chapter IV.

Scheme II with two deflecting screens and cylindrical shutters differs from Scheme I in the fact that the flaps rotate around an axis lying close to

[1] The values of $\bar{R}_{rev}$ cited in this section refer to $\pi^*_{nozzle} \approx 2.0$.

the rear channels of the screen. The moment required to rotate the shutters is greater under this scheme than under Scheme I. Some experimental data on a similar scheme are given in §2 of Chapter IV ($\bar{R}_{rev} \approx 0.63$).

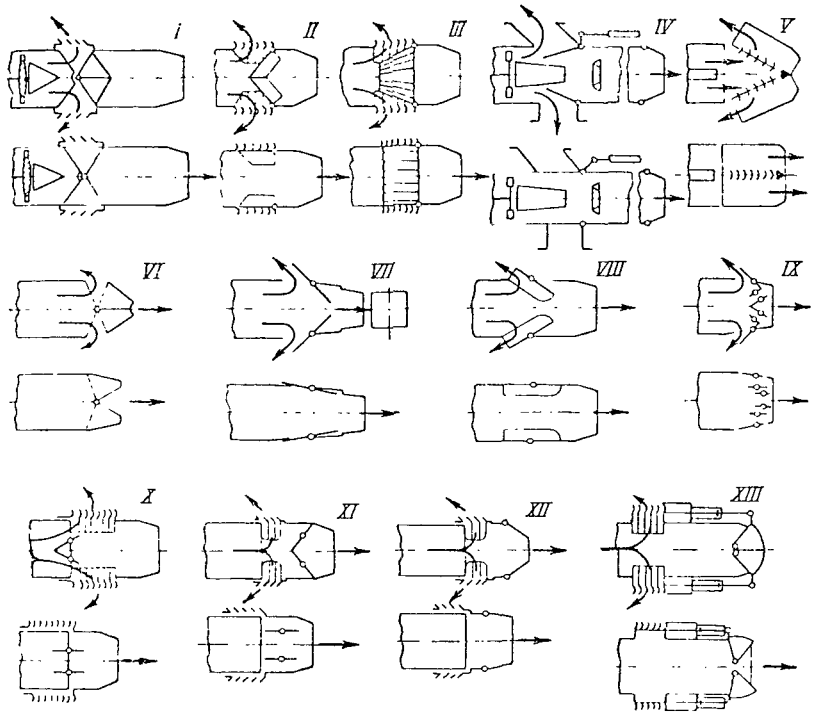

Figure 1.7. Schemes of Reversers Located Aft of the Exit Cross-Section of the Jet Nozzle: I, With Deflecting Screens (d.s.) and Cylindrical Throttling Shutters (t.s.) with Axis of Rotation Along the Jet Pipe Axis; II, With d.s. and Cylindrical t.s. With Axes Along the Rear Channels of the Screens; III, With d.s. and t.s. of the Reverse Regulated Nozzle Type; IV, With Nonsymmetrical Deflecting Connecting Pipes and Individual Small t.s. not Entering Into Coupling; V, With Deflecting Vanes and Tilting Shutters Comprising Part of the Jet Pipe; VI, With Hinged Shutters Constituting Part of the Jet Nozzle; VII, With Bypass Shutters and Parallel Lateral Walls; VIII, With Bypass Cylindrical Shutters; IX, With Tilted Throttling Vanes and Bypass Cylindrical Shutters; X, With d.s., Tilted Throttling Vanes, and Extensible Jet Pipes; XI, With d.s. Throttling Tilted Vanes-Baffles and Extensible Jet Pipes; XII, With d.s., Throttling Jet Nozzle, and Extensible Jet Pipes; XIII, With Throttling Bucket Shutters and Deflecting Screens Covering the Cylindrical Shutters Movable in the Longitudinal Direction.

Scheme III with deflecting screens is characterized by throttling shutter /31 of the reverse controlled nozzle type. The possibilities of using such

shutters for throttling the gas duct has been examined in §2 of Chapter IV, where experimental results based on this scheme are also given ($\bar{R}_{rev} \approx 0.82$).

Scheme IV has nonsymmetrical deflecting connecting pipes and individual throttling shutters that do not enter into coupling. The emergence of this scheme was caused by conditions of engine location on the aircraft (in the fuselage) and in order to avoid injection of heated gases into the engine inlet owing to the necessity of their nonsymmetrical exiting. In testing a model, $\bar{R}_{rev} \approx 0.5$. A reverser of this scheme with symmetrical exhaust of streams installed on the engine had $\bar{R}_{rev} \approx 0.5$; $\Delta\bar{R} \approx 0.01$ (when $\beta_{vane} = 40°$). The relative weight was 0.12. The results of model tests are given in §3 of Chapter IV. /32

Scheme V, developed by NASA (United States) has two series of deflecting vanes located along the tiltable shutters which are part of the engine jet pipe. In the direct thrust regime the vanes are located one behind the other, forming a stack that lies in the gas stream. Direct thrust losses amount to about 2%. When the reverser is switched on the vanes are tilted together with the shutters. When $\beta_{vane} = 50°$, the value $\bar{R}_{rev}$ up to 0.6 is attained. The design of the reverser of this scheme has been developed for the turbojet engine used in the fighter Republic F-84 "Thunderjet", which lands with use of a reverser[1].

Scheme VI with hinged shutters constituting part of the jet pipe, designwise is simple and easily allowed for in the over-all dimensions of the engine. This scheme is similar to Scheme V, differing from it in the absence of deflecting vanes. The relative weight of the reverser must be comparatively small, since its design makes use of part of the jet nozzle. According to the data of the Fairchild Corporation (United States), the design thrust reverse coefficient is 0.4[2]. There are no design developments and experimental verification of this scheme.

Scheme VII with bypass shutters and parallel lateral walls, as indicated in the introduction, has been implemented in an actual structure tested on an engine under stand conditions.

The reverser built under this scheme has a relatively simple design of working parts, however, owing to the rectilinear shape of the nozzle it is not covered conveniently within the over-all dimensions of the engine. Rectilinear-shaped nozzles are technologically unprogressive and warp in engine

---

[1] *American Aviation*, 1954, 21/VI, Vol. 18, No. 2, p. 21, 10/V, Vol. 17, No. 25, p. 20, 1954.
Interavia, 15/IV, No. 2947, 1954.

[2] *American Aviation*, Vol. 17, No. 25; Vol. 18, No. 2, 1954.

operation. The efficiency of the jet nozzle that is of square cross-section is lower than that of a round nozzle. In stand tests with different shutters (Figures 1.2, 1.4, Position II), values of $\bar{R}_{rev}$ = 0.12-0.24, were obtained, /33 with direct thrust losses up to 4.5% with the reverser not switched on.

Scheme VIII with bypass cylindrical shutters has a round cross-section jet nozzle. In model tests the value $\bar{R}_{rev}$ = 0.46 was obtained. One failing of this method is that the shutters occupy much of the surface of the jet pipe and reduced its rigidity. Owing to this shortcoming the scheme has not been given further design development.

Scheme IX with throttling tiltable vanes and bypass cylindrical shutters differs from Scheme VIII by the presence of tiltable throttling vanes with aerodynamic profile. In the direct thrust regime the vanes are placed along the stream. Installation of the vanes in the stream leads to up to 2% losses of engine direct thrust. In tests $\bar{R}_{rev}$ = 0.55 obtained.

Scheme X with tiltable throttling vanes and extensible jet pipes with deflecting screens installed in it.

In the direct thrust regime vanes with aerodynamic profiles are positioned as in Scheme IX, along the stream. Direct thrust losses rise to 4.5%. When the reverser is switched on, the jet pipe is shifted, the vanes are tilted, the gas duct is partially throttled, and the stream is directed onto the screens. From data of model studies (§4, Chapter IV) a reverse coefficient of up to 0.5 can be obtained for this scheme.

Scheme XI with deflecting screens, throttling tiltable vanes-baffles, and extensible jet tubes differs from Scheme X by the fact that the vanes-baffles almost completely partition the gas ducts in thrust reversal. This scheme, owing to fuller throttling of the gas duct, can have higher reverse coefficients than Scheme X, approximately the same as those that characterize Scheme II. However, in the direct thrust regime the large vanes-slide gates present in the stream inevitably lead to more perceptible losses in direct thrust than in Scheme X.

Scheme XII with deflecting screens, throttling the jet nozzle, and an extensible jet pipe is characterized by the fact that it has relatively uninvolved structure of working elements and is easily managed within the overall dimensions of the engine. Elongated shutters of an ordinary regulated jet nozzle are used for throttling. When the reverser is switched off, the jet nozzle connecting to the screens rests on the butt end of the jet pipe, but the screens extend across the pipe. Since there are no working parts in the stream, the reverser cannot effect the direct thrust produced by the engine. /34 Experimental investigations on models have shown that the reverse coefficient for this scheme when $\beta_{vane} = 40^\circ$ is approximately 0.4 (§3, Chapter IV).

Variants of Schemes X, XI and XII can be implemented without an extensible jet tube, which obviously complicates and weighs down the design. Interior or external cylindrical flaps with longitudinal displacement along the engine axis (Scheme XIII) or made to tilt about the engine axis (slide type) can be provided to cover screens in direct thrust regime. These methods of covering screens are shown in Figure 4.14 where the possible schemes of a reverser in a nozzle fitted with a central body are examined (§2, Chapter IV). Cylindrical flaps can hinge backward, as has been done in covering ports in engine nacelles and the fuselage of the Boeing 727 (cf. §5 of this chapter). The screens can also be covered by individual louver type flaps opening within the jet pipe of the engine or into the exterior outside the aircraft. Several schemes of reversers installed in the nozzle with a central body fitted with the first of these louver types have been investigated. The results of model tests are given in §2 of Chapter IV. A design using other louvers has been executed and is described in §5 of this chapter.

Scheme XIII with throttling bucket shutters located aft of the exit cross-section of the jet nozzle and with deflecting screens located on the jet pipe of the engine forward of the jet nozzle. In the direct thrust regime the deflecting screens are closed by cylindrical shutters which are capable of longitudinal displacement. The scheme belongs in the class of one of the earlier designs for reversers and is marked by high weight [27].

The variants of Schemes X, XI, XII and Scheme XIII examined below are examples of reversers in which the throttling of the gas ducts and closing of the deflecting elements in the direct thrust regime is carried out by different parts of the assembly.

Reversers Installed Aft of the Jet Nozzle Exit

Reversers with shutters (Figure 1.8).

Scheme I with shiftable, tiltable cylindrical shutters is one of the simplest. The shutters are relatively easily encompassed within the over-all dimensions of the engine nacelle. The over-all length of the engine fitted with a reverser under this scheme, as is true for most schemes of reversers located aft of the jet nozzle exit, is increased in the reverse regime. /35

Experimental verification on models (§1 and 3 of Chapter IV) have shown that reversers of this scheme can have high reverse coefficients ($\bar{R}_{rev}$ = 0.5-0.6).

Scheme II with tiltable shutters and deflecting flaps is suggestive of Scheme I in the method of screen deflection. However, in this scheme shutters constitute a hinged part of the engine nacelle and have additional deflecting tiltable flaps. Scheme IIa ($\bar{R}_{rev}$ = 0.5) has actually been built by General Electric Company (United States). A description of the reverser design of

this company is given in the next section. A similar scheme ($R_{rev} \approx 0.6$) was tested on a Curtiss-Wright (United States) engine[1].

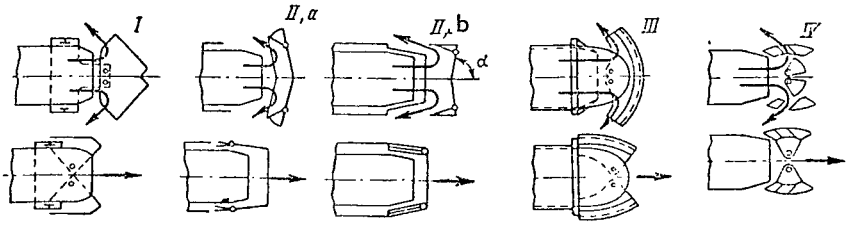

Figure 1.8. Reversers with Shutters Located Aft of the Jet Nozzle Exit; I, with Shiftable, Tiltable Cylindrical Flaps; II, with Tiltable Flaps and Deflecting Flaps; III, with Hinged Spherical Flaps; IV, with Ejector and Spherical Flaps.

Variant b of Scheme II differs in the angle α of the shutter inclination. From model tests data its reverse coefficient for a small enough angle of stream exit $\beta_{vane} = 15°$ and $\alpha = 85°$ is $\bar{R}_{rev} \approx 0.68\text{-}0.74$ (§1, Chapter IV). The reverser of this scheme with angles $\beta_{vane} = 48°$ and $\alpha = 55°$, tested by Boeing (United States) on models, has $\bar{R}_{rev} = 0.5$[2]. A similar scheme has been realized in the bypass Pratt-Whitney JT8D-5 engine[3] on a Douglas DC-9 ($\bar{R}_{rev} = 0.40\text{-}0.45$).

Scheme III with hinged spherical shutters was actually built (cf. Figure 1.1) and has undergone stand tests on an engine ($\bar{R}_{rev} \approx 0.35\text{-}0.4$).

Scheme IV with an ejector has spherical shutters which in thrust reversal direct the stream to the ejector ports. In direct thrust regimes the ports /36 are covered by the very same shutters. If a fixed ejector is used, the overall length of the engine in reverse regimes remains unchanged. A similar scheme [32] has found use on the Douglas DC-8 (United States) ($\bar{R}_{rev} = 0.43$).

---

1 *Aviation Week*, 11/III, Vol. 66, No. 10, p. 43, 1957.
2 *Flight*, 30/IV, No. 2362, pp. 540-541, 1954.
3 *Interavia*, Vol. XX, No. 6, p. 726, 1965.

Reversers with deflecting screens (Figure 1.9)

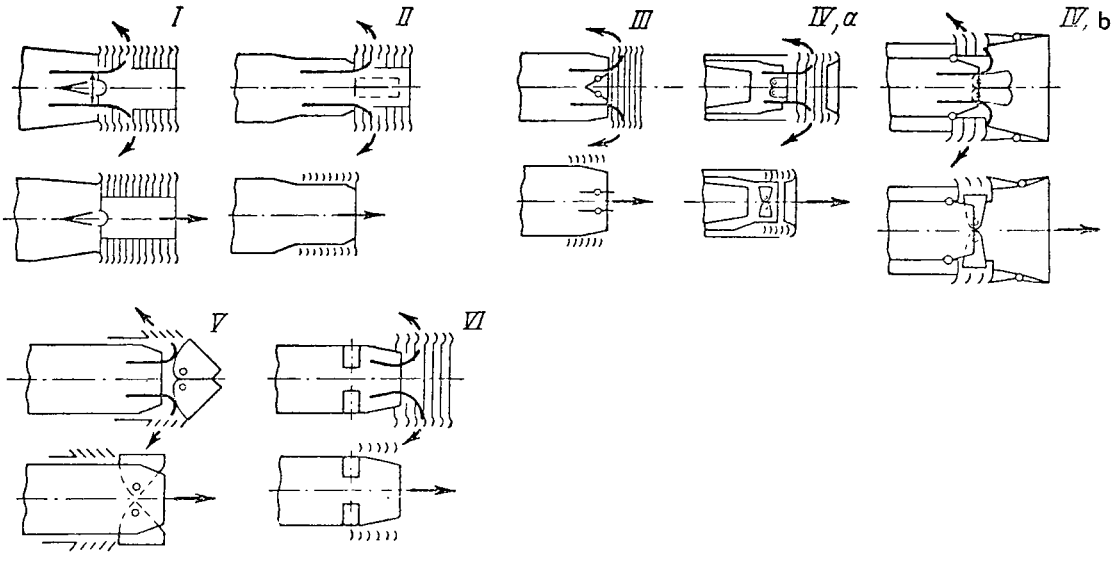

Figure 1.9. Schemes of Reversers With Deflecting Screens Located Aft of the Jet Nozzle Exit: I, with Fixed Deflecting Screens (d.s.) and Blow-through of Air Through Fairing in the Nozzle; II, with Movable d.s. and Tiltable Throttling Shutters; III, with Movable d.s. and Tiltable Vanes; IV, with Annular Tiltable Throttling Shutters and Movable d.s. (Variant a) and with Fixed d.s. (Variant b); V, with Movable Screens and Hinged Cylindrical Shutters; VI, with Movable Screens and Vanes Rotating the Exhaust Stream.

Scheme I developed by the amalgamation SNECMA (France), has fixed deflecting screens and fairing installed in the jet nozzle through whose slits air bled aft of the engine compressor is swept. The presence of fairing in the nozzle leads to direct thrust losses up to 4%. With 2-3% air bleeding, in this scheme the reverse coefficients can amount to 0.3.

Flight tests of reversers of this scheme on the Vampire aircraft made by De Havilland (Great Britain) have been conducted by the company. A modification of this scheme has shiftable deflecting screens [34].

Scheme II with shiftable screens and two tiltable throttling shutters, developed by Aerojet General (United States), is an advanced version of Scheme I. When the reverser is switched off, the shutters lie flush with the annular flaps covering the sides of the screen, and in reverse regimes they are tilted

along their axes and partition the gas duct, compelling the stream to be deflected to the screens.[1]

Scheme III developed by the amalgamation SNECMA (France), with shiftable deflecting screens has tiltable vanes with aerodynamic profile, which serve to deflect the stream to the screens. With the reverser switched off, the vanes remaining in the stream exert an effect on engine direct thrust. Based on SNECMA data, the reverser built under this scheme has $\bar{R}_{rev} \approx 0.20$ and $\Delta\bar{R} \approx 0.03$[2]

Scheme IV, developed by the amalgamation SNECMA (France) is characterized by deflecting screens and two annular tiltable throttling shutters. When the version a reverser is switched off, the shutters lie along the periphery of the ejector fitting and do not block the straight flow exit of the stream. When the reverser is switched on, the rear of the ejector and the screens associated with it are shifted, the shutters are tilted by 90°, the ejector fitting is partially covered, and the stream is deflected to the screens. The /38
reverser of this version of the scheme, according to SNECMA data, has a reverse coefficient of 0.5[3].

Variant b of Scheme IV, differing in its fixed deflecting screens ($\bar{R}_{rev}$ = = 0.4-0.5), is being developed by SNECMA for the power plant in the Anglo French supersonic Concord airliner [27].

Scheme V with movable screens and hinged cylindrical shutters was experimentally verified on models ($\bar{R}_{rev} = 0.40$). When not functioning, the reverser doesn't have any effect on engine parameters. As preliminary design developments have shown, this scheme is easily fitted into the middle of the engine nacelle or the fuselage.

Scheme VI with movable screens and exhaust-rotating vanes can be relatively easily fitted into the middle of the engine nacelle or the fuselage. The scheme has been developed and investigated in the Swiss Technological Institute [31]. Key shortcomings of the scheme include the severe effect of the reverser on pressure aft of the turbine in that it shows a characteristic with respect to the vane tilting angle with a jumplike variation in thrust. Thus, tests of numerous models have shown that when the vanes are rotated by an angle ranging from 0° to 50° the thrust remains positive. At large vane tilting angles the thrust becomes negative with a simultaneous abrupt climb in pressure aft of the turbine. The values of the reverse coefficient are 0.5-0.8. The smallest value of direct thrust losses is an impressive figure--10%.

---

[1] *Jet Propulsion*, IV, Vol. 25, No. 4, 1955.
[2] *Aeroplane*, Vol. 89, No. 2293, 1955.
[3] *Les Ailes*, No. 1887, p. 9, 1962.

§5. Description of Reverser Designs

Arrangements of reversers on aircraft are marked by diversity. Reversers located forward of the jet nozzle exit are part of the engine assembly and are made in the form of a separate compartment of the jet pipe, aft of which the noise suppressor is easily installed.

Reversers located aft of the jet nozzle exit in the form of flapwise structures are constructed as hinged parts of the aircraft fuselage or the engine nacelle.

When engines are installed on an aircraft in the wings close to the fuselage or on pylons along the fuselage sides, flaps of the reversers located aft of the jet nozzle exit can be reinforced directly on the fuselage (Figure 1.10). The reverser is automatically placed aft of the engine's jet nozzles /39 when there is compression of the aircraft landing strut shock absorbers following contact with the runway and throttling of the engines[1].

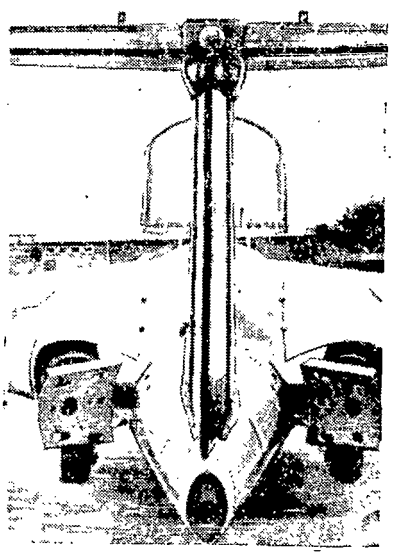

Figure 1.10. Reverser on the Bypass Engine Turbomek "Obisk" (740 kg Thrust) on the Military-Training Aircraft SAAB 105 (Sweden).

Reversers on the turbojet Rolls-Royce "Avon" and the bypass engine "Conway" (Great Britain), installed on airliners of De Havilland (Great Britain) "Comet" and Boeing 707 (United States), BAC VC-10, and BAC "Super VC-10" (Great Britain) have been executed, respectively, following the same scheme and differ in minor details. The design of reversers used in these engines is characterized by several interesting engineering solutions. The main assemblies--the reverser housing (made of the alloy Nimonic), the throttling shutters and the deflecting screens--are fabricated in welded form.

Throttling shutters 1 (Figure 1.11, a, b) are made of seamless sheet. The stiffness ribs 2 on the outer surface of the shutters are heated by the hot exhaust gases passing through them, emerging through openings in the upper side of the shutters and emitted at that point through the deflecting screens. The shutters have shoulders 3 and 4 in the form of flat semicircles which in direct thrust and reverse regimes abut against the corresponding gasket rings 5 and 6 of the housing. No special gaskets are provided for, for the surfaces of the shutter shoulders and housing semicircles in contact are

[1] *Interavia Review*, No. 12, p. 1,804, 1964.

processed mechanically. The front semicircles of the housing have an elastic reinforcement 7. The screen vanes are made of sheet material and are located in chessboard fashion (Figure 1.11 c). Thermal expansion of the deflecting screen is compensated by deformation of the supporting struts 8 in the rear of the screen.

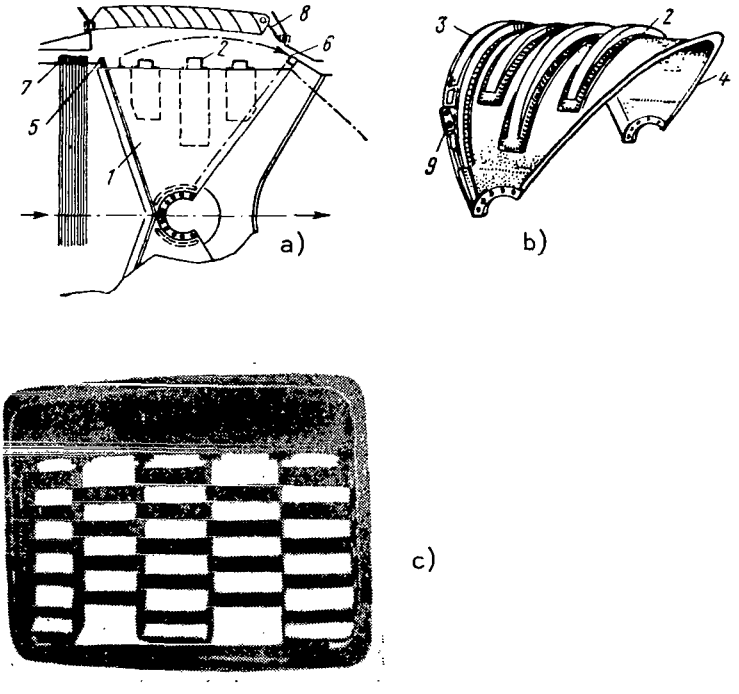

Figure 1.11. Reverser Used with Rolls'Royce Turbojet Engine and Bypass Engine. (a, Design Layout; b, Throttling Shutter; c, Deflecting Screen): 1, Throttling Shutter; 2, Rigidity Rib; 3, Front Gasket Shoulder; 4, Rear Gasket Shoulder; 5, Front Housing Semicircle; 6, Rear Housing Semicircle; 7, Elastic Reinforcement; 8, Maintenance Support; 9, Aperture.

Special "dry" antifriction roller bearings functioning without lubricant /40 and cooling at temperatures up to 600°C have been developed for reversers. Slipping bearings have also been investigated in the course of work with the reverser. However, they have been rejected owing to large frictional resistance which would lead to weighing down the control drive.

The shutters are secured by their flanges on two coaxial pivots between which two ball bearings are situated. The outer pivot rotates on ball bearings placed in the housing. To simplify the design, the rotational moment is transmitted to the shutters not through the pins: the outer pin is covered by

bushings, each of which has a two-arm lever; one arm of each of the levers is within the housing and a pin projecting from one end enters the aperture 9 (cf. Figure 1.11, b) in the lug on the shutter, and the other arm of the lever connects with a rod of the control drive system ("Avon" engine, Figure 1.12) /41
or with the rods of the pneumatic cylinders ("Conway" engine).

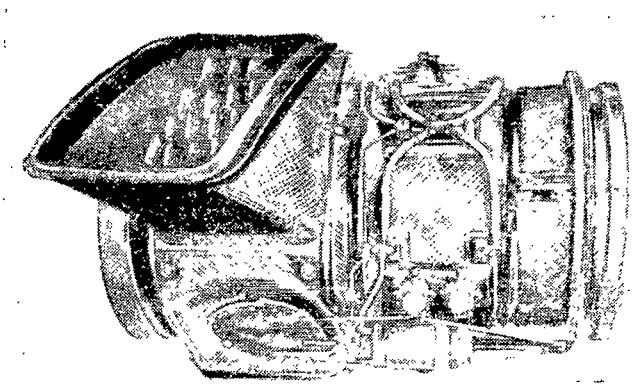

Figure 1.12. Reverser of the Rolls-Royce "Avon" Turbojet Engine Built for Installation on the Engine.

Pneumatic cylinders in which air bled from the compressor is fed are used in the drive controlling the shutters, affording a two-position placement of the shutters. The lever system of the drive is capable of developing great leverage even in high-cruise regime when the air pressure available is low.

As a whole, the structures of Rolls-Royce reversers, ensuring reverse coefficients within the limits of 0.45-0.56, are marked by compactness. Their relative weight is 0.10 (cf. Table 1) and direct thrust losses are not greater than 0.75%. The photograph above shows the reverser used on the "Avon" engine (cf. Figure 1.12), where we can see the pneumatic cylinder, the lever system of the drive, the heated-insulating coating, and the exhaust channel of the reverser.

Control systems exclude the possibility of switching on reversers owing to pilot error. On the "Comet" aircraft with four "Avon" engines, located in the wings, the levers used to control reversers installed on the other engines have such an arrangement that their movement is possible only in low-throttle regimes. On the Boeing 707 aircraft, in which all the four "Conway" engines installed in the underslung engine nacelles are equipped with reversers, each main lever of thrust control is equipped with an additional lever for control /42
of the reverser that lies within pilot reach only in the case when the main lever is shifted to the low-throttle position.

Drives used in controlling thrust produced by engines fitted with reversers are made in such a way that the possibiltiy of increasing engine rpm when reversers are switched on is obviated [25].

Figure 1.13 presents a design scheme of a reverser used on the "Spay" RB-163 Rolls-Royce bypass engine (flight thrust 4,560-5,170 kg), installed on

the airliners Hawker Siddeley HS-121 "Trident" and the BAC 1.11[1] (Great Britain) and on the Grumman administrative aircraft "Gulfstream" II (United States).

The reverser used on the Pratt-Whitney JT3C-6 turbojet engine (United States, thrust 5,080 kg), installed on the Boeing 707-120 airliner in underslung engine nacelles on all four engines, was built according to the same scheme as the one used by Rolls-Royce ($\bar{R}_{rev}$ = 0.40). The screen is made of individual sections (Figure 1.14). The vanes of the screen are nonprofiled, made of stainless steel sheet. The width of the central sections is 114 mm, and the rest 76 mm. The chord of the vanes is about 60 mm in length. The vanes are curved at the stream inlet. The angle of vane placement in the rear of the screen is constant (approximately 2/3 of the screen length), but is variable in the front section. The first two vanes are built without bends and are installed perpendicular to the engine axis. This screen design, as well as the individual flaps covering the screen from without and visible in the photograph, reduced to permissible limits the ingestion of heated gases at the engine inlet and on the structural members of the aircraft. Screen density is about 2.0.

Pilot instructions provide for switching on the reverser only after the nose wheel of the aircraft has touched ground. At an aircraft velocity greater than 110 km/hr, thrust reversal is carried out when the number of rpm of the high-pressure compressor rotor is not greater than 90% of the rated value. When the velocity is reduced to 110 km/hr, the negative thrust is brought down to a value corresponding to π^*_{nozzle} = 1.5. This negative thrust setting is kept until the aircraft comes to a full halt[2].

The reverser used on all the Pratt-Whitney JT8D-1 bypass engines installed on the Boeing 727 consist of throttling internal shutters similar to those used on the reversers described for the Rolls-Royce engines and their associated mechanically external shutters, forming in the direct thrust regime the surface of the engine nacelle(Figure 1.15). For the central engine installed in the rear of the aircraft fuselage, deflection of gases occurs in the horizontal plane, and for the two engines located on pylons along the aircraft sides--upwards and downwards[3]. /44

Figure 1.16 shows a photograph of shutter type reversers located aft of the jet nozzle of the Pratt-Whitney JT12A-A6 turbojet engines (thrust 1,360 kg). /45 The shutters are hinged parts of the engine nacelle. On the service aircraft Lockheed "Jet-Star" 329 (United States) all four engines installed on pylons in the rear section of the fuselage are fitted with these reversers [37].

Aircraft Engineering, No. 395, pp. 7-11, 1962.
Aviation Week, X, Vol. 81, No. 19, pp. 5[illegible] 53, 1964.
Flight, 7/XII, No. 2752, 1961; V, No.2826, pp. 681-682, 687-688, 1963.

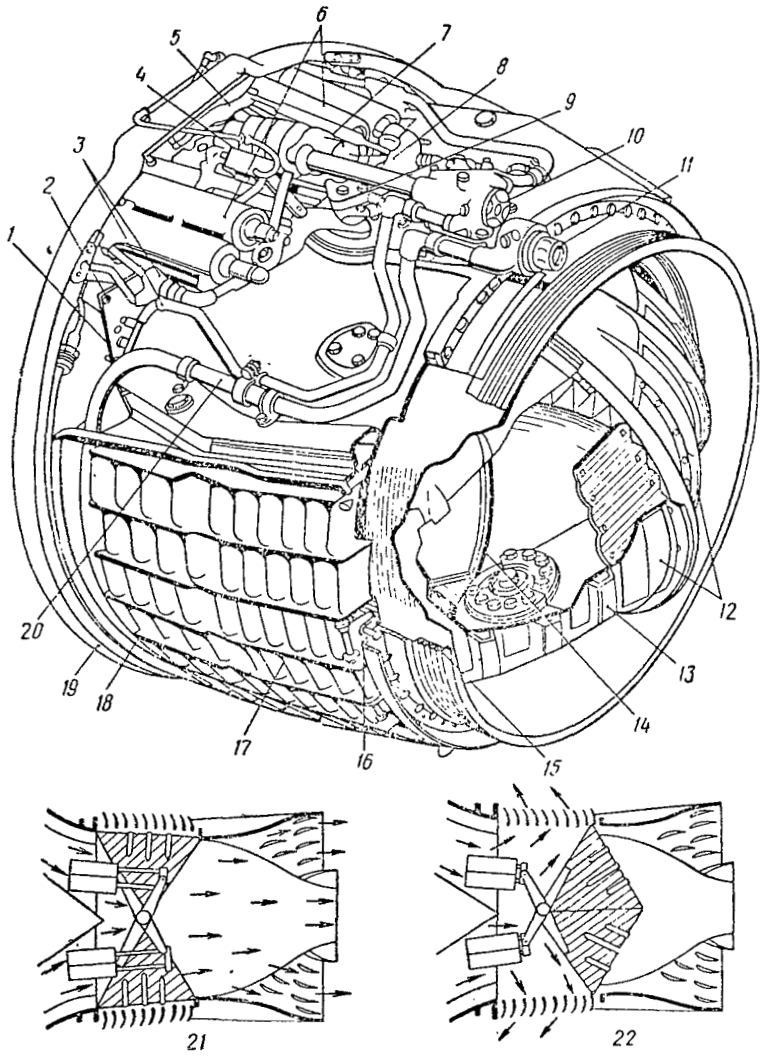

Figure 1.13. Design Layout of Reverser Used on the Rolls-Royce "Spay" Bypass Engine: 1, Assembly Flange; 2, Lifting Gear; 3, Distribution Tubing for Air; 4, Switch; 5, Lever of Control Relay; 6, Pneumatic Cylinders; 7, Locking Mechanism; 8, Floating Lever; 9, Control Lever; 10, Control Valve; 11, Bypass Valve for Pressure Reduction; 12, Throttling Shutters; 13, Rigidity Corrugations; 14, Front Semicircle of Housing; 15, Gasket; 16, Assembly Flange; 17, Screen Vanes; 18, Release Valve Wall; 19, Fairing Ring; 20, Air Tubing; 21, Direct Thrust Regime; 22, Thrust Reversal Regime.

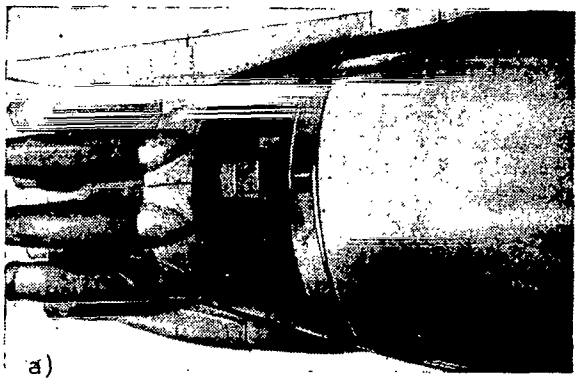

a)

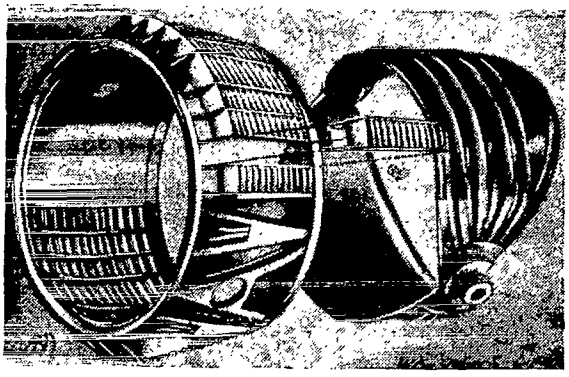

Figure 1.14. External Appearance of Reverser and Noise Suppressor Used on the Pratt-Whitney JT3C-6 Turbojet Engine (a). Housing of Reverser Fitted with Deflecting Screens and Throttling Shutters (b).

Interest has centered on the Pratt-Whitney JT3D-1 bypass engine (thrust 7,700 kg), in which the reversers are provided for both engine passes. These engines are installed in underslung engine nacelles on the airliners Douglas DC--8-50 "Jetliner" (United States)[1] and Boeing 707-120B[2]. /46

Throttling of the gas duct of the internal engine pass is provided by tilting vanes. The stream of the internal and external passes is deflected in the reverse direction by profiled screens. When the thrust is reversed on these aircraft by the covering screen of the internal pass, the housing of the engine nacelle is shifted downward along the streamline with the aid of a pneumatic drive, uncovering the shutters (Figure 1.17).

On the bypass engine used on the DC-8-50 aircraft cold air from a two-step fan in the direct thrust regime is issued through two ports that are crescent-shaped and located along both sides of the engine nacelle; on the Boeing 707-120B air from the fan is issued along the periphery. On the DC-8-50 aircraft the external pass screens in the direct thrust regime are covered by the external tilting vanes (louvers) located in the longitudinal direction. On the Boeing 707-120B these screens are covered by being shifted backwards by the engine nacelle housing. This housing is mechanically connected with the throttling vanes and is shifted simultaneously with their actuation.

The necessity for deflection of the outer pass thrust in the reverse direction in thrust reversal stems from the fact that direct thrust obtained by air escaping from the fan represents almost half of the over-all engine thrust. /47

[1] *Interavia*, No. 4672, p. 8, 1961.
[2] *Aeroplane*, No. 2553, p. 442, 1960.

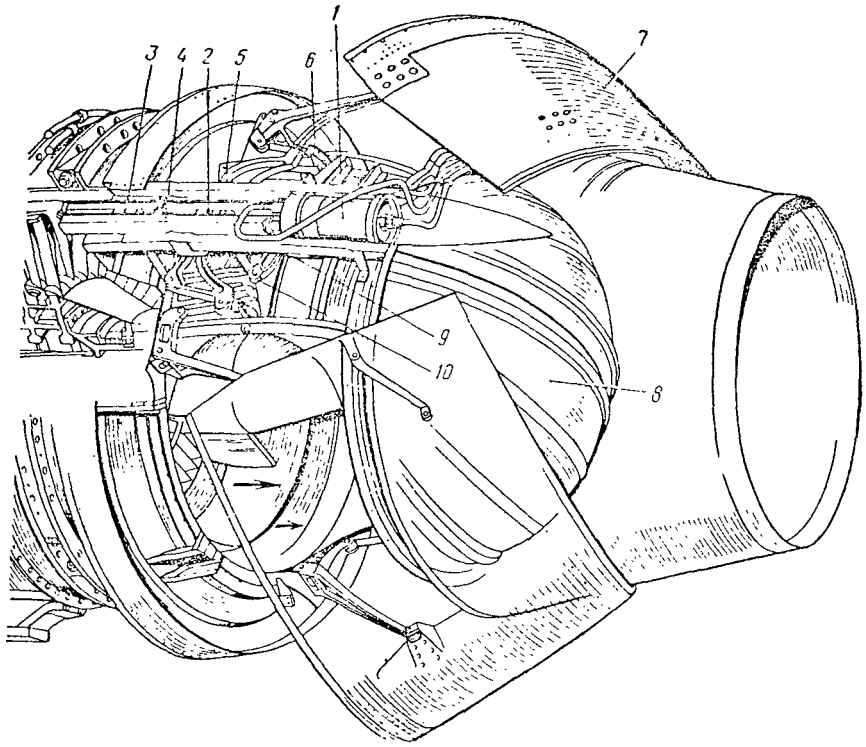

Figure 1.15. Design Layout of Reverser Used on the Pratt-Whitney JT8D-1 By-Pass Engine Installed on the Boeing 727: 1, Power Cylinder; 2, Slide for the Drive Controlling External Shutters; 3, Slide for Drive Controlling Internal Shutters; 4, Guide Slide; 5, Levers of External Shutter Drive; 6, Buffer Stop; 7, External Shutters; 8, Internal Shutters in Thrust Reversal Regime; 9, Support Bracket of Internal Shutters; 10, Internal Shutter Lever.

Figure 1.18 presents a photograph of the reverser on the TF33-P-7 bypass engine (thrust 9,525 kg) equipped on the Lockheed C-141 "Starlifter" transport $\overline{R}_{rev} = 0.45$). The reverser consists of tilting flaps, comprising part of the engine nacelle[1]. /48

Figure 1.19 shows the design layout of a reverser installed on the Pratt-Whitney JT8D-5 bypass engine (thrust 5,445 kg). Two such engines are installed in engine nacelles in the aft section of the fuselage of the Douglas DC-9 airliner. The reverse coefficient $\overline{R}_{rev} = 0.40\text{-}0.45$, and the switch on time of the reverser is 1.5-2 sec.[2]

[1] *Aviation Week*, 2/IX, Vol. 79, No. 10, pp. 69-70, 1963.
[2] *Interavia*, Vol. XX, No. 6, p. 728, 1965; *Flight*, 3/III, Vol. 89, No. 2973, p. 345, 1966.

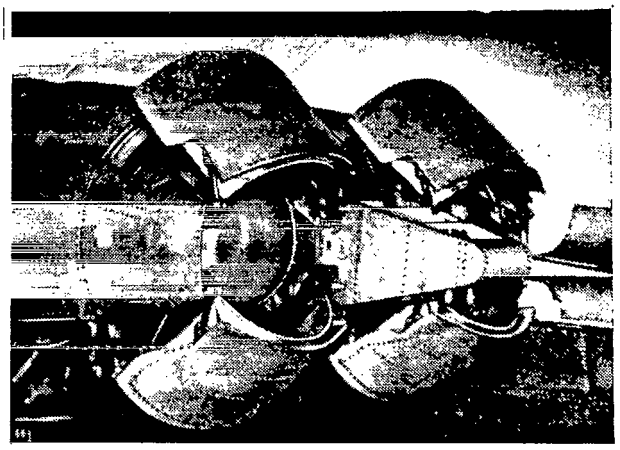

Figure 1.16. Reverser Used on the Pratt-Whitney JT12-A6 Turbojet Engine.

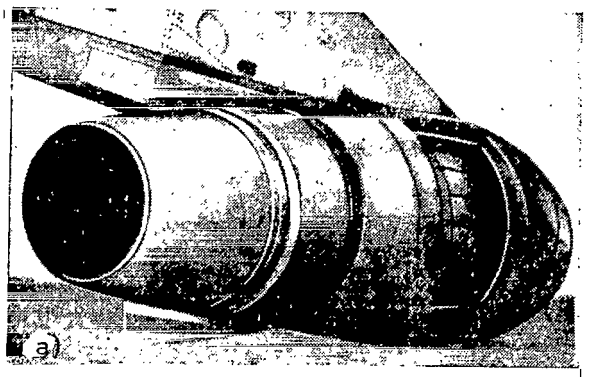

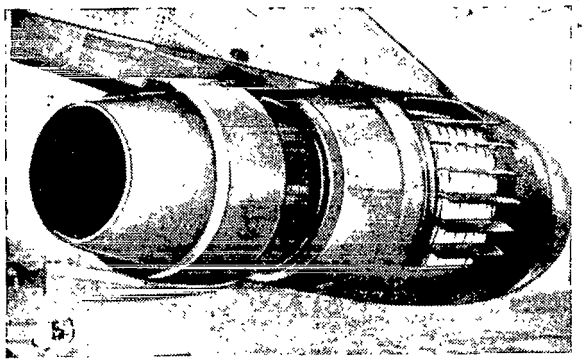

Figure 1.17. Engine Nacelle of the DC-8-50 Aircraft Equipped with a Pratt-Whitney JT3D-1 Bypass Engine: a, With Position of Engine Nacelle Housing and External Tilting Shutters in Takeoff and Cruise Mode Flight; b, With Position of Housing and Shutters in Thrust Reversal.

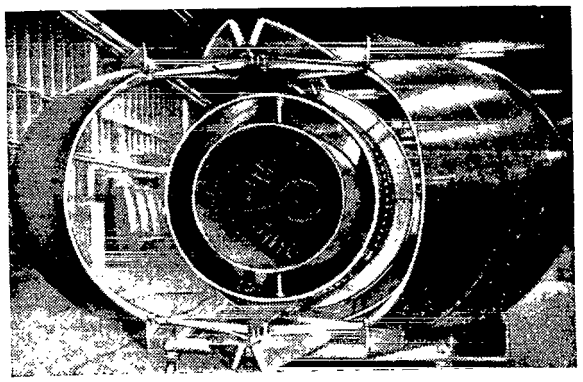

Figure 1.18. Reverser Used on the Pratt-Whitney TF33-P-7 Bypass Engine.

Figure 1.20 is a photograph of the aft section of the General Electric CJ805-3 (United States, thrust 5,285 kg) turbojet engine with a noise suppressor and a reverser equipped with throttling shutters and deflecting screens located forward of the nozzle exit ($\overline{R}_{rev} = 0.50$). The screen coverage angle is 120°. Direct thrust losses are less than 1%. Switch-on time for the reverser is 1 second.

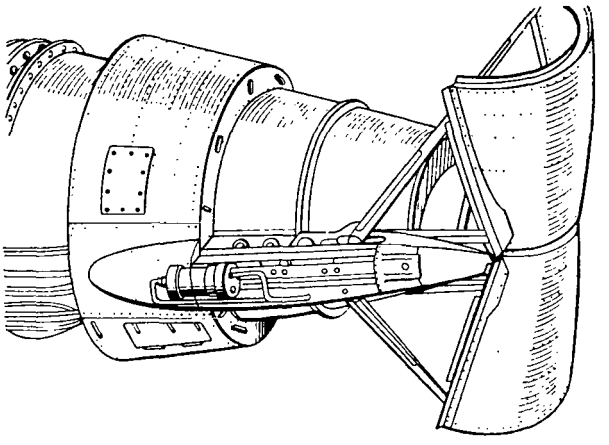

Figure 1.19. Design of Reverser on the Pratt-Whitney JT8D-5 Bypass Engine on the Douglas DC-9.

This engine has been installed on the Convair 880 airliner (United States). Switch-on of the reverser takes place after touchdown of the aircraft and velocity has been reduced to 220 km/hr. Maximum engine rpm is maintained down to a velocity of 110-120 km/hr. Then the rpm is reduced to a value 90% of the maximum and retained down to a velocity of 75 km/hr. Subsequently the engine is switched to low gas regime with /51 maintenance of the reverser in the reverse thrust position.

A special device obviates the possibility of landing with thrust reversal if on a given engine the throttling shutters do not move into the position required for thrust reversal.[1]

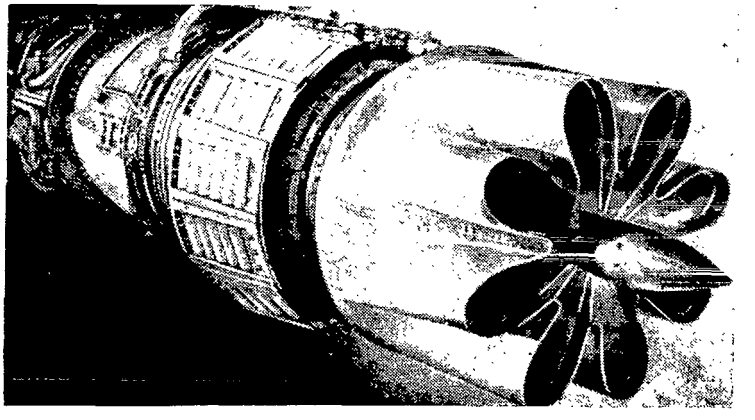

Figure 1.20. Reverser on the CJ805-3 Turbojet Engine

The reverser equipped on the General Electric CJ805-23 bypass engine (thrust 7,300 kg), a modification of the CJ805-3 turbojet engine with aft attachment, is located aft of the jet nozzles of both engine passes and consists of shutters and stream-deflecting slotted shutters, constituting hinged parts

[1] *Aviation Week*, Vol. 75, No. 3, p. 82, 1961; *Airlift*, Vol. 23, No. 4, pp. 65-68, 1959.

of the engine nacelle (Figure 1.21). On the Convair 990 airliner (United States) all four engines installed in suspended pods are equipped with reversers.

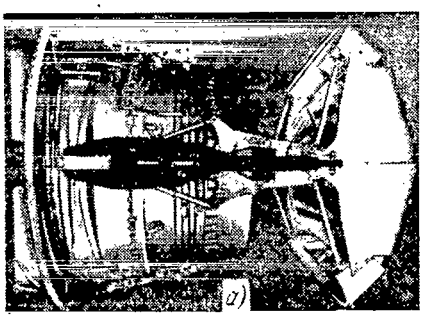

a)

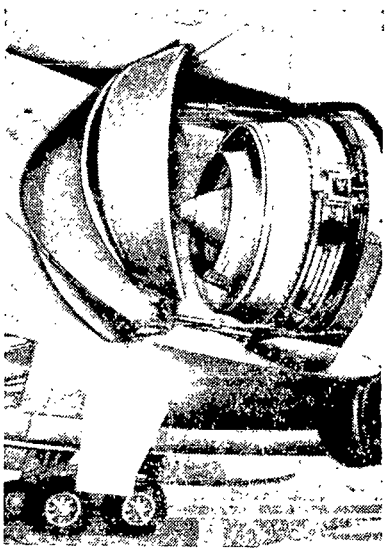

b)

Figure 1.21. Reverser on the CJ805-23 Bypass Engine: a, Side View; b, Position Under the Reverser on the Convair 990.

The reverser is oriented relative to the engines in such a way that gas escape proceeds in the horizontal plane (cf. Figure 1.21, b). The slotted flap inclination angle can be varied for attainment of the required negative thrust and to prevent impinging upstream on aircraft structural members. For the reverser shown in the figure, the reverse coefficient at a stream exit angle of about 45° is 0.50. Control of shutters and slotted flaps is accomplished via a system of levers using hydraulic powered cylinders. The kinematics of the lever system provides the shutters and slotted flaps simultaneous translational and rotational motion. For thrust reversal the shutters are shifted rearward about 685 mm along rails located beneath the pod pylon. In the event of control drive failure, a safety device holds the shutters and flaps in a working position. The maximum negative thrust is reached in 2 sec.

In the course of company improvement of the reverser, measurement of vibration was made and found to be slight; the range of vibrations did not exceed 1.3 mm [20].

CHAPTER II

FUNDAMENTALS OF GAS DYNAMIC CALCULATION OF REVERSERS AND EFFECT OF GEOMETRIC AND GAS DYNAMIC PARAMETERS ON REVERSE COEFFICIENT

§1. Fundamentals of Gas Dynamic Calculation of the Reversers

Let us examine a reverser whose diagram in generalized form is given in /52
Figure 2.1. Here the section 2-2 refers to the minimum cross-section of the deflecting screen, and section 3-3 corresponds to the stream at its exit from the screen, that is, after it has been tilted obliquely to the cross-section. Rotating of the stream obliquely to the cross-section is observed when the extent of pressure reduction is much greater than the working levels of pressure reduction for thrust reversal upon landing. When the reverser is cut in, the gas duct is partially blocked and some of the exhaust gases escape in the rear- /53
ward direction. Another part escapes into the atmosphere through deflecting screens. When the pressure reduction levels $\pi^*_{\text{nozzle}} \leq 2.2$, typical of working modes of reversers cut in upon aircraft landing, the escape velocity from the deflecting elements, considering the relatively high level of total pressure loss therein, is subsonic. Therefore we can assume that the velocity and the direction of the stream in the section 3-3 are equal to its velocity and direction in the section 2-2, but the static pressure at the exit from the deflecting elements is equal to the ambient pressure.

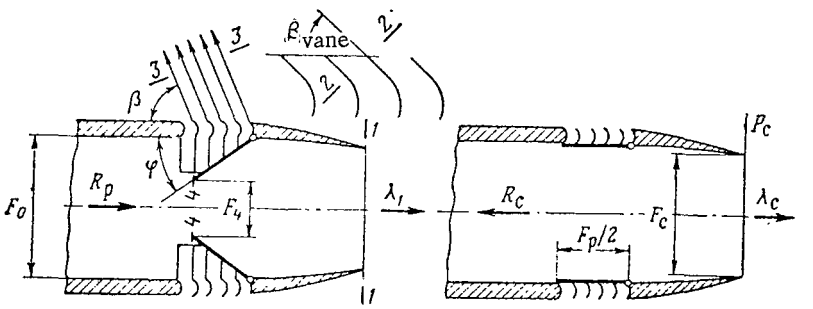

Figure 2.1. Diagram of Reverser and Symbols Used.

Experimental data given in Chapter V confirmed the validity of the foregoing.

The sum of the projection of reverse stream momentum in the engine axis and the momentum of air entering the engine, with subtraction of momentum of gas escaping from the nozzle, is the negative thrust P_{rev} of the engine:

$$P_{rev} = \frac{G_2}{g} v_2 \cos \beta_2 + \frac{G_{rev} V}{g} - \frac{G_1}{g} v_1, \tag{2.1}$$

where G_2 and v_2 = consumption through deflecting elements of the reverser and and flow rate at exit therefrom;

G_1 and v_1 = consumption through jet nozzle in reversal and velocity at exit therefrom;

β_2 = angle of gas stream exit from deflecting elements of the reverser relative to engine axis;

$G_{rev} = G_1 + G_2$ = total consumption through engine in reversal;

V = aircraft flight velocity

g = acceleration due to gravity.

Under stand conditions, the negative thrust of the nozzle is

$$R_{rev} = \frac{G_2}{g} v_2 \cos \beta_2 - \frac{G_1}{g} v_1. \tag{2.2}$$

Using the well-known gas dynamic relationship

$$p_0 f(\lambda) F = v \frac{G}{g} + pF,$$

we write out equation (2.2) and the value of consumption in terms of the coefficients of total pressure recovery σ_2 in the reverser and σ_1 in the jet nozzle when throttling elements have been installed in it:

$$\begin{aligned} R_{rev} &= P_H F_2 \cos \beta_2 \left[\pi^*_{noz} \sigma_2 f(\lambda_2) - 1\right] - p_H F_1 \left[\pi^*_{noz} \sigma_1 f(\lambda_1) - 1\right], \\ G_{rev} &= m \frac{p_H}{\sqrt{T_0}} \left[q(\lambda_2) \pi^*_{noz} \sigma_2 F_2 + q(\lambda_1) \pi^*_{noz} \sigma_1 F_1\right]. \end{aligned} \tag{2.3}$$

Here F_2 = minimum cross-sectional area of deflecting elements; /54

F_1 = jet nozzle area in reversal;

T_0 = temperature of gas braking in the nozzle;

$$m = \sqrt{k \left(\frac{2}{k+1}\right)^{\frac{k+1}{k-1}}} \cdot \sqrt{\frac{g}{R}},$$

where R = gas constant. For the products of combustion of a turbojet engine m = 0.389.

The values of gas dynamic functions $f(\lambda)$ and $q(\lambda)$ are found in the table listed by the following ratios

$$\Pi(\lambda_2) = \frac{1}{\pi^*_{\text{nozzle}}\sigma_2}, \quad \Pi(\lambda_1) = \frac{1}{\pi^*_{\text{nozzle}}\sigma_1}.$$

Here the extent of pressure reduction $\pi^*_{\text{nozzle}} = p_0/p_H$, where p_0 = total pressure at inlet to reverser.

In the case of nonuniform fields of total and static pressure and angles β_2 in the exit section of the deflecting elements of the reverser and nonuniform pressure fields in the exit section of the jet nozzle, equations (2.3) are written in integral form:

$$\begin{aligned} R_{\text{rev}} &= \int_{F_2} \cos\beta_2 [p_0\sigma_2 f(\lambda_2) - 1]\, dF_2 - \int_{F_1} [p_0\sigma_1 f(\lambda_1) - 1]\, dF_1, \\ G_{\text{rev}} &= \frac{m p_0}{\sqrt{T_0}} \left[\int_{F_2} q(\lambda_2)\, \sigma_2 dF_2 + \int_{F_1} q(\lambda_1)\, \sigma_1 dF_1 \right]. \end{aligned} \tag{2.4}$$

We can use equations (2.3) and (2.4) to conduct verification calculation of the reverser, that is, so-called "forward problem". Generalized data on σ_2 and other information on σ_1 are given in Chapter IV.

Let us denote by k the ratio of consumption through the deflecting elements of the reverser to the overall consumption through the engine:

$$k = \frac{G_2}{G_{\text{rev}}} = \frac{G_{\text{rev}} - G_1}{G_{\text{rev}}}$$

and we will introduce reduced velocities at the exit from the deflecting elements λ_2 and the valve in thrust reversal λ_1. Then equation (2.2) will become:

$$R_{\text{rev}} = \frac{kG_{\text{rev}}}{g} a_* \lambda_2 \cos\beta_2 - (1-k)\frac{G_{\text{rev}}}{g} a_* \lambda_1. \tag{2.5}$$

Here a_* = critical speed of sound.

To calculate the reverse coefficient $\bar{R}_{rev}$, we must know the direct thrust /55
of the nozzle, usually expressed by the coefficient $\bar{R}_{\text{specific nozzle thrust}}$ of the specific thrust:

$$R_{nozzle} = \bar{R}_{\substack{\text{spec. nozzle} \\ \text{thrust}}} \frac{G_{nozzle}}{g} a_* \lambda_{\text{ideal velocity}}, \qquad (2.6)$$

and for determination of the consumption coefficient in reversal $\bar{G}_{rev}$, we must know the value of the consumption through the nozzle in forward thrust:

$$G_{nozzle} = \mu_{nozzle} G_{\text{ideal velocity}}$$

Here μ_{nozzle} = consumption coefficient, $G_{\text{ideal velocity}}$ = ideal consumption

$$G_{\text{ideal velocity}} = m \frac{p_0}{\sqrt{T_0}} q\,(\lambda_{\text{ideal velocity}}) F_{nozzle}$$

where $\lambda_{\text{ideal velocity}}$ = reduced velocity at total expansion from total pressure p_0 forward of the nozzle up to the pressure p_H of the surrounding environment, F_{nozzle} = area of critical section of nozzle in forward thrust. It is assumed that the characteristics of the nozzle are known in the form of the function $\bar{R}_{\text{specific nozzle thrust}}$ and μ_{nozzle} with the extent of pressure reduction in the nozzle as the dependent variable

Consumption through the engine when the reverser has been cut in must equal the consumption through it in forward thrust, that is, the consumption coefficient $\bar{G}_{rev} = G_{rev}/G_{nozzle} = 1$. Then, by using equation (2.5), we express the reversal coefficient in the following form:

$$\bar{R}_{rev} = \frac{R_{rev}}{R_{noz.}} = \frac{1}{\bar{R}_{\substack{\text{spec. noz.} \\ \text{thrust}}} \lambda_{\text{ideal velocity}}} [k\lambda_2 \cos\beta_2 - (1-k)\lambda_1]. \qquad (2.7)$$

Thus, in calculating the reverser located forward of the exit section of the jet nozzle, in addition to characteristics of the nozzle $\bar{R}_{\text{spec.nozzle thrust}}$ and μ_{nozzle} we must yet have available the parameters σ_2, β_2, σ_1, k. When the entire consumption is deflected in the reverser, it is sufficient to have additionally only two parameters σ_2 and β_2:

$$\bar{R}_{rev} = \frac{\lambda_2 \cos\beta_2}{\bar{R}_{\text{specific nozzle thrust}}\,\lambda_{\text{ideal velocity}}} \qquad (2.8)$$

The negative thrust of the engine when external flow is present is written in the following form in terms of the reverse coefficient:

$$P_{rev} = \left(P + \frac{G_{nozzle}}{g} V\right) \bar{R}_{rev} + \frac{G_{rev}}{g} V, \qquad (2.9)$$

where P = forward thrust of engine.

In the actual practice of designing reversers, we encounter the so-called "reverse problem" which formulated thusly: for a reverse coefficient and known characteristics of the deflecting and throttling elements, we want to find the appropriate position of the latter and the required minimum cross-sectional area of the deflecting elements. /56

Using formulas (2.7) for the reverse coefficient and (2.6) for the forward thrust of the nozzle in terms of the coefficient of the specific thrust produced at the nozzle, we can derive an expression for the required value k necessary to ensure the specified reverse coefficient for given characteristics of the deflecting elements and of the nozzle when the throttling elements have been installed in the nozzle:

$$k_{required} = \frac{\bar{R}_{rev}\bar{R}_{\text{spec. nozzle thrust}} + \frac{\lambda_1}{\lambda_{\text{ideal velocity}}}}{\frac{\lambda_2}{\lambda_{\text{ideal vel.}}} \cos\beta_2 + \frac{\lambda_1}{\lambda_{\text{ideal velocity}}}} = k_1(\phi) \qquad (2.10)$$

The required value of k is a function of the position of the elements throttling the gas duct of the engine, for example, the tilting angle ϕ of the shutters, flaps, etc.

The variables λ_1, β_2 and λ_2 entering into expression (2.10) must be determined experimentally. We must also find from experiment the function of the assumed value of k:

$$k_{available} = k_2(\varphi). \qquad (2.11)$$

We will take as the assumed value of k the fraction of the over-all consumption that must be directed to the deflecting elements for the selected scheme of throttling elements. Since the functions $k_1(\phi)$ and $k_2(\phi)$ are

analytically unknown, combined solution of equations (2.10) and (2.11) for determination of the values of k and ϕ is best done graphically. Knowing the characteristics of the deflecting elements (σ_2, β_2) and the nozzle characteristics when the throttling elements have been installed in it (σ_1), we can for several positions of the throttling elements calculate from formula (2.10) the required value of the fraction of the over-all consumption which must be directed to the deflecting elements in order to obtain the desired reverse coefficient. The sought-for values of k and ϕ are found from the intersection of the curves $k_1(\phi)$ and $k_2(\phi)$ plotted in terms of the coordinates ϕ and k.

The necessary minimum cross-sectional area of the deflecting elements is calculated from the formula

$$F_2 = \frac{G_2}{m \frac{p_{02}}{\sqrt{T_0}} q(\lambda_2)}, \tag{2.12}$$

where $p_{02} = p_0\sigma_2$. We find the value $q(\lambda_2)$ from the known values of π^*_{nozzle} and σ_2.

§2. Effective Geometric and Gas Dynamic Parameters on the Reverse Coefficient /57

We will write the expression for negative thrust of the nozzle in the following form:

$$R_{rev} = F_2 \varrho_* a_*^2 q(\lambda_2) \sigma_2 \lambda_2 \cos\beta_2 - F_4 \varrho_* a_*^2 q(\lambda_4) \sigma_4 \lambda_4 \tag{2.13}$$

where $F_2 = F_{\text{screen}} \sin \beta_{\text{vane}}$;

β_{vane} = design angle of vane at exit from screen;

F_{screen} = area occupied by screen;

F_4 = area of clearances in the throttling element closing the nozzle;

$a_* = \sqrt{\frac{2k}{k+1} g R T_0}$ = critical speed of sound;

$\varrho_* = \left(\frac{2}{k+1}\right)^{\frac{1}{k+1}} \varrho_0$ = density of gas in the critical section;

$q(\lambda)$ = reduced consumption;

λ_1 = reduced velocity at exit from nozzle;

σ = total pressure recovery coefficient.

The index "0" denotes the braking parameters, and the indexes 1, 2, 3, and 4 denote the cross-sections shown in Figure 2.1.

In equation (2.13) it has been assumed that $\lambda_2 = \lambda_3$ and $p_2 = p_H$.

When the reverser has been cut out, the gas exiting from the nozzle produces positive thrust.

$$R_{nozzle} = F_{noz.}\rho_* a_*^2 q(\lambda_{noz.})\sigma_{noz.}\lambda_{noz.} + F_{noz.}p_0\left(\frac{p_{nozzle}}{p_0} - \frac{p_H}{p_0}\right), \qquad (2.14)$$

where p_{nozzle} = static pressure at nozzle cross-section,

p_H = ambient pressure.

Dividing equations (2.13) by (2.14), we get an expression of the reverse coefficient as a function of gas dynamic and geometrical parameters of the reverser:

$$\overline{R}_{rev} = \frac{F_1 q(\lambda_2)\sigma_2\lambda_2\cos\beta_2\sin\beta_{vane} - F_4 q(\lambda_4)\sigma_4(\lambda_1)}{F_{noz.}\left[q(\lambda_{noz.})\sigma_{noz.}\lambda_{noz} + \frac{p_0}{\rho_* a_*^2}\left(\frac{p}{p_0}_{noz} - \frac{p_H}{p_0}\right)\right]}. \qquad (2.15)$$

Let us consider the effect of geometric parameters of the reverser, that is, the area of the deflecting screens and the angle of gas escape β_2 on the reverse coefficient. Let us take as the optimal reversers the design for which at a given area occupied by the deflecting screens or the connecting pipes in the jet duct of the engine, the reverse coefficient will be at a maximum or for a given reverse coefficient the indicated cross-sectional area will be at a minimum. To exclude the effect of the reverser on the engine it is necessary to satisfy the following equality /58

$$F_4\sigma_4 q(\lambda_4) = F_{noz.}q(\lambda_{noz})\sigma_{noz} - F_{screen}\sin\beta_{vane}q(\lambda_2)_2. \qquad (2.16)$$

For simplicity in analysis, let us consider the case when $p_{nozzle} = p_H$, that is, for subcritical or near critical extent of pressure reduction or when

there is complete expansion of gas in the nozzle. Let us also assume that $\sigma_{nozzle} = 1$, that is, total pressure losses in the nozzle with the reversers cut out do not exist, and that $\beta_2 \simeq \beta_{vane}$. Then, substituting expression (2.16) in the relationship (2.15) we get

$$\overline{R}_{rev} = \overline{F}_{screen} \frac{q(\lambda_2)}{q(\lambda_{noz})}\sigma_2\frac{\lambda_2}{\lambda_{noz}}(\cos\beta_{vane}\sin\beta_{vane} + \xi\sin\beta_{vane}) - \frac{\lambda_1}{\lambda_{noz}}, \quad (2.17)$$

where $\overline{F}_{screen} = F_{screen}/F_{nozzle}$ = relative cross-sectional area of deflecting screens;

$$\xi = \lambda_1/\lambda_2.$$

The reduced velocities λ_1 and λ_2 depend on the total pressure recovery coefficients in the throttling and deflecting elements of the reverser, respectively. With a reduction in β_{vane} at $F_{screen} = const$, the minimum passage cross-sectional area of the deflecting element, and consequently, the gas consumption deflected to the reverse direction, is reduced. To satisfy condition (2.16), the amount of gas bypassed in the straight-flow direction for which the area F_4 must be increased must rise. Variation in the ratio F_4/F_{nozzle} will lead to a change in coefficient σ_4. Thus, in the general case the parameter ξ is a function of the angle β_{vane}. However, in the two cases of practical importance to us, we can assume that ξ does not depend on the angle β_{vane}. In the first case, when the throttling shutters are located at the exit section of the nozzle. Gas escaping through the gaps leaves the nozzle at a supercritical degree of pressure reduction at a reduced velocity $\lambda_1 = 1$. In the second, when the throttling shutters are located so far from the exit cross-section of the nozzle that they practically completely dissipate the axial velocity, such that $\lambda_1 << 1$, and within the limits $\lambda_1 = 0$.

Let us find the value of the angle β_{vane} that corresponds to the maximum reverse coefficient for the specified limiting cases when there is a fixed value of the parameter $\overline{F}_{screen}$, for which we will differentiate (2.17) in terms of the angle β_{vane}, assuming that $q(\lambda_2)$ and σ_2 do not depend on the angle β_{vane}.

Equating the product to zero, we get the optimal angle as a function of the ratio of velocities

$$\cos\beta_{\text{optimal vane angle}} = \frac{-\xi \pm \sqrt{\xi+8}}{4}. \quad (2.18)$$

In expression (2.18) we must take a plus sign in front of the root, which corresponds to the angle $\beta_{vane} < 90°$. /58

If the throttling elements are located close to the nozzle exit ($\xi = 1$), then the optimal angle of the exit of the stream from the screen is 60°. If the throttling elements are located remotely from the exit cross-section of the nozzle ($\xi = 0$) then the angle β_{vane} is 45°.

Results of calculating the reverse coefficient from formula (2.17) for the value $\xi = 1$ and $\xi = 0$ in the case of an absence of total pressure losses in the deflecting screens, that is, when $\sigma_2 = 1$, are shown in Figure 2.2. In the calculation, the value of $\bar{F}_{screen}$ is taken as a parameter. The maximum reverse coefficient corresponds to the optimal value of the angle β_{vane} at a given area $\bar{F}_{screen}$, and for a given reverse coefficient--for minimum $\bar{F}_{screen}$ (Figure 2.3). The maximum value of the reverse coefficient $\bar{R}_{rev} = \cos \beta_{vane}$, is plotted on the figure, corresponding to the case when the entire consumption passes through the screen and the losses of total pressure in the nozzle and in the deflecting on the screen are absent ($\sigma_{nozzle} = \sigma_2 = 1$).

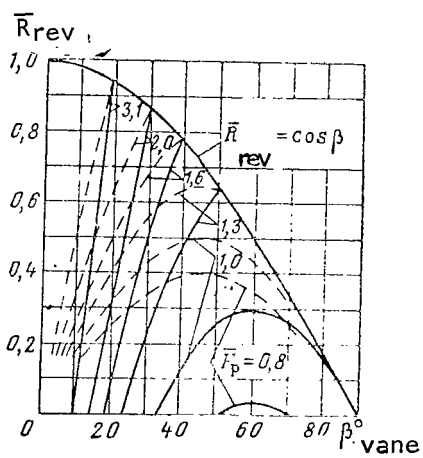

Figure 2.2. Reverse Coefficient as a Function of the Angle of Stream Exit at Constant Relative Area $\bar{F}_{screen}$ of the Deflecting Screen; $\pi^*_{nozzle} = 1.9$. (The Solid Curves Correspond to the Ratio of the Reduced Velocities $\lambda_1/\lambda_2 = 1.0$; and the Dashed--When $\lambda_1/\lambda_2 = 0$).

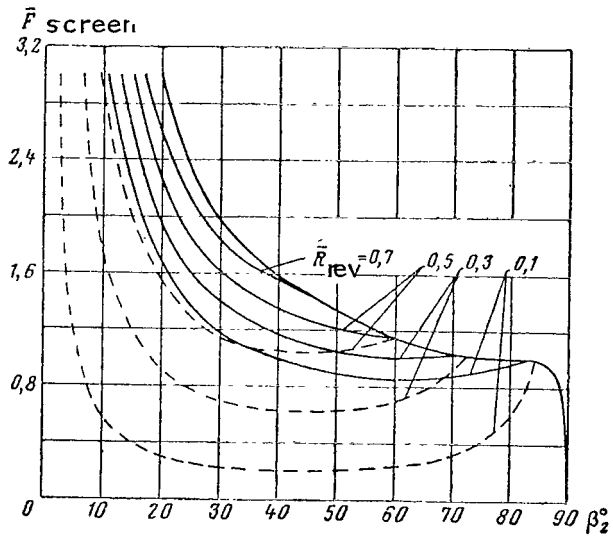

Figure 2.3. Relative Area of Deflecting Screens as a Function of Stream Exit Angle at Constant Reverse Coefficient. (The Symbols are the same as those in Figure 2.2.).

It follows from calculations that in the absence of total pressure losses the values of the reverse coefficients needed in practice (about 0.5) can be obtained when the stream angle at exit from the screen β_2 = 45-60°. It is obvious that it will be more profitable to have large stream escape angles since here the probability of the heated reverse stream sweeping over the engine nacelle, fuselage, or wing of the aircraft is reduced.

Let us consider the effect that the coefficient of total pressure recovery in the deflecting screen and the extent of pressure reduction have on the reverse coefficient.

For simplicity, let us consider the case when all of the gas passes through the reverser. Then it follows from the consumption equation that

$$\frac{F_{screen}\sin\beta_{vane}}{F_{nozzle}} \quad \frac{q(\lambda_2)}{q(\lambda_{nozzle})} \quad \sigma_2 = 1$$

and expression (2.15) can be transformed to the following form: /61

$$\overline{R}_{rev} = \frac{\frac{\lambda_2}{\lambda_c}\cos\beta_2}{1 + \frac{p_0}{\varrho_* a_*^2)_{nozzle} q(\lambda_{nozzle})}\left(\frac{p_{nozzle}}{p_0} - \frac{p_H}{p_0}\right)} \qquad (2.19)$$

If there are losses of total pressure, the reverse coefficient is reduced by a reduction in velocity at the exit from the screen.

The reverse coefficient as function of the coefficient of total pressure recovery σ_2 is shown in Figure 2.4. The calculation was based on formula (2.19) for $p_{nozzle} = p_H$. When there is an increase in the total pressure losses in the screen, the reverse coefficient decreases. Here, to retain the unchanged consumptions through the engine compared to the case $\sigma_2 = 1$, we must increase the exit cross-sectional area of the screen F_2 (Figure 2.5).

When some of the gas passes through the nozzle, the reverse coefficient is reduced by the amount

$$\Delta\overline{R}_{rev} = \frac{F_4\sigma_4 q(\lambda_4)\lambda_1}{F_{noz}\lambda_{noz} q(\lambda_{nozzle}) + \frac{p_0}{\varrho_* a_*^2}\left(\frac{p_{nozzle}}{p_0} - \frac{p_H}{p_0}\right)},$$

which is directly proportional to the gas consumption and its velocity at the nozzle exit.

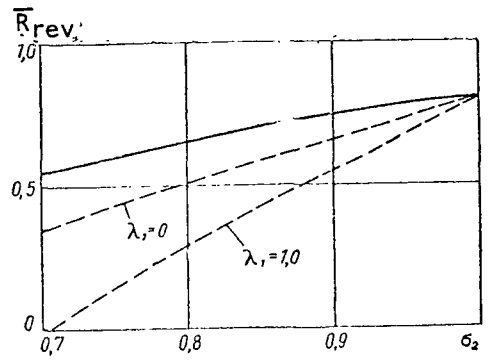

Figure 2.4. Reverse Coefficient as a Function of the Total Pressure Recovery Coefficient for $\beta_{vane} = 37°$ and $\pi^*_{nozzle} = 1.9$. (The Solid Curve Corresponds to the Absence of Gas Passing Through the Throttling Elements; Dashed Lines--for the Case of Constant Area $\bar{F}_{screen}$ Corresponding to $\sigma_2 = 1.0$).

If the exit cross-sectional area of this screen compared to the case $\sigma_2 = 1$ remains unchanged, then to retain the condition $\pi^*_{nozzle} =$ = const some of the gas must be released to the jet nozzle, which sharply reduces the reverse coefficient (dashed lines on Figure 2.4).

In this case, as has already been remarked, a reduction in the reverse coefficient depends strongly on the escape velocity of the gas from the jet nozzle. The limiting cases corresponding to $\lambda_1 = 0$ and $\lambda_1 = 1.0$ are plotted in the figure.

As has been indicated, for a critical degree of pressure reduction in the nozzle

$$\pi^*_{nozzle} \leqslant \left(\frac{k+1}{2}\right)^{\frac{k}{k-1}},$$

$p_{nozzle} = p_H$, the oblique cross-section does not function in the screen, and, consequently, we can assume that $\lambda_3 = \lambda_2$ and $\beta_3 = \beta_2$. The reverse coefficient when $\sigma_2 = 1$ and the independence of the angle β_2 on the extent of pressure reduction do not depend on π^*_{nozzle}.

If the extent of pressure reduction in the nozzle is supercritical, then /62 $\pi^*_{nozzle} > \left(\frac{k+1}{2}\right)^{\frac{k}{k-1}}$ and it is clear from the ratio (2.19) that the reverse coefficient depends on π^*_{nozzle}. Owing to the presence of an oblique cross-section in the screen the escape velocity from the screen and the stream angle at the exit are changed.

The stream angle at the exit from the screen, owing to tilting in the oblique cross-section, can, for example, be found from the consumption equation written for the cross-sections 2-2 and 3-3:

$$\sin\vartheta_3 = \frac{q(\lambda_2)}{q(\lambda_3)} \frac{\sin\beta_{vane}}{\sigma_3},$$

where $q(\lambda_2)$ and β_{vane} = stipulated geometrical and gas dynamic parameters of of the screen;

λ_3 = determined from extent of pressure reduction p_H/p_0 and the coefficient of total pressure recovery σ_3 in the oblique cross-section.

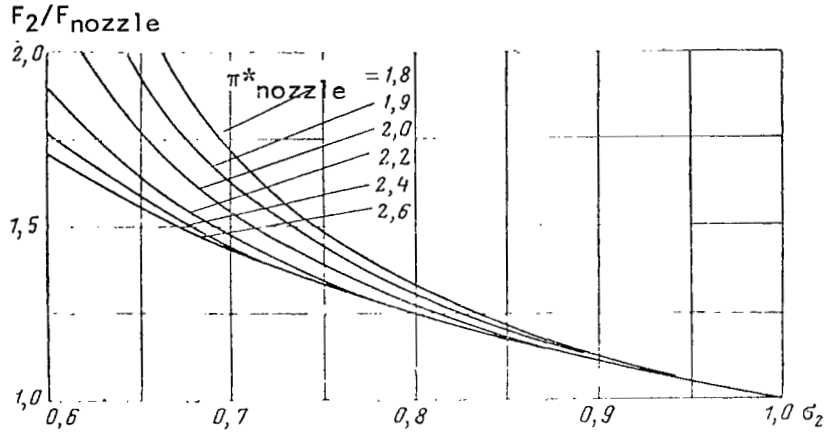

Figure 2.5. Relative Area of Deflecting Screens of the Reverser as a Function of the Coefficient of Total Pressure Recovery for Different π^*_{nozzle}.

The presence of losses in the oblique cross-section will lead to an increase in the angle β_2 and to a reduction in the velocity λ_2. The limiting value of the angle β_3 depends on the geometric parameters of the screen and the total pressure losses in it [5] and can be found without allowing for losses, from formula

/63

$$\sin\beta_3 = \frac{\sqrt{\frac{k-1}{k+1}}}{\sqrt{\sin\beta_2 - \frac{2(1-k)}{k+1}} - \frac{2}{k+1}}.$$

Here the limiting value of the pressure ratios is

$$\frac{p_3}{p_0} = \left(\frac{2}{k+1}\right)^{\frac{k}{k-1}} \sin\beta_3^{\frac{2k}{k+1}}.$$

A further reduction of this set of pressure ratios does not result in an increase of the angle β_3.

By way of example, Figure 2.6 presents the results of calculating the reverse coefficient for a single model. It was assumed in the calculation that the coefficient of total pressure recovery in the deflecting screens does not depend on the extent of pressure reduction. In this same figure experimental values of the reverse coefficient obtained from tests have also been plotted. Calculation of the reverser model with deflecting screens and throttling element in the form of a diaphrgam with opening equal to 25% of the nozzle cross-section escape area has been made on the assumption that $\lambda_1 = \lambda_{nozzle}$.

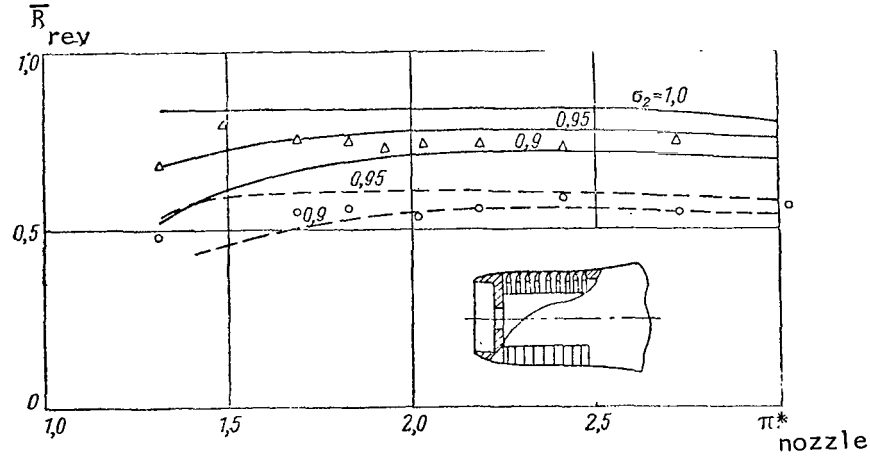

Figure 2.6. Reverse Coefficient as Calculated Functions of the Extent of Pressure Reduction for Different Total Pressure Recovery Coefficients and Comparison with Experiment for a Reverser Model when $\beta_{vane} = 37°$. (Solid Curves Correspond to the Case in Which There is no Passage of Gas Through the Throttling Diaphragm; Dashed Curves Correspond to the Presence in the Diaphragm of Openings Having an Area $F_4 = 0.25\ F_{nozzle}$).

Comparison of the calculated values of the reverse coefficient with experimental reveals that for the given simplest model calculation in general follows the reverse coefficient as a function of the extent of pressure reduction and as a function of distribution of consumption between the reflecting screen and the nozzle. /64

The smallest value of the total pressure recovery coefficient in the deflecting screen for this model is equal, evidently, to 0.9.

We must note that the reverse coefficient is the function of the extent of pressure reduction are marked by great diversity (Chapter IV). Design determination of the values of $\bar{R}_{rev}$ encounter certain difficulties which have necessitated in practice resorting to model tests of reversers.

CHAPTER III

STUDY METHODS AND EXPERIMENTAL FACILITIES FOR TESTING REVERSER AND DEFLECTOR MODELS

§1. Methods of Studying Reversers and Deflectors /65

Constructing reversers and deflectors requires comprehensive and careful experimental investigation. These investigations are conducted as follows:

-- on models in special experimental installations;

-- on small-scale engines in stand tests;

-- on models of aircraft in low velocity wind tunnels;

-- on full-scale engines in stand tests;

-- on aircraft in taxiing, test landings and takeoffs.

Studies on models allow us to explore the effect of design and gas dynamic parameters on characteristic coefficients, to determine the required passage cross-sectional areas of deflecting and throttling elements, to study on the basis of measurements of pressure fields and angle characteristics of the flow in elements of reversers and deflectors, to secure information about the size of hinge moments, data on distribution of pressure along streamlined surfaces, that is, to obtain the basic information required in building rational designs of these devices.

Let us dwell on several general problems in research on reversers and deflectors on models.

Experimental facilities are equipped with force-measuring devices (scales) that allow us to measure the direct thrust of the nozzle for negative thrust of the reverser, and also the vertical component of the thrust when we are /66 studying deflectors.

High requirements have been placed on precision of measurements on facilities intended for use in studying jet nozzles and deflectors. Usually consumption must be measured on such installations with a precision not less than ±1%, and thrust-- ±5%. The precision in measuring negative thrust of reversers, speaking generally, can be lower (±1-2%), since no unique criteria, as indicated in §3 of Chapter I, exists for the required value of the reverse coefficient that must be provided for the reverser. On the other hand, gas dynamic improvements of the reverser of any scheme or scheme modification is subordinate in importance compared to its other characteristics--envelope dimensions, weight, possibilities of realizing in an actual design, etc. However, in actual practice, investigation of reversers proceeds with high

measurement precision, since their tests are conducted on the same facilities as nozzle tests.

Experimental facilities for investigating models of jet nozzles, reversers and deflectors in the form of pipe bend that can be tilted have won acceptance. In several designs this bend is connected with a suspended force-measuring device that is not a structural part of the facility itself. In some installations a movable bend is directly connected with a lever on which a pan is provided for weights that equalize the measured force of thrust. Lately, units in which forces are measured by tensometry have been enjoying mounting acceptance.

Investigation of models of reversers and deflectors is usually conducted in air. We know that some studies of reverser models have been conducted on units equipped with the combustion chambers of air-jet engines [37]. However, conducting tests of reverser and deflector models in this way does not stem from necessity, since the data obtained from tests in cold air can be recalculated to natural conditions by a well-known method.

In order for the results of model tests to be transferred to full-scale application, we must satisfy similarity conditions, in particular, with respect to M and Re numbers. The first condition is met by testing models for given extent of pressure reduction that obtains in a full-scale engine. The second condition is more difficult to satisfy.

The Re number for a model must be higher than the critical Re number, which is approximately $3 \cdot 10^5$. The Re number must be calculated from the characteristic dimensions of the reverser or deflector, for example, from the chord of the vane of the deflecting screen or the pitch of the screen, and for the reverser with shutters, along the gap between the shutters and the jet nozzle (engine nacelle) forming a minimum passage cross-section of the reverser. Usually, when testing models the modeling scale is 1/5-1/8. Units in which the jet pipe diameter (critical nozzle cross-section) is about 100 mm have been widely accepted. These installations require a measured amount of air. On the other hand, for these dimensions of the shutter-type reverser model the characteristic Re number will prove to be higher than the critical. /67

Deflecting screens of reversers and deflectors in full-scale engines have vane chord dimensions within the range 50-70 mm. When modeling such screens in the scale indicated, the dimensions of the vane chord will be too small in order to satisfy the similarity condition in Re number. Estimates have shown that the size of the vane chord of the model for M_2 numbers of about 0.9 for the stream exit from the reverser are characteristic for improved reversers, and must be taken as equal to approximately 15 mm. On the other hand, when manufacturing vanes of deflecting screens with smaller dimensions their geometric shape can be improperly executed. Thus, when investigating models of reversers and deflectors with screens we have to resort to units of fairly large size.

Another method of insuring the required Re number is to conduct tests of reversers and deflectors with screens on small-size engines. In the course of the studies, just as when testing on full-sized engines, it appears possible to study not only gas dynamic problems, but also the temperature conditions of parts of assemblies, the working order of the structure, and so on.

Investigations of reversers and deflectors in location on the aircraft when there is external streamlining are of great importance. Studies are made on models of aircraft in wind tunnels during which the reversers and deflectors are modified in such a way as to preclude impinging of the deflected stream on the engine inlet and on the structural members of the aircraft. In these studies water vapor or heated air is passed through the model of the reverser, and as the temperature at the air scoop inlet rises, this increase is used to estimate the incursion into it of the deflected jet stream. In addition, when water vapor or smoke-filled air is used as the working fluid it /68
appears possible to conduct visual observation.

The final stage in the cycle of studies conducted in the building of reversers or deflectors is to refine them during taxiing and test landings and takeoffs at the airport. The same range of problems that was considered in model tests of an aircraft fitted with reversers and deflectors in the wind tunnel is also in general the object of this kind of research.

§2. Experimental Unit for Study of Reverser and Deflector Models

Description of the installation No. 1. The lever type unit No. 1 for studying models of reversers and deflectors is shown in Figure 3.1. This unit was used to conduct investigations whose main results are given in §3 of Chapter IV, in §2 of Chapter V and in Chapter VIII. The unit has a rocking tube and a lever weighing device that affords measurement of the positive thrust of the jet nozzle and the negative thrust of the reversers, and also /69
the vertical and horizontal components of thrust produced at the deflectors. The unit operates on high pressure air fed to the model through the airline 1, cylinder 2, bushing 3, two connecting pipes 4, and the rocking tube 5. Labyrinth sealing is provided in cylinder 2.

Present at the end of the rocking pipe 5 is a bracket pipe 6 with a flange to which the test model 7 is secured. The bushing 3 rests on the support 9 via the prism 8. A two-arm lever 10 is rigidly secured to the bushing 3; suspended from the lever are scale pans for measuring the thrust or its vertical and horizontal components by means of weights. A mercury th rmometer is placed in the rocking pipe at the entry to the test model to measure the braking temperature T_0 and Pitot tubes for measurement of total and static air pressure. The Re numbers determined from the dimensions of the vane chord of the screens in the reversers and deflectors lie within the limits $(2\text{-}3)\cdot 10^5$. Therefore, the results of model tests obtained on this unit can be extrapolated to full size with adequate precision.

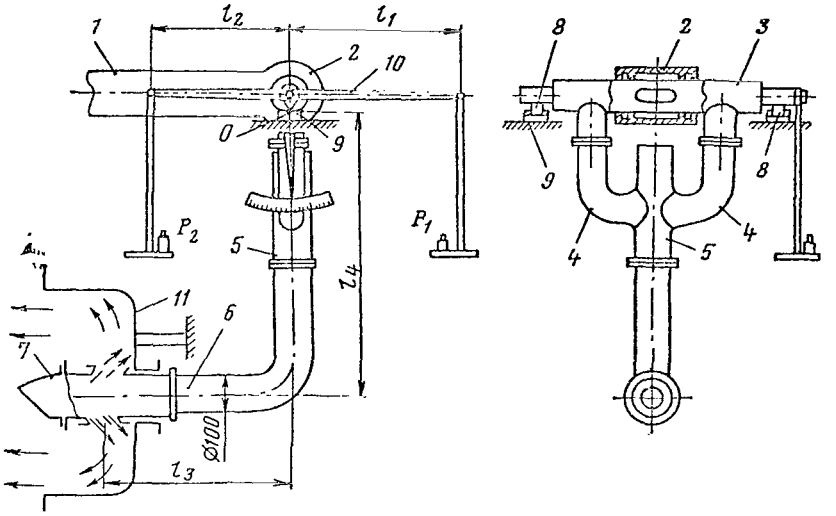

Figure 3.1. Diagram of Experimental Unit No. 1: 1, Airline; 2, Cylinder; 3, Bushing; 4, Connecting Pipes; 5, Rocking Pipe; 6, Bracket Pipe; 7, Test Model; 8, Prism; 9, Support; 10, Two-arm Weight Lever; 11, Deflector.

Method of conducting experiments and treatment of results. In tests of a model, the thrust in the steady-state regime is equalized by weights on the scale pans. The position of equilibrium is established by a pointer. The thrust of the model is determined from the equation of moments built up relative the point of rotation 0 of the system.

Direct thrust is determined from the equation

$$R_{nozzle} = P_1 \frac{l_1}{l_4},$$

where P_1 = weight on right pan of scale;

l_1 = right-arm of scale lever;

l_4 = vertical arm of rocking pipe.

Negative thrust of the reverser is determined from the equation

$$R_{rev} = P_2 \frac{l_2}{l_4},$$

where P_2 = weight on left pan of scale;

l_2 = left arm of scale lever.

The vertical and horizontal components of the thrust of deflectors are determined from the results of two experiments conducted with stream deflected downward and upward. The direction of the stream is varied by tilting the model by 180° on the flange about its horizontal axis.

If the thrust resultant, when the stream is deflected upwards, passes to the right of point 0 and when the stream is deflected downward to the left of 0, then the horizontal and vertical components of the thrust are determined, respectively, from the following equations: /70

$$R_{hor} = \frac{P_1 l_1 - P_2 l_2}{2 l_4},$$

$$R_{ver} = \frac{P_1 l_1 + P_2 l_2}{2 l_3}.$$

When the stream is deflected upward, the weights are loaded into the right pan of the scale, and when the stream is deflected downward--into the left pan. If the resultant passes to the right of point 0, then the force of the thrust is measured by a load only on the right pan of the scale when the stream is deflected upwards and downwards.

Equations for determining horizontal and vertical components of the thrust force in this case will be:

$$R_{hor} = l_1 \frac{P_1 + P_1}{2 l_4},$$

$$R_{ver} = l_1 \frac{P_1 - P_1'}{2 l_3},$$

where P_1' = load on right pan of scale with stream deflected downward.

If the resultant passes to the left of point 0, then the force of the thrust is measured by load on the left pan of the scale with the stream also deflected upward and downward. The equation of the horizontal and vertical components of the thrust force in this case are written, respectively:

$$R_{hor} = l_2 \frac{P_2 + P_2'}{2 l_4},$$

$$R_{ver} = l_2 \frac{P_2 - P_2'}{2 l_3},$$

where P_2' = load on left scale pan when the stream is deflected downward.

Air consumption is determined from the static p and the total p_{0i} pressures measured along the radius in the bracket pipe 6 in the center sections of five equally sized circular areas:

$$G = \frac{0,3965}{5\sqrt{T_0}} F \sum_{i=1}^{i=5} p_{0i} q(\lambda_i), \tag{3.1}$$

where F = area of bracket pipe.

The value of $q(\lambda_i)$ is determined with the aid of gas dynamic function tables from the following function calculated by relying on experimental data

$$\Pi(\lambda_i) = \frac{p}{p_{0i}}.$$

The total pressure p_0 at the inlet to the model is determined from the value of the measured static pressure p_{inlet} of the air from formula $p_0 = p_{inlet}/\Pi(\lambda_{inlet})$ in which the value of $\Pi(\lambda_{inlet})$ is found by using Table for the value of the function /71

$$y(\lambda_{inlet}) = \frac{G}{0,3965} \cdot \frac{\sqrt{T_0}}{F_{inlet} p_{inlet}}, \tag{3.2}$$

where F_{inlet} = area of inlet to the model.

Values of consumption and thrust are converted to standard atmospheric conditions.

Experimental characteristics of reversers are presented in the form of functions of the extent of pressure reduction π^*_{nozzle}, reverse coefficient $\bar{R}_{rev}$, and the consumption coefficient $\bar{G}_{rev}$, which are calculated from reduced thrust values:

$$\bar{R}_{rev} = \frac{R_{rev}}{R_{noz}}; \quad \bar{G}_{rev} = \frac{G_{rev}}{G_{noz}}; \quad \pi^*_{nozzle} = \frac{p_0}{p_H}.$$

The coefficients of vertical $\bar{R}_{ver}$ and horizontal $\bar{R}_{hor}$ components and the resultant $\bar{R}_{defl}$ of the thrust are calculated from data of experimental study of deflectors:

$$\bar{R}_{ver} = \frac{R_{ver}}{R_{id}}; \quad \bar{R}_{hor} = \frac{R_{hor}}{R_{id}}; \quad \bar{R}_{defl} = \sqrt{\bar{R}^2_{ver} + \bar{R}^2_{hor}}.$$

Here the indices "ver" and "hor", respectively, refer to the vertical and horizontal components of the thrust, and R_{id} is the ideal thrust of the nozzle

$$R_{id} = \frac{G}{g} a^* \lambda_{ideal} ,$$

where λ_{id} = reduced velocity corresponding to total expansion from pressure p_0 to p_H.

The consumption coefficients were calculated from the formulas:

$$\bar{G}_{deflecting} = \frac{G_{defl.}}{G_{nozzle}} ; \quad \bar{G}_{hor} = \frac{G_{deflecting}}{G_{hor}} .$$

The consumption coefficient $\bar{G}_{defl}$ was calculated for the deflectors for which in horizontal flight the jet stream escapes from the main nozzle, and the deflection of the stream is accomplished by throttling of the gas duct, that is, by the same method as in the reversers. The consumption coefficient $\bar{G}_{hor}$ was calculated for the deflectors with tilting nozzles, where G_{hor} = /72
= consumption upon escape of gas in the horizontal direction in the direct thrust regime.

The coefficient of total pressure recovery in the absence of direct thrust via bypassage of part of the consumption to the jet nozzle in the reverser was determined on the assumption that there is complete expansion of the thrust, based on the measured value of the negative thrust and the extent of pressure reduction π^*_{nozzle} by the method of successive approximations based on the following two equations:

$$R_{rev} = p_H F_2 \cos\beta_2 \left[\pi^*_{noz} \sigma_2 f(\lambda_2) - 1\right],$$

$$\Pi(\lambda_2) = \frac{1}{\pi^*_{noz} \sigma_2} .$$

In addition to obtaining overall characteristics of reversers and deflectors, it was of interest to investigate the stream when it exits from these devices. Study of the stream was based on measurement in different cross-sections of the total pressure fields and the stream exit angles. Analysis of total pressure fields aimed at establishing the nature of nonuniformity of the stream as it exits from the reversers and deflectors and at outlining ways of eliminating this nonuniformity. Study of fields of stream exit angles even under stand conditions is of great importance. Several measured total

pressure fields are listed in §3 of Chapter IV and the stream exit angles in §1 and 2 of Chapter V.

The total pressure fields were used also to calculate the coefficient of total pressure recovery in the reverser as the ratio of the averaged total pressure in the exit cross-section to the total pressure p_0 at the inlet to the reverser:

$$\sigma_2 = \frac{1}{F_2 p_0} \int_{F_2} p_{02} dF_2.$$

Comparison of σ_2 values calculated from thrust and from total pressure field at the exit has revealed their satisfactory convergence.

The total pressure recovery coefficient in the jet nozzle when throttling elements are installed in it was calculated in the thrust reversal regime as follows:

$$\sigma_1 = \frac{1}{F_1 p_0} \int_{F_1} p_{01} dF_1.$$

§3. Experimental Tensometric Type Unit for Studying Models of Reversers and Certain Methodological Problems in Research on Jet Nozzles and Reversers by the Scales Method /73

Description of Unit No. 2. This unit was used for experimental studies, the chief results of which are given in §1 and 2 of Chapter IV and §1 of Chapter V. The unit comprised a reverser, a scale section, and a silencer box.

An air bleed consisting of a disk with openings and a turbulentizing grid on a turning screen 3 were provided for organization of the stream in the reverser 1 (Figure 3.2). The scales section of the unit, designed to measure forces from the reverser or the jet nozzle under study by tensometry was mounted on the flange 10 of the reverser.

The housing 8 of a guidance device with vanes 9 located in the four ports of the housing was secured to the flange 10. Windows were also built in the sliding cylinder 19. In order to preclude stream momentum at the inlet, rational direction of the stream was provided by high screen density. The housing 8 had labyrinth gaskets designed to reduce leakage through gaps between housing and the sliding section of the unit. The sliding section consisted of a cylinder suspended on two weighing elements 7 and 12. The weighing elements consisted of laminar cross-pieces made out of single construction with inner

and outer flanges. The weighing elements allowed displacement of the cylinder in the axial direction, but secured it in the radial direction. The weighing element 7 was designed only for suspension of the cylinder in the sliding section. Resistance tensometers were riveted to the thick cross-pieces of the weighing element.

From the cylinder came air through the reducer 20 and arrived at the metered valve 14 ground according to the Vitoshinskiy curve. Drainage openings 16 were placed at the exit from the cylindrical section of the nozzle for static pressure measurement. A comb 15 was located in the reducer to measure total pressure.

The counter pressure chamber 6 with four pipes 17 serving to connect it with the space into which the gas is to escape was secured to the housing of the guide device. The dimensions of the chamber and the through sections of the pipe were chosen in such a way that the pressure in the chamber was equal to the pressure in the silencer box. This was done to prevent the pressure forces along both sides of the sliding cylinder to have an effect on the jet thrust. The pipes were sealed with rubber gaskets 18, and the face of the chamber with a rubber insert. The counter pressure chamber was covered with cowling 5. /75

The reverser or the jet nozzle under investigation was secured to the flange of the metered nozzle.

A collector 11 also fitted with a labyrinth gasket was installed to trap air streaming past the front labyrinth gasket. Bleeding of air from the connecting pipe proceeded in the radial direction.

The thickness of the thick cross-pieces of the weighing element 12 was 4.5 mm and for the thin cross-pieces--2.5 mm. The cross-pieces of the weighing element 7 were also made 2.5 mm in thickness. For a maximum load of 550 kg the bending stress in the cross-pieces did not exceed the permissible values for steel of grade 18KhNVA of which the weighing elements were fabricated. At a load of 550 kg the unbalance of the measuring bridge was about 17 millivolts. In nozzle tests the unbalance did not exceed 10-11 millivolts.

A comb 13 covering the unit was installed to reflect air escaping from the reverser under study. A thermometer 4 was installed on the reverser to measure the braking temperature. The bedplate 22, along the longitudinal guidewave of which the coordinate spacer can slide for shifting of the Pitot tubes, was secured to the unit's flange.

Calibration of the unit. Calibration of the weighing elements of the unit was conducted by means of model third-level dynamometers providing a precision of ±0.5% of the maximum measured value. An accessory consisting mainly of a nut and bolt was installed for weighing on the flange 23 of the bedplate 22 (cf. Figure 3.2). Turning the nut accomplished shifting of the screw and loading of the weighing element. The screw was kept from rotating with a cotter.

A universal dynamometer rated at 1,000 kg afforded calibration for performance in compression, (thrust) and in elongation (reverse).

Tensometers with resistances of about 90 ohms were connected in a Wheatstone bridge circuit, in the measuring diagonal of which the PP-type potentiometer affording a measurement precision of ±0.05 millivolt was connected. A variable resistance was inserted in one arm of the bridge. It afforded when necessary zeroing of the bridge. The bridge was connected to a battery. The feed voltage, 6 volts,was kept constant.

Calibrations showed that the unbalance of the measuring bridge as a function of force is satisfactorily approximated by straight line. In the calibrations the factory agreement of readings for forward and reverse movement when loads corresponding to reverse and thrust were applied was noted.

It was found that pressure in the receiver upset the equilibrium of the measuring bridge. Calibration was conducted to allow for the effect of pressure. To do this, the nozzle of the unit was covered by an end cap. /76

A comb was installed in the exit cross-section to measure total and static pressure levels in calibrating the measuring nozzle. Simultaneously, the difference between mean total pressure p_0 measured by the comb in the reducer and mean static pressure at the exit from the measuring nozzle Δp_{inlet} and the braking temperature T_0 were measured. Measurement of fields was conducted for two mutually perpendicular comb positions. Inspection showed adequate uniformity of total and static pressure fields.

Consumption was determined by the method stated in §2 of this chapter[1].

The calibration graph was plotted in the form of the function

$$G' = \frac{G}{p_0}\sqrt{T_0} = f(\Delta p_{inlet}/p_o).$$

Here p_0 = mean value of total pressure measured by the comb. The value of p_0 practically agrees with the total pressure values measured in the heart of the flow at the exit from the measuring nozzle. Examination showed that experimental values of G' differed only slightly from calculated values.

---

[1]We note that in this equipment as well as in the equipment described above, unit No. 1, consumption was not measured at the feed pipeline for which it is usually easy to attach standard instruments for measuring consumption, but directly in the movable part of the unit. This made it possible to ignore leakage through the laboratory field at the places where air is fed to the movable parts of the units.

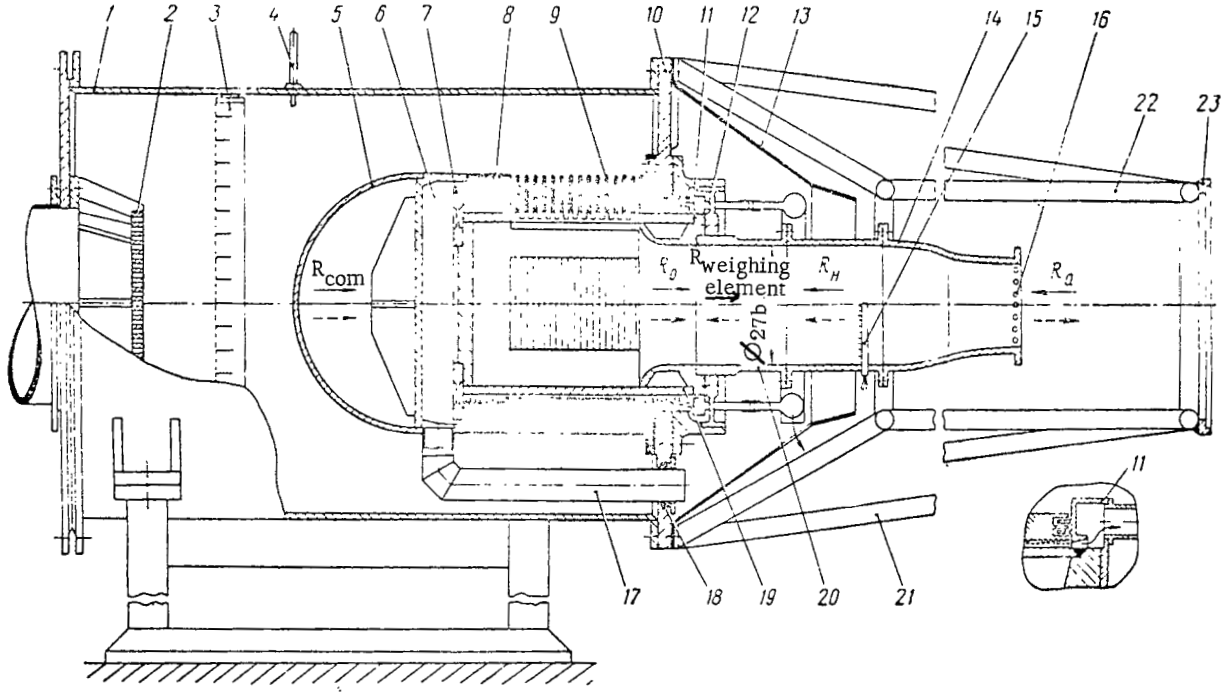

Figure 3.2. Design Schematic of Scales Section of Unit No. 2: 1, Reverser; 2, Baffle; 3, Screen with Grid; 4, Thermometer; 5, Cowling; 6, Counter Pressure Chamber; 7, Weighing Element; 8, Housing; 9, Vanes of Guide Device; 10, Flange; 11, Collector; 12, Weighing Element; 13, Reverberatory Housing; 14, Metered Valve; 15, Total Pressure Comb; 16, Metered Valve Drainage; 17, Counter Pressure Chamber Pipe; 18, Gasket; 19, Sliding Cylinder; 20, Reducer; 21, Bed Plate for Securing Coordinate Spacer and Calibrating Accessories; 22, Bedplate; 23, Flange.

Method of conducting experiments and treatment of results. In the test zone zone the nozzle and reversers are measured by the following variable :

1) mean value of total pressure in the reducer p_0;

2) static pressure in silencer box p_H;

3) difference between total pressure in reducer and static pressure at exit from metering nozzle Δp_{inlet};

4) difference between static pressure in counter pressure chamber and in silencer box $p_{chamber} - p_H$;

5) braking temperature T_0;

6) unbalance of measuring bridge $U_{weighing\ element}$.

To raise the reliability of results, the tests were conducted with a number of measuring bridges.

The forces acting on the sliding cylinder of the unit in the case of nozzle and reverser testing have been plotted in Figure 3.2. The solid arrows point to the direction of action of forces in testing of the jet nozzle, and the dashed lines--when the reversers were tested. /77

The forces are designated as follows:

1. R_k[1] = force of pressure on rear wall of sliding cylinder

$$R_k = F_k p_k,$$

where F_k = area of rear wall of sliding cylinder.

2. R_a = total momentum at exit

$$R_a = mw_a + p_a F_a,$$

where m = effective mass consumption through nozzle or reverser;

w_a = effective escape velocity;

p_a = pressure at exit from nozzle or reverser;

---

[1] k is arbitrary. Tr. note.

F_a = exit area of nozzle or projection of exit area of reverser in a direction perpendicular to the thrust.

3. R_H = force produced by the presence of pressure in the external pass pass of the sliding cylinder and the nozzle (reverser). In the case of the jet nozzle

$$R_H = p_H(F_к - F_a),$$

for the reverser

$$R_H = p_H(F_к + F_a).$$

4. $R_{\text{weighing element}}$ = force from weighing element.

5. R_0 = force acting on cylinder from the flange side.

From the condition of equality of the sliding cylinder, we have for the nozzle test

$$R_к + R_0 + R_{\substack{\text{weighing}\\\text{element}}} - R_H - R_a = 0.$$

Substituting the appropriate values, we get

$$R_a - F_a p_H = R_{\substack{\text{weighing}\\\text{element}}} + R_0 + F_к(p_к - p_H).$$

The expression

$$R_a - F_a p_H = m w_a + F_a(p_a - p_H)$$

represents the internal thrust R_{nozzle} of the jet nozzle. Consequently,

$$\begin{aligned} R_{\text{nozzle}} &= R_{\text{weighing element}} + R_0 + F_к(p_к - p_H), \\ R_{\text{nozzle}} &= k_{\text{nozzle}}(U_{\text{weighing element}} + U_0) + F_к(p_к - p_H), \end{aligned} \qquad (3.3)$$

where $U_{\text{weighing element}}$ = reading of potentiometer for tests in millivolts;

U_0 = reading of potentiometer in millivolts determined for the given bridge from the calibration curve for zero consumption; /78

k_{nozzle} = value of the calibration coefficient corresponding to the thrust of the jet nozzle.

When the reverser was tested, the directions of the action of the forces $R_{\text{weighing element}}$ and R_a were changed. Taking the same expression as for

positive thrust to be designated as internal negative thrust of the reverser R_{rev}, we get for determination of R_{rev} the following expression:

$$\begin{aligned} R_{rev} &= R_{\text{weighing elements}} - R_0 - F_к(p_к - p_H), \\ R_{rev} &= k_{\text{screen}} U_{\text{weighing element}} - k_{\text{noz.}} U_0 - F_к(p_к - p_H). \end{aligned} \tag{3.4}$$

When the experimental results were interpreted, determination of consumption was carried out under the formula

$$G = G' \frac{p_0}{\sqrt{T_0}},$$

where p_0 and T_0 = measured total pressure and braking temperature, respectively. The values of G' were found from the ratio $\Delta p_{inlet}/p_0$ from the calibration graph.

In nozzle testing the specific thrust coefficient $\overline{R}_{\text{specific nozzle thrust}}$ and the consumption coefficient μ_{nozzle} were calculated:

$$\overline{R}_{\text{spec.noz.thrust}} = \frac{R_{nozzle}}{\frac{G}{g} a_* \lambda_{\text{ideal velocity}}}, \quad \mu_{nozzle} = \frac{G_{nozzle}}{G_{\text{ideal velocity}}},$$

$$G_{\text{ideal velocity}} = 0.3965 \frac{p_0}{\sqrt{T_0}} q(\lambda_{\text{ideal velocity}}) F_{nozzle}$$

Here a_* = critical velocity of sound; $\lambda_{\text{ideal velocity}}$ = coefficient of velocity corresponding to total adiabatic expansion down to the pressure p_H.

The values of the reverse coefficient $\overline{R}_{rev}$ and the consumption coefficient $\overline{G}_{rev}$ were found for reversers.

Method tests. The aim of the initial methods tests of nozzles was comparison of characteristics with data obtained on other experimental stands.

The tests were conducted with different constricted nozzles. Figure 3.3 presents experimental data for several constricted nozzles of the reverser models investigated. A curve plotted from the numerous results of constricted nozzle tests on other weighing stands was drawn on the graph. This curve is valid for nozzles which have an angle of nozzle generatrix to its axis θ_{nozzle} = 0-20°. It is obvious that for certain measurements of the specific /79
thrust coefficient $\overline{R}_{\text{specific nozzle thrust}}$, the scatter of the points is about ±1%, while the average $\overline{R}_{\text{specific thrust values}}$ evidence the fully satisfactory

agreement of results. Since the stand was chiefly intended to test reversers, we can deem the precision of thrust measurement attained as wholly applicable.

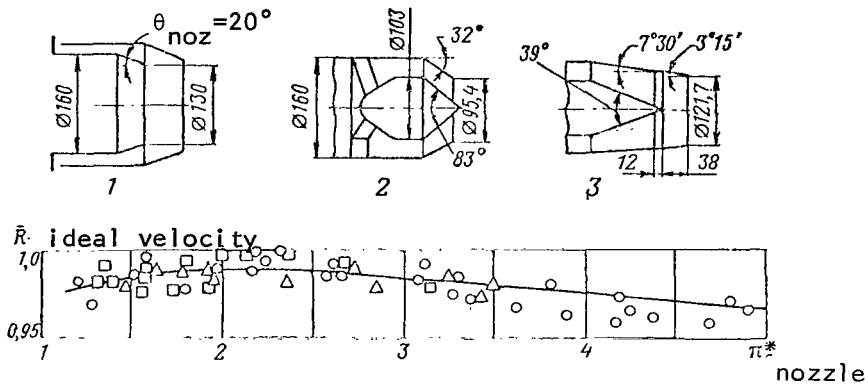

Figure 3.3. Specific Thrust Coefficient as a Function of Extent of Pressure Reduction for Several Constricted Nozzles: ———, Standard Curve ; Δ, Nozzle 1 of Reverser Containing Cylindrical and Conical Shutters; O, Nozzle 2 with Central Body Installed; □ , Nozzle 3 of Reverser with Connecting Pipes.

The curve plotted in Figure 3.3 can be considered as standard. Thrust characteristics of the corresponding constricted nozzles were determined from it in interpreting materials of reverser tests, which precluded errors in measurement of positive thrust associated with the data of a particular test.

Figure 3.4 presents a curve of the consumption coefficient as function of the angle of inclination of the generatrix of the conical nozzle to its axis for values of the extent of pressure reduction, upon the exceeding of which the value μ_{nozzle} did not depend on π^*_{nozzle}. Experimental data of G. Shirer and R. Gray, eminent from textbook literature were plotted on the graph (cf., for example, [5]), as well as data of tests conducted by other authors.

Points for the investigated nozzle 1 (Figure 3.3) with $\theta_{nozzle} = 20°$ and for a constricted profiled nozzle shown in Figure 3.4 were plotted on the graph. When $\theta_{nozzle} = 0$, the data was presented also for several supersonic nozzles tested on another stand by other authors.

As we know, the consumption coefficient of the supersonic nozzle depends on the method by which its subsonic section was profiled. If the contour of /80
the subsonic section was profiled. If the contour of the subsonic section

traced the Vitoshinskiy curve or was made of sections of arcs of circumference, the consumption coefficient will be a value on the order of 0.995-0.998.

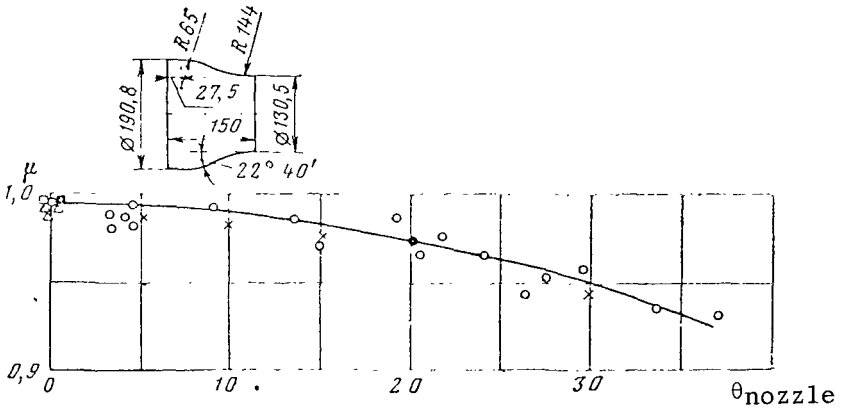

Figure 3.4. Consumption Coefficient as a Function of the Angle of Inclination of the Generatrix of the Conical Nozzle to its Axis: ×, Data of Shirer and Gray [5]; ●, Data for Nozzle No. 1 in Figure 3.3; ■, Data for the Nozzle Shown in the Figure; □, Data for this Nozzle Investigated on Another Stand; 0, Data of V. T. Zhdanov for Constricted Nozzles; Δ, Data of V. T. Zhdanov for Supersonic Nozzles.

It follows from the figure that the values of μ_{nozzle} of the nozzles studied satisfactorily fit the scattering band of the experimental points of a variety of authors (±1%).

Let us note one fact. Owing to the radial inlet of air into the rocking section of the unit, as indicated in describing the stand, the inlet momentum upon examination of forces acting on the sliding cylinder is excluded. Therefore, the value of the consumption does not enter into the expression for calculating thrust and the error in measurement of consumption does not have an effect on precision of thrust measurement. Error in consumption measurement does have a bearing in determination of the coefficients $\overline{R}_{spec.nozzle\ thrust}$, μ_{nozzle}, $\overline{R}_{rev}$, and $\overline{G}_{rev}$.

In the course of the study repeated tests were made of the same models. We will consider a few examples.

Figure 4.10, b and c present curves of the reverse coefficient as functions of the extent of pressure reduction for one of the reverser schemes investigated. The tests were conducted at different times for the same calibration of the stand. Similar curves are plotted in Figure 3.5 for another model. In constructing the curves, data of two different tests for different

calibrations of the stand were used. We can note the agreement of results fully satisfactory for practical use. It is obvious that in testing reversers /81
the absolute error in an individual measurement of the reverse coefficient is about $\pm 0.01\ \overline{R}_{rev}$ unit. However, the relative error obviously is higher owing to the lower values of the reverse coefficient compared to the thrust coefficients of the corresponding nozzles. The absolute error in measuring positive or negative thrust, determined from the result of repeated tests can be estimated as $\pm 0.005\ \overline{R}_{\text{specific nozzle thrust}}$ and $\overline{R}_{rev}$ unit. For the given reverser this is graphically evident upon comparing the curves shown in Figure 3.5.

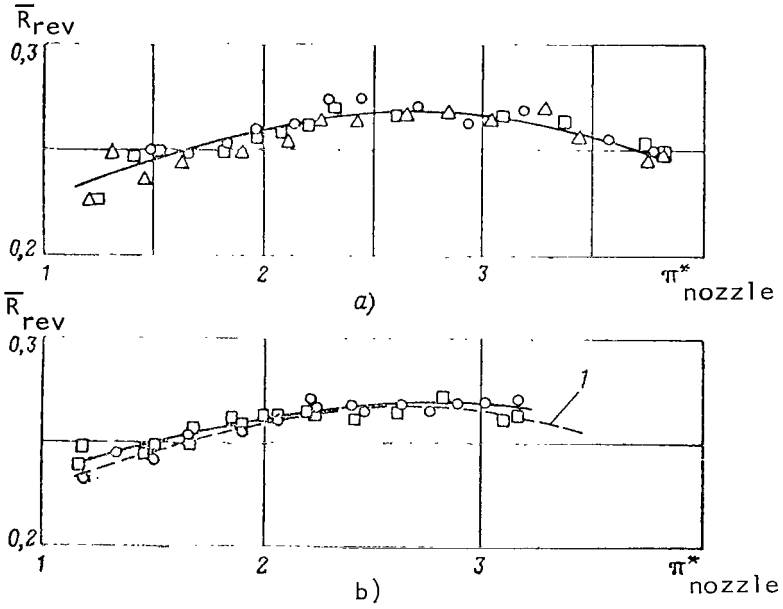

Figure 3.5. Reverse Coefficient as the Function of Extent of Pressure Reduction. Model of Reverser with Connecting Pipes: O, Measuring Bridge 1; Δ, Bridge 2; □, Bridge 3; a, First Test; b, Second Test; 1, Curve Based on Data of First Test.

Thus, method tests reveal the possibility of obtaining wholly reliable results on this stand.

§4. Exhaust Systems of Stands in Testing Engines Equipped with Reversers

The emission of gases in several directions is one characteristic of stands for testing engines equipped with reversers. The reception sections of the exhaust system of these test stands must effectively divert gases and must not have an effect on precision of thrust measurement. A diagram of such a stand is shown in Figure 3.6. Gases escaping from the deflecting screens 1

and the jet nozzle 2 are directed to the exhaust pipe 3. Owing to the high gas velocity in the entry section of the pipe 4 rarefaction can be induced. This may have an effect on precision of thrust measurement. This effect depends on the ratio of l/D_{nozzle}, where l = distance from end face of the exhaust pipe up to exhaust section of the jet nozzle, and D_{nozzle} = diameter of jet nozzle[1]. Precision of thrust measurement can also be effected by the distance a.

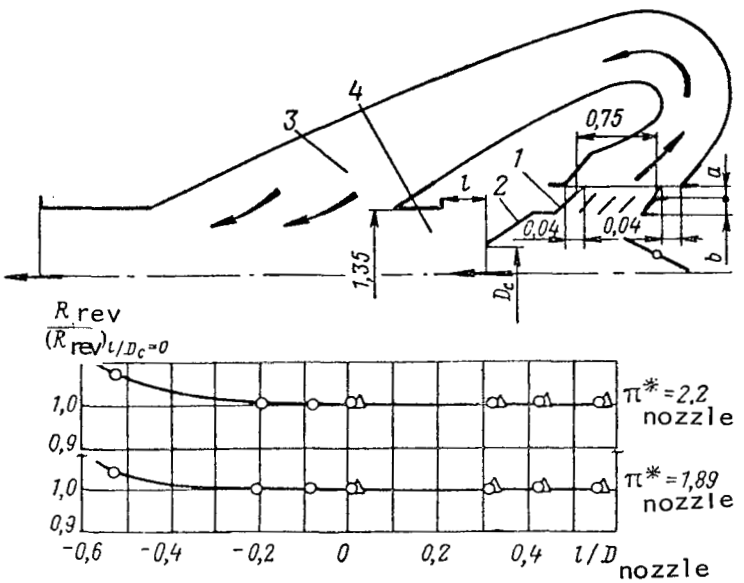

Figure 3.6. Diagram of Exhaust System of a Stand Used in Testing Engines Equipped with Reversers, and Relative Value of Negative Thrust as a Function of the ratio l/D_{nozzle} for Different Values of a/b and π^*_{nozzle}: 1, Deflecting Screen; 2, Jet Nozzle; 3, Exhaust Pipe of Stand; 4, Inlet Section of Pipe; O, a/b = 1.92; Δ, a/b = 0.40.

A reverser model around which the exhaust system was arranged was investi- /83
gated in determining the maximum values of the exhaust system parameter under which the effect of stand elements on thrust measurement precision would be absent. The tests of this model were conducted on a stand described in §3 of this chapter. The model made it possible to vary the dimensions l and a within wide limits. The results of the tests are plotted in the same figure where the relative values of the measured negative thrust as functions of the ratio

*The relative dimensions in fractions of D_{nozzle} are shown in the figure.

l/D_{nozzle} at π^*_{nozzle} = 1.89 and π^*_{nozzle} = 2.2 are given. The effect of the variable l/D_{nozzle} on the results of thrust measurement becomes appreciable only when the exhaust cross-section of the nozzle extends within the exhaust pipe and the ratio $l/D_{nozzle} < -0.2$.

It is also clear from the figure that when a/b = 0.4-1.9, the reception sections of the exhaust system do not have a bearing on the results of negative thrust measurements.

CHAPTER IV

EXPERIMENTAL STUDY OF REVERSERS ON MODELS

§1. Reversers with Shutters Located Aft of the Exit Section of the Jet Nozzle /84

Reversers with Cylindrical Shutters

This kind of reverser consists of cylindrical shutters, located in inoperative position in the space between the jet pipe of the engine and the engine nacelle. When the reversers cut in, the shutters are shifted aft of the exit section of the jet nozzle and are tilted, discharging the stream in the reverse direction (Figure 4.1).

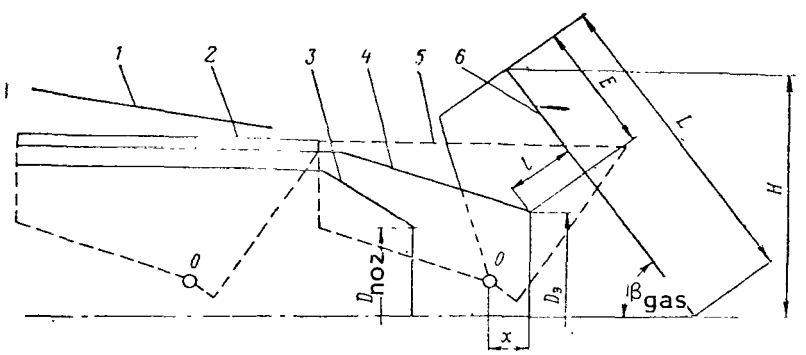

Figure 4.1. Diagram of Reverser with Cylindrical Shutters: 1, Engine Nacelle (Aircraft Fuselage); 2, Reverser Shutter in Gathered Position; 3, Jet Nozzle; 4, Ejector; 5, Shutter in Extended Position; 6, Shutter in Working Position; 0, Center of Rotation of Shutters.

Reversers of this type are applicable for thrust-augmented engines and engines without afterburner. In the absence of an ejector, the elements 4 can be considered to be the engine nacelle or the fuselage of the aircraft in the case of engine without afterburner.

Three reverser models with cylindrical shutters (Figure 4.2) investigated on stand No. 2 were built with an angle of shutter inclination β_{gas} of 30°, 45° and 60°. It is obvious that to ensure exiting of the thrust from the reverser of this type at a specific angle, the shutters must have some guide section of length E. To reduce the effect of this parameter on the results of investigation for different shutter arrangements relative to the exhaust section of the ejector, the length L was taken to be large enough in order that

for all values of x the value of E/l will be greater than zero. All the shutters have the same dimension $H(H/D_{nozzle} = 1.06)$. The fourth and fifth models with angles $\beta_{gas} = 30°$ and $40°$ $(H/D_{nozzle} = 1.8)$ were investigated on the stand No. 1(§3, Chapter IV).

The curves of the coefficient $\bar{R}_{rev}$ as a function of the extent of pressure reduction plotted in Figure 4.3 can be viewed as typical for the reversers investigated. For a certain value of the extent of pressure reduction a maximum reverse coefficient is observed. A trend toward shifting of the maximum toward the side of lower π^*_{nozzle} values with decrease in shutter inclination angle has been noted. /85

Tests of reversers for different shutter arrangements relative to the exit section of the ejector revealed that, starting with a certain value $\bar{x}$, a decrease in the consumption and reverse coefficients was observed (Figure 4.4). The reduction in the $\bar{R}_{rev}$ values was accounted for mainly by the drop in the consumption stemming from the variation in the minimum through cross-section. For values $\bar{x} \leq 0$, the minimum through section lies between the shutters and the ejector. The consumption coefficient $\bar{G}_{rev} < 1$. When the shutters are sufficiently removed from the exit cross-section of the ejector, the exit cross-sectional area of the nozzle proves to be critical. Therefore, the values of the consumption coefficient when $\bar{x} \geq 0.2$, equal 1.0. A reduction in the through cross-sections when $\bar{x} \leq 0$ leads to a rise in pressure in the jet pipe (Figure 4.5). Thus, reversers located aft of the exit cross-section of the nozzle are characterized by the fact that they deflect in the reverse direction the stream accelerated in the nozzle up to a high velocity.

When the shutters are sufficiently removed from the exit cross-section of the ejector ($\bar{x} \geq 0$, Figure 4.6), for the greater part of its length the pressures are almost identical, and the velocity is low. The velocity increases with increasing proximity to the exit from the reverser. As a whole, the pattern of pressure distribution is analogous to that observed for gas escape from a constricted nozzle. With increasing proximity of the shutters to the ejector, the zone with reduced pressure is widened, and the velocities at the exit sections rise. Consequently, the negative thrust built up by the reverser shutters is reduced. When $\bar{x} = -0.195$ and $\bar{x} = -0.39$ at the exit section of the shutters, re-expansion of the stream is observed. This stems from the fact that a constriction is formed between the shutter and the ejector, beyond which the through section becomes greater. There is a shock wave obviously located between the drainage points 5 and 6 ($\bar{x} = -0.39$). The situation here shows some parallel with escape from a Laval nozzle in nonrated regimes. The presence of shutter surfaces on which the pressure is less than in the surrounding environments naturally additionally reduces the negative thrust of the reverser. Reduction in the reverse coefficient proceeds to a greater /88

extent, the more sharply the consumption coefficient is reduced (cf. Figure 4.4).

The optimal shutter position must be held to be that at which the maximum reverse coefficient is attained for a consumption coefficient equal to unity. /89 In the case under consideration, this position corresponds to $\overline{x} \simeq 0.2$. In this position the shutters have a certain directing section at the exit for the shutters with β_{gas}, equal to 30°, 45° and 60°, equal to, respectively, L/l = 0.73, 0.50 and 0.35.

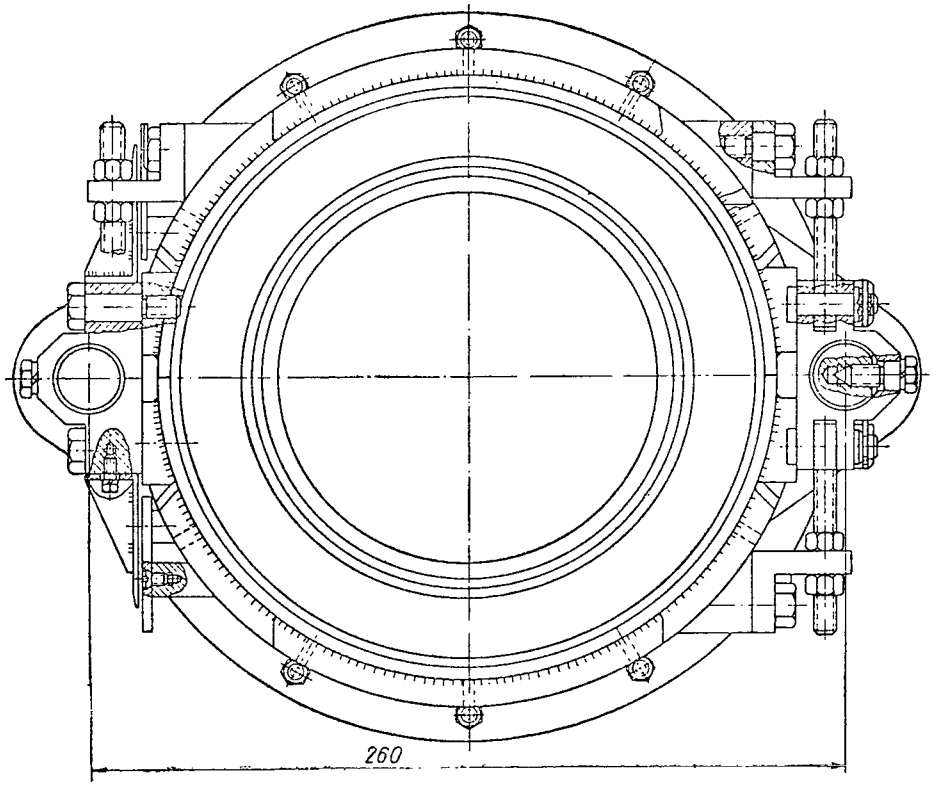

Figure 4.2. Experimental Model of the Reverser With Cylindrical Shutters Tested on Stand No. 2.

Figure 4.2 Continued on next page...

Figure 4.2. (Continued)

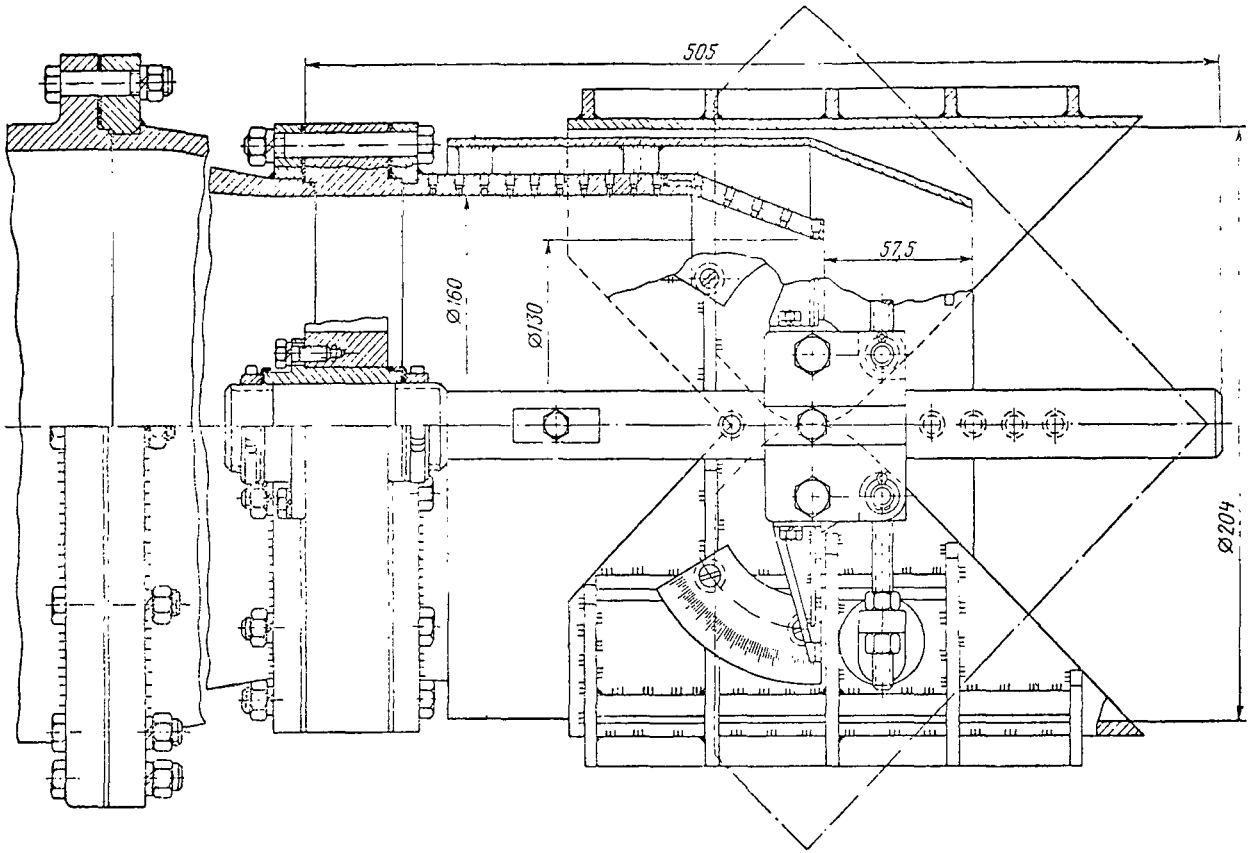

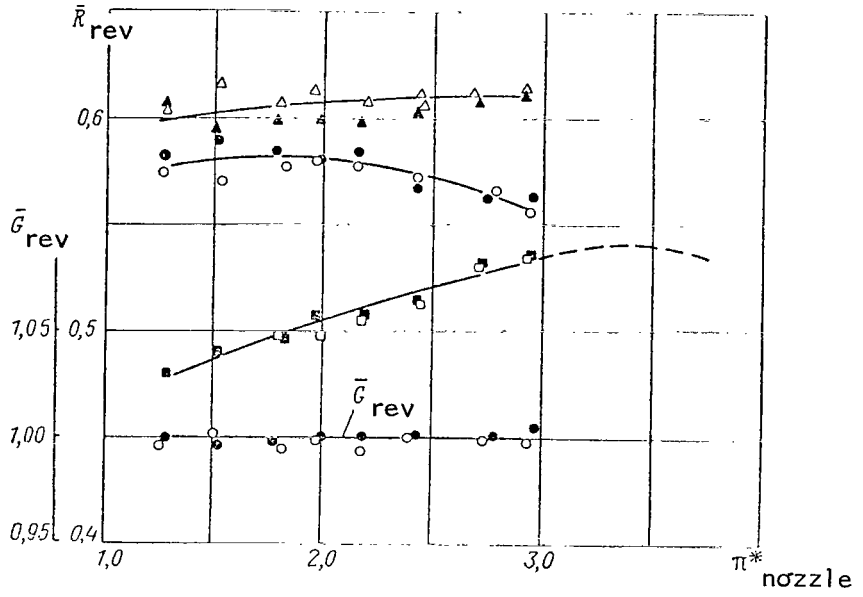

Figure 4.3. Reverse and Consumption Coefficients for a Reverser with Cylindrical Shutters as Functions of the Extent of Pressure Reduction: ○, ◉, β_{gas} = = 30°; △, ▲, β_{gas} = 45°; □, ■, β_{gas} = 60°. (The Blacked-in Symbols Refer to the Results of Repeated Tests).

For great separation of shutters from the ejector and when the guiding section of the shutters is reduced in extent, a reduction of the reverse coefficient is possible owing to streaming of the jet stream. However, this position of the shutters, leading to an increase in reverser over-all envelope dimensions, is not of practical interest.

When the angle of shutter inclination is reduced from 60° to 45°, the reverse coefficient rises (Figure 4.7). This figure shows plots of experimental points for reversers with cylindrical shutters β_{gas} = 30° and β_{gas} = = 40° tested on stand No. 1 in the absence of bypassing of gases in the straight-line direction through shutter slits. Without going into a detailed comparison of the results that stem from the difference between models in a number of geometric parameters, we merely observe that the resulting reverse coefficient values are close together. /90

Figure 4.8 presents data on the relative variation of the reverse coefficient $\Delta\bar{R}_{rev}$ as a function of relative consumption $\bar{G}_{slit}$ through the slit between throttling shutters:

$$\Delta\bar{R}_{rev} = \frac{(\bar{R}_{rev})_0 - (\bar{R}_{rev})_{slit}}{(\bar{R}_{rev})_0}, \quad G_{slit} = \frac{G_{slit}}{G_{nozzle}} = \frac{F_{slit}}{F_{nozzle}} \frac{\mu_{slit}}{\mu_{nozzle}}.$$

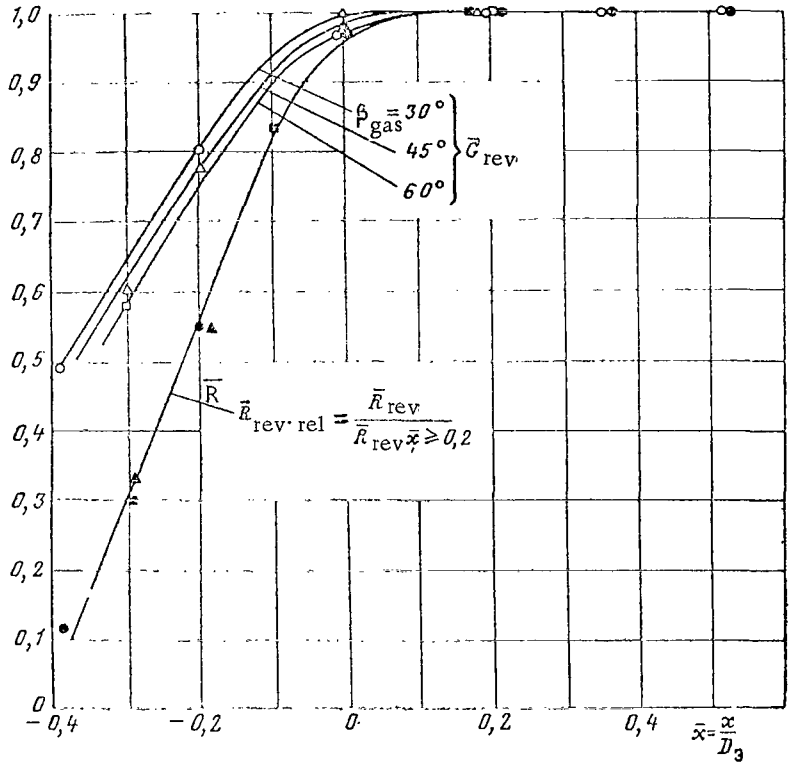

Figure 4.4. Consumption Coefficient and Relative Values of Reverse Coefficient for a Reverser with Cylindrical Shutters as Functions of the Parameter $\bar{x}$ (π^*_{nozzle} = 2.0). (The symbols are the same as those in Figure 4.2.)

Here the subscripts "0" and "slit" correspond to reverse coefficients without slit and with slit. In the calculations, the coefficients μ_{slit} of consumption through the slit and opening were based on the data of G. A. Dombrovskiy [5]--μ_{slit} = 0.75. Some mean value of the consumption coefficient was adopted for the nozzles (μ_{nozzle} = 0.98). It is clear from the figure that bypassing of gases in the straight-line direction, for example, owing to leakage through loosely collected shutters can substantially reduce the reverse coefficient. /91 /93

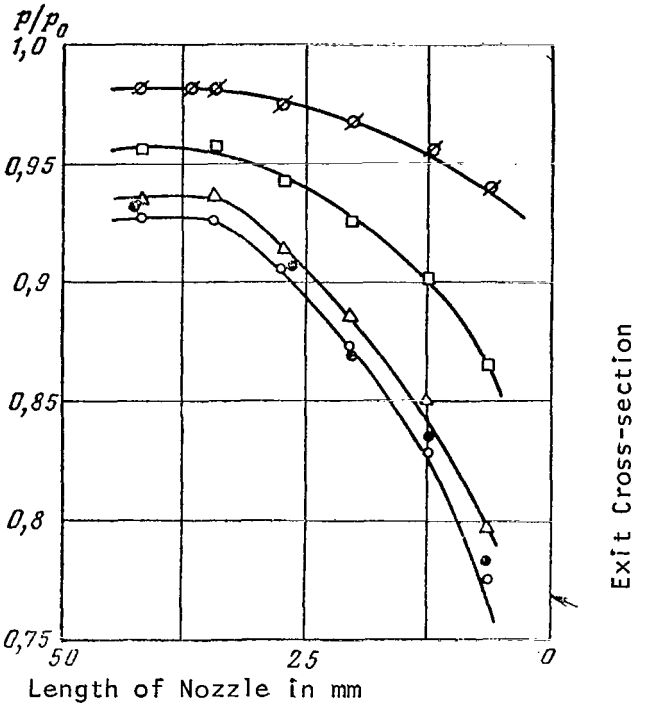

Figure 4.5. Distribution of Pressure Along the Nozzle of a Reverser with Cylindrical Parameters with β_{gas} = 30° for Different Shutter Positions. π^*_{nozzle} ≈1.8. ●, Without Shutters; o, $\overline{x}$ = +0.195; Δ, $\overline{x}$ = 0; □, $\overline{x}$ = -0.195; ø, $\overline{x}$ = -0.390.

Experimental points for a fourth and a fifth model were plotted on the graph. We can note the satisfactory convergence of the results. Also plotted on the figure were results of a test made of a model with deflecting screens and throttling diaphragm.

We can see that the functions $\overline{R}_{rev} = f(\overline{G}_{slit})$ are linear to the first approximation.

Reversers with Conical Shutters

A reverser of this type, whose diagram is shown in Figure 4.9, consists of part of the engine nacelle which is rotated and shifted aft of the nozzle in its working position. The rotating flap 5 discharges the stream in the reverse direction.

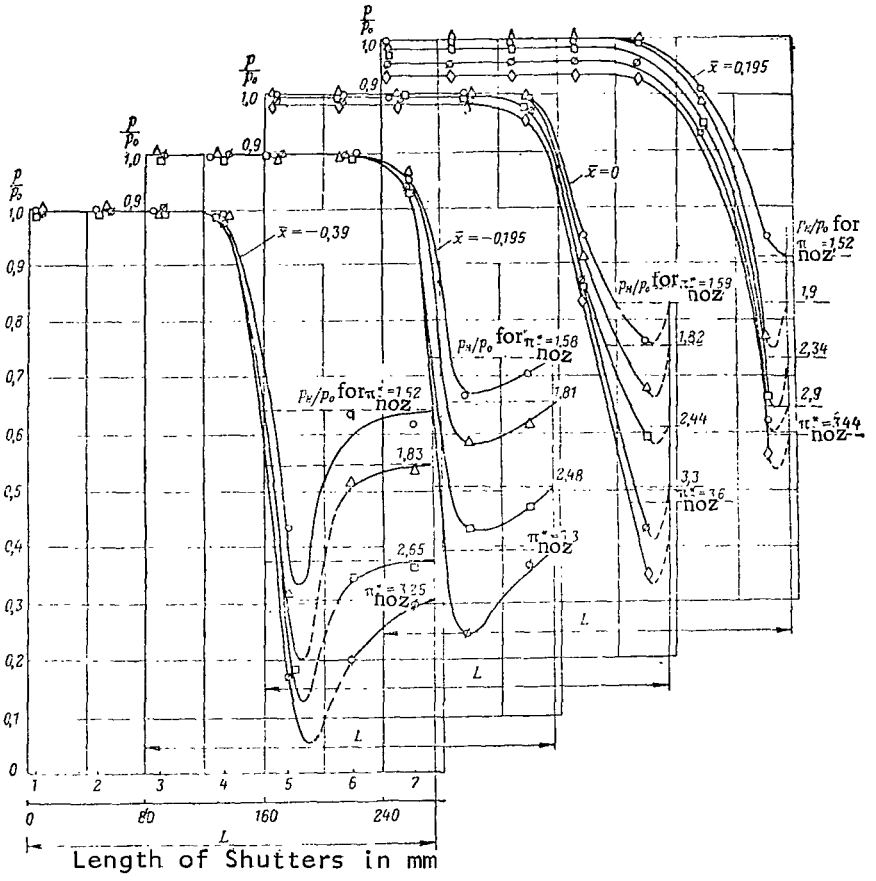

Figure 4.6. Distribution of Pressure Along Cylindrical Shutters with β_{gas} = = 30° for Different Shutter Positions.

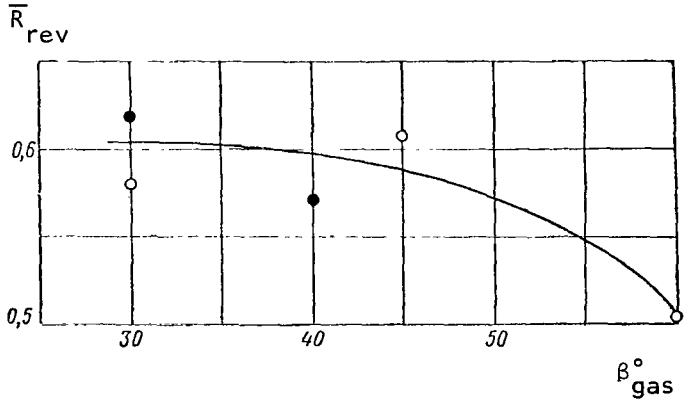

Figure 4.7. Reverse Coefficient as a Function of the Angle β_{gas} of Cylindrical Shutters (π^*_{nozzle} = 2.0): o, for Models Tested on Stand No. 2; ●, for Models Tested on Stand No. 1 ($\bar{F}_{slit}$ = 0).

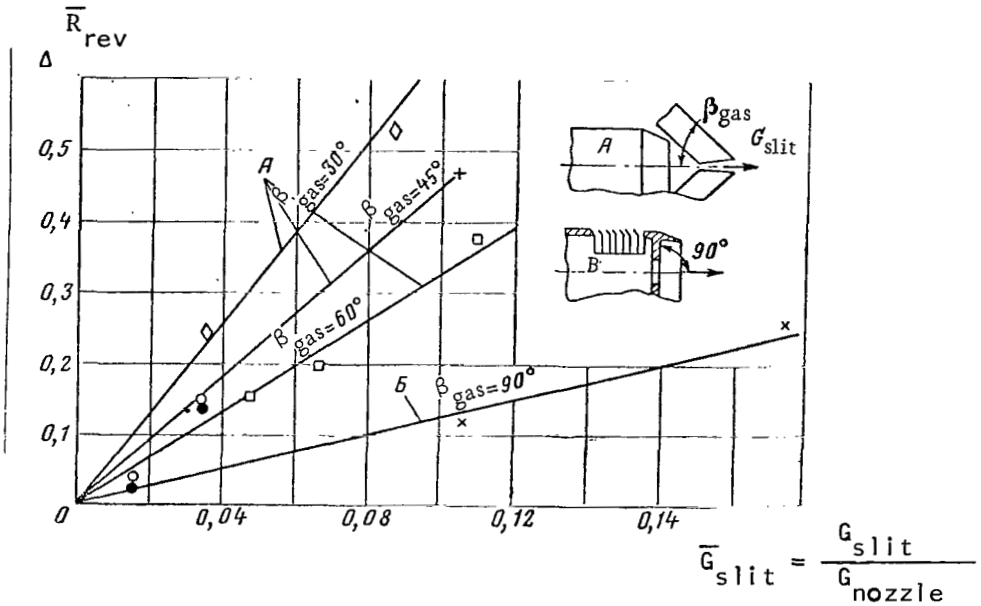

Figure 4.8. Relative Reduction in Reverse Coefficient as Functions of Relative Consumption Bypassed in the Straight-line Direction for Different Reverser Schemes: Models with Cylindrical Shutters (c. sh.), Tested on Stand No.2: ◇, $\beta_{gas} = 30°$; $\bar{x} = 0$; +, $\beta_{gas} = 45°$; $\bar{x} \approx 0.1$; □, $\beta_{gas} = 60°$; $\bar{x} \approx -0.1$. Models with c. sh. ($\beta_{gas} = 40°$) Tested on Stand No. 1: ●, $\bar{x} = 0$; o, $\bar{x} = 0.21$.

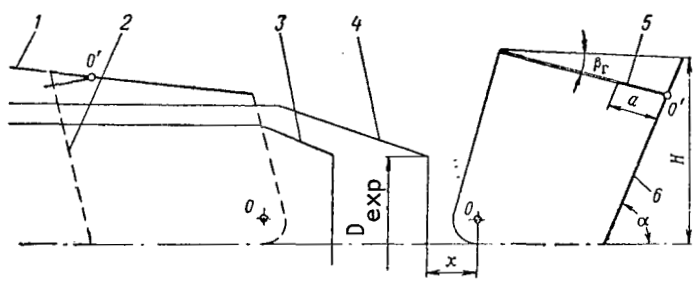

Figure 4.9. Diagram of Reverser with Conical Shutters: 1, Engine Nacelle (Fuselage of Aircraft); 2, Shutters in Non-working Positions; 3, Jet Nozzle; 4, Ejector; 5, Flap; 6, Shutters in Working Position; 0, 0', Centers of Rotation of Shutter and Flap, Respectively.

Taking account of the results of the studies of reversers with cylindrical shutters, tests with conical shutters were conducted for the values $\bar{x} = x/D_{exp}$ for which the equality $\bar{G}_{rev} = 1$ was satisfied ($\bar{x} \approx 0.2$). For $\alpha = 85°$ this is obvious for example, in Figure 4.10,a. The curves of the reverse coefficient is a function of extent of pressure reduction mainly run similar to those indicated earlier for cylindrical shutters. We must note the more appreciable reduction in the reverse coefficient when

π^*_{nozzle} > 2-2.2 in the case of a model with α = 55°, where the reduction of $\bar{R}_{rev}$ is the more noticeable the smaller the angle β_{gas} (cf. Figure 4.10, c). A tendency toward a shift in the maximum $\bar{R}_{rev}$ toward the side of lower π^*_{nozzle} with a decrease in β_{gas} was also noted in all the reversers. The effect of the /95 flap inclination angle shows up in reversers with conical shutters differently, depending on the shutter inclination angle (Figure 4.11).

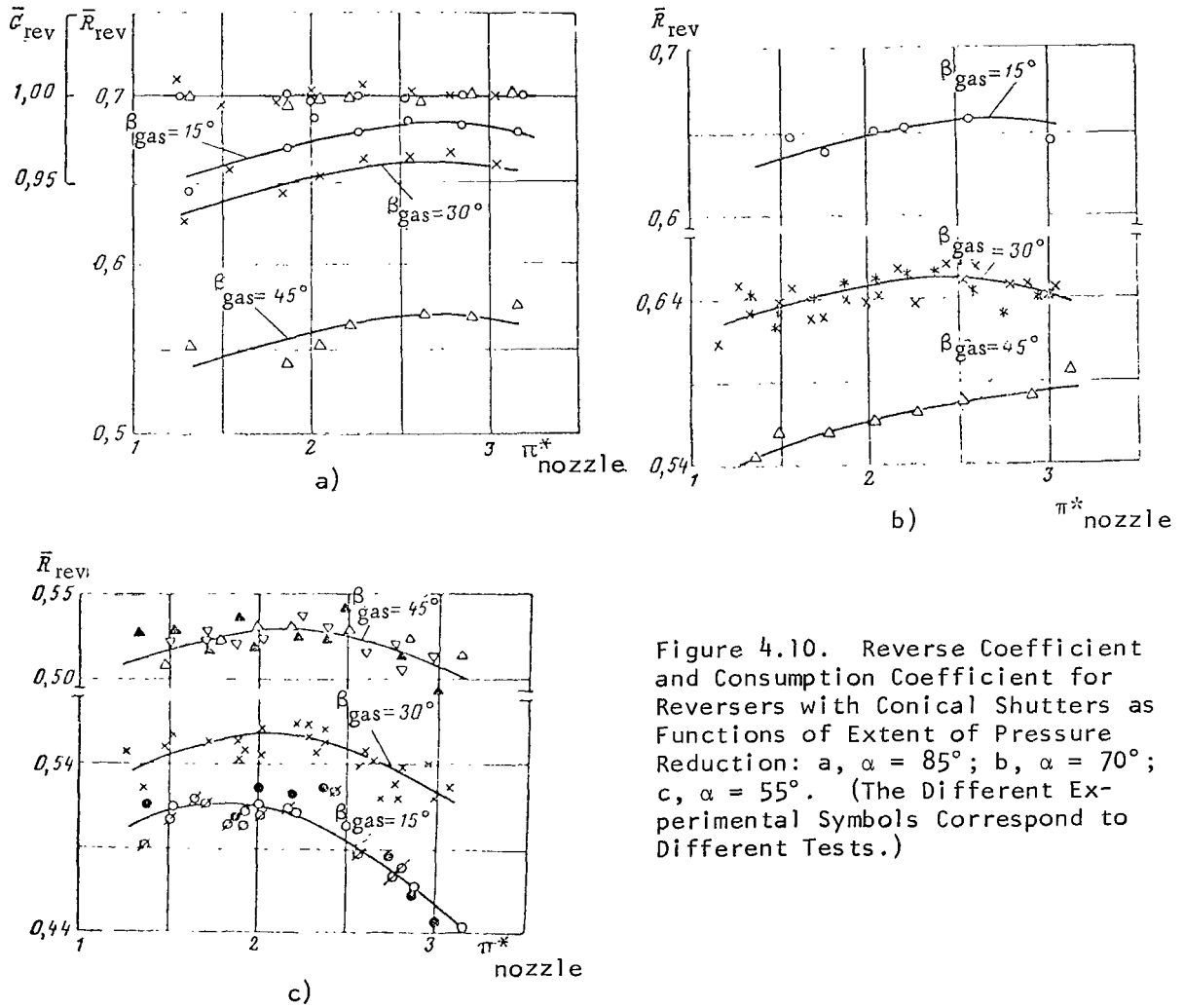

Figure 4.10. Reverse Coefficient and Consumption Coefficient for Reversers with Conical Shutters as Functions of Extent of Pressure Reduction: a, α = 85°; b, α = 70°; c, α = 55°. (The Different Experimental Symbols Correspond to Different Tests.)

Figure 4.11 shows plots of experimental points for a model tested on stand No. 1, and also based on material known from the literature[1]. The level of the attained reverse coefficient is approximately the same.

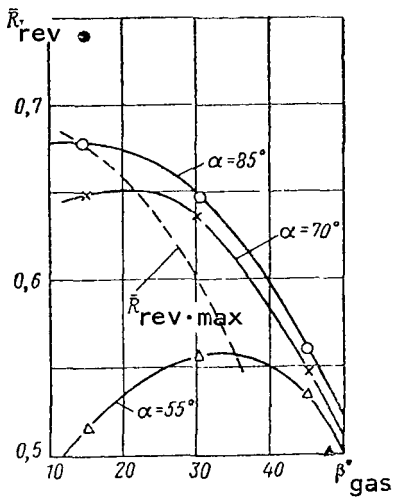

Figure 4.11. Reverse Coefficient as a Function of the Angle β_{gas} of Inclination of Reverser Flaps with Conical Shutters ($\pi^{*}_{nozzle} = 2.0$): ●, Results of Tests of the Model on Stand No. 1; ▲, Data Known from the Literature ($\alpha = 55°$, $\beta_{gas} = 48°$).

The maximum reverse coefficient values correspond to relatively small angles β_{gas}, which must be avoided in order to reduce the probability of the ingestion of exhaust gas at the engine inlet. However, in actual practice a reverse coefficient equal to about 0.5 is necessary, which can be attained in this scheme for values of β_{gas} applicable in practice. /96

§2. Reversers With Deflecting Screens Located Forward of the Exit Section of the Jet Nozzle

Schemes of Reversers in Nozzles Enclosing a Central Body

Figure 4.12, 4.13, 4.14 and 4.15 present several possible schemes of reversers for a nozzle enclosing a central body in which deflection of the stream is attained at the screen's 4 (Figure 4.12) with a subtended angle θ, located in the subsonic section of the nozzle, and covering of the screens in the direct thrust regime and partitioning of the gas duct in thrust reversal are accomplished mainly by shutters of the type used in nozzle regulation.

As we know, the control range of shutters characterized by the ratio of diameters D_0/D_1 (See Figure 4.12), depends substantially on the extent of overlapping δ of the shutters and on their number. For overlapping equal to zero, independently of the number of shutters the control range is 2.0. The necessity of overlapping of shutters reduces the possible control range. When special types of shutters affording limited overlapping are developed, the control range can be high enough. The D_0/D_1 values for a designwise minimal overlapping $\delta = eD_0$, where $e \sim 1/30$, are presented below for different numbers i of shutters. /97

[1] *Flight*, 30/IV, No. 2362, pp. 540-541, 1954.

i	8	10	12	14
D_0/D_1	1,84	1,81	1,77	1,64

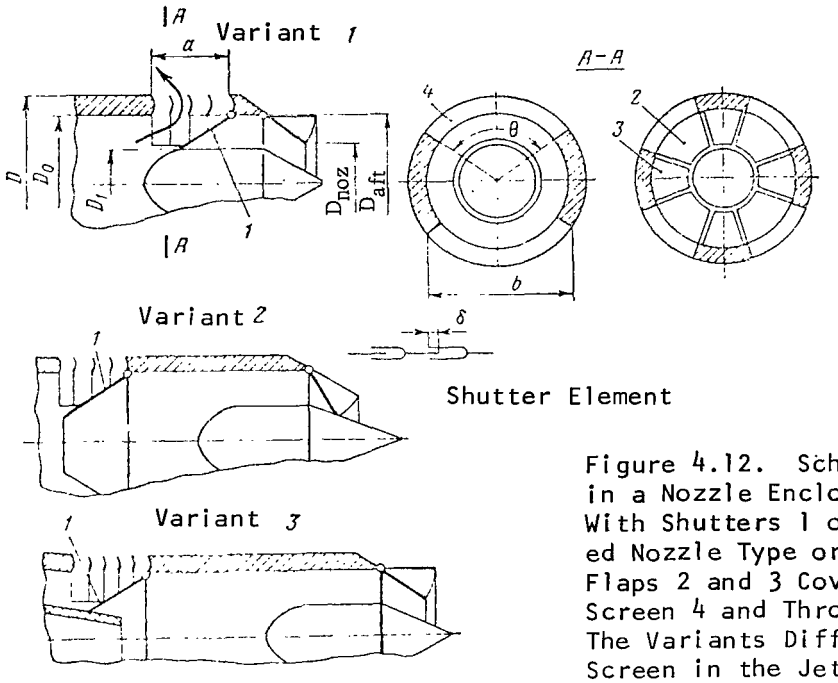

Figure 4.12. Scheme I of a Reverser in a Nozzle Enclosing a Central Body With Shutters 1 of the Reverse Regulated Nozzle Type or Individual Tilting Flaps 2 and 3 Covering the Deflecting Screen 4 and Throttling the Gas Duct. The Variants Differ in Placement of the Screen in the Jet Pipe: 1, Around the Central Body; 2, In the Jet's Tube; 3, Aft of the Turbine.

As the calculated extent of pressure reduction is reduced, the diameter of the central body rises, and consequently, the angles of shutter deflection in their extreme positions and the required control range are reduced. Therefore, in the schemes considered below practically the entire consumption can be used in producing negative thrust.

In scheme I (cf. Figure 4.12), the deflecting screens, when the reverser is not operative, are covered by the shutters 1 of the reverse control nozzle type, which upon cut-in of reverser also serve the function of a throttling element. Shutters covering the deflecting screens in Scheme No. 1 can be made also in the form of individual tilting flaps that do not interlock. Such flaps are also schematically shown in Figure 4.12. The main flaps 2 cover the inlet section of individual deflecting screens. Additional flaps 3 serve only to partition the gas duct. /98

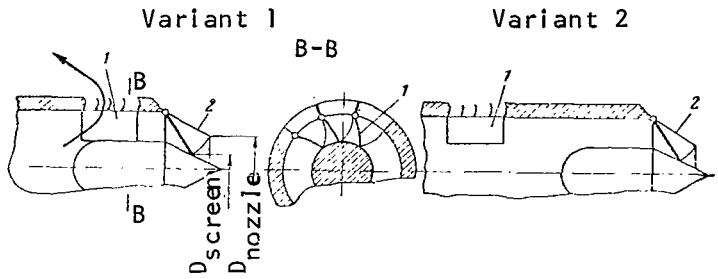

Figure 4.13. Scheme II of a Reverser Equipping a Nozzle Enclosing a Central Body Fitted with Tilting Flaps 1, Covering the Deflecting Screen, and with Flaps 2 of the Regulated Nozzle Throttling the Gas Duct. In Variant 1 the Screen is Located About the Central Body, and in Variant 2 in the Jet Pipe.

In Scheme II (Figure 4.13) the screens in the positive thrust regime are covered by flaps 1, located in this position flush with the jet pipe, and throttling of the gas duct is accomplished by shutters 2 of the controlled jet nozzle.

The reverser can be built without shutters or flaps (Figure 4.14). Screens in Scheme III can be covered by cylindrical flaps (slides) 1 tilting about the jet pipe axis or by cylindrical flaps 2 that are capable of longitudinal sliding, and the gas duct is throttled just as in Scheme II.

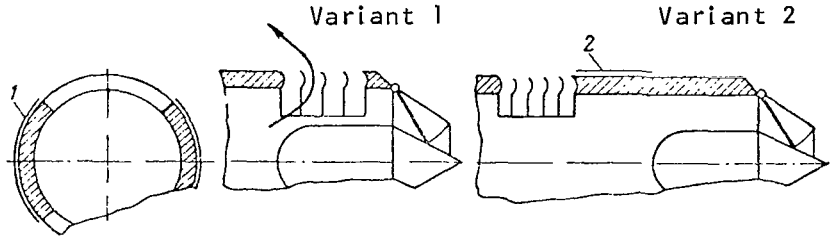

Figure 4.14. Scheme III of Reverser of Nozzle Enclosing Central Body With Tilting Cylindrical Flaps 1 or Cylindrical Flaps 2 that Move Longitudinally. In Variant 1 the Screen is Located Around the Central Body, and In Variant 2 -- in the Jet Pipe.

As variants of Schemes I, II and III, we can consider the placement of deflecting screens quite removed from the central body. In the case of Variant 2 of Scheme I (cf. Figure 4.12) throttling of the gas duct is accomplished by shutters of the jet nozzle. When the screens are placed in direct proximity aft of the turbine (Variant 3), throttling of the gas duct can be easily

achieved with the shutters 1 owing to the presence of a spinner. Then there is no need to partition the gas duct with jet nozzle shutters. In Variants 1 and 3 of this scheme, individual tilting flaps can also ensure practically complete partitioning of the gas duct. 99

One can imagine a scheme IV of a reverser in which the screens are covered by means of cylindrical shutters (Figure 4.15) tilting about axes lying in the rear section of the screens (Variants 1 and 2) or about axes situated near or on the engine axis (Variant 3). In the latter case, when the reverser is cut-in the flaps are tilted in the reverse position compared with Variant 1. /100 In Scheme IV the cylindrical flaps can be designed in such a way as to ensure complete (or almost complete) partitioning of the gas duct even without shutters of the jet nozzle.

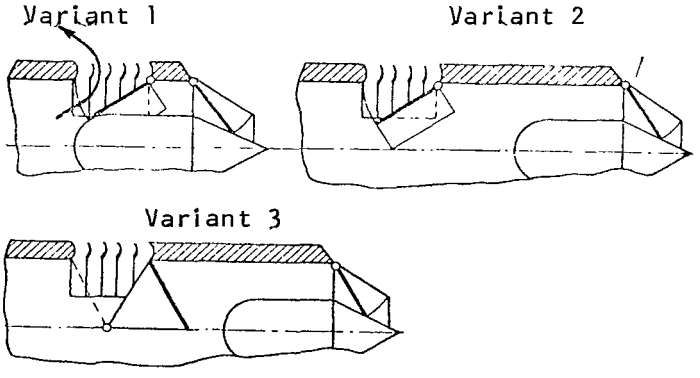

Figure 4.15. Scheme IV of Reverser of a Nozzle Enclosing a Central Body with Cylindrical Shutters Tilting about an Axis Lying in the Rear of the Screen (Variants 1 and 2) or about an Axis Lying in the Axis of the Jet Pipe (Variant 3).

Schemes of Reversers of a Constricted Nozzle

Figure 4.16 presents schemes of investigated reversers with deflecting screens in which the same throttling elements were used as in the investigated schemes of the nozzle with a central body.

In Scheme A when the deflecting screens are located aft of the turbine, shutters 1 of the reverse regulated nozzle type ensure total partitioning of the gas duct. When the deflecting screens are placed in the jet pipe far removed from the turbine, these shutters do not partition the gas duct completely (Scheme B). Thus, when there are eight shutters about one-third of the gas duct proves to be unpartitioned.

In Schemes C, D, and E with cylindrical shutters as indicated above, it appears possible to attain practically complete throttling of the gas ducts.

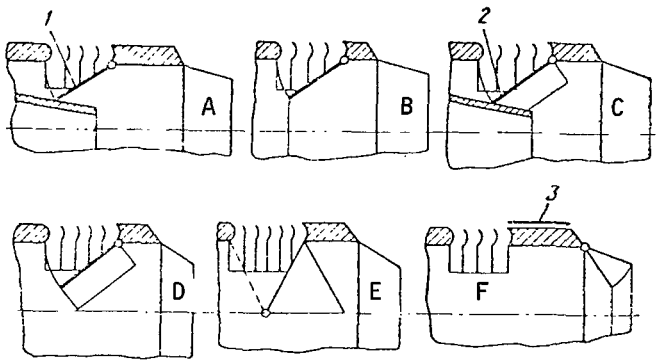

Figure 4.16. Schemes of Investigated Reversers of a Constricted Nozzle: A, B, With Shutters 1 of the Reverse Regulated Nozzle Type; C, D, E, With Cylindrical Shutters 2; F, With Cylindrical Flaps 3.

In Scheme F with cylindrical flaps and throttling of gas duct with jet nozzle shutters just as in Scheme B, bypassing of gases in the straight-line direction remains.

Experimental Models /101

Experimental studies were conducted on models shown in Figures 4.17 and 4.18. In the models of group No. 1 (Figure 4.17) the screens were made of leaf-type profiles, and in models of group No. 2 (Figure 4.18)--of profiled vanes. The central body in the nozzle of the model was made in a simplified form. Experiments showed that replacement of a profiled central body with a contour close to the calculated design did not lead to an appreciable variation in thrust characteristics of the nozzle. We also know that complete removal of the supersonic section, and also the subsonic section, and placement instead of a central body of a disk increases thrust losses at the design point by approximately 1.5%. To reduce the nozzle envelope, the central body was selected with a truncated cone. The cone was built in such a way that its tangency with the jet nozzle shutters for the permissible shutter control range was ensured.

A cylindrical section, where the deflecting screens were located, was situated forward of the critical section of the nozzle. It was assumed that the cylindrical position of the necking [shell] of the models in group No. 1 corresponded to performance of an engine with afterburner. The operating regime of the reverser is the usually rated engine performance regime in which the area of the critical nozzle section is about 1.7 times less than the nozzle area with afterburner. This was how the critical nozzle section of the model was estimated and how the appropriate shutter position was found.

From the viewpoint of weight reduction, it is desirable to have short shutters. However, when these shutters are used the tilting angles are increased, which gives rise to difficulties in production of required seals and in prevention of leakage. In addition, when the shutters are too short it can prove impossible to partition the gas duct of the engine. In this model, the center of shutter rotation is taken in such a way that the angle of shutter deflection from the position corresponding to afterburner up to the rated value is about 30°. Here the control range $D_{aft}/D_{nozzle} \approx 1.8$ (cf. Figure

4.12). When the reverser was built under Scheme II, D_{nozzle}/D_{screen} also ≈ 1.8. In Scheme II, when the shutters were tilted in the afterburner position, gaps inevitably appeared between the shutter strips. This scheme, with the value of the D_{nozzle}/D_{screen} ratio limited in practice, can be viewed as applicable to engines without afterburner.

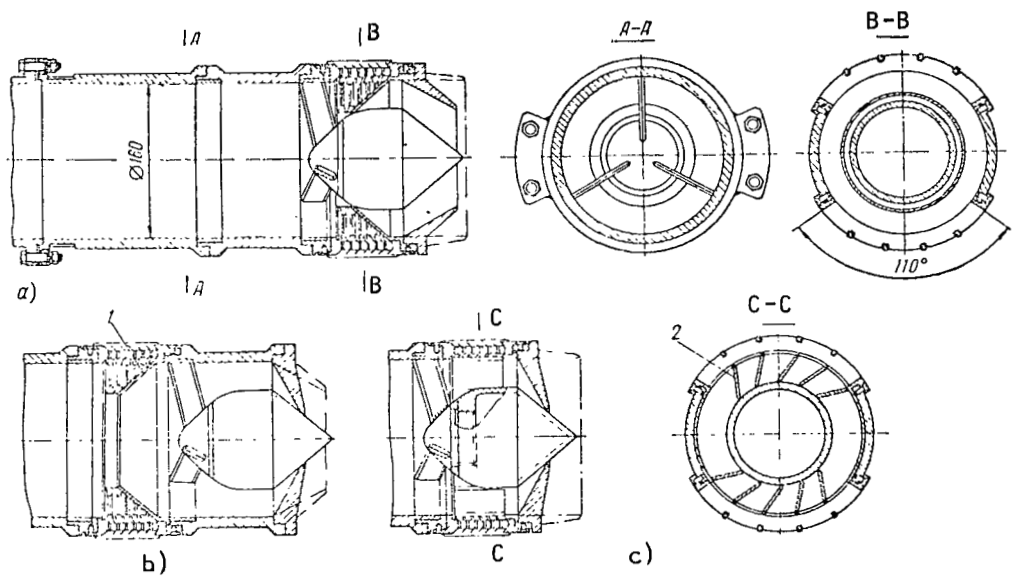

Figure 4.17. Experimental Models of Group No. 1 With Deflecting Screens Made of Leaf-Type Vanes: a, Scheme I, Variant 1; B, Scheme I, Variant 2; c, Scheme II, Variant 1; 1, Cone Modeling Shutters of the Reverse Control Nozzle Type; 2, Strips Modeling Tilting Flaps.

The models were built dismountable, which made it possible to place the cylindrical part of the models with deflecting screens in different positions.

Effect of Angle of Stream Exit from Deflecting Screens on $\bar{R}_{rev}$ /104

Screens with design angles β_{vanes} of vanes at an exit equal to 35° (Screen I), 50.5° (screens II and III), and 67° (screen IV) were constructed for models in group No. 1. The vane profiles were constructed leafwise, that is, of sheet material. The area of the exit sections of the screens compared with the nozzle cross-sectional area was increased for the screens I, II, and

IV by 1.3; 1.2, and 1.1 times, respectively. For all the models the subtended angle θ was taken as 110°.

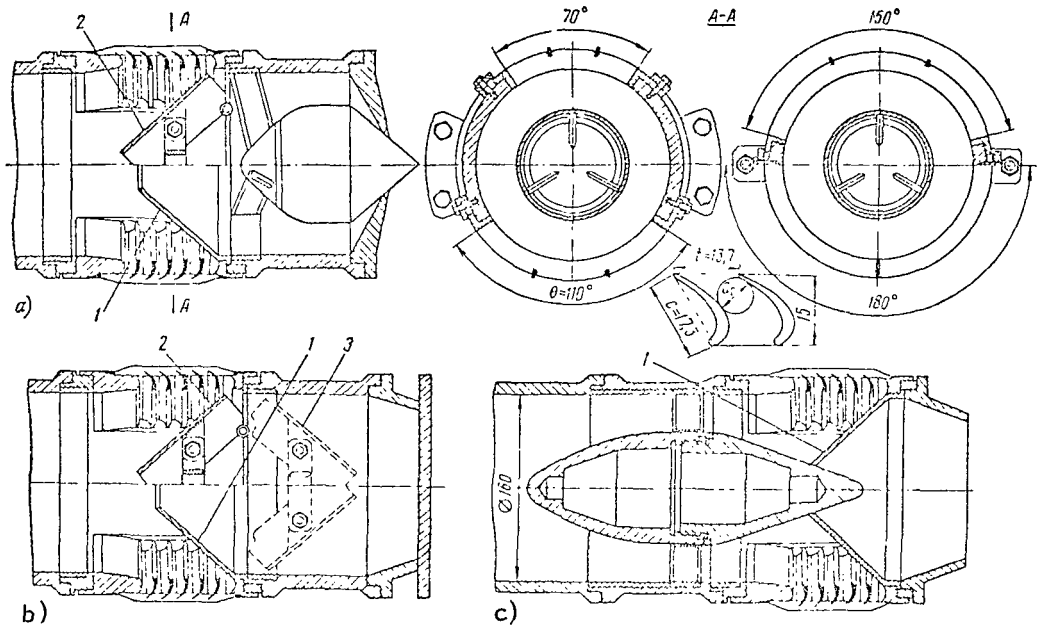

Figure 4.18. Experimental Models of Group No. 2 With Deflecting Screens Made of Profiled Vanes: a, Scheme I, Variant 2; Scheme IV, Variant 2; b, Scheme B, D, E, (Figure 4.16); c, Scheme A (Figure 4.16); 1, Cone Modeling Shutters of the Reverse Regulated Nozzle Type; 2, 3, Cylindrical Shutters; (3c in Turned Position).

The inlet section of the duct was profiled to ensure shockless stream inflow. The angle β_{inlet} of the vane at the inlet was taken as equal to the angle of a cone modeling shutters of the reverser: for screen I--40°, and for screens II and IV--56° (Figure 4.19). The angle of profile placement ϑ was taken as 10°. The number of ducts was selected in such a way as to have closely grouped values of screen density c/t.

A variant of screen II was constructed--screen III, differing from the former in the number of vanes. Two vanes were installed instead of three.

Geometric parameters of the screens of group No. 1 models are listed in Table 2.

Here z = number of ducts; F_{inlet}/F_2 = ratio of areas of inlet and exit cross-sections. It is obvious that all screens,with the exception of screen IV, formed convergent ducts as a whole. /105

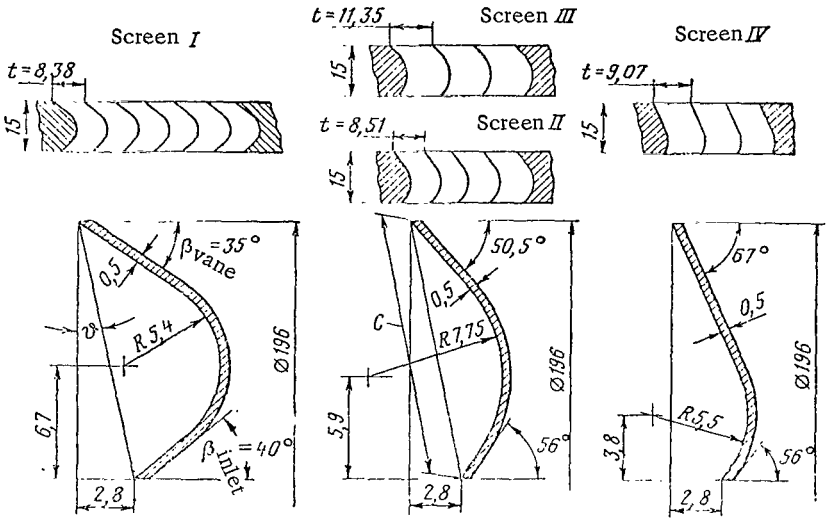

Figure 4.19. Sketches of Deflecting Screens and Vanes of Group No. 1 Models.

TABLE 2

Screen.	β_{vane}	β_{inlet}	c/t	z	F_{inlet}/F_2
I	35	40	1,81	6	1,12
II	50,5	56°	1,79	4	1,075
III	50,5	56°	1,34	3	1,075
IV	67	56°	16,8	3	0,912

Tests of Group No. 1 models revealed that consumption through reversers proved to differ for all screens from the consumption through the nozzle when the nominal shutter position was adopted. Since this investigation was not related to any specific equipment layout, the characteristics of the corresponding nozzle were determined by calculation based on the measured consumption through the reverser and on the $\overline{R}_{specific\ nozzle\ thrust}$ values obtained from the curve in Figure 3.3.

Curves of the reverse coefficient as a function of extent of pressure reduction are plotted in Figure 4.20 for a model constructed under Scheme I, Variant 1, with screens I, II, III and IV. As indicated, provisionally $\overline{G}_{rev} = 1$. Since the entire consumption in the model was directed to the deflecting

screens, the resulting values of the reverse coefficient for this structure are the maximally obtainable.

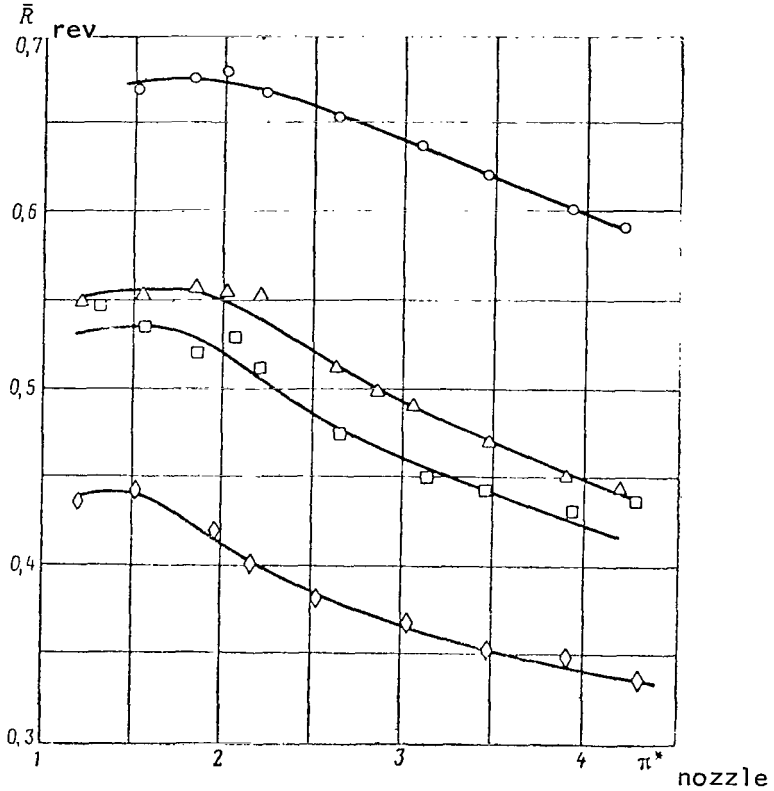

Figure 4.20. Reverse Coefficient as a Function of Extent of Pressure Reduction for a Reverser of a Nozzle Enclosing a Central Body with Different Deflecting Screens. Scheme I, Variant 1. Mean Values of Two Tests: o, screen I; Δ, Screen II; □, Screen III; ◇, Screen IV.

From inspection of the curves it is clear that smooth maxima of the reverse coefficient are noted at low degrees of pressure reduction. When the extent of pressure reduction rises past $\pi^*_{\text{nozzle}} = 2.0$ (for most screens), the reverse coefficient is markedly reduced. The curves are representative of a reverser with deflecting screens made of leafwise profiles constructed under Scheme I. The greater the angle of stream exit from the screens, the lower the values of the reverse coefficient. In a reverser with screens III that have lower density compared to screens II and as a consequence somewhat greater diffusivity, the reverse coefficient in the entire range of π^*_{nozzle} is lower than with screens II. This pattern in the curves that we have noted is accounted

for by variation in the angle of stream exit from the reverser (cf. Figure 5.5). Analysis reveals that a reduction in the reverse coefficient occurs to a lesser extent than a reduction in the cosine of the angle of stream exit. This means that losses of total pressure are reduced with a reduction in the angle of stream deflection in reverser screens. /106

Effect of the Ratio of the Sides of Deflecting Screens on $\bar{R}_{rev}$

When building a reverser the given area of the deflecting screen exit cross-section can be obtained for different ratios of the screen length a (in the direction of the engine axis) and its width b (Figure 4.12). For a given screen density, its elongation involves increasing the number of ducts in it. /107 Widening the screen leads to a transition to large subtended angles θ. Screen width is related to subtended angles by the self-evident ratio $b = D/\sin \theta/2$, where D = external diameter of the screen (jet pipe).

The effect of the subtended angle of the screen and of the number of channels in the screen was explored on Group No. 2 models (cf. Figure 4.18), corresponding to Variant 2 of Scheme I. The deflecting screens in this model group were composed of profiled vanes. A turbine screen of the jet type with a design screen angle $\beta'_{screen} = \text{arc sin } a_{gas}/t \approx 31°$, was selected, that is, a value close to the angle β_{vane} for the screen with the leafwise profile.

The density of the deflecting screens of well-known reversers varies within wide limits--from 1 to 2.0. Some mean value c/t = 1.26 (t = 13.7 mm) was selected, which from data of a study made of a series of flat turbine screens, for a constant angle of stream exit corresponds to the minimum total pressure losses. Intervane channels formed by these profiles are smoothly constricted and have a ratio of inlet and exit section areas of about 1.25.

Since the exit section area of the deflecting screens for reversers differing in the reverse coefficient will be different, the effect of the a/b ratio was conducted with deflecting screens for a series of relative area values $\bar{F}_2 = F_2/F_0$, where F_0 = cross-sectional area of jet pipe (Table 3).

TABLE 3

$\bar{F}_2$	0.235	0.470	0.465	0.720	0.707	0.996	0.996	0.958	0.885
θ	35	110	110	110	55	180	150	110	55
z	6	4	6	6	12	5	6	8	15

A screen built of circular vanes, that is, with a subtended angle for both screens of $2\theta = 360°$, will scarcely be of practical importance, though it does afford some interest as a limiting case of the screen in which the effect of end faces is done away with and circular symmetry ensured.

Figure 4.21, 4.22 and 4.23 present plots of curves of the reverse coefficient as functions of the extent of pressure reduction for model reversers differing in the ratio of deflecting screens sides, that is, in the subtended angle and in the number of channels in the screens. We can see that when π^*_{nozzle} is increased there is a general tendency toward a reduction in reverse /108
coefficients. Comparing these curves with similar functions for reversers constructed under the same scheme, but in which screens are made of leafwise profiles, we can spot several points of difference. Minima of the reverse coefficient, whose positions vary depending on the subtended angle of the screens and the number of channels they inclose, is observed on several curves constructed from the results of repeated experiments, in the range of pressure decreases $\pi^*_{nozzle} = 1.7\text{-}2.5$. These minima are found at smaller π^*_{nozzle} values, the smaller the relative area $\overline{F}_2$: when $\pi^*_{nozzle} \approx 1.7\text{-}2.0$ and $\overline{F}_2 \approx 0.470$ (cf. Figure 4.21); when $\pi^*_{nozzle} \approx 2.2\text{-}2.5$ and $\overline{F}_2 \approx 0.72$ (cf. Figure 4.22) and when $\pi^*_{nozzle} \approx 2.5$ and $\overline{F}_2 \approx 1.0$ (Figure 4.23). The sizeable decrease in the reverse coefficient when short screens with a small number of channels ($\theta = 110°$, $z = 4$, Figure 4.21) are used is quite marked.

Available experimental material does not allow us thus far to give a /110
satisfactory explanation of these features of the characteristics. In fact, the subsequent reduction of the reverse coefficient finds an explanation in the tilting of the stream in the oblique cross-section of the screens (cf. §1, Chapter V).

A rise in the reverse coefficient is observed for all values of the relative area $\overline{F}_2$ when the screens are elongated, that is, when the subtended angle is reduced (see Fig. 4.21) and with a reduction in subtended angle and an increase in number of channels (cf. Figures 4.21, 4.22, and 4.23). This is graphically evident from Figure 4.24, where the values $\overline{R}_{rev}$ are given in the functions of the screen subtended angle for different relative area values. It also logically follows from this figure that for a given screen subtending angle, higher values for the reverse coefficient are reached in reversers that have /111
large $\overline{F}_2$ values.

The material given here allows us to draw a conclusion about what the rational ratio of the deflecting screen sides for reversers of the type under consideration is. To reach high reverse coefficient values it is best to use screens that are extended along the engine axis (Figure 4.25). We can see in this figure that starting with the value $a/b \approx 1$ a further rise in a/b does not give us much added advantage. We take note that from the design point of view use of screens that extend along the engine axis is not favorable, since this

leads to higher longitudinal overall dimensions of the engines and hampers closure of screens in direct thrust regimes. The screen subtended angle is best chosen as not greater than 110-120°

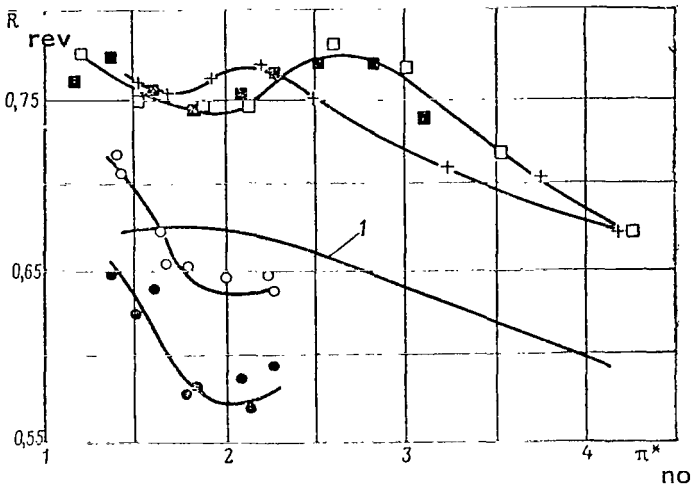

Figure 4.21. Reverse Coefficient as Functions of the Extent of Pressure Reduction for Reversers of the Nozzle in Closing a Central Body and for a Constricted Nozzle for Different Subtended Angles of the Deflecting Screen and for Different Numbers of Channels Inclosed in the Screen ($\bar{F}_2 \leqslant 0.47$). Scheme I, Variant 2: ○ — $\theta = 35°$, $z = 6$ ($\bar{F}_2 = 0{,}232$); □ — $\theta = 70°$, $z = 6$ ($\bar{F}_2 = 0{,}465$); ◐ — $\theta = 110°$, $z = 4$ ($\bar{F}_2 = 0{,}470$). Scheme IV, Variant 2: ● — $\theta = 110°$, $z = 4$ ($\bar{F}_2 = 0{,}470$). Scheme A (Fig. 4.16): ■ — $\theta = 70°$, $z = 6$ ($\bar{F}_2 = 0{,}465$). 1, Curve for the Reverser Constructed Under Scheme No. 1, Variant 2, with Screen 1 Made of Leafwise Profile.

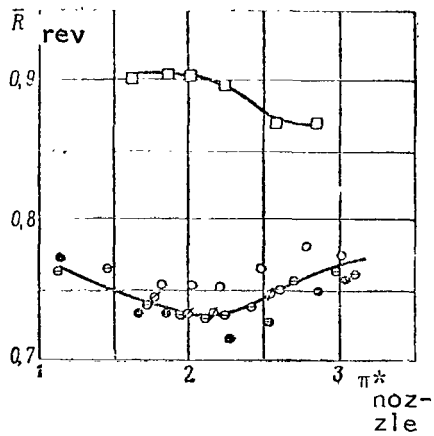

Figure 4.22. Reverse Coefficient as Function of the Extent of Pressure Reduction for Reversers of a Nozzle Enclosing a Central Body and for a Constricted Nozzle for Different Subtended Angles of the Deflecting Screen and the Number of Channels Enclosed Therein. ($\bar{F}_2 \approx 0{,}7$). Scheme I, Variant 2: □ — $\theta = 55°$, $z = 12$ ($\bar{F}_2 = 0{,}707$); ○, ⊙, ⊘ — Different Tests $\theta = 110°$, $z = 6$ ($\bar{F}_2 = 0{,}720$) Scheme A, (Fig. 4.16): ⊘ — $\theta = 110°$, $z = 6$ ($\bar{F}_2 = 0{,}720$)

Effect of the Method of Profiling Deflecting Screen Vanes on $\bar{R}_{rev}$

The material we have looked at allows us to determine whether it is profitable to use profiled vanes instead of leafwise vanes in the deflecting screens of reversers. For any given degree of pressure reduction the reverse coefficient in the absence of direct thrust and when equal to the value of the total pressure recovery coefficient in the deflecting screens is proportional /112 to the cosine of the angle of the stream exit:

$$\bar{R}_{\text{reverse, profiled}} = \bar{R}_{\text{reverse, leaf type}} \frac{\cos \beta_{\text{profiled}}}{\cos \beta_{\text{leaf type}}}.$$

Here the indices "pr" and "vane" refer, respectively, to screen made of profiled and those made of leafwise vanes.

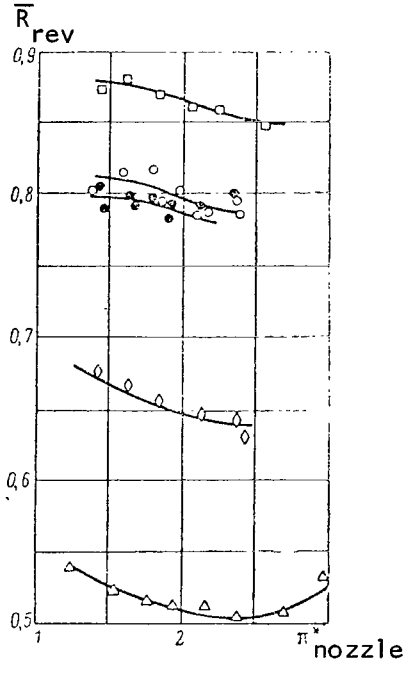

Figure 4.23. Reverse Coefficient as a Function of the Extent of Pressure Reduction for a Reverser Equipped in the Nozzle with a Central Body for Different Subtended Angles of the Deflecting Screen and the Number of Channels Enclosed Therein ($\bar{F}_2 \approx 1$). Scheme I, Variant 2:

□ — θ = 55°, z = 15 ($\bar{F}_2$ = 0,885); ○ — θ = 110°, z = 8 ($\bar{F}_2$ = 0,958); ◇ — θ = 150°, z = 6 ($\bar{F}_2$ = 0,996); △ — θ = 180°, z = 5 ($\bar{F}_2$ = 0,996).

Scheme IV, Variant 2:

● — θ = 110°, z = 6 ($\bar{F}_2$ = 0,958)

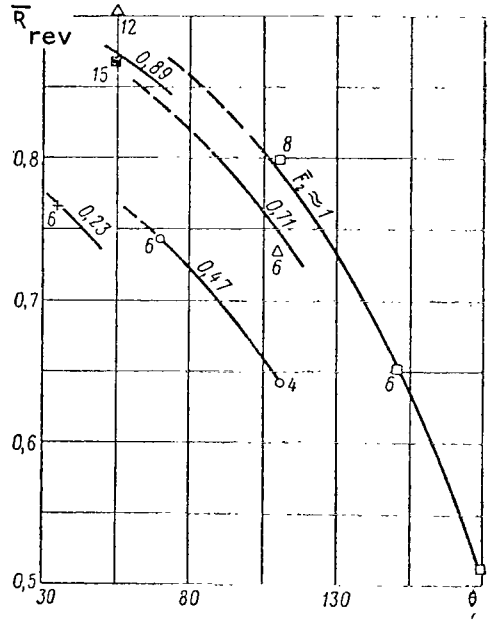

Figure 4.24. Reverse Coefficient as the Function of Subtended Angle of Screen for a Reverser INstalled in a Nozzle with a Central Body for Different Relative Areas of Minimum Through Cross-section of the Screens When π^*_{nozzle} = 2.0. Scheme I, Variant 2. (The number of channels in the screen is indicated close to the experimental symbol.)

Relying on the results of measuring the stream exit angle for a reverser constructed under Scheme I (§1, Chapter V) with deflecting screens at θ = 110° and z = 6, it is easy to calculate the values of

$\bar{R}_{reverse,\ profiled}$ listed below in Table 4. This table also gives us for comparison experimental values based on data in Figure 4.22.

TABLE 4.

π^*_{nozzle}	1,25	1,5	1,75	2,0	2,25
$(\bar{R}_{reverse\ profiled})_{experi.}$	0,760	0,750	0,740	0,732	0,735
$(\bar{R}_{rev.\ profiled})_{calculated}$	0,700	0,700	0,700	0,696	0,692
$\Delta\bar{R}_{rev}$ %	9,0	7,4	5,9	5,7	6,5

Tr. note: Commas indicate decimal points.

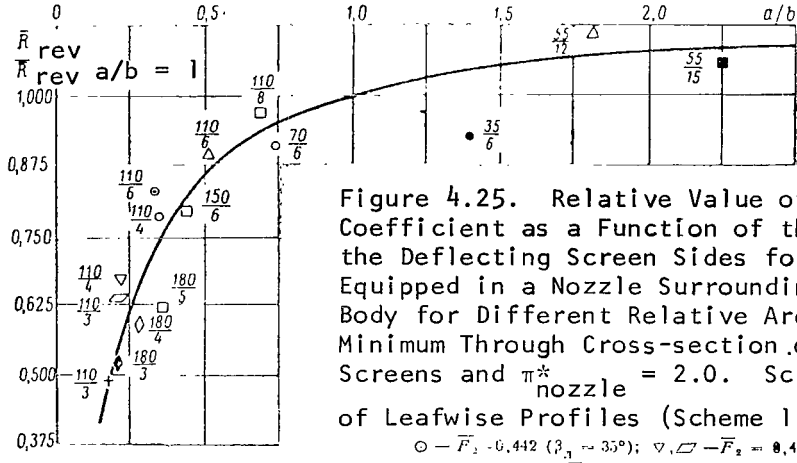

Figure 4.25. Relative Value of Reverse Coefficient as a Function of the Ratio of the Deflecting Screen Sides for a Reverser Equipped in a Nozzle Surrounding a Central Body for Different Relative Areas of the Minimum Through Cross-section of the Screens and π^*_{nozzle} = 2.0. Screens Made of Leafwise Profiles (Scheme 1, Variant 1) ○ – $\bar{F}_2$ = 0,442 (β_{vane} = 35°); ▽, ▱ – $\bar{F}_2$ = 0,425 (β_{vane} = 50,5°); ◇ – $\bar{F}_2$ = 0,375 (β_{vane} = 67°) Screens made of Profiled Vanes: (Scheme 1, Variant 2): ● – $\bar{F}_2$ = 0.232; ⊙ – $\bar{F}_2$ ≈ 0,47; △ – $\bar{F}_2$ ≈ 0,7; ◆ – $\bar{F}_2$ = 0,61; ▲ – $\bar{F}_2$ = 0,81; ■ – $\bar{F}_2$ ≈ 0,89; □ – $\bar{F}_2$ ≈ 1. (The values of the subtended angles and the number of channels enclosed in the screens are given next to the experimental symbols).

It follows from the table that the difference $\Delta\bar{R}_{rev}$ in the reverse coefficients when the extent of pressure reduction corresponds to working conditions of a reverser does not go beyond 6.5%.

So, the method of vane profiling in reversers that include deflecting screens is not the governing factor in total pressure losses. Therefore, we can use vanes of the simplest type, made of sheet material, in screens of reversers without any detriment to their efficiency.

Effect of Method of Closure of Deflecting Screens and Their Placement in the Jet Duct [Pipe] of an Engine on $\overline{R}_{rev}$

When a reverser of a nozzle that includes a central body is constructed under Scheme II, that is, when flaps are placed forward of the screens 1 made of leafwise profiles instead of a cone, the character of the curves describing the reverse coefficient as a function of the extent of pressure reduction is somewhat modified: the maximum of the reverse coefficient shifts to large /113
π^*_{nozzle} values (Figure 4.26, a). The results of testing a reverser with remotely-located flaps (Scheme III) are plotted in Figure 4.26, b. We can easily see that the reverse coefficient increases. This stands to reason, since the Scheme II flaps, located as they are in the stream, introduce certain losses of total pressure which are not to be found in Scheme III.

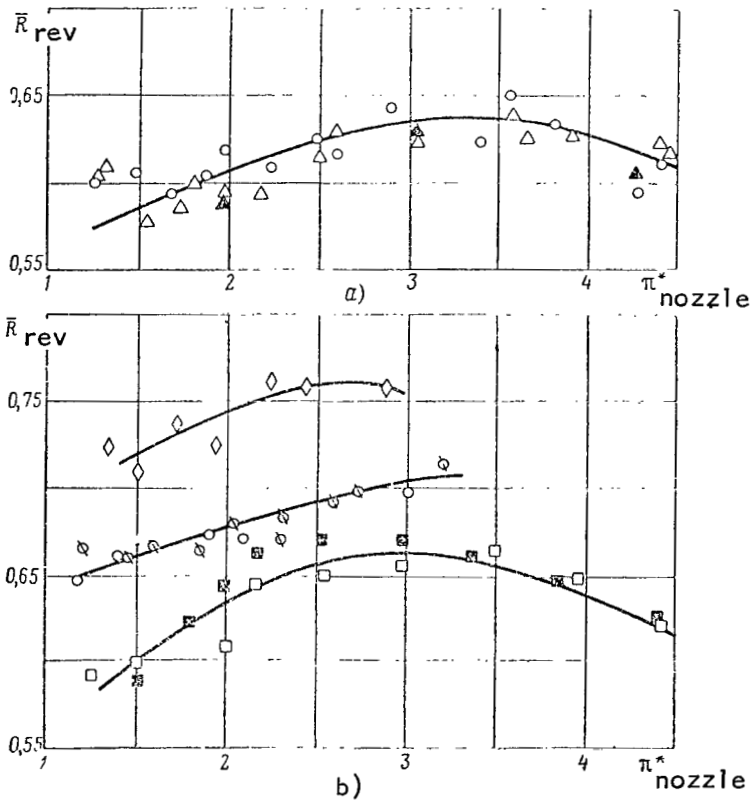

Figure 4.26. Reversing Coefficient as a Function of Pressure Drop for Reverser With Central Body:
a, Diagram II with Lattice 1 of Vane Profiles: Δ Δ, Various Diagram IV, Variant 2; **0**, Variant 2; b diagram III with Lattice 1 of Vane Profiles; Variant 1; □, Variant 2. Diagram III, Variant 2 With Lattice of Shaped Vanes; ◊, θ = 70, z = 6 ($\overline{F}_2$ = 0.465); 0, Ø, Various Tests, θ = 110°. z = 6 ($\overline{F}_2$ = 0.720)

Tests of a reverser constructed under Scheme I with screen remotely located from the central body (Variant 2) showed that the characteristics remain practically as before (Figure 4.27). The thrust characteristic does not change as the result of relocating the screens in Scheme II (Variant 2) and in Scheme III (Variant 2), which we can see in Figure 4.26. /114

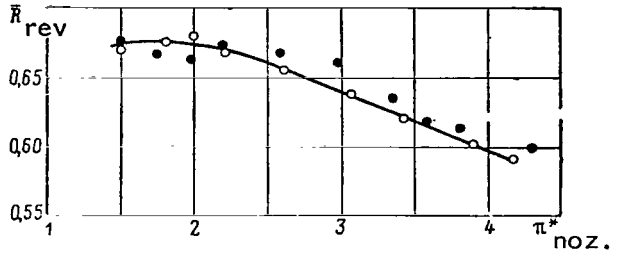

Figure 4.27. Reverse Coefficient as the Function of Extent of Pressure Reduction for the Reverser of a Nozzle that Includes a Central Body with Screen I. Scheme I: o, Variant 1; ●, Variant 2.

Figure 4.26, b also gives us data for a reverser constructed following Scheme III of Variant 2 with screens made of profiled vanes. We can see that in Scheme III use of profiled vanes in the deflecting screens does not bring about change in the qualitative pattern of the reverse coefficient as a function of extent of pressure reduction.

And so, the elements (shutters, flaps) located in direct proximity about the screens, and not the placement of the screens relative to the central body, is what has a bearing on the size of the reverse coefficient and on the appearance of the function $\bar{R}_{rev} = f(\pi^*_{nozzle})$ and, in particular, on the location of the maximum $\bar{R}_{rev}$ on the curve.

When cylindrical shutters are placed forward of the deflecting screens (Figure 4.28), that is, when the reverser is built according to Scheme IV, Variant 2, the nature of the function $\bar{R}_{rev} = f(\pi^*_{nozzle})$ is kept about the same as when shutters of the reverse regulated nozzle type are positioned forward of the screen (Figure 4.22). This is also to be seen when we compare the corresponding curves in Figure 4.21 and 4.23. The values of the reverse coefficient attained prove to be lower, since the cylindrical shutters provide, obviously, better organization of the stream at its inlet into the screen. However, the difference between the $\bar{R}_{rev}$ values for $\bar{F}_2 \approx 0.72\text{-}1.0$ values that are of interests in actual practice is not very great. This is a favorable turn of events, giving the designer some freedom in choosing a method of screen closure in the direct thrust regime. /115

Let us turn to some results of a study made of reversers with constricted nozzles. Figures 4.21 and 4.22 present plots of data for a model corresponding to Scheme A (cf. Figure 4.16) of a reverser used with a constricted nozzle when the screens made of profiled vanes were placed directly aft of the turbine and when shutters of the reverse regulated nozzle type were located forward of the screens. We can see that placing deflecting screens in the region of increased velocities does not lead to a change in the pattern of the curve describing the reverse coefficient as a function of extent of pressure reduction

compared with Scheme I, Variant 2 of a reverser for a nozzle that includes a central body.

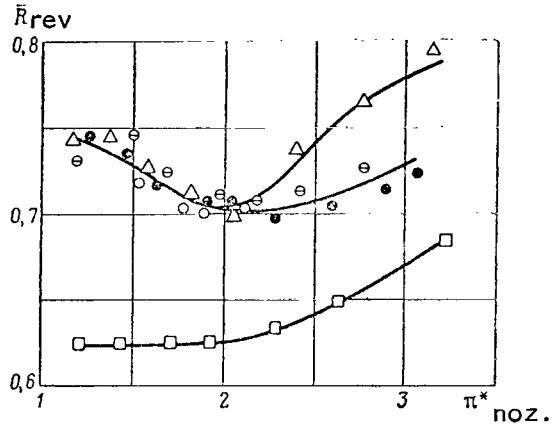

Figure 4.28. Reverse Coefficient as Functions of Extent of Pressure Reduction for Reversers Used with a Nozzle Enclosing a Central Body and for a Constricted Nozzle. Screen θ = = 110°, z = 6: 0, θ , Different Tests Scheme IV, Variant 2; Δ, Scheme D (Fig. 4.16); ●, Scheme V; □, Scheme E.

When, instead of shutters of the reverse regulation nozzle type, cylindrical shutters are positioned forward of the deflecting screens, the values of the reverse coefficient in the range π^*_{nozzle} = 1.8--2.2 prove to be almost the same. This is to be seen for Schemes C and D (Figure 4.16) from Figure 4.28.

When cylindrical shutters are positioned forward of the deflecting screens in the turned position (Scheme E, Figure 4.16), the pattern of the curve describing the reverse coefficient in function of extent of pressure reduction varies /116 but little, however the resulting values are appreciably lower. This is explained by a decrease in the coefficient of total pressure recovery in the screen. It must be pointed out that when the shutters are arranged in this position, experiments have revealed a considerable jarring of the unit, evidently produced by the instability of the flow. This phenomenon has also been observed in tests made of a reverser model incorporating deflecting screens in which the gas duct is throttled by a diaphragm. (cf. Figure 2.6). Therefore, in these models, when schemes C, D and E are studied, the gas duct was not completely partitioned, therefore in order to exclude the effect of direct thrust of the nozzle on test results and in order to secure comparable data, the nozzle was closed over with an end cap, as shown in the sketch (cf. Figure 4.18).

It follows from the foregoing that in the reverser schemes of a nozzle incorporating a central body and a contracted nozzle high reverse coefficients can be obtained. The values $\bar{R}_{rev} \approx 0.5$ that are needed in practice are attained for an applicable value of the design angle of the shutters at the exit from the deflecting screen, equal to approximately 50°.

Effect of Density of Deflecting Screens on $\bar{R}_{rev}$

At a given a/b ratio the screen can be made in a variety of densities. When a/b ≈ 0.5 (θ = 110°) screens can be made of profiled vanes with different densities:

z	4	5	6	7	8	10
c/t	0.835	1.05	1.26	1.47	1.68	2.10

In all these screens the overall screen length was taken at the same value as in the original variant where c/t = 1.26 and z = 6. For screens built in this way the exit area differed by about ±17.5% from the F_2 of the original variant.

Tests with these deflecting screens were conducted on a reverser model of a contracted nozzle when a cone was positioned forward of the screen, that is, on the nozzle corresponding to Scheme B (cf. Figure 4.16). The nozzle was covered with an end cap. Inspection of the curves describing the reverse coefficient as a function of the extent of pressure reduction showed that when the screen densities increased, at a given constant ratio of screen sides a/b, an almost equidistant shifting of the curves toward the side of large $\bar{R}_{rev}$ values takes place. For reversers with screens made of leafwise profiles this /117 can be seen from Figure 4.20. A rise in the reverse coefficient that occurs when the density is increased (Figure 4.29) is accounted for by a climb in the coefficient of total pressure recovery in the screen. The figure gives plots of the results of a test made of a reverser incorporating screens made of leafwise profiles and data known from the literature [38]. It is obvious that the effect of density shows up qualitatively the same.

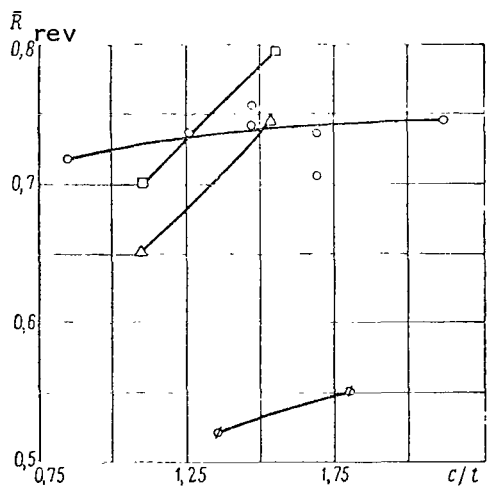

Figure 4.29. Reverse Coefficient as a Function of Density of Deflecting Screen when a/b = const and π^*_{nozzle} = 2.0: o, Reverser of a Contracted Nozzle Incorporating Shutters of the Reverse Regulated Nozzle Type (Scheme B, Fig. 4.16) With Screens a/b ≈ 0.50 Made of Profiled Vanes: □, Δ, the Same Scheme Based on the Data in the Study [38]; ϕ, Reverser of a Nozzle Incorporating a Central Body (Scheme I, Variant 1) With Screens a/b ≈ 0.25 Made of Leafwise Profiles.

We must direct attention to the fact that based on the results of this study the very considerable variation in density leads not only to an appreciable deviation in values of the reverse coefficient. Consequently, the density of the deflecting screens can be selected without detriment to the efficiency of the reverser quite arbitrarily, guided by design considerations.

Effect of Decrease in Exit Section of Deflecting Screens on $\bar{R}_{rev}$ /118

In a number of tests made of a reverser installed in a nozzle incorporating a central body that included screens made of leafwise profiles, the minimum screen exit area was reduced by installing longitudinal inserts along the margins of the screens. It follows from Figure 4.30 that installation of the inserts 4 substantially varies both the pattern of the reverse coefficient as a function of extent of pressure reduction, as well as the value $\bar{R}_{rev}$. The inserts led, evidently, to flow separation in the end face sections, building up appreciably as the extent of pressure reduction grew. As a result of flow separation large losses of total pressure are induced. Figure 4.30 presents this curve for one of the tested variants of a reverser model incorporating deflecting screens and throttling tilting vanes (§4, Chapter IV). Without delving into a detailed comparison of the results, since in this model bypassing of part of the gases to the jet nozzle was executed, we observed that for /119 these models the nature of the reverse coefficient as a function of extent of pressure reduction must be deemed unfavorable owing to considerable reduction of $\bar{R}_{rev}$ as π^*_{nozzle} is made greater.

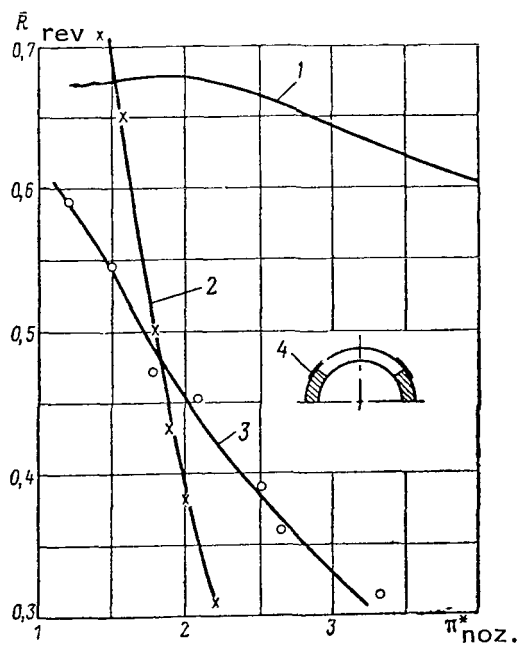

Figure 4.30. Comparison of Reverse Coefficients as Functions of Extent of Pressure Reduction for a Reverser Built Into a Nozzle Incorporating a Central Body and Screen I with Data for a Reverser (cf. Figure 4.51) of a Contracted Nozzle Incorporating Deflecting Screens (β_{screen} = 36°, c/t = = 1.5) and Throttling Tilting Vanes (Curve 2): 1, Scheme I, Variant 1 and 2; 3, Scheme I, Variant 1, Screen with Inserts 4.

The effect on the reverse coefficient of reducing the screen exit area, the longitudinal end face walls of which were made parallel to the vertical plane of symmetry, was investigated. The space around the longitudinal walls were lined with Wood's alloy. The screens produced had an area ratio F_{inlet}/F_2 of about 1.5.

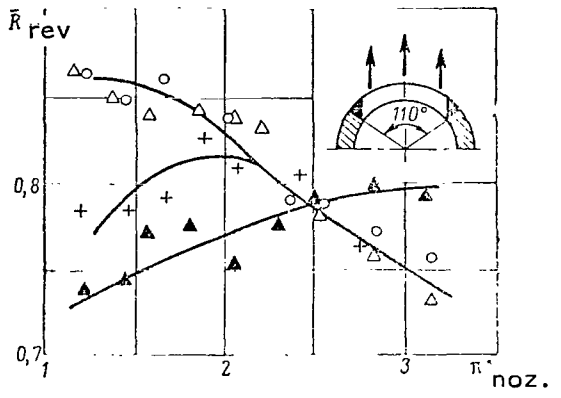

Figure 4.31. Reverse Coefficient as the Function of Extent of Pressure Reduction for a Reverser Incorporated in a Contracted Nozzle with Parallel Longitudinal Walls of the Deflecting Screens: o, with Shutters of the Reverse Regulated Nozzle Type (Scheme B, Figure 4.16); Δ, with Cylindrical Shutters (Scheme D); ▲, with Cylindrical Flaps (Scheme E); +, without Shutters (Scheme F).

The results of testing the reverser incorporated into a contracted nozzle with different throttling devices made up of screens of profiled vanes of density c/t = 1.26, subtended angle θ = 110°, and number of channels z = 6 are plotted in Figure 4.31. In these tests the exit area of the nozzle was closed over with an end cap. We can see that increasing the convergence of the intervane channels of the screen has a very favorable effect on the reverser characteristics. The curves testified to a marked rise in the reverse coefficient for all methods of throttling the gas ducts compared to the reverser employing radially positioned end walls of screens. /120

We must however, take note that the above-indicated value F_{inlet}/F_2 in actual reverser designs cannot be attained owing to the small radial dimension of the deflecting screens. Therefore, the gain from this placement of the end walls of the screens will evidently be less tangible.

§3. Reversers Positioned Forward of the Exit Area of the Jet Nozzle and Aft of it

Reversers Positioned Forward of the Jet Nozzle Exit

Reversers incorporating deflecting connecting parts and throttling shutters

A reverser of this type (Figure 4.32) is installed aft of the turbine ahead of the afterburner chamber. The parts of the reverser are not subjected to high gas temperatures in the afterburner regimes. Gases emitted into the atmosphere through four connecting pipes (nozzles). The connecting pipes have cross-pieces 4 forming a critical cross-section, and guide vanes 5

The principal shutters 2 directing the gas into the connecting pipes when the reverser is cut-in are installed at an angle to the engine axis. The reverser, in addition to the principal shutters, has two small auxiliary shutters 3 which serve to boost gas duct acceleration. Some of the gas is bypassed into

the jet nozzle through the slits between the shutters, the area of which F_4 is about 20% of the area F_{nozzle} of the critical area of the jet nozzle. When the reverser has been cut-in, the principal and auxiliary shutters are rotated simultaneously. Control of shutters is executed by means of levers connected to the pushrods of the control drive hydrocylinders.

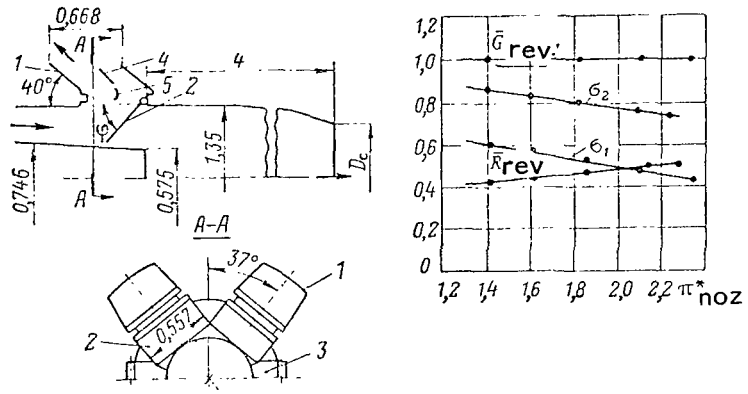

Figure 4.32. Reverser with Deflecting Connecting Pipes and Throttling Shutters and its Experimental Characteristics When $\bar{F}_4 = F_4/F_{nozzle} = 0.2$: 1, Connecting Pipes; 2, Principal Shutters; 3, Auxiliary Shutters; 4, Cross-piece; 5, Guide vane.

Shutters can have three characteristic positions. The first position is reverser not cut-in. The principal shutters cover the inlet sections of the connecting pipes and together with the auxiliary shutters lie flush with the jet pipe surface. The second position is partial reversal, in which /121 the engine operating at rated rpm provides a thrust equal to the thrust at low throttle. The second position is complete reversal. The flaps are tilted by an angle of $\phi = 46°$.

The characteristics of the reverser built with geometrical dimensions of the flow section shown in the figure[1] have been determined experimentally.

The figure also gives the main characteristics.

The values of relative thrust $\bar{R}_{rel}$ and consumption $\bar{G}_{rel}$, the reverse coefficients, and the consumption coefficients as functions of the angle ϕ of shutter tilting when the extent of pressure reduction $\pi^*_{nozzle} = 2.23$, corresponding to maximum engine regime, are shown in Figure 4.33. The thrust variation takes place smoothly, which is characteristic for all reverser schemes in which throttling of the gas ducts is accomplished mechanically.

In model tests, relative consumption in the process of cutting-in and cutting-out of the reverser increases owing to the fact that the through cross-sectional areas of the exhaust system become greater, since the connecting

[1]The relative dimensions in this section are given in the figures in fractions of diameter D_{nozzle} of the critical nozzle cross-section in direct thrust regime.

pipes into the jet nozzle are partially open simultaneously. Consequently, the cutting-in and cutting-out of the reverser must not induce any difficulties in performance of the turbo compressor group of the engine, since the stable performance margin of the compressor in the engine system here then increases. It is clearly seen in the figure that the thrust at low throttle ($\bar{R}_{rel} \approx 0.15$) is attained when the shutters have been turned by an angle $\phi \approx 25°$. /122

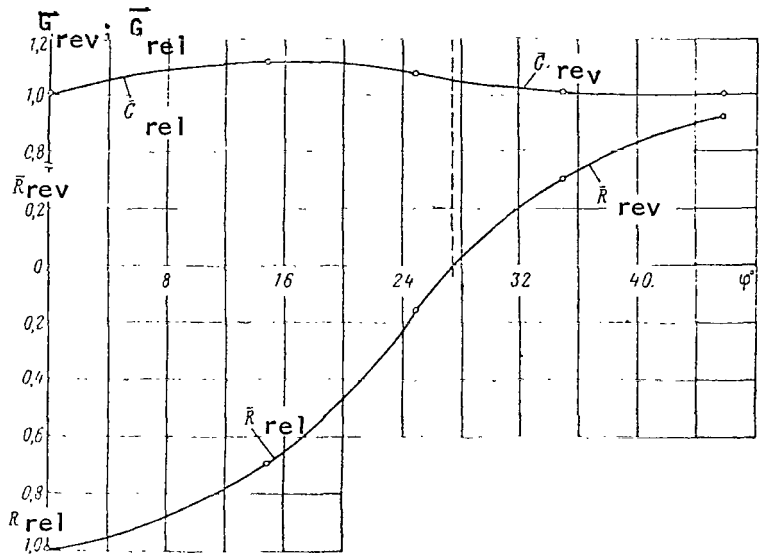

Figure 4.33. Relative Thrust $\bar{R}_{rel}$ and Relative Consumption $\bar{G}_{rel}$, Reverse Coefficient and Consumption Coefficient as Functions of the Angle of Shutter Turning ϕ ($\pi^*_{nozzle} = 2.23$) for a Model of a Reverser Incorporating Connecting Pipes and Throttling Shutters.

Figure 4.34 presents the distribution of total pressure in the inlet section $p_{0,inlet}$ and the exit area of the connecting pipe p_{02}, measured by the comb 6. We can clearly see that in the inlet section the total pressure $p_{0,inlet}$ is below the atmospheric at the front wall 1 of the connecting pipe. this drop in pressure was brought about by flow separation induced in the inlet section of the connecting pipe at the location of an abrupt turn. The pressure $p_{0,inlet}$ at some distance from the front wall is comparable with the atmospheric, further rises, and reaches the maximum close to the rear wall 2 where the flow is more organized, since it is directed by the principal shutter 3. The total pressures $p_{0,2}$ in the exit areas also characterized by appreciable

nonuniformity. The total pressure $p_{0,2}$ in the direction running from the front to the rear walls varies from p_H to the maximum. With the exception of the section adjoining the front wall, the total pressure at the exit has less than the total pressure at the inlet, owing to losses in the connecting pipe. By the front wall the value $p_{0,2}$ is greater than $p_{0,inlet}$. This is so because stream once again fills the entire cross-sectional area. The cross-piece 4 and the guide vane 5 have a marked effect on flow structure: aft of these elements a sharp drop in total pressure is observed. /124

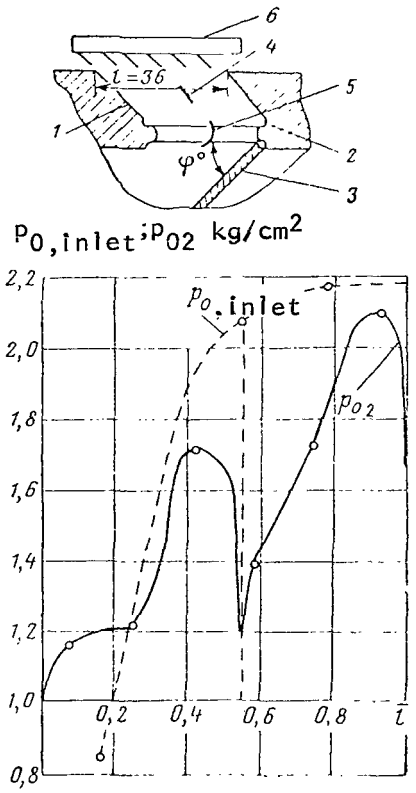

Figure 4.34. Distribution of Total Pressure in the Inlet and Exit Sections Along the Middle of the Connecting Pipe when $\pi^*_{nozzle} = 2.23$ and $\phi = 46°$: 1, Front Wall; 2, Rear Wall; 3, Principal Shutter; 4, Cross-piece; 5, Guide Vane; 6, Comb.

Measurements showed that the distribution of total pressure across the cross-sectional area of the jet nozzle located remotely from the reverser is quite uniform, since the flow along the path from the shutters to the exit area of the jet nozzle becomes equalized. Coefficients of total pressure recovery σ_2 in the connecting pipe and σ_1 in the jet nozzle in reversal, determined from the result of measuring total pressure, are also plotted in Figure 4.32[1].

Also tested was the effect on reverser parameters of the following design changes in the starting model:

a) Elimination of the cross-piece 4 (cf. Figure 4.32) and the guide vane 5 of the connecting pipes (Variant a);

b) use of nonsymmetrical design of shutters, as the result of which the auxiliary shutters were done away with and the area of gas bypass to the jet nozzle was brought down from 20 to 13% (Variant b);

c) Variation in the bypass area from 13 to 22% in the design incorporating nonsymmetrical shutters (Variant c);

d) a reduction in the height of the rear wall of the connecting pipe by 0.306 D_{nozzle} (Variant d).

[1]The data on σ_2 presented below in this section have been based on measurement of total pressure fields at exit from deflecting elements of reversers.

Investigation of the variant a showed that when the consumption coefficient $\bar{G}_{rev} = 1$ the reverse coefficient when $\pi^*_{nozzle} = 2.2$ was lowered from 0.50 to 0.48. This decrease in the reverse coefficient can be explained by the fact that in eliminating the cross-piece and the guide vanes in the connecting pipe a flow separation area was built up and total pressure losses mounted.

When the bypass area was reduced (Variant b) the reverse coefficient rose up to about 0.55.

In Variant c a reverse coefficient of 0.50 was obtained, that is, it agreed with the value of $\bar{R}_{rev}$ of the starting model when $\bar{F}_4 = 0.20$.

In Variant d the reverse coefficient proved to be equal to 0.40. A reduction in the value of $\bar{R}_{rev}$ compared to variants a and c were due to the fact that as the height of the rear wall of the connecting pipe was decreased, some of the flow escaped from the connecting pipes at a large angle to the engine axis.

Reversers with annular deflecting screens and with a throttling jet nozzle /125

A reverser with throttling jet nozzle was developed for one of the domestic engines. Tests of a series of variants of this scheme on models was conducted aiming at determining the chances of obtaining a reverse coefficient 0.35-0.40.

When the reverser was cut-in, the shutters 1 (Figure 4.35) of the jet nozzle throttled the exit area of the nozzle and a large part of the gas exited through the extended deflecting screen 2, building up negative thrust. When the reverser was not cut-in, the screen was shifted to the left (pushed along the surface of the jet pipe) and the through section of the jet nozzle was expanded to normal. Here the jet nozzle, rigidly mounted to the screen, rests at the face of the jet pipe 4 ensuring tightness of the butt.

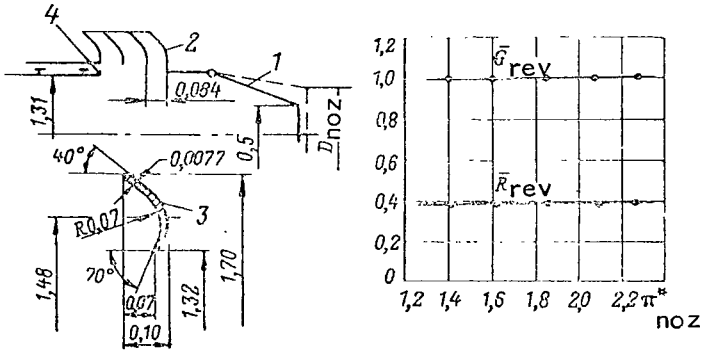

Figure 4.35. Reverser with Annular Deflecting Screen and with Throttling Jet Nozzle and its Experimental Characteristics at $F_1/F_{noz.} = 0.25$: 1, Jet Nozzle Shutters; 2, Screen; 3, Screen Profile; 4, Jet Pipe.

Reverser models were constructed suitably for the maximum engine regime (Figure 4.35 and 4.36) and for the afterburner regime (Figures 4.37 and 4.38). The extent of pressure increase in the afterburner regime $T_{0,aft}/T_0$ for the models tested was taken as equal to two. Here $T_{0,aft}$ = braking temperature in the jet nozzle in the afterburner regime, and T_0 = braking temperature in the jet nozzle in maximum engine regime. The tests showed that of the variants constructed for the maximum engine regime, the required $\bar{R}_{rev}$ value was provided by the variant shown in Figure 4.35. The fairly high reverse coefficient /126 ($\bar{R}_{rev}$ = 0.39) compared with the other variant was attained owing to the considerable throttling of the gas duct by the jet nozzle. The jet nozzle diameter here was reduced in half, that is, F_1/F_{nozzle} = 0.25. This decrease in diameter was attained by using a jet nozzle structure with stepped shutter cross-section (Figure 4.39).

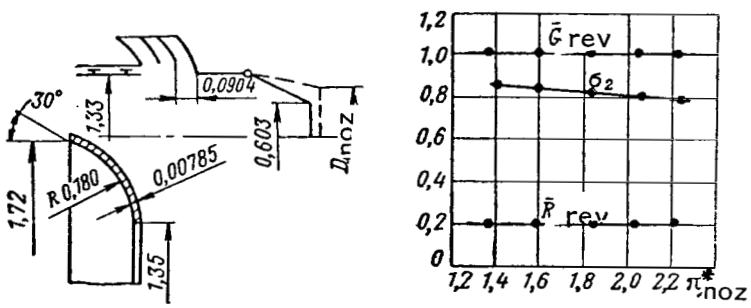

Figure 4.36. Reverser with Annular Deflecting Screen and with Throttling Jet Nozzle and Its Experimental Characteristics at F_1/F_{nozzle} = 0.364.

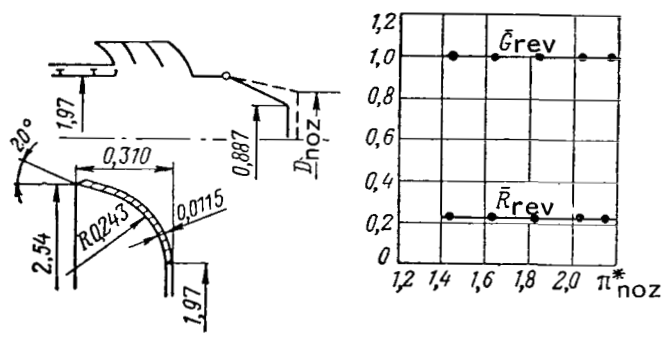

Figure 4.37. Reverser with Annular Deflecting Screen with Throttling Jet Nozzle and Its Experimental Characteristics at F_1/F_{nozzle} = 0.79.

When F_1/F_{nozzle} = 0.31, the value $\bar{R}_{rev}$ = 0.20 was obtained. For the maximum possible extent of gas duct throttling F_1/F_{nozzle} = 0.36 in the jet nozzle that did not incorporate stepwise cross-section of shutters, a reverse coefficient of $\bar{R}_{rev} \approx 0.2$ (cf. Figure 4.36) was achieved.

In the afterburner regime the reverse coefficient value of $\bar{R}_{rev} \approx 0.22$ /127 is attained at a relatively small decrease in diameter D_{nozzle} of the jet nozzle, approximately down to 0.887 D_{nozzle}, that is, when $F_1/F_{nozzle} \approx 0.79$ (cf. Figure 4.37). As the diameter of the jet nozzle is reduced down to a value close to the minimum, 0.594D_{nozzle}, which can be attained without stepwise shutter cross-sectioning, and with simultaneous increase in the angle β_{vane} from 20° to 40°, the reverse coefficient is $\bar{R}_{rev}$ = 0.55 (cf. Figure 4.38).

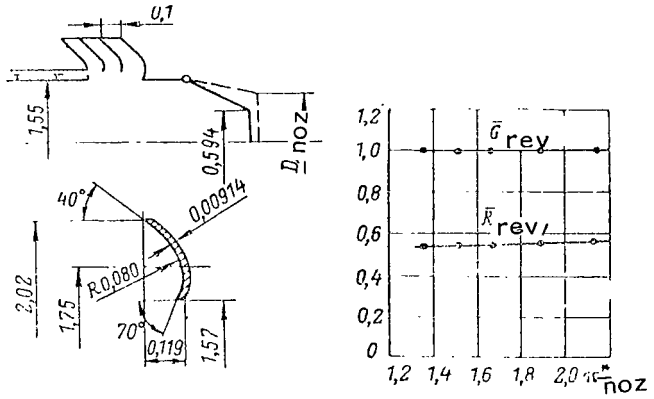

Figure 4.38. Reverser with Annula Deflecting Screen and With Throttling Jet Nozzle and Its Experimental Characteristics at F_1/F_{nozzle} = = 0.35.

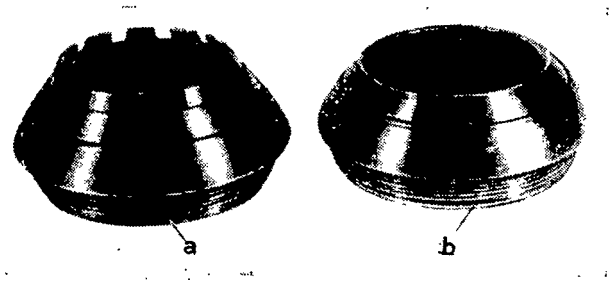

Figure 4.39. Models of Jet Nozzles: a, Throttling Jet Nozzle with Stepwise Cross-sectioning of Shutters; b, Ordinary Jet Nozzle.

Investigation of the effect that the deflecting screens have on direct nozzle thrust with reverser not cut-in revealed that direct thrust of the nozzle /128 with externally closed screen does not change compared to the thrust produced by nozzle that has no screens.

Reverser with Deflecting Screens and Throttling Shutters of a Bypass Engine

Two cylindrical shutters 1 (Figure 4.40) rotating on pins uncovered the screens 2 and locked exit of the stream in the straight-line direction. Streams from both passes of the engine are deflected by the shutters to streams that direct the flow to the opposite side. Some of the flow has direct exit through the slit between the shutters. The slit area is about 6% of the jet nozzle area. When the reverser is not cut-in, the shutters

area. When the reverser is not cut-in, the shutters close over the screens and do not block direct exiting of the stream[1].

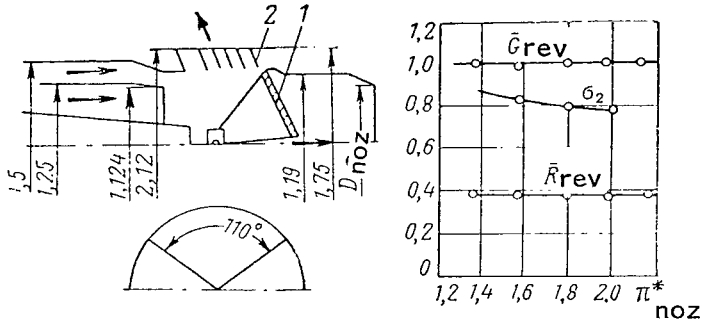

Figure 4.40. Reverser with Deflecting Screens and Cylindrical Throttling Shutters of a By-pass Engine and Its Experimental Characteristics, F_4/F_{nozzle} = 0.06: 1, Shutter; 2, Deflecting Screen.

The through sections of the reverser and gas consumption through it vary as a function of the shutter tilting angle. Relative thrust and relative consumption and reverse coefficient and consumption coefficients as functions of the angle ϕ of shutter rotation are shown in Figure 4.41.

Distribution of total pressure along the length of the deflecting screeen in the exit cross-section is shown in Figure 4.42.

Figure 4.43 presents distribution of pressure along the shutter in the form of a function of the ratio $p/p_{0,inlet}$ (p = static pressure at shutter and $p_{0,inlet}$ = total pressure of stream in inner pass).

When the shutter rotation angle ϕ = 30°-40°, we have a maximum variation /131
in pressure. The dashed line shows the distribution of pressure along the shutter when the jet nozzle has been capped. In this case pressure distribution is more uniform.

Reverser with nonsymmetrical discharge

Conditions of engine placement on an aircraft, and also the possibility of injection of gas from the reversers in the air scoop of an engine often do not permit organization of symmetrical gas discharge.

Figure 4.44 shows the scheme of a reverser with nonsymmetrical discharge. In the case of one-sided discharge of the gas through the upper (reverse) con- /133
necting pipe 2 at a design angle 40°, vertical component of thrust is built up, and this can be compensated by gas discharge to the opposite side through the lower (deflecting) connecting pipe with a design angle of 90°. Throttling of the gas duct makes use of the shutters 1. Some of the gas is bypassed to the

[1]Design of reverser was developed for one of the domestic engines produced by a group of designers lead by N. D. Kuznetsov.

jet nozzle via the gaps between the shutters 1 and the cowling 4. In the direct thrust regime the shutters are positioned flush, by means of hydrocylinders 5, with the walls of the jet pipe and partitioned off the connecting pipes 2 and 3.

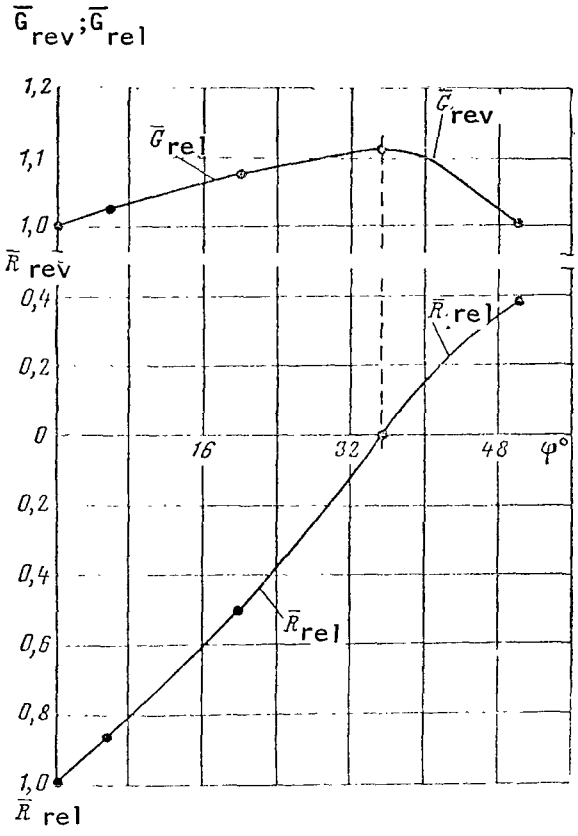

Figure 4.41. $\bar{R}_{rel}$, $\bar{G}_{rel}$, $\bar{R}_{rev}$ and $\bar{G}_{rev}$ as Functions of the Angle of Shutter Rotation for the Reverser Shown in Figure 4.40.

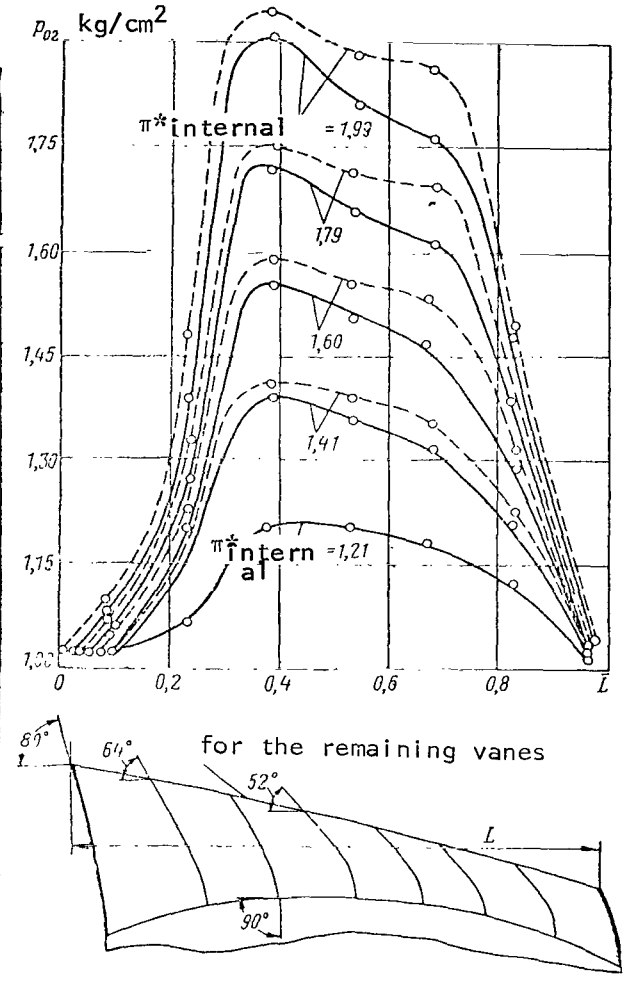

Figure 4.42. Distribution of Total Pressure in Average Cross-section Along Screen Length for Exiting from the Reverser Shown in Figure 4.40: ———, with Bypassing of Part of the Gas to the Jet Nozzles; -----, Without Bypassing.

The relative vertical component of thrust $\bar{R}_{ver} = R_{ver}/R_{nozzle}$ and the reverse coefficient were found as functions of the through cross-section of the deflecting connecting pipe for bypass areas that amount to 5 and 17% of jet nozzle area. The experiment was

limited to three values of the deflecting connecting pipe area, 15, 25 and 46% of the jet nozzle area. This stemmed from the necessity of obtaining a satisfactory reverse coefficient at minimum vertical thrust component. An area of the reverse connecting pipe was selected for the listed values of the deflecting connecting pipe area that would ensure simultaneous consumption with the reverser cut-in or cut-out, that is, $\bar{G}_{rev} = 1$.

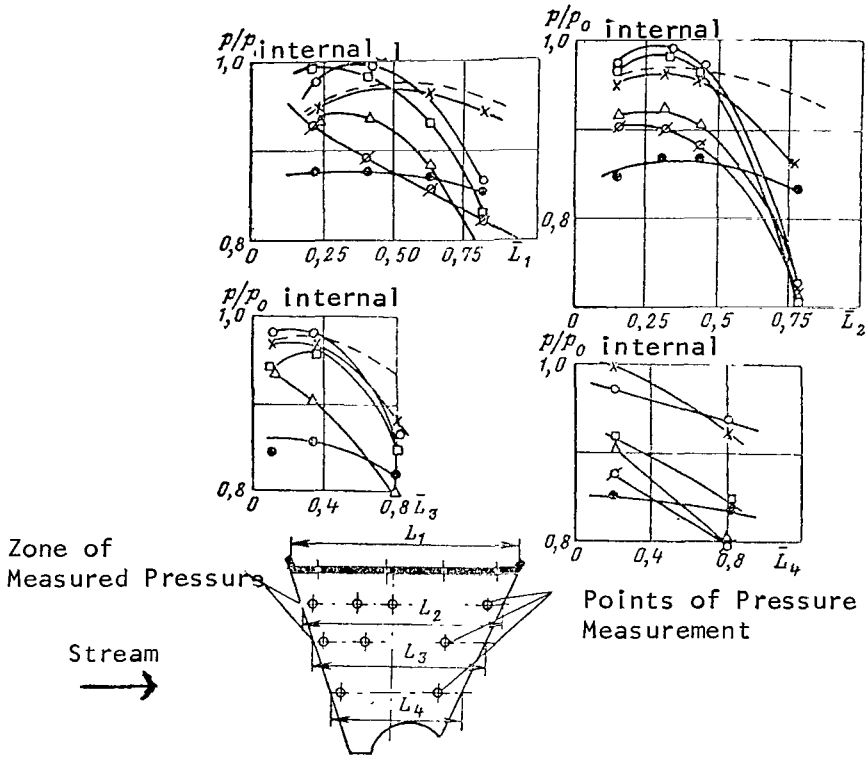

Figure 4.43. Curves of Pressure Distribution Along Shutter of the Reverser Shown in Figure 4.40; ●, $\phi = 0°$; Direct Thrust Regime; ⌀, $\phi = 10°$; Δ, $\phi = 20°$; □, $\phi = 30°$; 0, $\phi = 40°$; ×, $\phi = 50°$; Reverse Regime; -----, Capped Jet Nozzle.

With one-sided discharge and when $\bar{F}_4 = 0.05$, a reverse coefficient $\bar{R}_{rev} = 0.51$ and a relative vertical component of thrust $\bar{R}_{ver} = 0.41$ (Figure 4.45) were attained, respectively. For $\bar{F}_4 = 0.17$, $\bar{R}_{rev}$ was 0.42 and $\bar{R}_{ver} = 0.32$. The reverse coefficient can be determined from the resulting curve when there is a permissible value of the relative vertical thrust component.

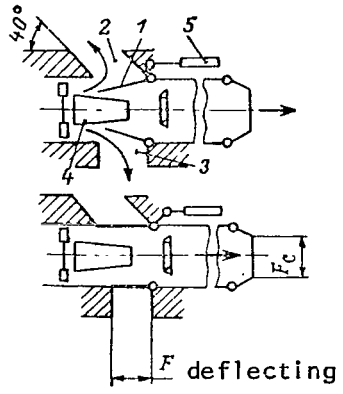

Figure 4.44. Reverser with Nonsymmetrical Discharge: 1, Shutters; 2, Reverse Connecting Pipe; 3, Deflecting Connecting Pipe; 4, Cowling; 5, Hydrocylinder.

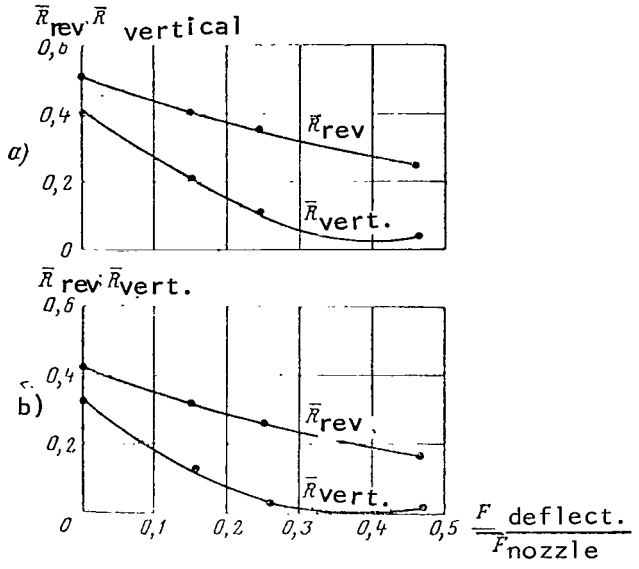

Figure 4.45. $\bar{R}_{rev}$ and $\bar{R}_{ver}$ as Functions of the Relative Area of the Connecting Pipe Deflecting the Stream Downward (F_{defl}/F_{nozzle}) for a Reverser with Nonsymmetrical Discharge When $\pi^*_{nozzle} = 2.2$; a, $\bar{F}_4 = 0.05$; b, $\bar{F}_4 = 0.17$.

Reversers Located Aft of the Jet Nozzle Exit Area

Reverser with cylindrical shutters

When the reverser is in the working position, the shutters 1 (Figure 4.46) direct the stream to the opposite side, producing negative thrust. With the reverser cut-out, the shutters are rotated on pins 2, fixed in the horizontal position, are extended beyond the limits of the nozzle 3, and do not block direct flow exit.

This scheme has been considered in detail in §1 of this Chapter. In this section we will present data for a model differing from the above-described in a number of parts, in particular, by the presence of bypass in the straight-line direction. The change in basic data of the reverser is shown in Figure 4.47 as a function of the angle ϕ of shutter rotation. The angle at which the thrust is equal to zero is approximately 28°. When the angle of shutter rotation is changed, the relative gas consumption remains constant ($\bar{G}_{rev} = 1.0$), /134

since the minimum through section of the gas duct is the exit section of the

jet nozzle. This property of reversers located aft of the exit section of the jet nozzle is their advantage compared with reversers located forward of it in which the exit cross-section of the engine is varied with change in the angle by which the throttling elements are rotated.

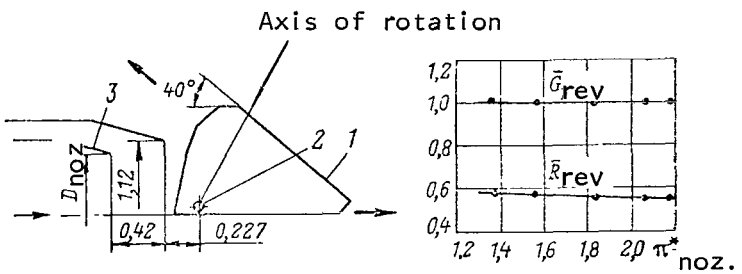

Figure 4.46. Reverser with Cylindrical Shutters and Its Experimental Characteristics when F_{slit}/F_{nozzle} = 0.05: 1, Cylindrical Flap; 2, Axis of Shutter Rotation; 3, Jet Nozzle.

Reverser with shutters constituting part of the engine nacelle surface

The design of this reverser (Figure 4.48) is characterized by the fact that its shutters 1 constitute part of the engine nacelle surface 2 and have tilting flaps 3, which provide the required angle of reverse stream exit. The relatively high reverse coefficient $\bar{R}_{rev}$ = 0.74 is obtained owing to the fact that the stream of gases exits at a relatively small stream exit angle. This scheme has been considered in more detail in §1 of this chapter.

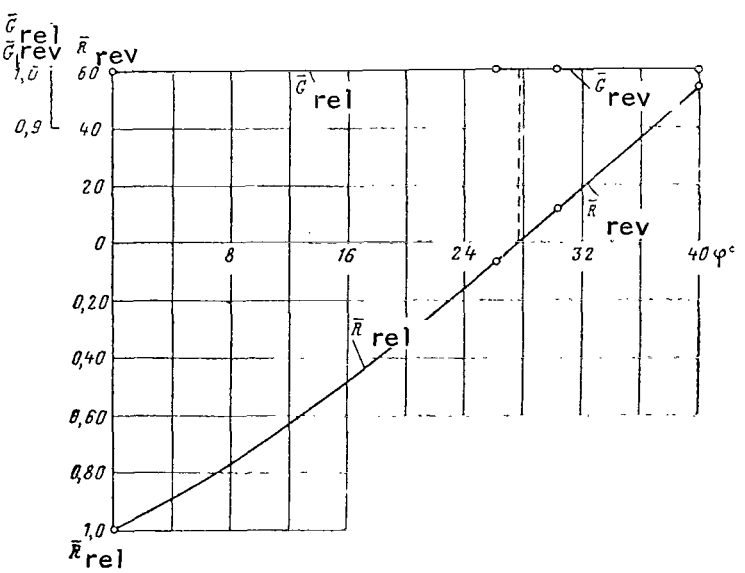

/135

Figure 4.47. $\bar{R}_{rel}$, $\bar{G}_{rel}$, $\bar{R}_{rev}$, $\bar{G}_{rev}$ as Functions of the Angle of Shutter Rotation (π^*_{nozzle} = 2.2).

Reverser with deflecting screens and external cylindrical shutters

In the working position of the reverser (4.49) shutters 1 are located aft of the jet nozzle 2 and direct stream to the deflecting screens 3 at a subtended angle of 120°. With the reverser not cut-in, the shutters tilting on pins are fixed horizontally over the screens and together with them are extended beyond the limits of the jet nozzle. The reverse coefficient attained is 0.4.

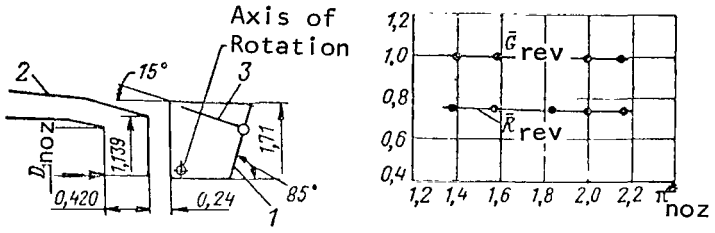

Figure 4.48. Reverser with Shutters Comprising Part of the Engine Nacelle Surface, and Its Experimental Characteristics: 1, Shutters; 2, Engine Nacelle; 3, Tilting Flaps.

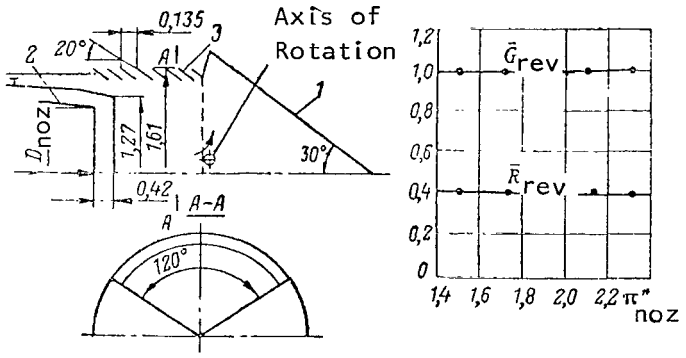

Figure 4.49. Reverser with Deflecting Screens and External Cylindrical Shutters and Its Experimental Characteristics: 1, Shutters; 2, Jet Nozzle; 3, Screen.

Reverser with annular deflecting screen and internal cylindrical shutters /137

In thrust reversal, shutters 1 (Figure 4.50) located aft of the jet nozzle 2 direct the flow to the annular screen 3. With the reverser not cut-in, the shutters are fixed in the horizontal position and do not block the direct exit of the stream. The screen connected to the shutters occupies a position in which it does not have an effect on the jet nozzle parameters. The reverse coefficient achieved is 0.51.

§4. Reverser with Deflecting Screens and Throttling Tilting Vanes

The reverser consists of extensible screens of the active profile type occupying two windows symmetrically over a 120° angle spread and two stream throttling tilting vanes both located in the jet pipe of the engine (Figure 4.51). The vanes are made in the form of symmetrical profiles with relative thickness 10%. In the direct thrust regime the vanes are located along the stream. Experimental studies have shown that minimum thrust losses in the

nozzle are obtained for the case when the trailing edges of the vanes are so aligned that between them a slightly constricted channel is formed ($\alpha = 4°$). Thrust losses here amount to 4-4.5% of the thrust of the ideal nozzle, that is, the nozzle without total pressure losses. When the reverser is cut-in, the vanes are deflected and direct the gas stream toward the screens. In this case the critical section for the nozzle are those running across the trailing edges /138 of the vanes and the beginning of the deflecting screens.

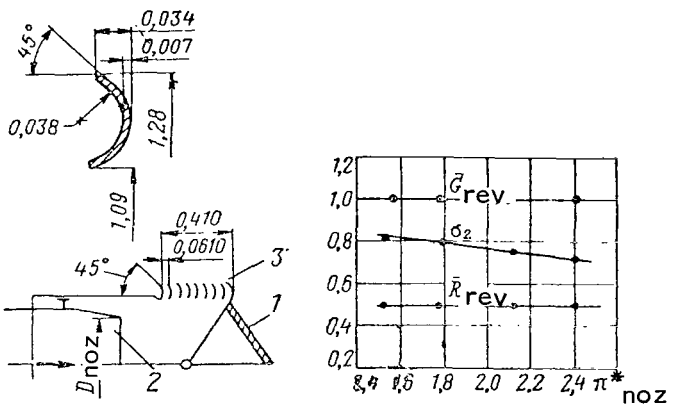

Figure 4.50. Reverser with Annular Deflecting Screen and Internal Cylindrical Shutters and Its Experimental Characteristics: 1, Shutters; 2, Jet Nozzle; 3, Screen.

The reverse coefficient and the consumption coefficient as functions of the extent of pressure reduction for different angles of throttling vane tilting and for fully extended deflecting screens are shown in Figure 4.52. For small angles of the throttling vanes $\alpha < 20°$, the thrust remains positive, but the air consumption is increased by 20-30%.

In order that the consumption of air through the engine remain unchanged, it is necessary that the extention of screens into the working position be /139 coordinated with vane tilting. In the model tested the consumption coefficient $\bar{G}_{rev} = 1.0$ was attained when the vanes were rotated by an angle of 40-42°. An increase in the chord of the tilting vanes led to a reduction in the tilting angle at which the consumption coefficient $\bar{G}_{rev} = 1.0$.

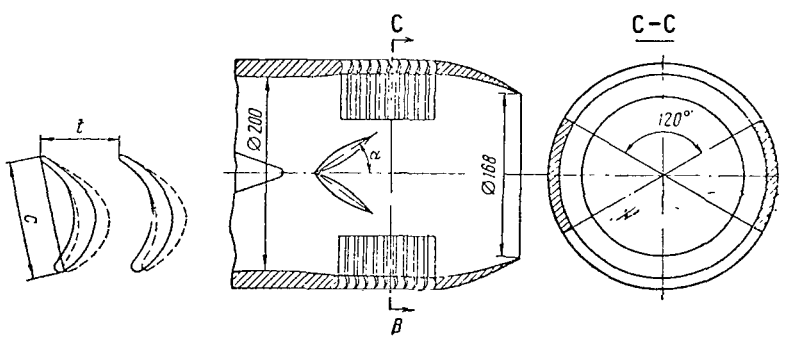

Figure 4.51. Scheme of Experimental Model of a Reverser with Deflecting Screens and Throttling Vanes.

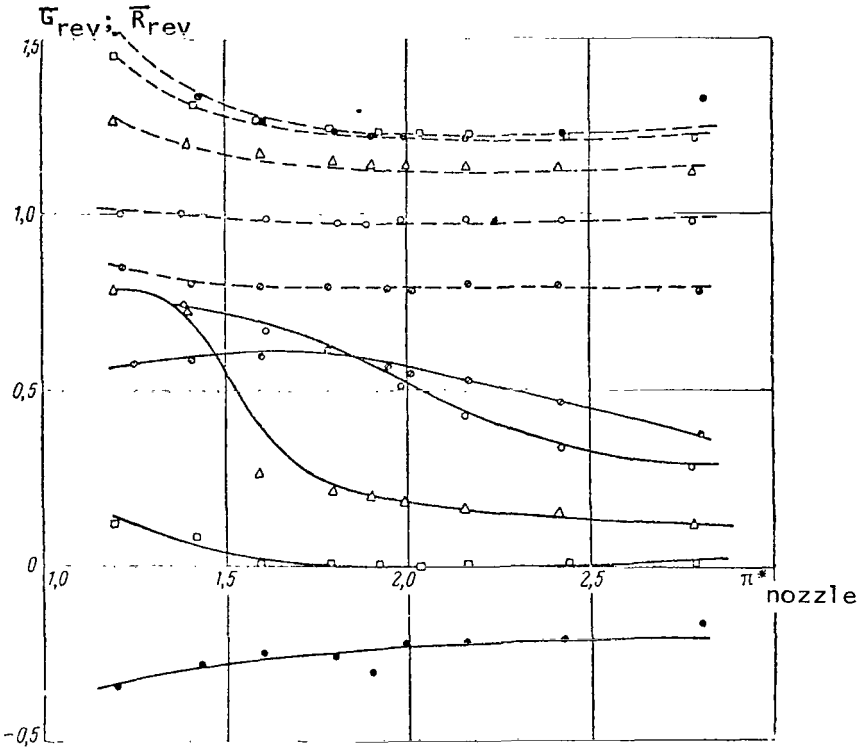

Figure 4.52. Reverse Coefficient and Consumption Coefficient as Functions of the Extent of Pressure Reduction for Different Angles of Rotation α of the Throttling Vanes, $\beta_{screen} = 36°$. The Solid Lines Correspond to a Reverse Coefficient $\overline{R}_{rev}$, and the Dashed Lines Correspond to the Consumption Coefficient $\overline{G}_{rev}$: ● — α = 10°; □ — α = 20°; △ — α = 30°; ○ — α = 40°; ⊘ — α = 50°

The effect of deflecting screen length on reverse coefficient with consumption coefficient remaining unchanged $\overline{G}_{rev} = 1.0$ and for different degrees of pressure reduction is shown in Figure 4.53. When $\pi^*_{nozzle} \leq 1.6$, an increase in screen length above a certain value still does not bring about a rise in reverse coefficient. This evidences that part of the screen channels lie in the zone of separation induced aft of the throttling vanes, and these channels are not operative. As the extent of pressure reduction becomes greater, the flow rate at the inlet to the screens rise, the screen resistance increases, the stream within the jet nozzle begins to be partially deflected toward the side of the nozzle axis, filling the entire intervane channels of the screen. With further increase in π^*_{nozzle} deflection of the stream leads to a situation in which an ever increasing fraction of consumption begins to

escape not through the deflecting screens, but through the jet nozzle. Therefore, the reverse coefficient is reduced with an increase in the extent of pressure reduction.

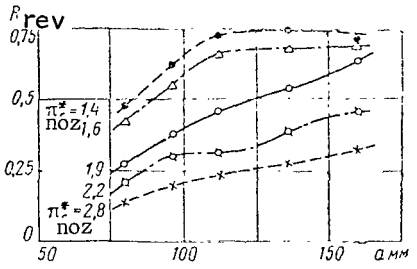

Figure 4.53. Reverse Coefficient as Function of Screen Length for Different Degrees of Pressure Reduction and for the Consumption Coefficient $\bar{G}_{rev} = 1.0$.

Figure 4.54 compares the values of reverse coefficients obtained for different deflecting screens. These screens differed in the shape of the profile and in the design angles β_{screen} of the screens, equal to 36° and 30°. The density of the screens differed but slightly and amounted to c/t = 1.5 and 1.54, respectively. When screens with large design angle were used with the same consumption coefficient, appreciably greater values of the reverse coefficient were obtained. This was accounted for by the fact that the ratio between consumption through the screens and the nozzle when the screens were used differs. Large consumption through the screens with simultaneous reduction in gas passage through the nozzle provides, when $\beta_{screen} = 36°$, a larger reverse coefficient than when $\beta_{screen} = 30°$, inspite of an increase in the angle of inclination of the reverse stream to the engine axis in the first case.

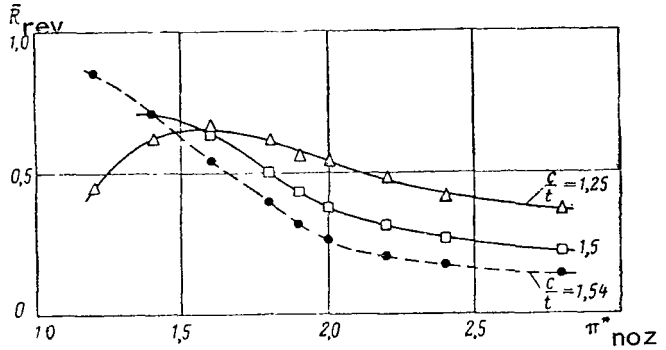

Figure 4.54. Reverse Coefficient as a Function of Extent of Pressure Reduction for Different Screen Densities c/t and for the Consumption Coefficient $\bar{G}_{rev} = 1.0$. The Solid Lines correspond to Screens with a Design Angle $\beta_{screen} = 36°$, and the Dashed Lines, $\beta_{screen} = 30°$.

The effect of screen density on the reverse coefficient for screens with design exit angle $\beta_{screen} = 36°$ is shown in Figure 4.54. A 20% reduction in screen density with screen length unchanged led to an appreciable rise in the reverse coefficient when $\pi^*_{nozzle} > 1.6$. Similar results are obtained also for a screen with a design angle $\beta_{screen} = 30°$. The investigation showed that for this scheme of reverser the density of the deflecting screens must be selected for

/140

the chosen engine performance regime, since the effect of the c/t on reverse coefficient varies with change in the extent of pressure reduction.

When $\pi^*_{nozzle} = 2.0$, this scheme of the reverser can provide a reverse coefficient within the limits of 0.4-0.5.

§5. Development of a Reverser Based on Experimental Test Data

We will illustrate a method of calculation earlier presented in §1 of Chapter II by the example of using a reverser with connecting pipes and throttling shutters.

The reverser (Figure 4.55) consists of four connecting pipes covered in the nonworking position with tilting shutters. When the reverser is cut-in, the shutters throttle the gas duct of the engine and direct the flow to the connecting pipes. The connecting pipes consist of contracted channels with an /142 area ratio of about 1.7.

In the calculation of the original variant the following data were adopted: reverse coefficient--0.3, extent of pressure reduction--2.01, ratio of consumption through connecting pipes in terms of over-all consumption--k = = 0. 68. The minimum diameter D of the ends of the throttling shutters (for the model) was 58 mm.

Tests of the original variant (model No. 1) revealed that the reverser does not provide either the desired reverse coefficient nor the consumption coefficient equal to unity. When the shutters are in the design position, the reverse coefficient is about 0.2 for a consumption coefficient equal to approximately 0.9. When there is complete consumption through the model (D = 83 mm) no negative thrust is produced, since even at D $\approx$ 75 mm the thrust is zero. Additional throttling of the gas duct when the shutters are in the maximum position ($D_{max} \approx$ 51 mm) cannot be viewed as a measure that ensures higher reverse coefficient. A test was made in which the effect of direct thrust was eliminated. To do this, the nozzle was covered with an end cap. Reduction of direct thrust down to zero naturally will lead to a rise in the reverse coefficient, however, the consumption coefficient is made still lower: $\overline{R}_{rev} = 0.43$, $\overline{G}_{rev} = 0.625$, $\mu_2 = 0.810$ ($\pi^*_{nozzle} = 2.01$). Here μ_2 = consumption coefficient through the connecting pipes:

$$\mu_2 = \frac{G_2}{G_{ideal,2}}, \quad G_{ideal,2} = 0.3965 \frac{p_{0,inlet}}{\sqrt{T_0}} q(\lambda_{ideal,2}) F_2.$$

Results of measuring the stream exit angle by using a dummy target goniometer at one of the connecting pipes in several cross-sections are given in detail below (§2, Chapter V). We note only that the stream exit angle averaged

over the entire connecting pipe cross-section proved to be about 1° greater than the angle of vane inclination at the exit. When results of measuring consumption through the connecting pipes with nozzle capped were used, it was found possible to estimate the total pressure recovery coefficient in the connecting pipes. By knowing the calculated extent of pressure reduction and assuming that the static pressure at the exit from the connecting pipes is equal to the static ambient pressure, we get for $\pi^*_{nozzle} = 2.01\ \sigma_2 = 0.805$[1].

Characteristics of the nozzle when throttling shutters were installed in it were obtained via weighing tests with connecting pipes capped (Figure 4.56). /143
We can see that the coefficient of total pressure recovery of the valve is the smaller, the more the shutters throttle the gas duct.

Analysis of the results showed that the total of consumption through the connecting pipes and the nozzle determined in separate tests did not equal the consumption through the model. This shows that the characteristics obtained in these separate tests must be viewed as approximate. Precise characteristics of the deflecting connecting pipes and the nozzle in which throttling shutters were installed could be determined if it were possible to simultaneously, but separately weigh the deflecting connecting pipes and the nozzle. To do this /144
would require complicating the weighing section of the stand and the experimental models. Nonetheless, with such approximate data available to us, it appears possible to carry out preliminary calculations of the reverser (Figure 4.57).

The coefficient of total pressure recovery in the connecting pipes must in general, depend on the position occupied by the shutters. It is obvious that when the shutters are used to block out the inlet section of the connecting pipes the values of σ_2 must be reduced. It can be assumed that in some range of change in shutter position around the limiting position the value of σ_2 will not vary appreciably. In the calculation σ_2 was taken as equal to 0.80. The intersection of the lines of the required and the available values of k determined the sought-for calculated diameters of the shutter end D_{calc} = =56.6 mm and the fraction of the over-all consumption that must be directed to the deflecting device, $k_{screen} = 0.722$.

The values of σ_2 are easily calculated from the ratio $\sigma_2 q(\lambda_2) = \mu_2 q(\lambda_{ideal\ 2})$, obtained from the expression for consumption expressed in terms of σ_2 and $q(\lambda_2)$. We noted that the values of σ_2 and μ_2 when $\pi^*_{nozzle} \approx 2.0$ in the range $\mu_2 = 0.8$-1.0 are numerically almost equal. We can also obtain the values of σ_2 from the function y (cf. Formula (3.2) on p.60.).

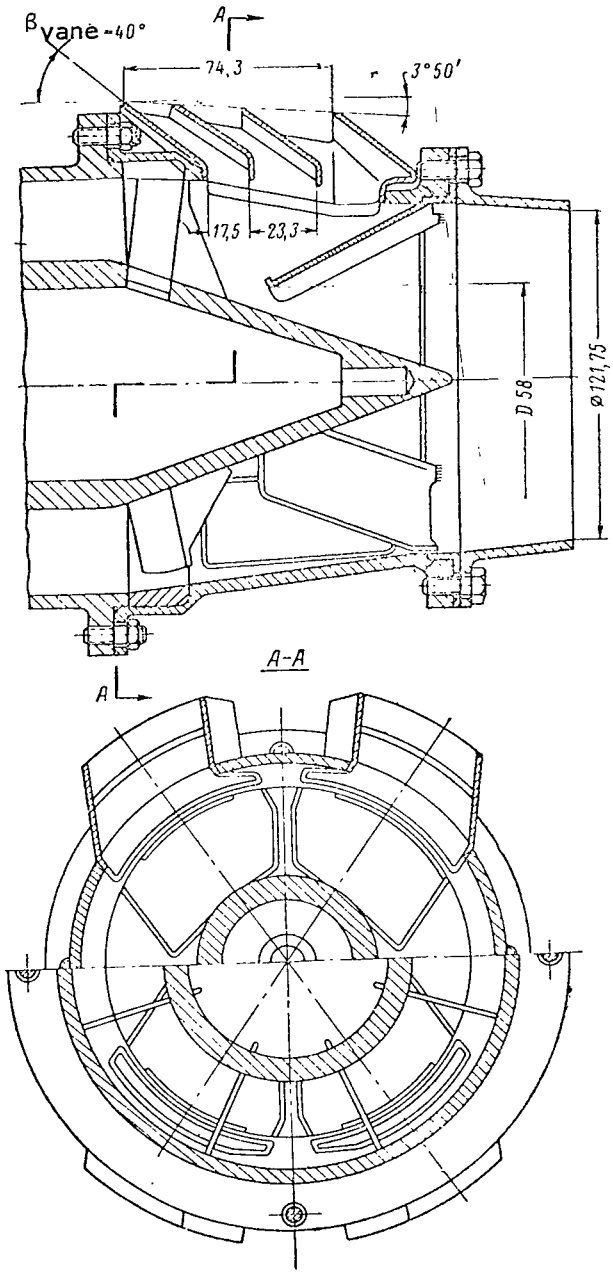

Figure 4.55. Sketch of Original Variant of the Reverser (Model 1).

Figure 4.57 also presents the ordinates D_{req} of the maximum shutter position when they rest on each other and D_0 obtained from intersection of the lines of the available and the required k values when $\overline{R}_{rev} = 0$.

We can differentiate four regions: I. $D < D_{req}$; II. $D_{req} < D < D_{available}$; III. $D_{req} < D < D_0$; IV. $D_0 < D$.

In region I it is impossible /145 to build the reverser because of design considerations. In region II, when $\sigma_2 = 0.8$ higher reverse coefficient values can be obtained since a larger consumption can pass through the connecting pipes than is required to obtain $\overline{R}_{rev} = 0.30$. In region III the desired reverse coefficient cannot be provided, since the required consumption is greater than the available, however, in this region of shutter positions a reverser can be built with a reverse coefficient less than 0.30. To the right of the ordinate D_0 (region IV) the reverser cannot be built. When $D > D_0$, positive thrust is in fact produced.

As calculations showed, the highest reverse coefficient for maximum shutter positioning and when $\sigma_2 = 1$ cannot exceed values of about 0.5. It is clear from the graph that when the coefficient of total pressure recovery in the connecting pipes is reduced, the desired reverse coefficient is ensured with lower consumption

through the nozzle. Into section of the ordinate D_{max} with the curve of the available value k determines the line of minimum σ_2 at which it is still possible to build a reverser with $\bar{R}_{rev} = 0.30$. In this scheme, for the indicated reverse coefficient σ_2 must not be less than 0.67. Thus, the range A of possible variation in diameter D for a given reverse coefficient, shown in Figure 4.57, constitutes a fairly narrow region.

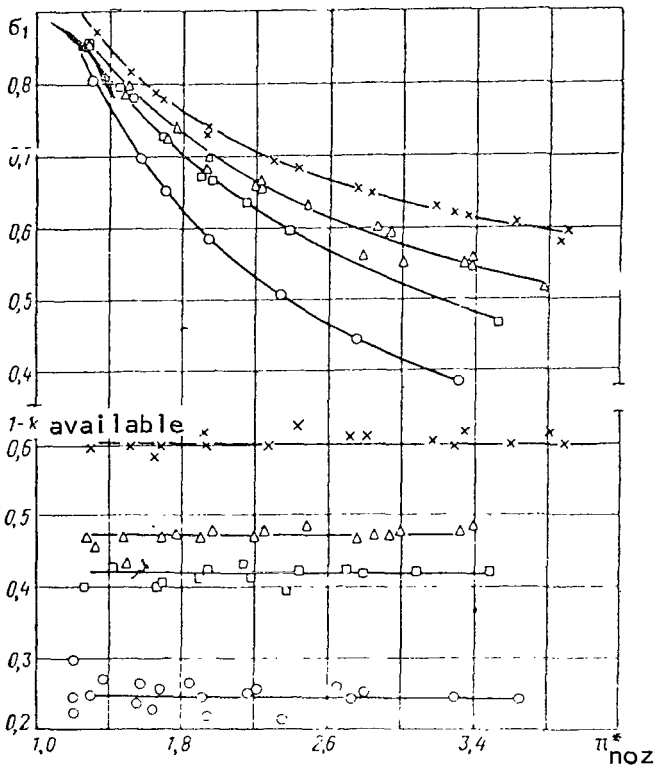

Figure 4.56. Total Pressure Recovery E Coefficient in the Nozzle of Model No. 1 as a Function of Extent of Pressure Reduction, When Throttling Shutters were Installed in the Nozzle and When the Coefficient $1-k_{available}$ was as Follows:

○ —D=51,2 мм; □ —D=66 мм; △ —D=72,2 мм; × —D=82,2 мм

Let us determine the exit area of the connecting pipes

$$F_2 = \frac{G_2'}{0,3965\sigma_2 q(\lambda_2)}.$$

Here $G_2' = (G_2/p_{0,inlet})\sqrt{T_0}$ -- reduced consumption through the deflecting connecting pipes

$G_2' = k_{screen} G_{nozzle} = k_{screen} \frac{G_{nozzle}}{p_{0,inlet}} \sqrt{T_0}$,

The reduced consumption through the nozzle

$G'_{nozzle} = 0.3965 \mu_{nozzle} q(\lambda_{ideal\ velocity}) F_{nozzle}$,

where μ_{nozzle} = coefficient of consumption through the nozzle determined when the latter was tested ($\mu_{nozzle} = 0.956$ when $\pi^*_{nozzle} = 2.01$); F_{nozzle} = critical area of the nozzle in the model, $F_{nozzle} = 116.5$ cm^2.

Finally, we get

$$F_2 = \frac{k_{screen}\mu_{nozzle}F_{nozzle}}{\sigma_2 q(\lambda)_2} = \frac{0,722 \cdot 0,956 \cdot 116,5}{0,80 \cdot 0,981} = 102,6\ см^2;\ \frac{F_2}{F_2^0} = \frac{102,6}{87,5} = 1,17.$$

Here F_2^0 = 87.5 cm^2 --the exit area of the connecting pipes in the original variant of the model. Thus, based on an approximate calculation, to attain the required reverse coefficient the exit area of the connecting pipes must be increased by 1.17 times. The resulting value of the exit area of the connecting pipes is less than the inlet cross-sectional area. With the existing inlet preserved and, consequently, with unchanged status of existing throttling shutters, it is still possible to build a constricted channel with an area ratio of about 1.3 (Model No. 2). /146

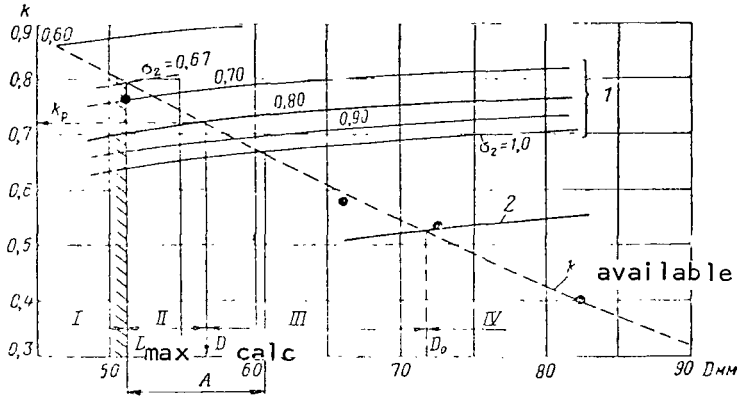

Figure 4.57. Calculated-Theoretical Study of Reverser Incorporating Connecting Pipes and Throttling Shutters (π^*_{nozzle} = 2.01): •, Experimental Points $k_{available}$; 1, $k_{required}$ for $\bar{R}_{rev}$ = 0.30; 2, $k_{required}$ for $\bar{R}_{rev}$ = 0 When σ_2 = = 0.8; D_{max} = Diameter of Ends of Shutters Corresponding to Their Limiting Position; D_{calc} = Calculated Diameter of Shutter End; D_0 = Diameter of Ends of Shutters Corresponding to Zero Thrust for σ_2 = 0.8; A = Range of Possible Shutter Positions.

The meridional cross-section of the connecting pipes was kept as before. An increase in the area was attained by using connecting pipes with walls turned parallel to their axis and with some displacement in the outer walls of the upper and lower connecting pipes in order to increase the through-passage cross-section. The throttling device remains unchanged. With π^*_{nozzle} = 2.01 and the calculated shutter position, a reverse coefficient was attained that was close to the required values, however the consumption coefficient was not equal to unity ($\bar{R}_{rev}$ = 0.28, $\bar{G}_{rev}$ = 0.91). This indicates that the effective throughput area of the connecting pipes proved to be inadequate.

Thus, the method of calculation based on an independent determination of the characteristics of the deflecting connecting pipes and the nozzle incorporating throttling shutters gives only a first approximation. Application of this method can be useful in the initial orientation calculation of a reverser.

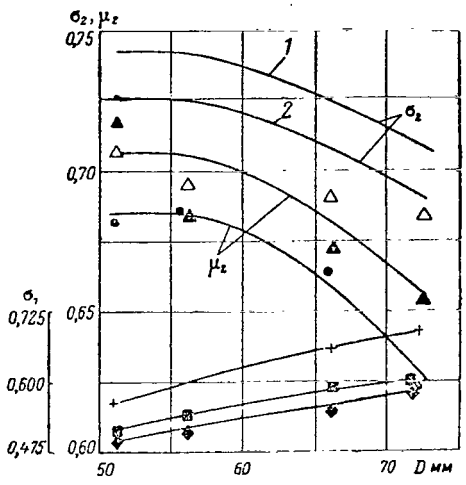

Figure 4.58. Consumption Coefficient Through Connecting Pipes, Coefficient of Total Pressure Recovery Varying, and Coefficient of Total Pressure Recovery in the Nozzle When Throttling Shutters Were Installed in it, as Functions of the Minimum Diameter of the Shutter End (π^*_{nozzle} - 2.01). Model No. 1:Δ.First Test; ▲, Second Test; ●, Model No. 2 1, Model No. 1: 2, Model No. 2; Results of Calculation of σ_1: +, Tests of Nozzle With Connecting Pipes Capped; ■, Based on Tests Made of Model No. 1; ◆, Based on Tests Made of Model No. 2.

To obtain refined characteristics of the reversereelements, a special test was held. On the nozzle used in Models No. 1 and 2 a pipe about 7 calibers in length was installed. Four grids were placed in the pipe in order to provide additional equalizing of the flow. Placement of the pipe made it possible to equalize the substantially nonuniform velocity flow aft of the throttling shutters. By means of combs the total pressure field at the exit from the pipe were measured in two mutually perpendicular directions. At the exit from the pipe measurement was made also of the static pressure through the wall drainage. From the results of these measurements the consumption G_1 was determined. /147

Based on the consumption through the connecting pipes $G_2 = G_{rev} - G_1$ the values of the consumption coefficient μ_2 were calculated, and from them the coefficients of total pressure recovery in the deflecting devices σ_2 (Figure 4.58). Examination showed that the values of μ_2 (σ_2) proved to be less than the values determined from the measured consumption through the connecting pipes with the nozzle capped. In addition, with increasing closure of the shutters the coefficient of total pressure recovery is markedly decreased.

Using the resulting functions of σ_2, and also the data on the consumption through the deflecting device and the nozzle, the values of the coefficient of total pressure recovery in the nozzle when throttling elements were installed therein were determined. The calculations of σ_1 were made according to the formula obtained from formula (2.10) on text page 46. Refined values of σ_1 were lower than those on which the calculation was made in designing Model No. 2. The substantial decrease in the coefficient of total pressure recovery in the nozzle σ_1 compared with the initial calculated values accounted for by

the fact that with lower σ_2 in Model No. 2 a reverse coefficient close to the required was nonetheless still obtained.

The areas of the throughput cross-sections of the connecting pipes in Model No. 3 were calculated based on the method described earlier, and the shutter position at which a reverse coefficient $\bar{R}_{rev} = 0.30$ was attained was determined.

Original Data	D мм	F_2 см²
For Model No. 1	55.5	109.5
For Model No. 2	59	112.5

In designing a larger value of F_2 was adopted.

A sketch of the housing of Model No. 3 with connecting pipes is shown in Figure 4.59. To obtain the required throughput cross-sectional area the areas at the inlet to the connecting pipes were considerably enlarged. The throttling shutters were retained unchanged.

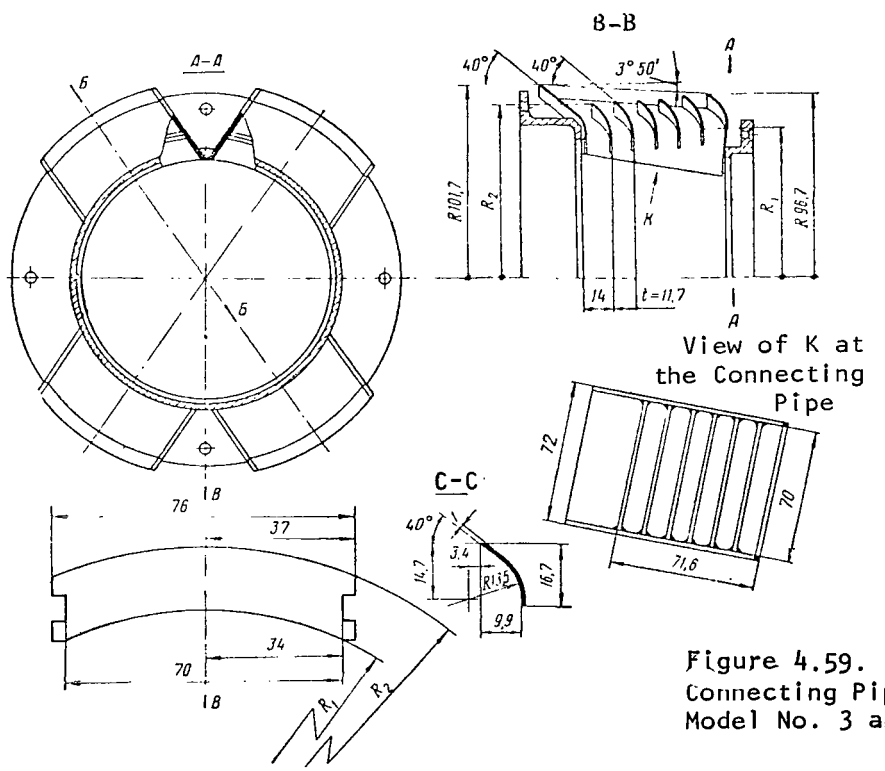

Figure 4.59. Housing with Connecting Pipes of Model No. 3 and Sketch of Vanes.

The resulting reverse coefficient is close to the calculated value, but the consumption coefficient differs from unity by approximately 2% (Figure 4.60). Taking account of the precision of measurement in thrust arrangement and consumption, these values can be recorded as satisfactory. /148

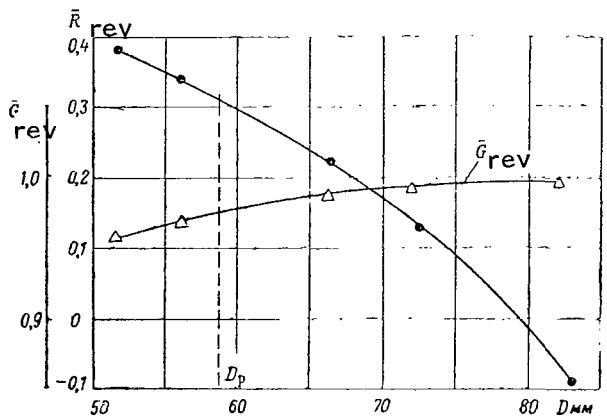

Figure 4.60. Reverse Coefficient and Consumption Coefficient as Functions of the Minimum Diameter of Shutter Ends for a Calculated Extent of Pressure Reduction (Model No. 3).

Thus, the method set forth in §1 of Chapter II can be used in analyzing reversers and in making practical calculations. Generalized data given in §6 of this chapter can also be employed for this purpose.

These studies also showed that when building a reverser of a given scheme the required reverse coefficient cannot be ensured with the inlet areas into the connecting pipes remaining unchanged, that is, the shutter areas. Enlargement /149 of the shutter surfaces is expressed in a redistribution of consumption between deflecting connecting pipes and the jet nozzle and in changed coefficient of total pressure recovery in the nozzle and, naturally, entails reexamination of the design developed.

§6. Generalized Data on Reversers

Data on the coefficient of total pressure recovery in the deflecting elements of reversers obtained as a result of direct measurement of total pressure are not numerous owing to the laboriousness of making such measurements.

It is easy to compare reversers in which the entire consumption was used to build up negative thrust. In this case direct-line thrust produced by bypassage of some of the gas into the jet nozzle does not show up.

Figure 4.61 shows plots of calculated curves of the reverse coefficient as functions of the stream angle at the exit from the reverser for different coefficients of total pressure recovery in the deflecting elements. Calculation was made for $\pi^*_{\text{nozzle}} = 2.0$ based on formula (2.8) in text page 46 with $\bar{R}_{\text{specific nozzle thrust}} = 0.99$. This is a π^*_{nozzle} value that is close to the calculated for turbojet engines at velocities corresponding to landing of an aircraft. The figure gives plots of experimental data of the authors and /150

data available from the literature for reversers located forward of the exit area of the jet nozzle and aft of it.

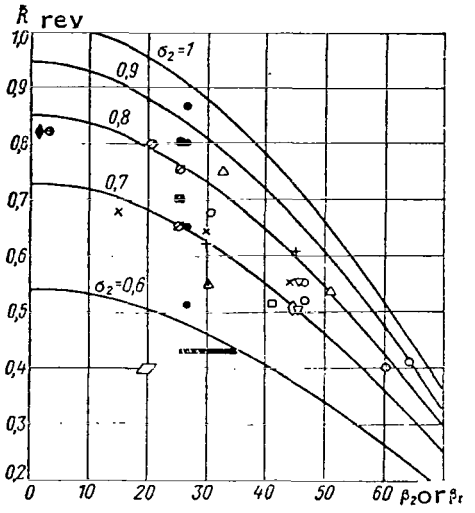

Figure 4.61. Reverse Coefficient as a Function of the Effective Angle of Stream Exit from the Reverser or as a Function of the Design Angle of Shutter or Flap Inclination for Different Values of the Coefficient of Total Pressure Recovery Therein (π^*_{nozzle} = = 2.0). The Reversers Positioned Forward of the Exit Area of the Jet Nozzle are Explained as Follows:

Δ, With deflecting screens made of profiled vanes and throttling diaphragm (cf. Figure 2.6); o, Nozzles incorporating a central body, Scheme I, Variant 1, with screens made of leafwise profiles (cf. Figure 4.12); •, as above, Scheme I, Variant 2 with screens made of profiled vanes for $\bar{F}_2 \approx$ ≈ 1; ϕ, Scheme A with screens made of leafwise profiles (cf. Figure 4.16) based on data of the report [37]; ■, the same Scheme, incorporating screens made of profiled vanes based on the same data; ▱, incorporating screens and external cylindrical shutters (cf. Figure 4.49); ◻, with screens and internal cylindrical shutters (cf. Figure 4.50); ∇, Scheme E incorporating screens made of leafwise profiles (cf. Figure 4.16); based on data full-scale tests [25]; ⊕, as above, based on data of full-scale tests [22, 44]. The reversers positioned aft of the exit area of the jet nozzle are explained as follows: +, incorporating cylindrical shutters (cf. Figure 4.1); χ, with conical shutters and tilted flaps (cf. Figure 4.9). The data in the report [37]: ⊕, hemispherical reverser; ♦, semicylindrical reverser; ⩚, with cylindrical internal throttling and external deflecting shutters; ▬ Scheme IV (cf. Figure 1.8) based on data of full-scale tests [32] [32]; , scheme II, but with cylindrical shutters and deflecting flaps (cf. Figure 1.8) based on data of full-scale tests [20].

For models of reversers incorporating deflecting screens positioned forward of the exit area of the jet nozzle, the $\bar{R}_{rev}$ values relate to the actual stream exit angles β_2 obtained with account taken of the correction for the angle $\Delta\beta$, by which the angle β_2 differs from the design angle β_{vane} of the screen (§3, Chapter V).

The results of full-scale tests of Scheme E (cf. Figure 4.16) of a reverser incorporating deflecting screens and cylindrical throttling shutters based on the data of the reports [25, 22, 44] refer to $\beta_2 = 45°$. In stand tests of engines, aft of the deflecting screens with $\beta_{vane} = 45°$ were installed exit ducts (cf. Figure 1.12, text page 34), and there were no wing (or engine nacelle) elements. Therefore, as noted by the author of the study [25], flowing of the stream was not observed, and consequently, no deviation of the stream toward the side of lower exit angles cropped up. The correction for the angle $\Delta\beta$ was also not introduced for results of full-scale tests in [22, 44], since the design was developed in such a way as to preclude angling of the reverse stream toward the side of the engine nacelle (§3, Chapter VI). /151

Data of tests made of models and full-scale reversers incorporating shutters positioned aft of the exit cross-section of the jet nozzle refer to design angles β_{gas} of the shutter or flap inclination. For reversers incorporating cylindrical and conical shutters, the results of their tests are presented in §1, and the maximum values of $\overline{R}_{rev}$ were plotted, respectively, from data in Figure 4.7 and 4.11. Data of the report [37] for hemispherical and cylindrical reversers located aft of the exit area of the jet nozzle was plotted on these figures. The first type of reverser consists of a hemisphere, the second of a semi-cylinder with walls perpendicular to the cylinder axis. The data for these models are given for optimal ratios of geometric parameters at which the maximum reverse coefficients were obtained. These reverser schemes are not devoid of practical interest, as a limiting case when the exit edges of the deflecting elements are parallel to the engine axis. The $\overline{R}_{rev}$ values for these models relate provisionally to $\beta_{gas} \approx 0$. The data of full-scale tests of the reverser of Scheme IV (Figure 1.8, text page 29) also provisionally refers to a certain probable range of angles β_{gas}, since the report [32], does not contain any concrete information about the parameters of the deflecting elements of this reverser.

Let us look at experimental data for models of reversers incorporating a central body (Scheme I, Variant 1) with deflecting screens made of leafwise profiles, with deflecting screens made of profiled vanes and a throttling diaphragm, Scheme A with deflecting screens made of leafwise profiles positioned aft of the turbine, as well as data for reverser models incorporating cylindrical and conical shutters.

We can see in Figure 4.61 a trend toward an increase in coefficient of total pressure recovery in the deflecting elements when the angle of stream exit is increased. The fact of reduction in total pressure losses with decrease in angle of stream rotation is well-known from screen tests. Still, the level of σ_2 varies not very greatly in this case, which evidences that the main fraction of total pressure losses in stream rotation is attributable not to precisely deflecting elements, but to the rotation of the stream forward

of these elements. This is also evident from the data given in Figures 4.32, 4.36, 4.40 and 4.50 on the coefficient of total pressure recovery σ_2 obtained on the basis of measurement of total pressure field at the exit from the deflecting elements of the reversers differing not only in geometric parameters of the deflecting elements, but also in fundamental design features. The values of σ_2 prove to be closely grouped in the range of angles $\beta_{vane} = 30°-50°$. /152

Inspection of the figure shows us that most of the investigated reversers are situated in a not very wide band of σ_2 values.

Approximately speaking, the σ_2 values for the reversers we have studied lie within the limits 0.7-0.8. We must note that the σ_2 values for reversers incorporating deflecting screens that are located forward of the exit cross-sectional area of the jet nozzle and those incorporating shutters positioned aft of the exit nozzle area, given optimal geometric parameters at which high values of the reverse coefficient are attained, prove to be approximately of the same level. In a range of stream exit angles of interest in actual practice, $\beta_2 = 30°-60°$, the lower limit of σ_2 can be adopted for smaller angles of β_2 and the upper for larger. In designing reversers incorporating shutters positioned aft of the exit area of the jet nozzle for design considerations, we do not preclude the possibility of choosing even nonoptimal geometric parameters of the reverser. If we look at the results obtained with reversers of this type that do not exhibit optimal geometric parameters, the values of $\bar{R}_{rev}$ and correspondingly σ_2 values prove to be lower than those examined. In the range of angles $\beta_{gas} \approx 30°-60°$ for reversers incorporating shutters positioned aft of the jet nozzle exit area, we can take $\sigma_2 \approx 0.65$, roughly speaking.

We must note that the generalized data of model tests agreed satisfactorily with individual results of full-scale tests.

How essential rational profiling of the throughput section of the reverser is, is demonstrated by the results of tests made of a scheme incorporating screens and external cylindrical shutters in which a very low reverse coefficient was attained, which is accounted for by the unsuccessful profiling of the deflecting screens. The low level of $\bar{R}_{rev}$ and σ_2 is characteristic also for a reverser incorporating shutters positioned in the ejector. Still, as was emphasized in §1 and 2 of this chapter and as we can plainly see from the figure, rational choice of reverser parameters and, in particular, their deflecting elements will allow us to attain an appreciable rise in σ_2. For reversers incorporating deflecting screens, rational choice of the ratio of deflecting screens sides is, for example, one of the avenues of boosting reverser efficiency.

Owing to the relatively moderate gas dynamic improvement of reversers, compared with other elements of turbojet engines, attaining the reverser coefficient values in the reverse direction that we actually need in practice /153
necessitates deflecting almost all the consumption. Therefore, the data given above on the coefficient σ_2 of total pressure recovery and the data about the stream exit angle (Chapter V) in most cases is sufficient to make approximate calculations when designing reversers.

If there is a need to attain lower $\bar{R}_{rev}$ values, some of the gas can be directed to the nozzle. In this case, as shown in §1 of Chapter II, when we make calculations we have to know the value of the coefficient σ_1 of total pressure recovery in the nozzle when throttling elements have been installed in the gas duct. Some data on σ_1 has been given above (Figures 4.32, 4.58, text pages 104 and 124). Since at present we do not have fuller data on σ_1, an attempt was made to generalize data on the reverse coefficient given the presence of gas bypassing in the straight-line direction.

The limited data available on the effect of gas consumption bypassed into the nozzle on the reverse coefficient are wholly comparable. Some results were given above (Figure 4.8). When we eliminated bypass through the slit between the shutters in the reverser scheme shown in Figure 4.40, the reverse coefficient when $\pi^*_{nozzle} = 1.8$ rose by 8-10% with a 4-5.5% decrease in the consumption coefficient. The report [32] contains an indication that in the reverser built under Scheme IV (Figure 1.8, text page 29) a 1% nonoverlapped area of the ejector insert led to a 2% drop in the negative thrust (evidently for a rated $\bar{R}_{rev}$ value = 0.43 when $\pi^*_{nozzle} \cong 2\text{-}2.5$).

Relying on these materials, curves have been plotted for the function of /154
the tangent of the slope of straight lines (Figure 4.8), that is, the ratio $\Delta\bar{R}_{rev}/\bar{G}_{slit}$ in the function of the angle of throttling shutter inclination. (See Figure 4.62). We can see a trend towards decrease in the $\Delta\bar{R}_{rev}/\bar{G}_{slit}$ with a concommittant increase in the angle β_{gas}, where the effect of bypassing in the straight-line direction on the reverse coefficient is expressed more weakly when the reversers are positioned forward of the nozzle exit area. The numerical difference in $\Delta\bar{R}_{rev}/\bar{G}_{slit}$ is not very great and is commensurable with the error introduced by errors in measuring consumption and thrust on experimental stands.

The data in the figure can be used for estimational calculations when designing reversers.

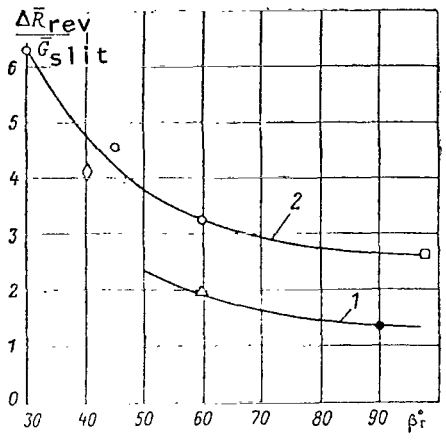

Figure 4.62. $\Delta\overline{R_{rev}}/G_{slit}$ as a Function of the Angle of Throttling Shutter Inclination. $\pi^*_{nozzle} \approx 2.0$; $\overline{R}_{rev} = 0.4$-0.75: 1, Reversers Positioned Forward of the Jet Nozzle Exit Area; Δ, the Scheme Shown in Figure 4.40; ●, Scheme Incorporating Deflecting Screens and Throttling Diaphragm: 2, Reversers Located Aft of the Jet Nozzle Exit Area; o, Reverser Incorporating Cylindrical Shutters (§1); ♦, as Above (§3 of Chapter IV); □, Scheme IV (cf. Figure 1.8) Based on Data in the Report [32].

The sizeable effect of gas bypassing in a straight-line direction compels us to focus the most serious attention on careful partitioning of the gas duct of the engine if we desire to arrive at a high reverse coefficient.

CHAPTER V

STREAM ESCAPE FROM DEFLECTING SCREENS AND CONNECTING PIPES OF REVERSERS /155

§1. Stream Escape from Deflecting Screens

Variation in the stream escape angle in the center cross-section along the length of screen I made up of leafwise profiles ($\beta_{vane} = 35°$) of Scheme I, Variant 1 of a reverser installed in a nozzle incorporating a central body is shown in Figure 5.1. The angles were measured at a distance of about 1 pitch (8 mm) from the exhaust edges of the vanes[1].

The curves presented allow us to note several interesting features. We can anticipate that in streaming over a convex surface of a wall in the front channel there will be flow separation much like what takes place in streaming past the extreme vanes of flat screens in a wind tunnel. However, at low degrees of pressure reduction ($\pi^*_{nozzle} = 1.2\text{-}1.5$) this is not observed. The values of the stream exit angle in the last channel somewhat exceed the design angle of the vane at the exit from the screen β_{vane} or are close to it, and for the greater part of the screen length are less than β_{vane}. Experimental points near the convex surface of the front channel were not plotted owing to the fact that the small stream exit angles were found impossible to measure.

This pattern in the curves is accounted for by the ejector action of the reverse stream, leading to the appearance of rarefaction along the margins of the stream.

As the extent of pressure reduction became greater, the stream exit angle /157
was observed to increase ($\pi^*_{nozzle} = 1.8;\ 2.2$). With an increase in the extent of pressure reduction the escape rate from these screens rose and the rarefaction induced proved to be inadequate to retain the rotation of the stream toward the side of the engine nacelle. This feature is not associated with the action of the oblique cross-section. Owing to large losses in the screen even at $\pi^*_{nozzle} = 2.2$ the escape rate practically speaking does not exceed the supersonic level. The rise in the stream escape angle was not noted in the front channel, to which the action of the induced rarefaction was extended.

---

[1]Measurement of the stream angles as the stream exited from the reversers, the results of which have been set forth in this chapter, were conducted with dummy target goniometers made of capron threads, has well recommended itself in the practice of investigating flat compressor screens.

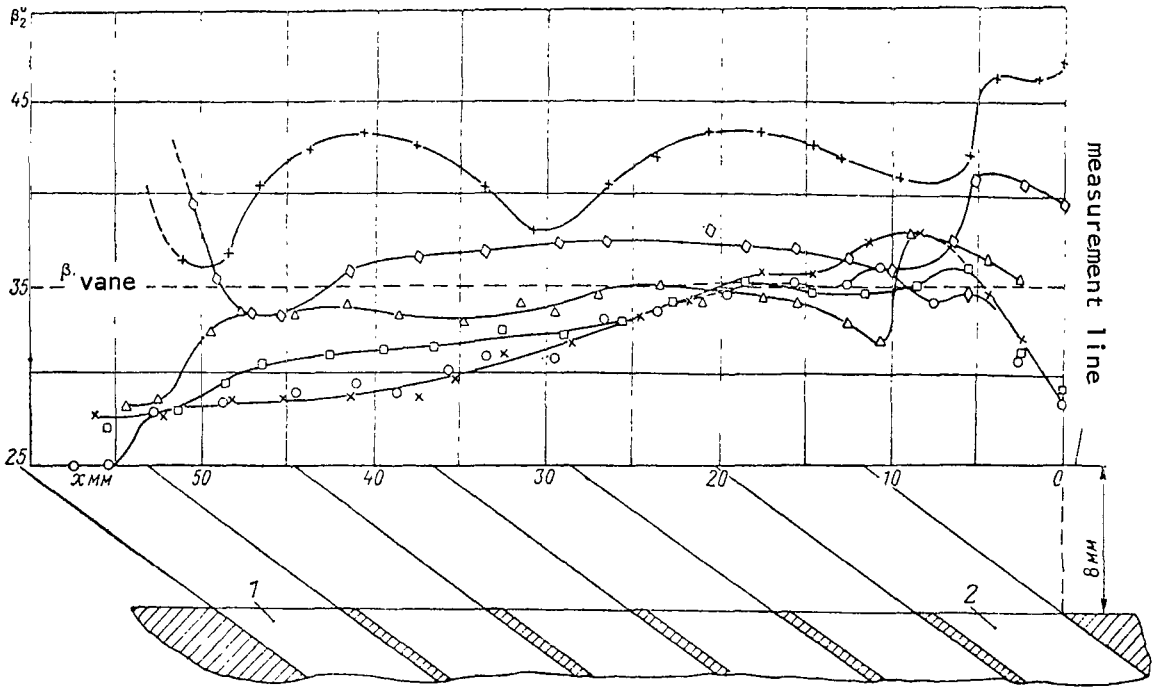

Figure 5.1. Variation in the Stream Exit Angle in the Central Cross-Section Along the Length of Screen I of the Model of a Reverser for a Nozzle Incorporating a Central Body. Scheme I, Variant 1: 1, Front Channel; 2, Last Channel; χ, $\pi^*_{nozzle} \approx 1.2$; o, $\pi^*_{nozzle} \approx 1.5$; □, $\pi^*_{nozzle} \approx 1.8$; Δ, $\pi^*_{nozzle} \approx 2.2$; ♦, $\pi^*_{nozzle} \approx 2.7$; +, $\pi^*_{nozzle} \approx 3.2$.

When there was a substantial rise in the extent of pressure reduction ($\pi^*_{nozzle} \geq 2.7$), along the entire length of the screen the increase in the stream exit angle owing to rotation in the oblique cross-section is evident. In the front channel and along the convex surface of the profile of the second channel stream separation was observed, which shows up also in a higher stream exit angle. In experiments considerable fluctuation and torsion of the goniometer threads occurred in this area, while at the same time this was not observed in the central channels for the given regimes.

Distribution of the difference in static pressure p_2 at the exit from this same screen and ambient static pressure p_H is shown in Figure 5.2. In static pressure measurements the aim of obtaining data that would explain the above-described pattern of change in the stream exit angle along the length of the screen was pursued. Information about the value of the static pressure at the exit from the reverser was also of interest in itself, since it is usually assumed in calculations that the pressure p_2 = pressure p_H. The figure makes clear that when $\pi^*_{nozzle} = 1.3$, over the entire length of the screen the static pressure is practically equal to p_H, while in the front part of the screen rarefaction is observed. The extent of this rarefaction increases with greater reduction of pressure down to $\pi^*_{nozzle} = 1.9$, then varies only slightly. In the central section of the screen the static pressure proves to be greater than the ambient pressure. In the rear of the screen, near the last channel, a rarefaction region is also induced. Averaging showed that the mean value of the difference $p_2 - p_H$ is practically equal to zero, at least as far as $\pi^*_{nozzle} = 2.2$.

Results of measuring the stream exit angle along the length of the annular screen made up of leafwise profiles ($\beta_{vane} = 20°$) of a model of a reverser incorporating throttling jet nozzle and pressure distribution along the engine nacelle are described in Figure 5.3. A decrease in the design angle of the vanes at the exit from this screen leads to a situation in which the ejecting action of the jet stream is manifest up to higher degrees of pressure reduction: the flow pattern for degrees of pressure reduction equal to 1.8-2.5 is /160 similar to that described for the angle $\beta_{vane} = 35°$ when $\pi^*_{nozzle} = 1.2$-1.8 in the last channel of the screen the stream exit angle is somewhat larger than the design angle of the vanes at the exit. In the other remaining channels the angle β_2 is smaller than the angle β_{vane}. The angle β_2 attains its smallest value in the front channel. Rarefaction is observed forward of the screen on the engine nacelle surface. Rarefaction is reduced with increasing distance from the screen. At some distance from it the ratio p/p_H becomes equal to unity. It is also clear from the figure that pressure on the engine nacelle in some range of pressure reduction values remains unchanged, which does agree with the results of measurements on screen I.

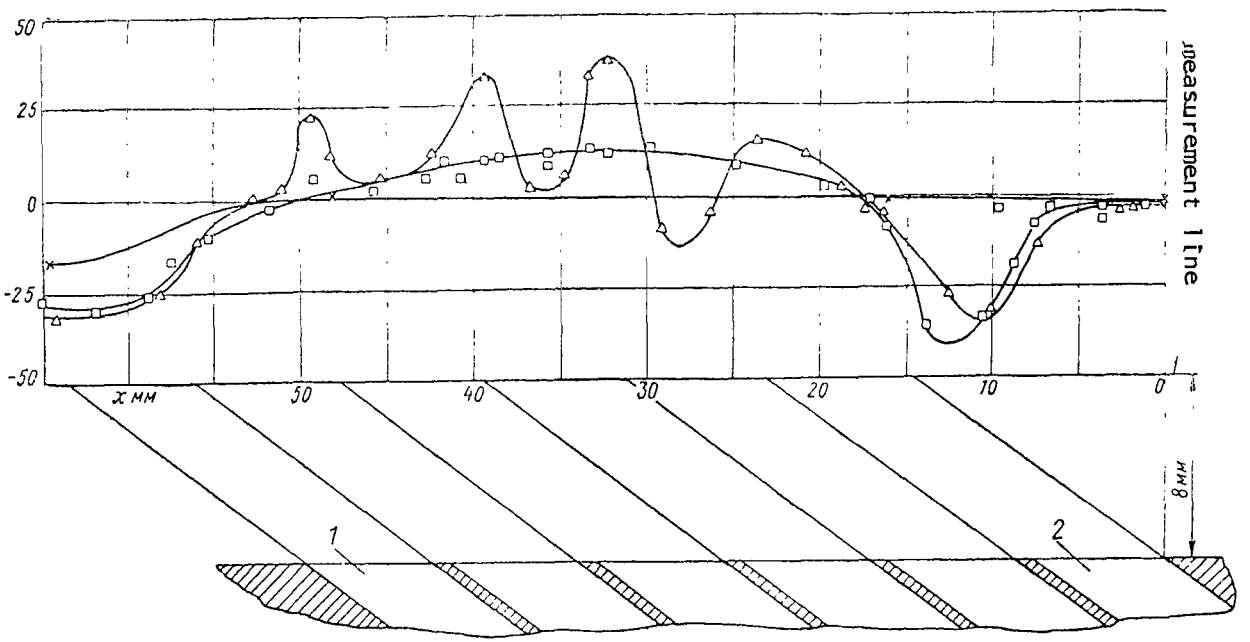

Figure 5.2. Variation in Difference Between Static Pressure at Exit From Screen p_2 and Ambient Pressure p_H in the Central Section Along the Length of the Screen 1 of a Model of a Reverser in a Nozzle Incorporating a Central Body. Scheme 1, Variant 1, 1, Front Channel; 2, Last Channel. X, $\pi^*_{nozzle} = 1.3$; □, $\pi^*_{nozzle} = 1.9$; Δ, $\pi^*_{nozzle} = 2.2$.

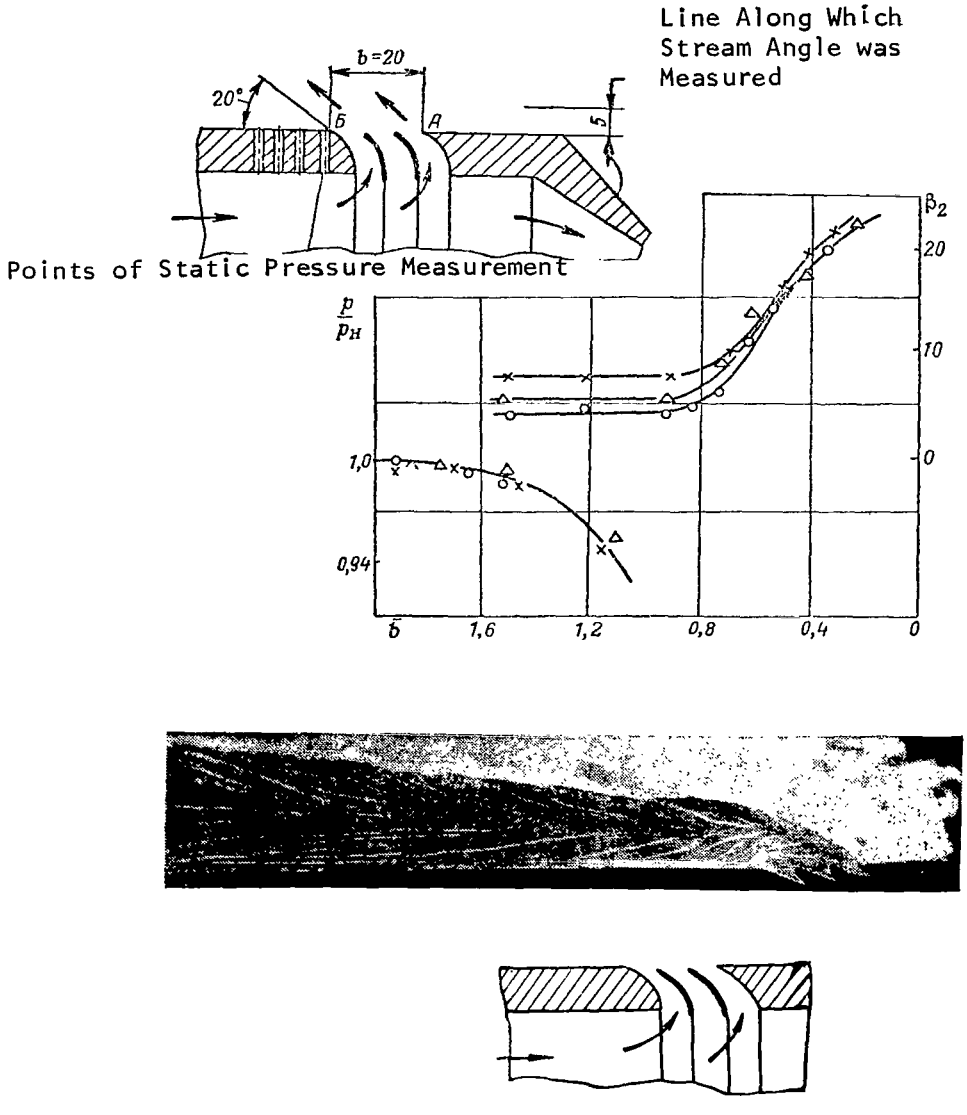

Figure 5.3. Variation in Stream Exit Angle Along Length of Annular Screen of a Reverser Incorporating a Throttling Jet Nozzle and Pressure Distribution Along Engine Nacelle Surface: o, $\pi^*_{nozzle} = 1.8$; x, $\pi^*_{nozzle} = 2.2$; Δ, $\pi^*_{nozzle} = 2.5$.

Thus, we see that the stream escaping from the front channel of the screen exhibits the greatest deviation from the design angle as it immediately adjoins the rarefaction area.

To clarify the qualitative structure of the stream, a strip of organic glass coated with a thin layer of liquified white gauche was placed at the exit from the screen. Black gauche was applied on this layer at several points. When streamlining passed over this strip the liquid dye was swept along by the stream leaving distinctive traces in the direction of the streamline.

Naturally, these traces reflect the over-all flow pattern during the period of change in the extent of pressure reduction down to the highest value in testing. Application of this method allows us to clarify the stream direction in direct proximity to the engine nacelle where measurement with accessories is difficult.

We can see in the photograph obtained for an increase in π^*_{nozzle} up to 2.0 the influence of the ejecting effect on the deviation of the stream as it exits from the screen. The stream flows along the surface of the engine nacelle.

For a vane exit design angle equal to 50°.5 (Screen II of the reverser model of a nozzle incorporating a central body), the flow pattern differs somewhat from that described above (Figure 5.4). When $\pi^*_{nozzle} \leq 1.8$, the stream exit nozzle along the length of the screen changed only slightly. There was no such decrease in the angles in the front channels as was the case in the screen I. But the values β_2 were also less than the design angle. When $\pi^*_{nozzle} = 2.2$, we can see an increase in the stream exit angle owing to its separation in the front channel. When $\pi^*_{nozzle} = 3.2$, the effect of the oblique cross-sectioning of the screen is marked.

Angling of the stream escaping from the slit at an acute angle to the surface toward the side of the latter is known by the Coanda effect and has been observed in several other textbook problems.[1] We know, for example, that a stream escaping from a screen of a finite number of profiles in the stages of turbines with partial feed of working fluid deviates toward the side of the diaphragm [4].

The curves describing the stream exit angle β_{2a} averaged over the screen /161
length for the central section of the screen as a function of the extent of pressure reduction is:

[1]Many theoretical and experimental studies deal with the Coanda effect, and of these a large number is given in the report [47].

$$\beta_{2a} = \frac{1}{a}\int_0^a \beta_2 dx,$$

where a = length of screen, are plotted in Figure 5.5. We note that with a decrease in the density of screens made of leafwise profiles (Screen III) for degrees of pressure reduction greater than 1.5, there is a certain increase in the stream exit angle compared to the value for the screen that has higher density (Screen II). Data is also plotted in the figure for screens made of profiled vanes in which the number of channels z = 6, differing in the subtended angle. It is evident that in these screens as well, for degrees of pressure reduction corresponding to the working regimes of reversers, the /162
stream in the central section also exits at angles less than the design angle of the screen $\beta_{screen} = \text{arc sin } a_{gas}/t$.

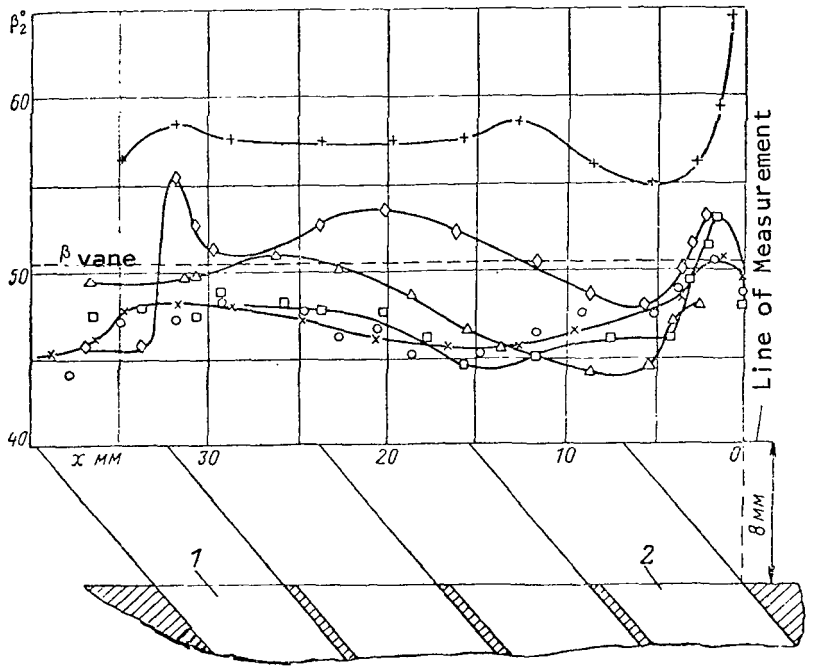

Figure 5.4. Variation in the Stream Exit Angle in the Central Cross-Section Along the Length of Screen II of the Model of a Reverser Installed in a Nozzle Incorporating a Central Body. Scheme I, Variant 1. The symbols are the same as those in Figure 5.1.

The stream at its exit from the deflecting screens of a reverser is three-dimensional in character. Distribution of stream exit angle averaged over screen lengths in the cross-sectional area of the screen IV made of leafwise

profiles ($\beta_{vane} = 67°$) and for screens made of profiled vanes ($\beta_{screen} \approx 31°$, $\theta = 110°$, $z = 6$) is plotted in Figure 5.6. We can see that the stream at the extreme section exits as smaller angles than in the center sections. This can be explained by the fact that the rarefaction induced along the margins of the stream turns the stream along the margins. When the extent of pressure reduction in the screen IV is increased, the difference between the angles β_{2a} in the central section of the screen and in the extreme sections is reduced. The difference between angles β_{2a} in these sections varies only slightly in a screen that has smaller stream exit angles.

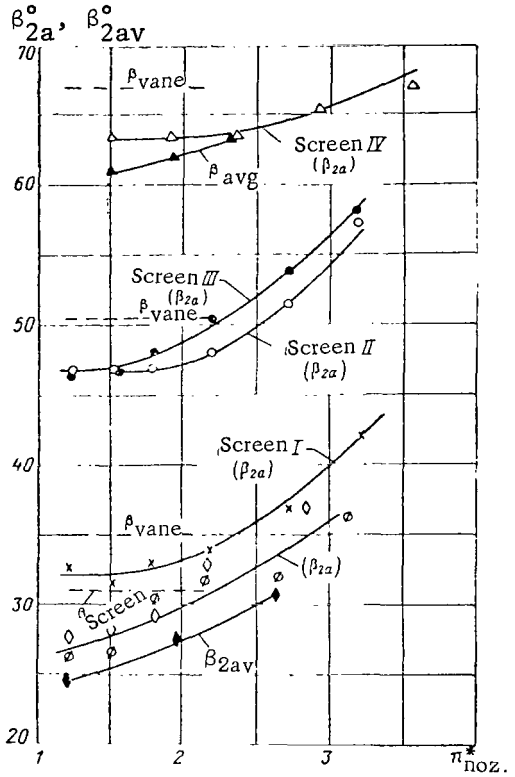

Figure 5.5. Pressure Reduction Dependence of Stream Exit Angles Averaged Over Screen Length β_{2a} in the Central Section of the Screens and the Angle $\beta_{2,av}$ Averaged Over the Screen as a Whole for a Model of a Reverser Built as Part of a Nozzle Incorporating a Centarl Body: Scheme I, Variant 1, With Screens I, II, III, and IV, Made of Leafwise Profiles; Scheme I, Variant 2, with Screens Made of Profiled Vanes (z = 6): ⌀ — θ=70°; ◆, ◇ — θ=110°

Thus, the average value of the stream exit angle for the screen as a whole

$$\beta_2 = \frac{1}{\theta}\int_0^{\theta} \beta_{2a} d\theta$$

is less than the angle β_{2a} in the central section averaged over the screen length. Thus, in working regimes of the reverser, for the angle $\beta_{2,av} \approx 62°$ (cf. Figure 5.5) the angle $\beta_{2,av}$ differs on the average by about 1° from the angle β_{2a}, while in the case when the stream exit angle $\beta_{2,av}$

25°--30°, the difference is about 2°. This difference is the smaller, the smaller the subtended angle of the screen, which does follow from inspection of the arrangement of experimental points for θ = 70° and 110°. Owing to symmetry, the stream exit angle averaged over screen length for annular screens agrees with the mean value of stream exit angle for the screen as a whole. The angle $\beta_{2,av}$ remains practically unchanged for the model

/164

of a reverser incorporating a throttling jet nozzle with such screens in the investigated range π^*_{nozzle} = 1.8-2.5.

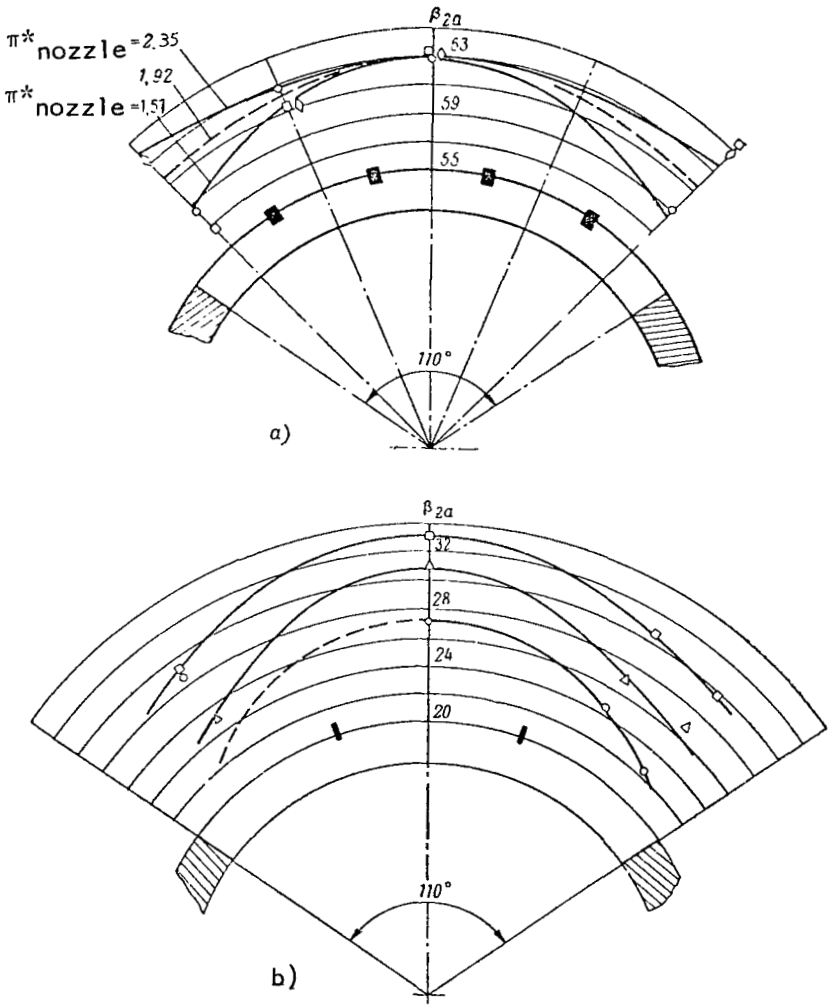

Figure 5.6. Variation of Stream Exit Angle Averaged Over Screen Length in the Cross-sectional Area of Screens that are Part of a Reverser in a Nozzle Incorporating a Central Body: a, Screen IV Made of Leafwise Profiles; Scheme I, Variant 1: o, π^*_{nozzle} = 1.51; □, π^*_{nozzle} = 1.92; ◇, π^*_{nozzle} = 2.35;

b, Screen Made of Profiled Vanes with θ = 110° and z = 6, Scheme I, Variant 2: o, π^*_{nozzle} = 1.18; △, π^*_{nozzle} = 1.95; □, π^*_{nozzle} = 2.64.

§2. Escape of Stream from Deflecting Connecting Pipes

Figure 5.7 shows, for π^*_{nozzle} = 2.2, the variation of stream exit angle along length of deflecting connecting pipe in a reverser incorporating throttling shutters, as well as distribution of pressure along the engine nacelle. The flow pattern at the exit from a connecting pipe of a reverser and pressure distribution at the engine nacelle are qualitatitively similar with that described above for deflecting screens when β_{vane} = 20° and 35°. The figure makes clear that in the rear half of the exit cross-section of the connecting pipe the stream exit angle is greater than the connecting pipe design angle at its exit, but in the front half it is less. The stream exit angle is smaller in the extreme sections of the connecting pipe than in the central section. The smallest values of the stream exit angles are found in the longitudinal section around the inner side of the connecting pipe, which is more closely situated to the other connecting pipe of the reverser. As a result, the stream exit angle averaged for the connecting pipe as a whole is less than the design exit angle of the connecting pipe.

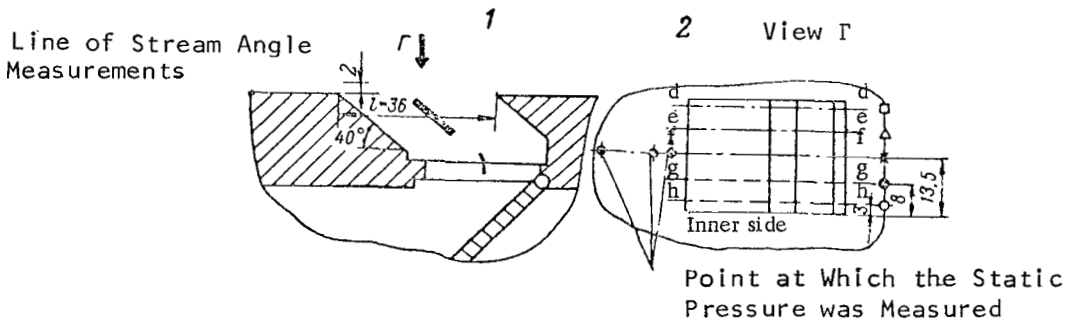

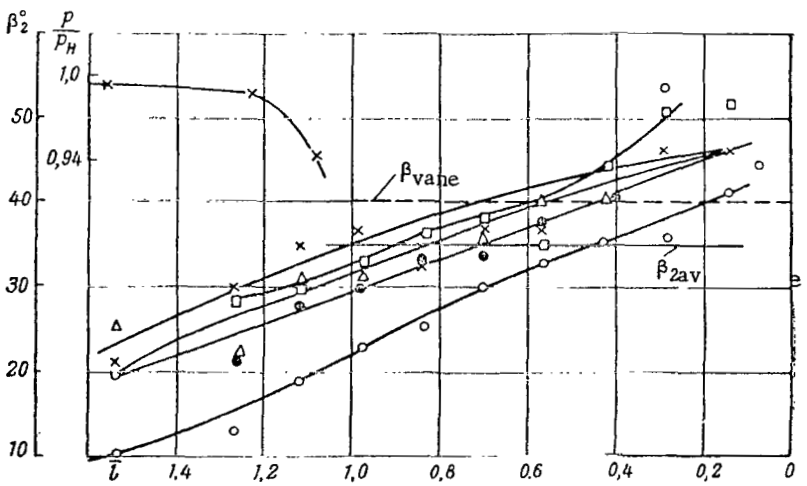

Figure 5.7. Variation of the Stream Exit Angle Along the Length of the Deflecting Connecting Pipe of a Reverser (cf. Figure 4.32), π^*_{nozzle} = 2.2.

Figure 5.8 presents a photograph of the flow pattern at the exit from the connecting pipe as π^*_{nozzle} is increased to 2.0. We can graphically see the fan-shaped pattern of the stream. It is easily discerned that the stream flows along the engine nacelle surface.

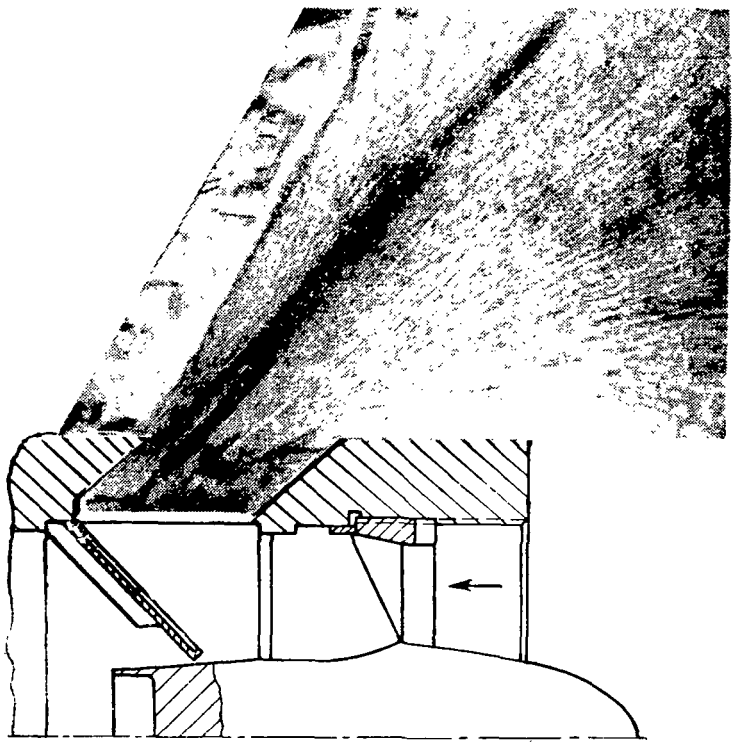

Figure 5.8. Pattern of Flow Exiting from Deflecting Connecting Pipe of a Reverser (Figure 4.32).

The results given above for measurement of the stream exit angle pertain to models of reversers in which the surface of the oblique cross-section of the deflecting screens or connecting pipes lies flush with the surface of the engine nacelle. If the surface of the oblique cross-section of the deflecting connecting pipe will project substantially, then it is obvious that, independently of the angle at which this connecting pipe projects, there will be no rarefaction induced along the engine nacelle which had brought about turning of the stream toward the engine nacelle side.

Studies of a model of a reverser incorporating deflecting connecting pipes and throttling shutters, described above in §5 of Chapter IV (cf. Figure 4.55), have show that even when the engine nacelle surface is removed about

1/3 the length of the deflecting connecting pipe from the surface of its oblique cross-section differences are observed in the distribution of stream exit angles (Figure 5.9). We can see from the figure that in all the cross-sections of the deflecting connecting pipe the stream around the external wall 1 over the entire cross-sectional area in the rear channel 2 extends at angles that are greater than the design angle of the connecting pipe and the guide vanes at the exit, which is explained by flow separation from the vane backs. This pattern of the curves agrees with the results of measurement of total pressure at exit from connecting pipes. Stream exiting at angles less than β_{vane} has been observed in the first two channels only from the inner side of the connecting pipe, to which evidently the influence of rarefaction induced in the zone between connecting pipes had extended. The value of the stream angle obtained by averaging over the entire exit cross-section proved to be about 1° greater than the angle β_{vane} in the range of degrees of pressure reduction that are of interest in actual practice: /165

π^*_{nozzle}	1.64	2.04	2.47
$\beta_{2,av}$	41.5	40.5	41.6

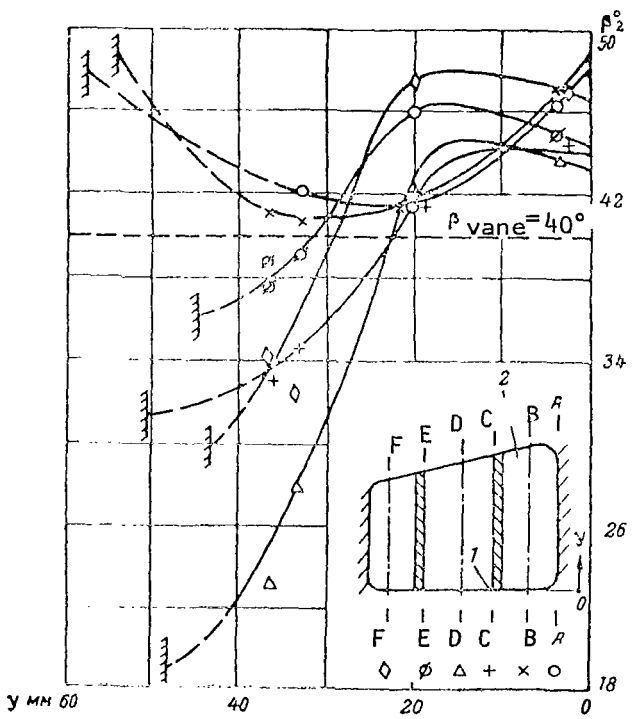

Figure 5.9. Variation in Stream Exit Angle Athwart the Deflecting Connecting Pipe of a Reverser (Figure 4.55), $\pi^*_{nozzle} = 2.0$.

§3. Generalized Data on the Angle at Which a Stream Exits from Deflecting Screens and Connecting Pipes of Reversers /168

Figure 5.10 presents the values of the difference $\Delta\beta$ between the design angle of vanes (connecting pipes) or the design angles of screens and the angle $\beta_{2,av}$ of exiting stream averaged for the screen as a whole:

$$\Delta\beta = \beta_{vane} = \beta_{2,av}, \quad \Delta\beta = \beta_{screen} = \beta_{2,av}$$

as a function of the M_2 number at the exit. The figure presents the data for deflecting screens of a reverser for a nozzle incorporating a central body, and for a reverser incorporating connecting pipes and throttling shutters. In plotting the graph we also used data for reversers incorporating an annular screen and a throttling jet nozzle.

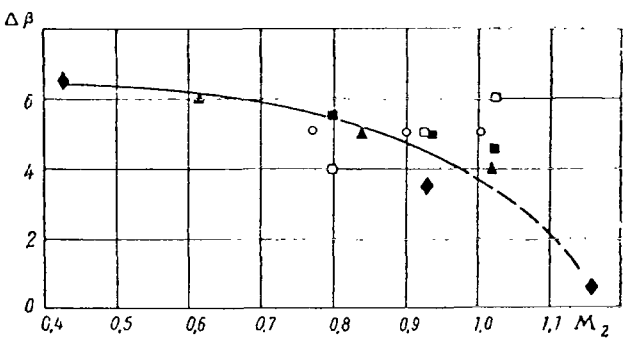

Figure 5.10. Angle $\Delta\beta$ as a Function of the M_2 Number at the Exit from Deflecting Screens and Connecting Pipes Under Stand Conditions. Reverser of a Nozzle Incorporating a Central Body: ♦, Screen made of Profiled Vanes (θ = = 110°, z = 6); ▲, Screen IV Made of Leafwise Profile. The Reverser Incorporating Annular Screens and a Throttling Jet Nozzle: □, β_{vane} = 20°; ■, β_{vane} = 30°; o, Reverser Incorporating Connecting Pipes and Throttling Shutters (Figure 4.32).

From the literature we are acquainted with the so-called Ainley curves (cf. for example, [15]), according to which, at subsonic velocities of escape from turbine screens of a reactive type the stream is not rotated up to the design angle of the screen by some angle ($\Delta\beta < 0$). In contrast to turbine screens, escape of a stream from deflecting screens of reversers is characterized by an increase in the angle of stream deviation ($\Delta\beta > 0$).

We can clearly see from the figure that when there is an increase in M_2 we observe a certain trend toward a reduction in the angle $\Delta\beta$. However, when $M_2 = 1$, the value of $\Delta\beta$, generally speaking, does not equal zero, as in the case of turbine screens, owing to the features of flow exiting from the screens and connecting pipes of reversers noted above. Bearing in mind the precision at which angles were measured, estimated at not higher than ±1°, the figure presents a plot of some averaged curve for deflecting screens and connecting pipes at stream exit angles in the range of approximately 15° to 65°. To the first approximation the curve in Figure 5.10 can be used in estimating the correction $\Delta\beta$ on the stream exit angle for streams exiting from deflecting screens and connecting pipes of reversers when their oblique cross-section surfaces located flush with the engine nacelle for stand performance, that is, without external flow. /169

Figure 5.11 presents a curve of the angle $\Delta\beta$ as a function of the angle β_{vane} (β_{screen}) for π^*_{nozzle} = 2.0, corresponding to the M_2 number $\simeq$ 0.9.

Also plotted in the figure are data for the reversers not considered above, incorporating connecting pipes and throttling shutters at β_{vane} angles equal to 20°, 30°, 50°, 60° and 70°, as well as data for a reverser incorporating annular screens with $\beta_{vane} = 50°$. For these models, measurement was made of static pressure at the engine nacelle surface under the reverse stream, along with measurement of angles. As the angle β_{vane} is increased, static pressure at the point near the front wall of the connecting pipes (screen) draws closer to the value of the ambient pressure, but when $\beta_{vane} = 70°$ it is practically /17
equal to the pressure p_H. When $\beta_{vane} = 70°$ the angle $\Delta\beta$ proves to be equal to zero. It is obvious that $\beta_{vane} = 70°$ is some limiting design angle of the connecting pipe at which the stream exits along the connecting pipe walls and does not deviate toward the engine nacelle side. However, for the close value of the angle $\beta_{vane} = 67°$ for deflecting screens with a subtended angle $\theta =$ $= 110°$, the angle $\Delta\beta$ differs markedly from zero. Thus, the limiting design angle at which $\Delta\beta = 0$ depends not only on the angle β_{vane}, but obviously also on the number of reverse streams and their mutual disposition. Some average curve is presented in the figure to the first approximation. The value $\Delta\beta$ in the range of angles β_{vane} (β_{screen}) = 30°-50° that is of practical interest to us, depends only weakly on β_{vane}, where $\Delta\beta \approx 4°$.

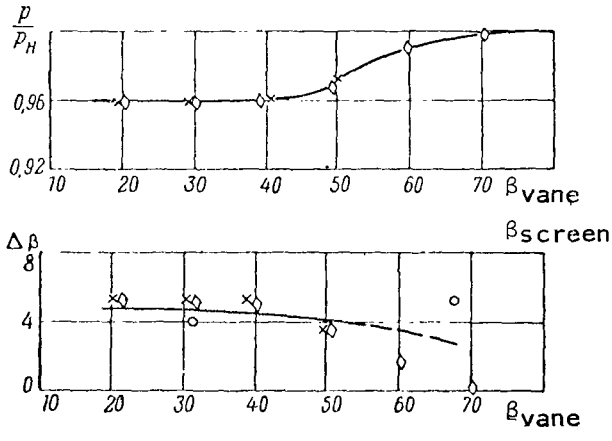

Figure 5.11. Angle $\Delta\beta$ and Pressure on Engine Nacelle Around the Front Wall of the Connecting Pipe as Functions of the Angles β_{vane} or β_{screen} of the Deflecting Screens and Connecting Pipes of Reversers Under Stand Conditions ($\pi^*_{nozzle} = 2.0$): o. Reverser with Screens IV of Nozzle Incorporating a Central Body; ◊, Reverser Incorporating Connecting Pipes and Throttling Shutters; χ, Reverser Incorporating Screens and Throttling Jet Nozzle.

In conclusion we will make a few remarks. Data on the stream exit angle for stream exiting from reversers has been obtained under stand conditions, that is, without external flow. The presence of external flow can have a bearing on the flow direction as it exits from the reverser. Experiments with

jets was distributed at an angle to the entraining stream have shown that at the front side of the jet, owing to flow stagnation increased pressure is built up [7, 19, 24]. The rise in pressure along the margin of the jet can reduce the rarefaction in the region between the engine nacelle and the front part of the jet and lead to a reduction in the angle $\Delta\beta$. Studies of reversers in an external flow, described below (§2, Chapter VI), as well as experiments with jets have revealed that when external flow is present, owing to rotation of the jet a rarefaction zone is located aft of the stream. This rarefaction leads to the appearance of a negative thrust component. Thus, in external flow the possible reduction of the angle $\Delta\beta$ is compensated by a rise in negative thrust applied on the surface of the engine nacelle. Studies conducted with models of reversers allowed us to establish that when an external flow passes over them at velocities corresponding to aircraft landing conditions the reverse coefficient is not only not reduced, but, on the contrary, is increased by several percent (§1, Chapter VI).

Relying on these results in estimational calculations of reversers, usually no correction on the angle $\Delta\beta$ is introduced. We will assume $\beta_2 \approx \beta_{vane}$ (β_{screen}).

CHAPTER VI

EXPERIMENTAL STUDY OF REVERSERS ON MODELS PAST WHICH EXTERNAL FLOW IS STREAMLINED AND STUDY OF A TURBOJET ENGINE INCORPORATING A REVERSER INSTALLED ON AN AIRCRAFT /171

§1. Effect of External Flow on Reverse Coefficient

The value of negative thrust acting on an aircraft depends not only on the inlet impulse of air passing through the engine and the design of the reverser itself, but also on how the engine incorporating this unit is arranged on the aircraft. The reverse stream can substantially alter aircraft streamlining and the resistance of certain of its parts. For example, in calculating the aerodynamic resistance of an aircraft equipped with reversers we must take account of the increased resistance of the engine nacelle that stems from bottom rarefaction induced in the exit area of the jet nozzle in the absence of engine gas exhaust.

An investigation of the effect of external flow on the reverse coefficient was conducted on a simplified model of the reverser, described above (§4, Chapter IV). In place of throttling tilting vanes, the gas duct was partitioned with a diaphragm. Tests showed that the negative thrust of the nozzle rose somewhat with increase in velocity of external flow. The rise in external thrust with increase in velocity is explained by the induction of rarefaction along the external surface of the conical part of the nozzle lying beyond the deflecting screens. The appearance of rarefaction at the tail end of the nozzle is associated with angling of the reverse stream by the external /172 flow: the streamlines of the reverse flow become twisted and a pressure difference shows up at the external and internal margins of the stream , which equalizes the centrifugal forces induced in the motion of particles along the curved sections of the trajectories. The increase in external resistance of the engine nacelle that shows up with the appearance of a reverse stream swept along by the flow can be viewed as an increase in negative thrust of the nozzle.

The values of the reverse coefficient obtained for different streamlining velocities without allowing for the inlet impulse are shown in Figure 6.1 in the form of experimental points. Thus, in the absence of external flow (V_H = = 0) and when the extent of pressure reduction $\pi^*_{nozzle} = 2.0$, the reverse coefficient $\bar{R}_{rev} = 0.6$. When the velocity of the external flow is 45-60 m/sec, the reverse coefficient rose to 0.65, that is, by 8.5%. The increase in the reverse coefficient was observed also for other values of π^*_{nozzle}. Based on the results of nozzle testing in the presence of external flow the values of engine reverse coefficient $\bar{P}_{rev}$ were calculated with account taken of inlet

impulse for different V_H values. The results of the calculation is shown in the figure with solid lines. The reverse coefficient of the engine increases with increasing aircraft velocity. Thus, while when $\pi^*_{nozzle} = 1.9$ and $V_H = 0$, the reverse coefficient $\bar{R}_{rev} = 0.6$, when $V_H = 60$ m/sec $\bar{P}_{rev} = 1.05$, that is, larger than the direct thrust produced by the engine.

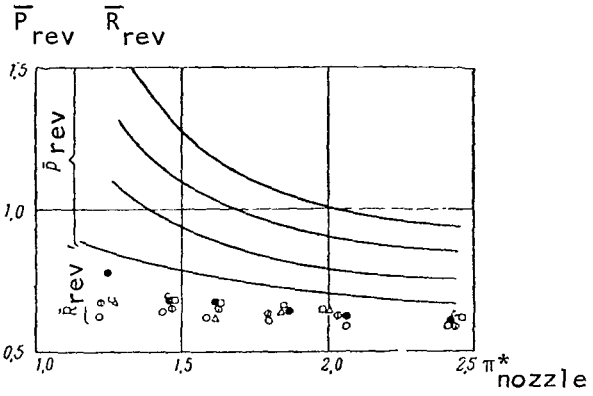

Figure 6.1. Reverse Coefficient $\bar{R}_{rev}$ and $\bar{P}_{rev}$ as Functions of the Extent of Pressure Reduction for Different External Flow Velocities: o, $V_H = 0$ m/sec; o, $V_H = 15$ m/sec; •, $V_H = 30$ m/sec; □, $V_H = 45$ m/sec; Δ, $V_H = 60$ m/sec.

§2. Flow Past a Model of a Nozzle Equipped with a Reverser /173

Side-by-side with investigating characteristics of reversers, study of the propagation of the reverse of stream in the external flow, whose velocity varies from zero to the aircraft landing velocity (wind velocity) is of great interest. The region of reverse stream propagation depends on the ratio of the velocity in the stream to the velocity of the external flow.

The reverse stream impinging the airport must not errode the airport paving and, spreading along the ground surface forward and to the side must not be ingested into the aircraft's air scoops or reduce visibility from the pilot's cabin.

The pattern of reverse flow propagation can be studied on models of reversers in wind tunnels that model the external flow when an aircraft is landing. Velocity flows in the vicinity of the reverser are shown in Figures 6.2 and 6.3 in the form of lines of equal values of the ratio $\bar{V} = V/V_H$ of local velocity to the velocity of the unperturbed flow streaming past the model.

The reverser consists of a cylindrical nozzle 48 mm in diameter, two windows symmetrically positioned in the lateral walls of this structure. Deflect-screens with a subtended angle of 120° are located in the windows.

Velocity fields are determined by means of a comb with T-shaped fittings insensitive to downwash up to ±15°. When measurements were made in the reverse stream zone the fittings were not oriented along the stream, therefore all results relating to severely tortuous sections of the stream must be viewed as approximate. Owing to symmetrical streaming past the model, the velocity fields are represented only in one-quarter of the coordinate plane /174

positioned perpendicularly to the nozzle axia at distances x = 0, 260 and 550 mm from the exit area of the jet nozzle and also in the upper half of the plane yx passing through the nozzle axis.

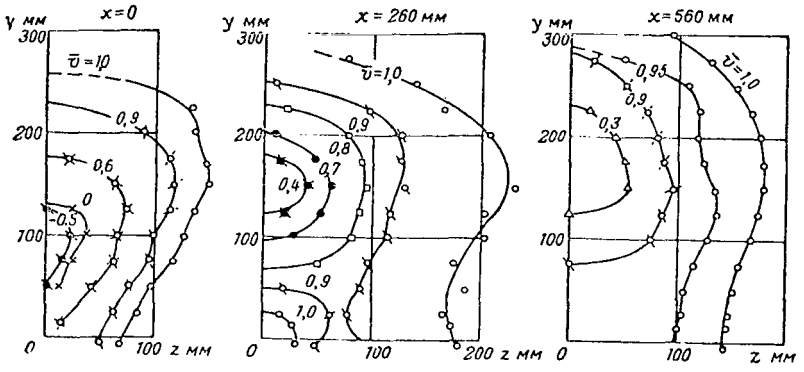

Figure 6.2. Velocity Field $\bar{V} = V/V_H$ in the Reverse Stream in the Plane yz when the Velocity of the External Flow V_H = 40 m/sec and the Extenf of Pressure Reduction in the Reverser. π^*_{nozzle} = 1.9 for Different Distances From the Nozzle.

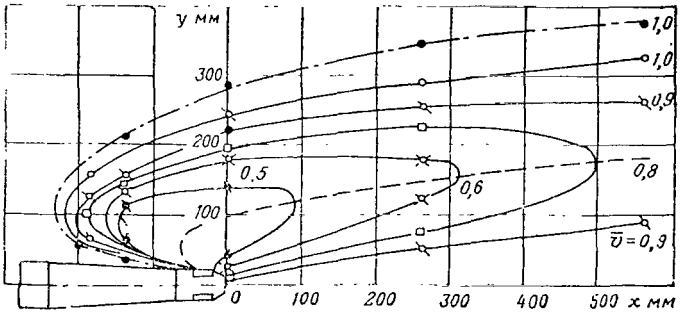

Figure 6.3. Velocity Fields in the Reverse Stream in the Plane yx When the External Flow Velocity V_H = 40 m/sec: ———, When π^*_{nozzle} = 1.9; — . — . — . , π^*_{nozzle} = 2.5; - - - - -, Stream Axis.

The extent of pressure reduction in the nozzle was π^*_{nozzle} = 1.9, that is, the gas escape rate from the nozzle was close to the speed of sound. With increasing separation from the nozzle the velocities in the entrained reverse stream become equalized and the stream widens. In direct proximity to the deflecting screen exist regions with negative velocities.

A reduction in the velocity of the unperturbed flow or an increase in the extent of pressure reduction (dash - dot line in Figure 6.3) leads to an enlargement of the region occupied by the reverse stream. The stream in this case penetrates somewhat further ahead.

The line of minimum velocities can be called the axis of the reverse stream. The axis of the stream at a considerable distance from the nozzle is not parallel to the nozzle axis, that is, the reverse stream retains vertical escape velocity components from the screen.

If we look at the velocity profile in the upper stream relative to the axis in a nondimensional form, then it turns out that the shape of the velocity profile is practically independent on the distance from the nozzle exit section, or on the velocity of the external flow. Figure 6.4 presents a profile of dimensionless velocities in the entrained reverse stream. As dimensionless variables the following were taken: the ratio $V_H - V/V_H - V_{min}$ and $y - y_0/y' - y_0$, where V_H = rate of impinging flow; V = velocity at point with coordinate y; V_{min} = velocity at stream axis in a given section; y_0 = distance from nozzle axis to stream axis; y' = distance from nozzle axis to the point at which the velocity is equal to the half-sum of the velocities $V_H + V_{min}/2$. Consequently, in the reverse stream similarity of velocity fields similar to the similarity of the profile in the wake after a body exists [1]. /175

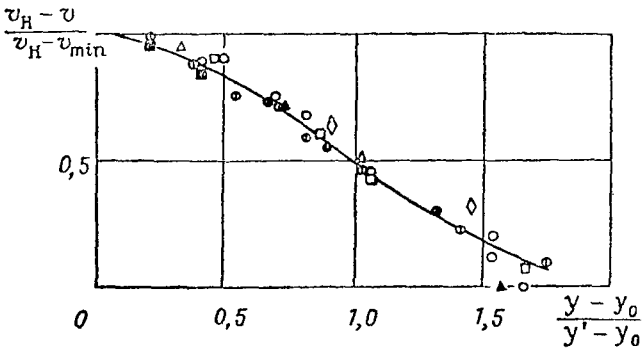

Figure 6.4. Profile of Dimensionless Velocities in the Reverse Stream When $\pi^*_{nozzle} = 1.9$:

V_H = 60 m/sec ○ — x = 560 мм; □ — x = 260 мм; V_H = 40 m/sec; ⊙ — x = 0 мм; ▣ — x = 260 мм; V_H = 25 m/sec: ● — x = 0 мм; ◇ — x = 260 мм; ▲ — x = 560 мм

Beyond the bounds of the reverse stream it is conventional to take a line along which the velocity is equal to the velocity of the unperturbed flow, that is, $\bar{V} = 1.0$.

A photograph of streamlining of the reverse stream is shown in Figure 6.5 for two values of external flow velocity V_H = 29 and 38 m/sec. The ratio of the reduced escape velocity from the screen λ_2 to the velocity of the impinging stream λ_H is, respectively, $\bar{\lambda}_2$ = 4.8 and 3.6. We can see that the stream penetrates forward several nozzle calibers and becomes greatly dilated. The distance from the nozzle axis to the margin of the reverse stream $\bar{y}$ and the distance to which the stream penetrates forward $\bar{x}$ measured in calibers of a critical nozzle section, vary linearly as a function of the ratio of the reduced velocities $\bar{\lambda}_2$ (Figure 6.6). Here the boundaries of the stream, determined from photographs of stream propagation in the impinging flow, agree well with the boundaries determined from changes in the velocity fields, where the /176

line $\overline{V} = 1.0$ is taken as the boundary. At small and high degrees of pressure reduction in the nozzle, the results proved to be similar for the same ratios of reduced velocities. This betokens the small influence of compressibility on screen dimensions. Consequently, many studies of propagation of the reverse stream in the impinging flow can be conducted without setting up full-scale conditions as to pressure. In tests, geometric similarity and the similarity of the reduced velocities in the reverse stream and the impinging flow must be retained.

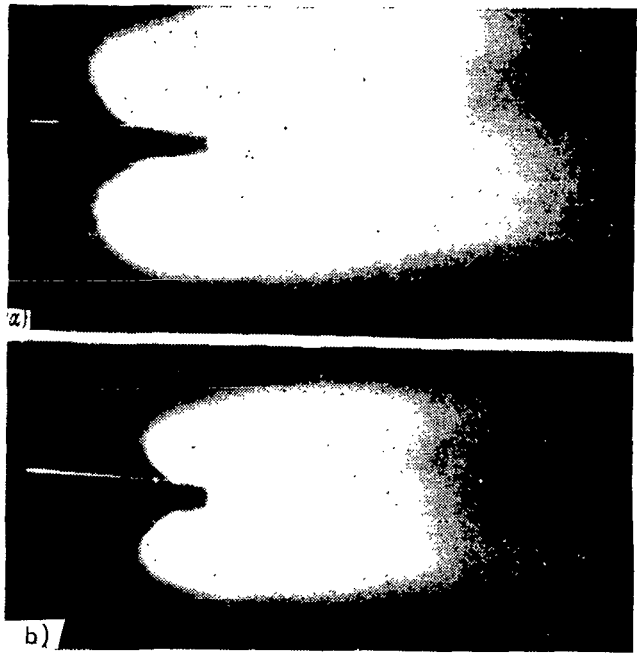

Figure 6.5. External Flow Past an Isolated Nozzle Equipped with a Reverser: a, V_H = 29 m/sec, $\overline{\lambda}_2 = \lambda_2/\lambda_H = 4.8$; b, V_H = 38 m/sec, $\overline{\lambda}_2 = 3.6$.

If the nozzle is oriented at some angle of attack to the impinging flow, then the symmetry of propagation of reverse streams is violated. From the side of increased engine stream exit angle, measured from the direction V_H, the reverse stream propagates more towards the side /177 from the nozzle, and from the side of reduced engine stream exit angles the reverse stream propagates more in the forward direction. After the reverse stream has been rotated by the external flow their direction approximates the direction of the impinging flow.

The effect of the angle at which the stream exits from the deflecting screens on the form and dimensions of the reverse stream entrained by the flow are shown in Figure 6.7. The lines of equal velocities in the reverse stream cross-section in the play xy where z = 0, plotted in the figure were obtained for escape from screens that had a design angle of vanes at the exit point of, respectively, 37°, 55° and 90°. In this case the length of the screen was varied in such a way that consumption through the reverser remained unchanged. The escape velocities differed only owing to deviations in the value of losses in the screens that had different angles β_{vane}. As the stream exit angle was increased, the transverse dimensions of the reverse stream initially rose, but then decreased. The depth of stream penetration forward decreased with increase in stream exit /178 angle and is equal to zero for escape perpendicular to the impinging flow.

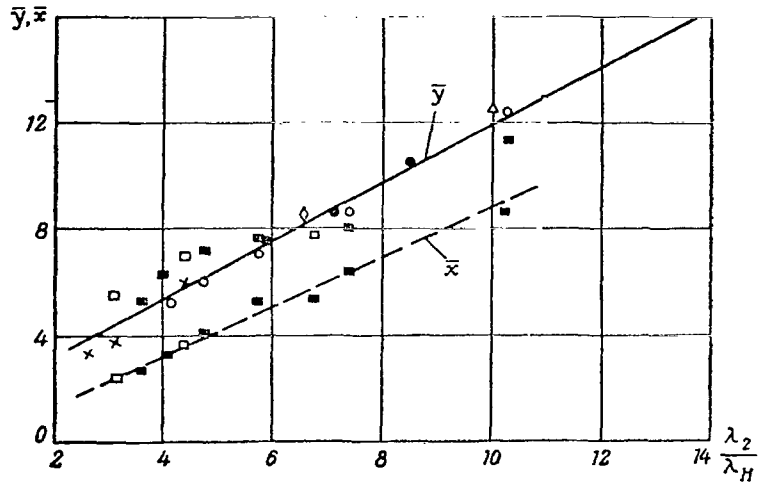

Figure 6.6. Distance by Which the Reverse Stream Penetrated Forward $\bar{x}$ and upward $\bar{y}$ in Calibers of the Critical Nozzle Cross-section as a Function of the Ratio of the Reduced Velocities for Different Degrees of Pressure Reduction. Distance up to the Line $\bar{V} = 1.0$; ×, $\pi^*_{nozzle} = 1.05$; o, $\pi^*_{nozzle} = 1.12$; ◇, $\pi^*_{nozzle} = 1.5$; ●, $\pi^*_{nozzle} = 1.9$; △, $\pi^*_{nozzle} = 2.5$. Distance up to the Boundary of the Stream Judging from Photographs: □, $\pi^*_{nozzle} = 1.05$; ■, $\pi^*_{nozzle} = 1.12$.

From the viewpoint of the arrangements on the aircraft, the substantial penetration of the stream forward can be detrimental. For example, if the reverser is located in the wing, then there is the probability that the gases will be thrown into the engine inlet. Additionally, the reverse stream extending closely over the wing can bring about substantial change in circulation over the wing. For the case when the reverser is installed in the tail end of the fuselage heated gases can reach the trailing edge of the wing and the landing strut, which will result in their heating. Therefore, for identical values of reverse coefficients preference must be given to the reversers that have large angles of stream exits.

Increasing screen length for a given β_{vane} leads to variations in the momentum in the reverse stream owing to an increase in gas consumption and also has the same effect on stream dimensions as an increase of the velocity at which the stream escapes from the screen or a decrease in the velocity of the impinging flow (Figure 6.8). We can also discern from the figure that a sizeable increase in screen length will lead to a sharp change in reverse stream shape and dimensions. Doubling screen length brings about an approximately 1.2 times greater increase in reverse stream width. This is accounted for by the fact that the momentum in the reverse stream is proportional to the linear

dimension (screen length), but the momentum of the external flow acting on the reverse stream is proportional to the square of the reverse stream radius. /180

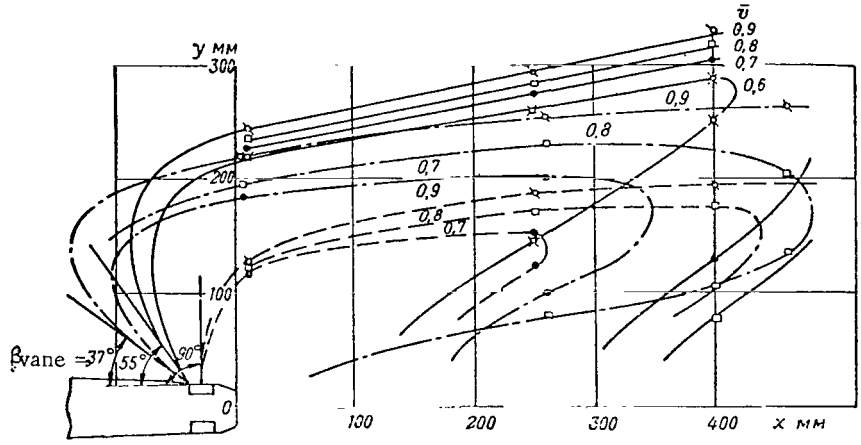

Figure 6.7. Form of Reverse Stream in the Plane yx when the External Flow Velocity V_H = 40 m/sec and for Different Design Angles of Vanes in Deflecting Screens, π^*_{nozzle} = 1.9.

When the number of channels in the screen is increased from z = 2 to z = = 7 and when there is a corresponding increase in consumption aft of the nozzle, a region appears where the velocities in absolute value are greater than the velocity of the unperturbed flow. In the plane yz these regions girdle the zone of reduced velocities (cf. Figure 6.9). The upper part of the reverse stream, the region of increased velocities rapidly disappears, and along the sides of the reverse streams these regions can be traced, at low external flow velocities, for sizeable distances from the nozzle.

Consequently, the reverse stream not only is retarded by the oncoming stream, but is also rotated rearward, retaining a higher velocity than the velocity of the impinging stream.

Photographs of the reverse stream in the presence of a screen modeling the "ground" are shown in Figure 6.10. The stream escaping downward spreads along the sides and in the forward direction upon striking against the screen. Propagation of the stream along the screen depends on the ratio of the reduced velocities $\bar{\lambda}_2$ of escape from the nozzle and of the impinging flow, and also depends on the angle at which the stream exits from the reverser. At low external flow velocities, the stream reverberating from the screen envelopes the nozzle from the top and penetrates far forward. Increasing the stream exit

angle will lead to a reduction of reverse stream propagation along the screen, /181
as can be seen from comparing Figure 6.10a ($\beta_{vane} = 55°$) and Figure 6.10 b ($\beta_{vane} = 90°$).

§3. Flow Past a Model of an Aircraft Equipped With a Reverser

Figure 6.11 presents the scheme of aircraft model placement in a wind tunnel with an exposed working section. In this case one of two engines located in the wings of the aircraft near the fuselage, one wing, and all of the tail assemblies are modeled. Compressed air, modeling the reverse stream is fed to the nozzle along the tube that has a flexible section in order that, when the angle of aircraft attack is varied the angle between the fuselage axis and the engine nacelle will remain unchanged. The model is secured to /182
three supports that make it possible to vary the aircraft's angle of attack.

Figure 6.12 presents the velocity field in the reverse stream for a 4° angle of attack of the model aircraft in the absence of the screen modeling "ground". Used as the angle of attack of the aircraft model was the angle between the direction of the external flow (axis of pipe) and horizon line of the aircraft's fuselage. The results of measuring the velocity fields are /183
given in the flow system of coordinates. The origin of coordinates lies at the aircraft's center of gravity, and the axis z is directed toward the side of the semiwing on which the nozzle model is mounted. The graphs also present plots of fuselage cross-sections and the control surface planes parallel to the plane yz for the corresponding values of the coordinate x. In the section of the plane x = 230 mm the projection of the nozzle is shown arbitrarily, since it does not extend into the section.

As in the case of flow past an isolated nozzle, as the impinging flow velocity rises the region in which the reverse stream propagates becomes narrower. Since the reverse nozzle is located at an angle both with respect to the fuselage as well as to the wing chord, the reverse stream is not symmetrical relative to the horizontal coordinate plane, but is somewhat shifted downward. The presence of circulation around the wing distorts the lower part of the stream more strongly than the upper.

The velocity near the tail assembly, with variation in the velocity of the impinging flow from 15 to 55 m/sec, changes but slightly. However, there does exist a velocity gradient within the framework of the tail assemblies. With a strong side wind this velocity gradient can lead to the induction of asymmetrical load on the tail assemblies.

The variation in the flow rate at the tail assembly associated with change /184
in the aircraft's angle of attack is limited.

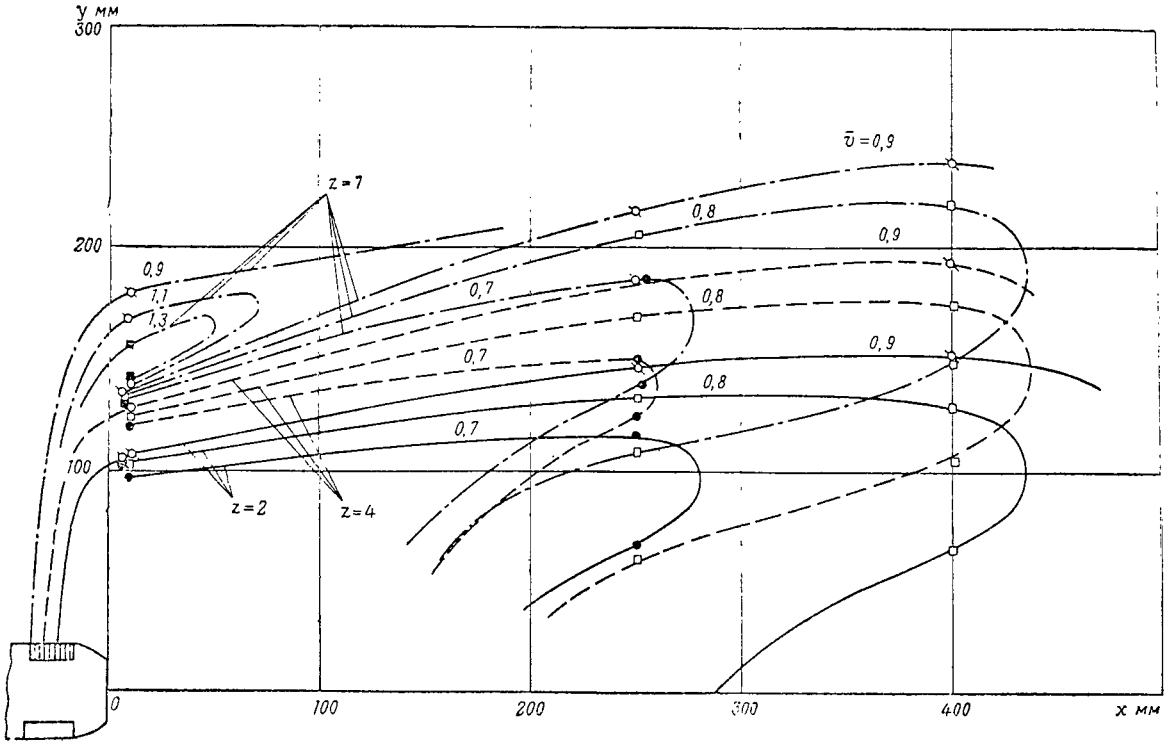

Figure 6.8. Form of Reverse Stream in the Plane of yx for an External Flow Velocity V_H = 40 m/sec and for Different Numbers z of Channels in the Deflecting Screen, π^*_{nozzle} = 1.9.

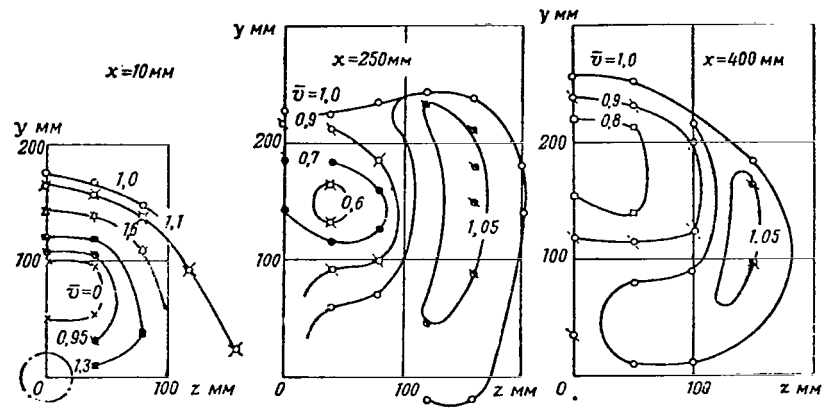

Figure 6.9. Velocity Fields in the Reverse Stream in the Plane yz for an External Flow Velocity V_H = 40 m/sec and for Different Distances from the Nozzle. The Number of Channels in the Screen z = 7, the Design Angle of the Screen Vanes β_{vane} = 90°, and π^*_{nozzle} = 1.9.

a)

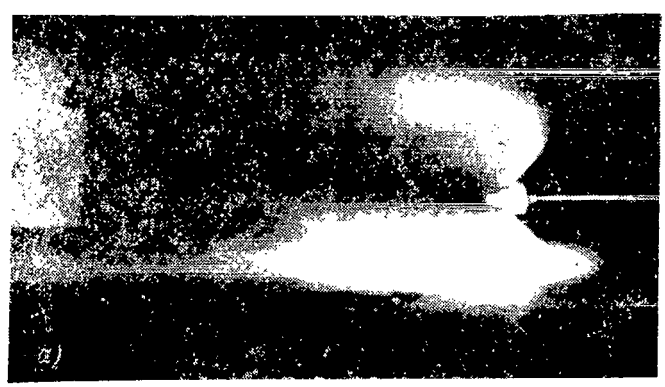

b)

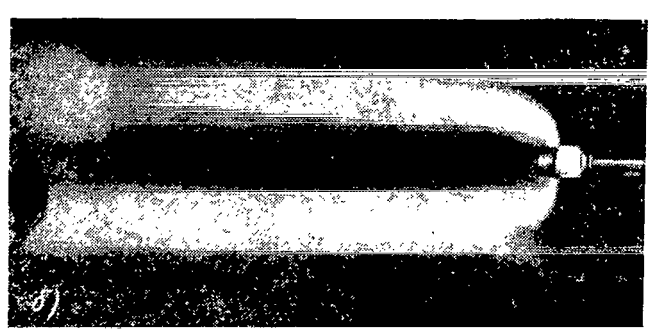

Figure 6.10. Reverse Stream Subjected to Streamlining by the External Flow in the Presence of a Screen Modeling "Ground": a, V_H = 65 m/sec; $\bar{\lambda}_2$ = 4.75; β_{vane} = 55°; b, V_H = 65 m/sec; $\bar{\lambda}_2$ = 4.75; β_{vane} = 90°.

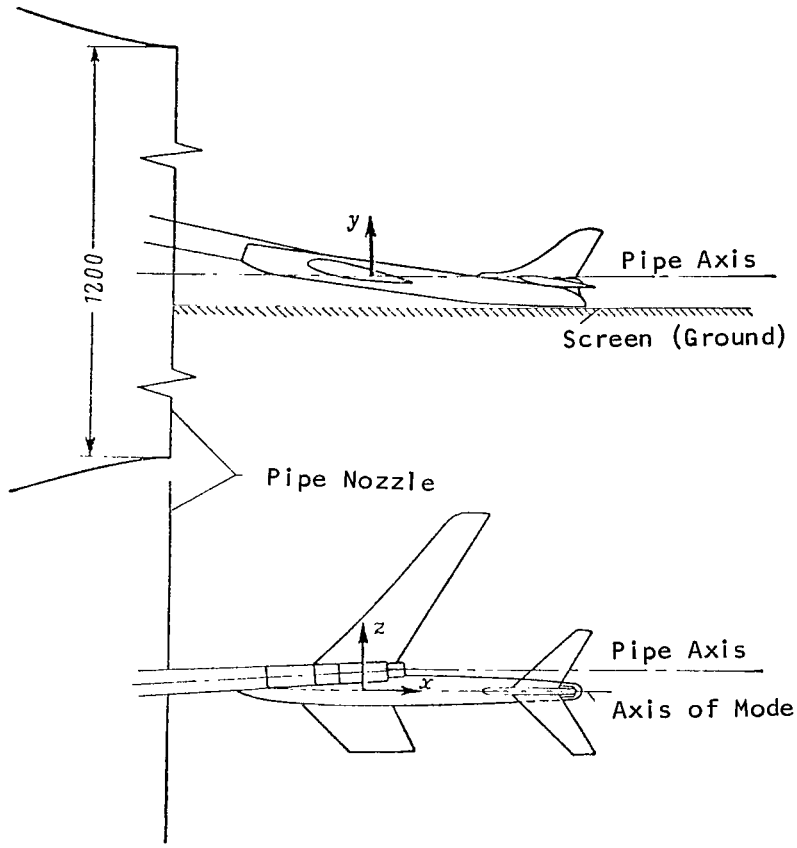

Figure 6.11. Positioning Scheme of a Model of an Aircraft Equipped with a Reverser, in a Wind Tunnel.

Relative velocity fields in a study of the aircraft model close to "ground" are shown in Figure 6.13. When the external flow velocity $V_H \leq 50$ m/sec, the reversed stream strikes the "ground" and spreads along it. At high velocities the reverse stream is situated between "ground" and the wings and slightly spread along the latter. Velocities are lower at the tail assembly than for tests without a screen. Below Table 5 lists values of the relative velocity $\overline{V}$ at the horizontal control surfaces obtained from testing an aircraft model.

At low external flow velocities the lower stream extends out from under the wing and envelopes it from above. In this case discharge of gases and dust from the airport to the engine's air intake is possible. /185

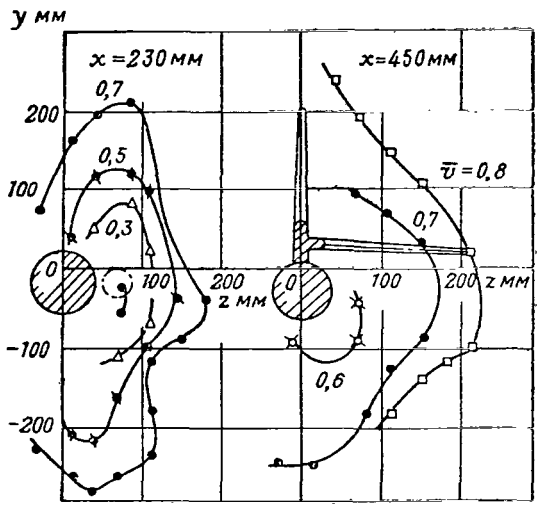

Figure 6.12. Velocity Fields in the Reverse Stream of a Nozzle Mounted in the Wing of an Aircraft When V_H = = 40 m/sec, π^*_{nozzle} = 1.9, and the Aircraft's Angle of Attack α = 4°.

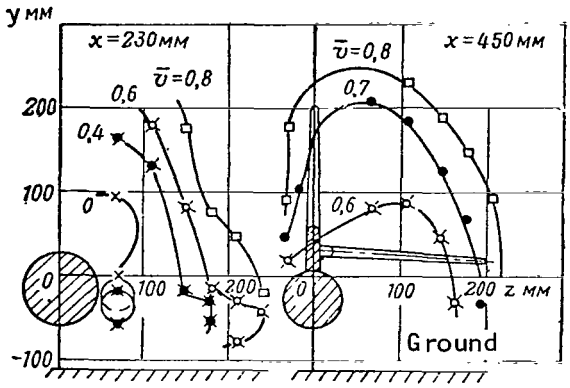

Figure 6.13. Velocity Fields in the Reverse Stream of a Nozzle Mounted on the Wing of an Aircraft When the Aircraft is Running Along "Ground" V_H = 40 m/sec, π^*_{nozzle} = 1.9, α = = 4°.

In order to reduce the probability of ingestion of the stream reflected from the ground into the engine's inlet, the reverse stream can be angled to one side away from the fuselage. For example, double angling of the stream can be accomplished by means of a special screen of vanes: first in the vertical plane passing through the nozzle axis, and then in the plane perpendicular to the nozzle axis.

TABLE 5.

V_H m/sec	$\alpha = 0°$		$\alpha = 4°$		$\alpha = 8°$	
	Distance to Screen					
	∞	100 мм	∞	100 мм	∞	100 мм
15	0,65	0,40	0,70	—	—	—
25	0,70—0,75	—	0,70—0,80	0,50	0,68	0,50—0,60
40	0,75—0,80	0,55—0,70	0,60—0,75	0,55—0,70	0,65—0,80	0,50—0,70
55	0,70—0,80	0,45—0,70	0,55—0,80	0,47—0,70	0,50—0,65	0,45—0,60

The velocity fields for this case are given in Figure 6.14 for aircraft past which an unbounded flow streams, and in Figure 6.15 for the aircraft close

to "ground". Angling of the stream occurs at an angle of 30° to the vertical plane running through the nozzle axis.

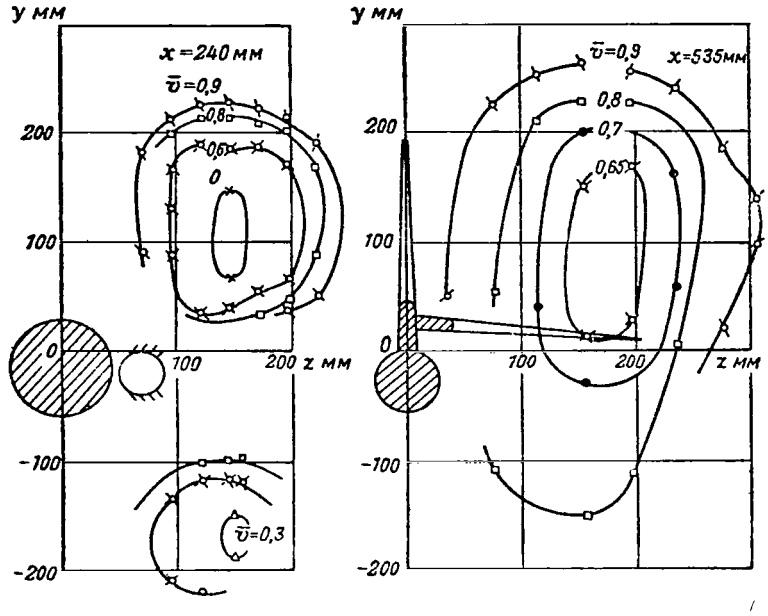

Figure 6.14. Velocity Fields in the Reverse Stream Additionally Deflected Toward the Wing Tip by an Angle of 30°: v_H=40 м/сек, π_c^*=1,9, α=4°

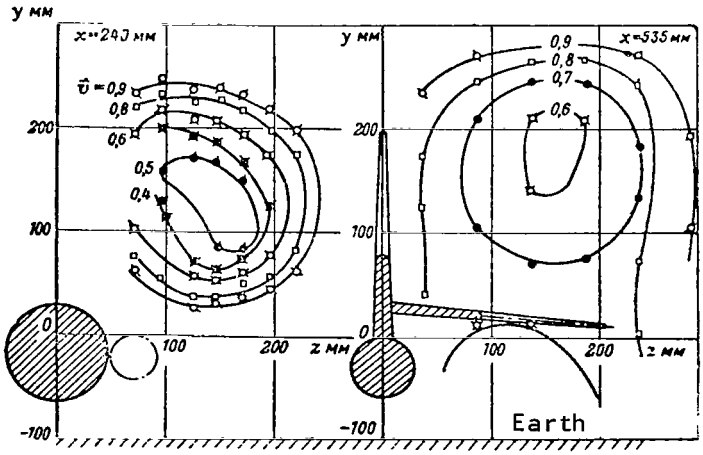

Figure 6.15. Velocity Fields in the Reverse Stream Additionally Deflected to the Wing Tip by an Angle of 30°, for Travel Along the "Ground": v_H=40 м/сек, π_c^*=1,9, α=4°

We can see from the figures that the center of the reverse stream is shifted by some distance from the fuselage compared with the earlier examined velocity fields in similar stream cross-sections. By the tail assembly the velocities varied only slightly.

Angling the way of the /186
stream led to the situation in which it was propagated along the "ground" not under the fuselage, but under the wing in which the reverser was located. Here the velocity of the aircraft at which the start of possible

ingestion of gases into the engine inlet occurs is reduced, and the amount of gases striking the engine is also decreased, since it is not the center of the stream but only its blurred margin strikes the air intake zone.

§4. Several Results of Investigating the Turbojet Engine Equipped with a Reverser and Experience in Final Adjustment of Reversers on an Aircraft

The basic problems that have to be solved in final adjustment of a reverser on an aircraft, as stated in §1 of Chapter III, include the ingestion of the reverse stream into the engine inlet and the temperature conditions of the aircraft structural assemblies close to the reverse stream.

The operating conditions of an engine equipped with a reverser depends quite heavily on the engine's location in the aircraft. However, relying on the example of a number of studies it appears possible to outline several general principles.

NASA (United States) has conducted studies [33] of a hemispherical reverser located aft of the jet nozzle exit of an engine installed in the engine nacelle on the B-47 (Figure 6.16). If the aircraft is immobile (Figure 6.17), then in the course of cutting-in the reverser, owing to ingestion of the reverse stream into the engine inlet the inlet temperature climbs rapidly, and does so to a greater extent the higher the engine rpm setting. Subsequently, the inlet temperature continues to rise slowly, associated with increase of the temperature over the entire gas-air duct of the engine. /187

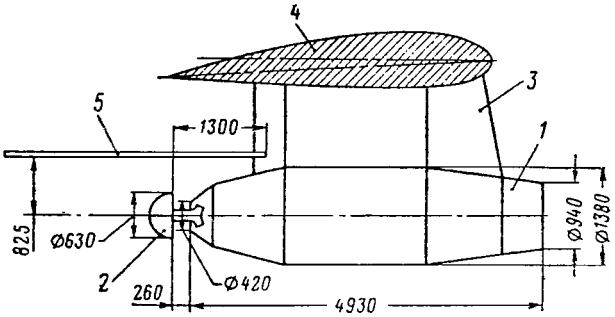

Figure 6.16. Installation of a Hemispherical Reverser on an Aircraft [33]. 1, Engine Nacelle; 2, Reverser; 3, Pylon; 4, Aircraft Wing; 5, Screen.

In the landing run of the aircraft, the inlet temperature remains unchanged as the reverser is cut-in (Fig. 6.18). This means that some of the gas deflected in the reverse direction is swept along by the oncoming flow and does not enter into the engine inlet. When the reverser has been fully cut-in, some time has elapsed during which the reverse stream does not enter the inlet and the inlet temperature remains constant. Then, as the aircraft slows down an intense temperature rise sets in. For a given placement of an engine on an aircraft and when it operates at maximum regime, the reverse stream does not enter into the inlet if the aircraft's landing run speed is greater than 115 km/hr. As the rpm setting goes down we

observe a trend toward a reduction in maximum inlet temperature; a decrease in the landing run velocity at which the reverse stream enters into the inlet is also graphically evident. This latter fact is associated with a decrease in the long ranging status of the stream as the engine rpm settings are reduced and is in accord with the results given in §2 of this chapter. A rise in the /188
inlet temperature leads to compressor stalling and reduces the reverse thrust of the engine and the braking effect of the reverser. The inacceptability of exceeding some fixed temperature at the inlet limits the time during which the thrust can be reversed. At a specific landing run velocity the reverser must be cut-out or the engine must be switched over to a lower rpm setting. Thus, for example, the operating time of the reverser installed in the Avon Rolls-Royce turbojet engine on the De Havilland Comet IV at an rpm setting of approximately 0.5 of maximum is 15 sec.

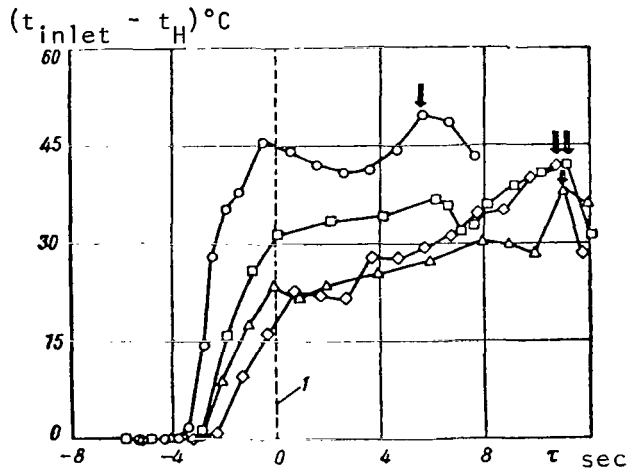

Figure 6.17. Increase in Air Temperature at Engine Inlet for a Reversers (Figure 6.16) as Functions of Time for an Immobile Aircraft, at Different Engine rpm Settings: o, number of rpm, $n = n_{max}$; □, $n = 0.9n_{max}$; Δ, $n = 0.75n_{max}$; ◇, $n = 0.6n_{max}$; 1, Point of Total Cut-in of Reverser; ↓, Point at which Reverser Cut-out Begins.

The minimum landing run velocity at which the reverse stream still does not strike into the engine inlet depends on a multiplicity of factors associated with the placement of the reverser in the aircraft. Figure 6.19, borrowed in modified form from the /189
report [37] gives for several aircraft equipped with reversers the reverse coefficient as a function of this velocity.

Also plotted in the graph are the data of the works [33]. We can see that these experimental points lie in a common band of data cited by the author of the report [37]. Using this graph to the very first approximation we can form a general idea about the possibility of using any particular reverser on an aircraft.

Measurements conducted on a full-scale reverser have shown that the temperature in the reverse stream at a distance of 1,200 mm from the nozzle axis is reduced down to one-third, but with further separation from it is reduced gradually (Figure 6.20). At a distance of 3 m the temperature in the stream is equal to about 150°C. These data are in accord with the results of temperature measurement at the screen positioned around the hemispherical reverser, shown in Figure 6.21. We can also see from the diagram that

increasing the temperature over part of the screen located aft of the shutters of the reverser is slight.

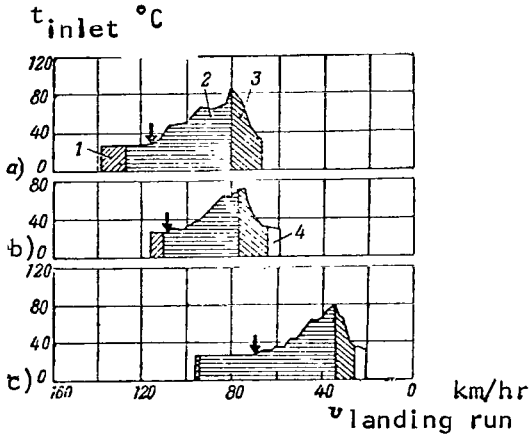

Figure 6.18. Air Temperature at the Inlet to an Engine Equipped with a Reverser (Figure 6.16) as Functions of the Landing Run Velocity of the Aircraft for Different Engine rpm Settings: a, $n = n_{max}$; b, $n = 0.9n_{max}$; c, $n = 0.75n_{max}$. 1, At Cut-in; 2, In the Working Position; 3, At Cut-off; 4, Reverser in Gathered Position (the Arrow indicates the initial moment at which the reverse stream is ingested into the engine inlet).

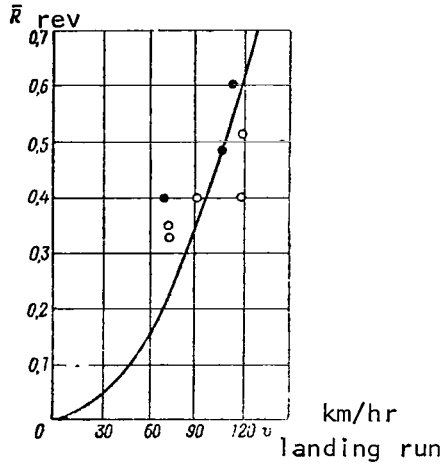

Figure 6.19. Reverse Coefficient as a Function of Maximum Aircraft Landing Run Velocity at which the Reverse Stream does not Become Ingested into the Engine Inlet: o, Data of the Report [37]; •, Data of the Report [33].

To avoid ingestion of the reverse stream into the engine inlet and on to the structural assemblies of the aircraft, discharge of gases from the deflecting elements does not proceed strictly in the vertical or horizontal planes. Thus, for example, to provide normal operating conditions of the wheels and landing struts, and also of the fuselage on the Comet IV, the reverser is discharged at a 20° angle to the vertical, and in this case upwards--to one side of the fuselage. On the BAC VC-10 (Great Britain) in which the reversers are installed in the two outermost Conway RCo. 42 engines of the four installed on pylons in the rear of the fuselage, the reverse streams are emitted as follows: the upper--in the vertical plane and forward at an angle of 45° to the horizon, the outermost halves of the lower streams--at an angle of 35° to the vertical to one side of the fuselage and forward at an angle of 45°, and the inner halves of the lower-streams--at an angle of 20° to the vertical to one side of the fuselage and rearward at an angle of 105°. /191

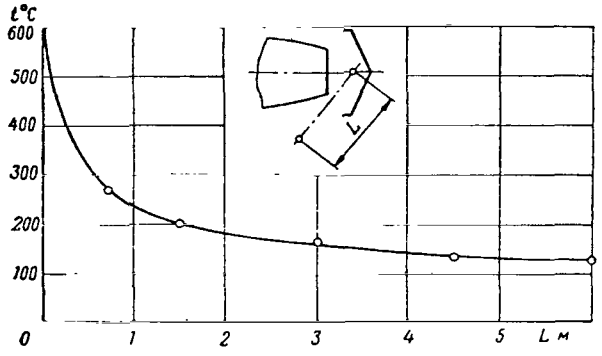

Figure 6.20. Temperature in Reverse Stream as a Function of Distance From Nozzle Axis for a Reverser Equipped with Cylindrical Shutters and Deflecting Flaps [37] (π^*_{nozzle} = 2.2).

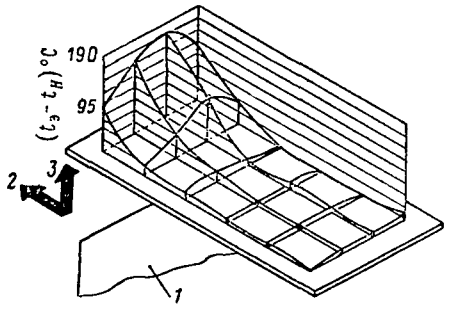

Figure 6.21. Distribution of Temperature Along the Stream Situated Around the Hemispherical Reverser (Figure 6.16) When the Aircraft is Taxiing 15 sec. After Thrust Reversal at $n = n_{max}$ [33]. 1, Plane of Symmetry of the Hemispherical Reversers; 2, "Forward"; 3, "Upward".

An experiment in final adjustment of a reverser on the Boeing 707 is of interest [22]. The initial variant of the reverser was made in simplified form: the gas duct was throttled with a series of strips forming a diaphragm; the deflecting screens made of annular vanes with a design angle of 55° at the exit were covered above and below with screens. Ingestion of exhaust gases at the engine inlet was observed in stand tests, which led to compressor stalling. When a deflector 125 mm high was installed on the engine nacelle ahead of the reverser, this did not do away with gas ingestion into the inlet. Framing of two front series of vanes, ensuring exiting of the stream at right-angles to the engine axis, did prove successful. The reverse coefficient proved to be 0.40-0.45 as compared to the value 0.30-0.35 required for safe halting of the aircraft.

The wing of the Boeing 707 has a large sweepback and the inner engines are shifted far forward compared with the outer engines, which promotes ingestion of the left reverse stream of the inner engine in the inlet of the outer, and also forcing back of the right reverse stream of the outer engine by the left reverse stream of the inner engine and the incursion of the latter into the inlet of the inner engine. Tests of these reversers installed on the two left engines on a prototype aircraft revealed that when the reverser of the left of the engines operating at low throttle regime is cut-in, ingestion of the reverse stream at the inlet and compressor stalling of the engine is observed for an immobile aircraft. To verify the effect that the entraining flow has on gas ingestion into the engine inlet, the aircraft was accelerated

to 185 km/hr using the two right engines, and then they were shifted to low throttle regime and the reversers of the left engine were cut-in. At a landing run velocity greater than 150 km/hr, the exhaust gases did not strike the enging inlet. At lower velocities continuous compressor stall occurred. The inner engine proved to be under worse conditions. Compressor stalling of the inner engine was eliminated by varying the design angle at the exit of part of the screen vanes facing the inner engine on the reverser of the outer engine, which led to a change in the reverse stream exit angle. Compressor stalling of the outer engine at a landing run velocity greater than 75 km/hr was eliminated by reworking part of the inner engine screen vanes. When the reverser from the left outer engine was installed in the inner right engine, ingestion of exhaust gases in engine inlets was not observed. /192

In this way it was established that ingestion of exhaust gases at engine inlets causes engine compressor stalling in a few seconds. In several cases severe compressor stalling developed in the absence of an appreciable rise of inlet temperature, which was associated with disturbance of the velocity field at the inlet. These tests showed that eliminating ingestion of exhaust gases at an engine inlet must be conducted individually for each engine and separately for each specific engine layout on an aircraft.

As the result of the final adjustment, a series-produced design of a reverser was developed and the order in which the reversers are cut-in when an aircraft is landing was drawn up.

CHAPTER VII

DEFLECTORS USED IN TURBOJET ENGINES

§1. Present Status of Research and Development of Deflectors /193

The idea of using a jet stream to produce a lift force was born simultaneously with the introduction of turbojet engines to aviation. One of the early domestic proposals, made in 1945, was a scheme of a turbojet engine incorporating N. Ye. Kitanin tilting nozzles for a vertical takeoff and landing aircraft.

Reports on gas dynamic studies of deflectors are not numerous. Several studies have been published in which a variety of schemes of deflectors used in turbojet engines intended to produce lift force, control and balancing, etc. moments are examined. The results of experimental research on a number of schemes of such devices has been published by A. A. Svyatogorov and N. I. Khvostov in 1959. The article [39] examines schemes of devices for deflecting turbojet engine jet stream, as well as aerodynamic and design problems of building deflectors. Figure 7.1 presents, based on data in the report [29] schemes of deflectors that can be used to solve different problems. These schemes have been developed based on a group of possible fields of application. Naturally, some judgement about the suitability of any particular scheme for specific needs can be made only after experimental research and design development that is suitable for the given aircraft. Based on a consideration of the schemes it is clear that the transverse force can be produced in two ways: by introducing into the jet stream some surfaces (flaps, shutters) or by angling /194 the stream forward of the nozzle exit area, that is, by the very same devices as are used in building negative thrust produced by turbojet engines. However, in contrast to reversers, production of a transverse force requires nonsymmetrical discharge of gas.

Transverse force is built up when the area of the jet nozzle is regulated by advancing a flap into the plane of the exit cross-sectional area [43]. Thrust losses are observed when this is done. A similar idea was realized on an experimentally vertically lifting device "Atar Volain" (France) incorporating a turbojet engine [14]. The gas control surfaces of the flying vehicle consisted of four flaps that were advanced into the jet stream and which deflected it toward the required side. Each pair of oppositely positioned flaps was connected with the power control cylinders governing course and pitching. With the simultaneous advance of all flaps into the stream, the nozzle exit area can be cut by 10% and the thrust of the engine change, which ensures control over the vertical translations of the vehicle. We note that the method of producing transverse forces by advancing your flap into the nozzle cross-section area across the stream has found application in developed projects for flying craft using rocket engines and is now being studied experimentally.

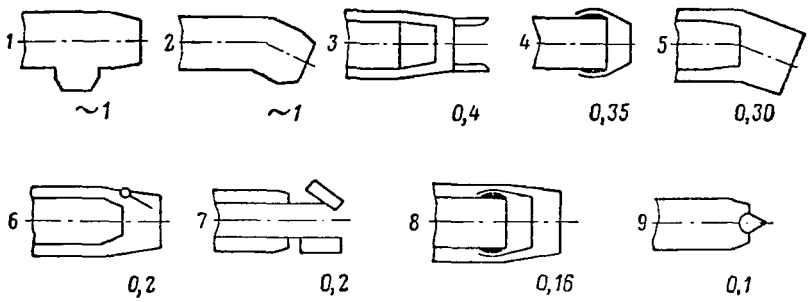

Figure 7.1. Scheme of Devices for Increasing Lift, Control of Flying Craft, and Its Balancing (from Data in the Study [29]). The Permissible Value of Lateral Force in Fractions of Nozzle Thrust is Indicated Next to the Sketches. The Schemes for Increasing Lift and Control are as Follows: 1, Nozzle at an Angle of 90°; 2, Tilting Exhaust Pipe; 3, External Flaps; 4, Tilting Nozzle; 5, Tilting Rings. The Schemes for Control and Balancing are as Follows: 6, Internal Flaps; 7, Cylindrical Reversers; 8, Tilting Valve in Fixed Engine Nacelle; 9, Shifting Central Body.

Gas control surfaces, which are planes with aerodynamic profiles, have been used in the domestic experimental flying stand "Turbojet" on which research studies on vertical takeoff and landing have been conducted. /195

Practical developments of turbojet engine deflectors intended for vertical takeoff and landing aircraft have been conducted in a number of countries following the accumulation of some experience with reversers, with which deflectors have features in common. Experimental-design developments and gas dynamics research on deflectors have been conducted relevantly to two-deflector schemes: Scheme I with two-tilting nozzles and shutters throttling the gas duct (cf. Figure 7.8). We know of variants of Scheme I. Four nozzles, one pair in each pass (cf. Figure 7.5), can be installed on a bypass engine. When two engines are located in the engine nacelle (fuselage) of an aircraft, one-sided discharge of gases at each engine through a single tilting nozzle can be executed.

We find interest in the report [21] that presents results of model studies of a deflector of Scheme II in an installation equipped with a force-measuring instrument, and also data of flight tests made of an aircraft equipped with a turbojet engine that is fitted with a deflector. The articles [23, 35] present several results of studies made of pressure losses occurring in the cleavage and partial angling of the flow in Scheme I and of thrust losses in the tilting nozzle equipped with a deflecting screen.

The study [36] gives a comparative analysis of the deflectors built under Schemes I and II. We know of a number of reports devoted to design-theoretical examination of ways of improving the takeoff and landing characteristics of

aircraft that have deflected gas streams [3, 41]. The report [13] describes several schemes of deflectors, examines power plants for vertical takeoff aircrafts, as well as problems associated with building and operating such aircraft.

We must emphasize that deflectors have not yet gone beyond the stage of experimental-design work. The only foreign aircraft with a power plant equipped with deflectors that can be cut-in serieswise is the British VTO fighter-bomber Hawker P-1127, the "Castrel".

§2. Efficiency of Deflecting a Jet Stream Downward to Shorten Takeoff and Landing Distances for an Aircraft

If the jet stream of an engine is deflected downward at an angle β with respect to the horizon and if at the moment of takeoff or landing of an aircraft vertical and longitudinal accelerations are equal to zero, then the following relationships must be satisfied: /196

$$\left(P+\frac{G}{g}V_H\right)\sin\beta=Q-\frac{c_y\varrho V_H^2}{2}S; \tag{7.1}$$

$$\left(P+\frac{G}{g}V_H\right)\cos\beta-\frac{G}{g}V_H=c_x\frac{\varrho V_H^2}{2}S, \tag{7.2}$$

where P = engine thrust;

G = weight consumption of gas through the engine;

V_H = takeoff or landing velocity;

Q,S = weight of aircraft and wing area.

Here it is assumed that deflection of the stream occurs without loss in thrust force, and that the deflected stream does not have an effect on the aerodynamic characteristics of the aircraft.

We introduce several symbols:

$\overline{P}_0 = P_0/Q$ - thrust-to-weight ratio of aircraft, that is, the ratio of the engine thrust when performing in place close to the ground to the aircraft's weight;

$f_1=\frac{P}{P_0}$; $f_2=\frac{G}{G_0}$ - ratio of thrust and consumption of air through the engine in the landing run to the thrust and air consumption when performing in place, respectively;

$P_{0,ideal} = P_0/G_0$ - specific thrust produced by an engine when performing in place;

$K = c_y/c_x$ - aerodynamic characteristic of the aircraft;

$\bar{Q} = Q/S$ - specific wing loading.

Substituting the symbols given above into the equalities (7.1) and (7.2) we get

$$\bar{P}_0\left(f_1+\frac{f_2V_H}{P_{\text{ideal}}g}\right)\sin\beta=1-c_y\frac{\varrho V_H^2}{2\bar{Q}}; \tag{7.3}$$

$$\bar{P}_0\left(f_1+\frac{f_2V_H}{P_{\text{ideal}}g}\right)\cos\beta-\frac{\bar{P}_0f_2V_H}{P_{\text{ideal}}g}=\frac{c_y\varrho V_H^2}{2K\bar{Q}}. \tag{7.4}$$

We can use the ratio (7.3) expressing the equality of the aircraft's weight to its lift at the moment of touchdown or liftoff to find the landing velocity or the takeoff velocity as a function of the angle at which the jet stream is deflected /197

$$\sin\beta=\frac{1-\frac{c_y\varrho V_H^2}{2\bar{Q}}}{\bar{P}_0\left(f_1+\frac{f_2V_H}{P_{\text{ideal}}g}\right)}.$$

The landing velocity of the minimum liftoff velocity as a function of the angle by which the jet stream is deflected is shown in Figure 7.2 for the specific loading $\bar{Q}$ = 300 and 600 kg/m^2. The values of the function f_1 were taken from the study [6] for compressor ratio $\pi_{\text{compressor}}$ = 8 and the temperature forward of the turbine equal to 1,200°K, the function $f_2 = (1 + 0.2M^2)^{2.5}$. We can see from the graph that the efficiency with which the jet stream is deflected rises with increase in the deflection angle β and with increase in the thrust-to-weight ratio of the aircraft $\bar{P}_0$. Thus, for a specific loading /198 $\bar{Q}$ = 300 kg/m^2, thrust-to-weight ratio $\bar{P}$ = 0.6, and when the stream is deflected by an angle β = 85°, the landing and takeoff velocity is reduced approximately from 70 to 40 m/sec, and when $\bar{Q}$ = 600 kg/m^2--from 100 to 60 m/sec.

However, when the jet stream is deflected by an angle β < 90°, a horizontal component of the engine thrust appears, which can prove to be greater than the aerodynamic resistance of the aircraft at the landing velocity. In this case the aircraft will pickup in velocity and the landing will prove impossible. From the ratio (7.4) that expresses the equality of the force of gravity to the aerodynamic resistance of the aircraft we can find the value of the deflection angle β_1 at which the aerodynamic resistance of the aircraft is equal to the thrust, as a function of flight velocity

$$\cos\beta_1 = \frac{\frac{c_y \varrho V_H^2}{2K\overline{Q}} + \frac{\overline{P}_0 f_2 V_H}{P_{0\text{ideal}}\, g}}{\overline{P}_0\left(f_1 + \frac{f_2 V_H}{P_{0\text{ideal}}\, g}\right)}.$$

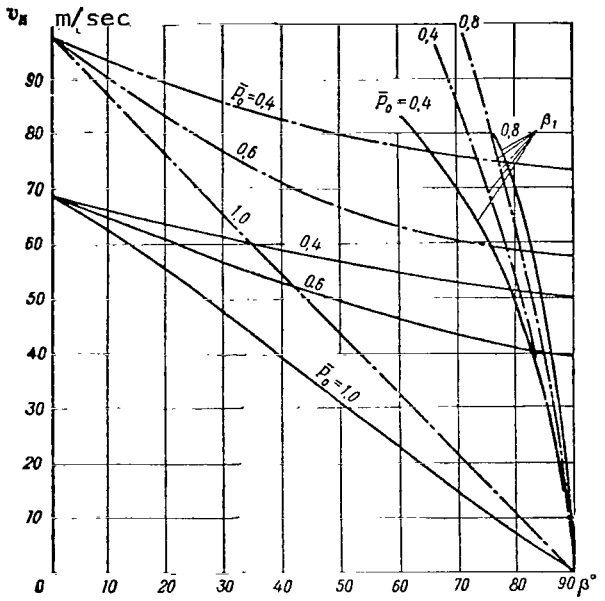

Figure 7.2. Minimum Separation Velocity and Landing Speed as a Function of Deflection of Jet and Angle β_1 at Which Thrust Is Equal to Drag of Aircraft for Various Values of Power and Specific Load on Wing $\overline{Q}$:

———— $\overline{Q}$ = 300 kg/m^2

-.-.-.-. $\overline{Q}$ = 600 kg/m^2

β_1 as functions of flight velocity have been plotted in Figure 7.2 for the appropriate values of the thrust-to-weight ratios and specific loadings. When the jet stream is deflected by an angle $\beta < \beta_1$ aerodynamic resistance of the aircraft is less than the force of gravity and landing is not possible. For deflection at an angle $\beta > \beta_1$, the aircraft reduces the flight velocity and landing does become possible. And, in contrast, in the takeoff run the jet stream cannot be deflected at an angle $\beta > \beta_1$, since if this is done takeoff velocity cannot be attained.

Thus, calculation shows that in landing it is necessary to turn the jet stream by an angle close to 90°.

If following landing of an aircraft with deflected jet stream engine thrust reversal is executed, the length of the aircraft's landing run will be substantially reduced. Figure 7.3 plots the length $L_{\text{landing run}}$ for the landing of an aircraft as a function of the reverse coefficient. The calculation was made for stream deflection angles and landing velocities corresponding to the points of intersection of the curves of V_H and β_1 in Figure 7.2.

Figure 7.3 presents, for comparison, a dashed line to indicate the landing run distances for an aircraft that does not use jet stream deflection. We can see

from the comparison that even without subsequent thrust reversal ($\bar{R}_{rev} = 0$) stream deflection is a highly effective means of reducing the aircraft landing run distance.

As was indicated above, the aircraft liftoff velocity in the takeoff run can be substantially reduced by deflecting the engine's jet stream. However, in takeoff runs with deflected streams the horizontal component of thrust is reduced, which leads to an increase in the distance over which the liftoff velocity is attained. In order to analyze the effect of the angle by which the resulting thrust of the engine is deflected, on the takeoff landing distance, we will write out the equation of aircraft movement in the takeoff run /200

$$\frac{Q}{g}\frac{dV_H}{dt}=\left(P+\frac{G}{g}V_H\right)\cos\beta-\frac{G}{g}V_H-\frac{c_x\varrho V_H^2}{2}S-$$
$$-\mu\left[Q-\frac{c_y\varrho V_H^2}{2}S-\left(P+\frac{G}{g}V_H\right)\sin\beta\right].$$

$L_{landing\ run}$

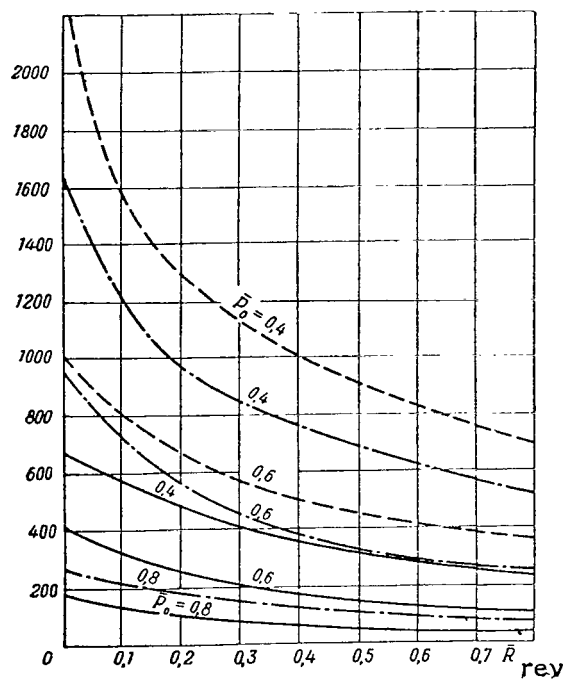

Figure 7.3. Landing Run Distance of an Aircraft as a Function of Reverse Coefficient: ———, Landing with Jet Stream Deflected and with Specific Wing Loading $\bar{Q}$ = 300 kg/m^2; - • - • ; Q = 600 kg/m^2 ; - - - -, Landing with Undeflected Jet.

Using the earlier introduced symbols, after transformations we arrive at an equation for aircraft acceleration $\ddot{x} = dV_H/dt$ in the following form:

$$\ddot{x}=\bar{P}_0 g\left[f_1(\cos\beta+\mu\sin\beta)-\frac{f_2 V_H}{p_0\cdot_{ideal}\ g}(1-\cos\beta-\mu\sin\beta)\right]- \quad (7.5)$$
$$-\left[\frac{c_y\varrho V_H^2}{2\bar{Q}}\left(\frac{1}{K}-\mu\right)+\mu\right]g,$$

where g = acceleration due to gravity;

μ = coefficient of frictional force of aircraft when making a landing or takeoff run on an airport.

The takeoff distance that must be traveled prior to attaining the liftoff velocity can be found by integrating the expression

$$L=\int_0^{V_H}\frac{VdV}{\ddot{x}}, \tag{7.6}$$

where $\ddot{x}$ = acceleration of aircraft, a familiar function of the velocity, determined by formula (7.5).

Results of graphic integration of the expression (7.6) for an aircraft with specific loading $\overline{Q}$ = 600 kg/m^2 for a coefficient of friction μ = 0.02 are shown in Figure 7.4 in the form of the takeoff run distance as a function of the angle by which the jet stream is deflected (solid curves). From inspection of the figure it is clear that the takeoff run distance has a minimum at some deflection angle β. This, as has already been remarked, is accounted for by the fact that as the angle of stream deflection is increased the liftoff velocity is reduced, as is the accelerating force. When the angle $\beta \geq \beta_1$, liftoff becomes impossible ($L \to \infty$). Thus, calculation shows that the takeoff run must be made, when the jet stream is not deflected, and the stream deflection mechanism cut-in only after the liftoff velocity has been attained. Here the takeoff run distances is considerably reduced and has a minimum at $\beta \approx 90°$ (dashed curves in Figure 7.4). However, here also it makes no sense /201 to deflect the jet stream by an angle greater than β_1 shown in Figure 7.3, since when this is done the aircraft following liftoff will be slowed down and cannot proceed to gain altitude.

For turbojet engine aircraft the engine axis is usually located in the plane of the wing chord and, consequently, in takeoff the turbojet engine stream is deflected by an angle β_1 that is approximately equal to the aircraft angle of attack. If the aircraft's angle of attack in liftoff is 10°, then the additional deflection of the jet stream by 20-25° with respect to the wing chord for aircraft that have a specific wing loading $\overline{Q}$ = 600 kg/m^2 will lead to a 6% reduction in takeoff run distance when the thrust-to-weight ratio $\overline{P}_0$ = 0.4, and a 20% reduction when the thrust-to-weight ratio $\overline{P}_0$ = 0.6 compared to the takeoff run distance without additional deflection of the jet stream. For the case of additional deflection of jet stream, only at the moment of aircraft liftoff, the reduction in takeoff run distance under these same conditions will be, correspondingly, 30-50%.

When there is a weak dependence of f_1 and f_2 as functions of velocity during the aircraft acceleration period, the expression (7.6) can be integrated

$$L_{\text{takeoff run}} = \frac{1}{2gA}\left[\ln\left(1+\frac{AV_H^2+BV_H}{C}\right)+\right.$$
$$\left.+\frac{2B}{\sqrt{B^2-4AC}}\operatorname{Ar\,th}\frac{V_H\sqrt{B^2-4AC}}{-(2C+BV_H)}\right],$$

where

$$A=-\frac{c_y\varrho}{2\overline{Q}}\left(\frac{1}{K}-\mu\right);$$

$$B=-\frac{\overline{P}_0 f_2}{P_{0\text{ ideal g}}}[1-(\cos\beta+\mu\sin\beta)];$$
$$C=\overline{P}_0 f_1(\cos\beta+\mu\sin\beta)-\mu;$$

V_H - aircraft liftoff velocity at the jet stream deflection angle of β.

Expanding in the series $\frac{V_H\sqrt{B^2-4AC}}{-(2C+BV_H)}$ and retaining only the first member of the series, we derive an approximational formula for calculating the takeoff run distance with jet deflected:

$$L_{\text{takeoff run}} = \frac{1}{2gA}\left[\ln\left(1+\frac{AV_H^2+BV_H}{C}\right)-\frac{2BV_H}{2C+BV_H}\right]. \tag{7.7}$$

The approximate value of the aircraft takeoff run distance when the stream is not deflected can be gotten from the relationship (7.7) by introducing in the appropriate coefficients $\beta = 0$,

$$L_{\text{takeoff run}} = \frac{1}{2Ag}\ln\left(1+\frac{AV_H^2}{C}\right), \tag{7.8}$$

where A has its former value but $C = \overline{P}_{0f_1} - \mu$.

The approximate expressions (7.7) and (7.8) determine the takeoff run distance of the aircraft with precision that is good enough for practical purposes. The total length of the takeoff run is defined as the distance over which the aircraft gains a specific altitude (about 15-25 m). This distance depends on the rate of climb near the ground at the takeoff weight of the aircraft. With the symbols we have already adopted, the angle of inclination γ of the aircraft trajectory is expressed via its characteristic as follows:

$$\tan\gamma = \frac{\frac{c_y \varrho V_H^2}{2\bar{Q}} + \bar{P}_0\left(f_1 + \frac{f_2 V_H}{P_{\text{ideal}}\, g}\right)\sin\beta - 1}{\frac{c_y \varrho V_H^2}{2K\bar{Q}} - P_0\left(f_1 + \frac{f_2 V_H}{P_{\text{ideal}}\, g}\right)\cos\beta + \frac{\bar{P}_0 f_2 V_H}{P_{0\text{ideal}}\, g}}. \qquad (7.9)$$

It is clear from expression, (7.9)that when the stream is deflected ($\beta > 0$) the rate of climb under otherwise equal conditions increases and the distance over which the altitude gain is made can also be shortened. However, we must also bear in mind that in calculating the takeoff run distance we have not allowed for losses of turbojet engine thrust that are associated with angling of the jet stream. The thrust losses will lead to an increase in the distance over which the liftoff velocity and altitude of 15-25 m are attained. /203

§3. Requirements Imposed on Deflectors Used on Lift-Thrust Turbojet Engines

To ensure maximum vertical thrust component, turning of the jet stream in the deflector must be executed with minimum losses of total pressure.

To avoid the effect of the deflecting device on performance of the turbocompressor group of the engine, gas pressures aft of the turbine with deflector cut-in and cut-out must be equal. Losses of positive engine thrust with deflector cut-in arise in devices used for deflecting jet thrust, constructed under Scheme II (cf. Figure 7.8), owing to gas leakage at the seal areas. These losses, as well as those in the reversers, must not be greater than 1%.

The operating conditions of vertical takeoff and landing aircraft show that a jet stream deflected downward can strike the engine inlet, boost the temperature of the inlet stream, and produce compressor stalling of the engine. If the stream deflected by the device escapes at an acute angle to the surface of the aircraft or the engine nacelle, then it flows along this surface, just as in the case of the reverser. Therefore, exiting of the stream must be organized in such a way that ingestion of gases at the engine inlet and along structural parts of the aircraft will be at a minimum.

The condition of stepless turning of the stream is extended also to deflectors. With the deflector cut-in there must not be any erratic variation of thrust and consumption. To cut down the takeoff distance when taking off with a short run the transition from horizontal thrust to vertical must be executed in 1-2 sec.

Just as for reversers, deflectors must be of minimum over-all dimensions and weight and must not increase the side resistance of the aircraft in horizontal flight. When the deflector is cut-in on an aircraft equipped with one or a number of engines, to avoid building up pitching, yawing and rolling moments, no asymmetrical thrust must be produced. This requirement is /204

achieved by synchronicity of the performance of deflectors. Deflectors must ensure maximum safety and reliability in operation.

Thus, the following main requirements are imposed on deflectors used on lift-thrust turbojet engines:

1. Ensuring high vertical component coefficient, and consequently, high coefficient of total pressure recovery.

2. The absence of any effect on normal functioning of the engine's turbocompressor group. In deflectors constructed under Scheme II (cf. Figure 7.8) thrust losses in horizontal flight must be at a minimum, not more than 1%.

3. Ingestion of the deflected jet stream at the engine inlet and along the structural parts of the aircraft must be at a minimum.

4. Stepless regulation of the turning of the jet stream must be provided.

§4. Description of Designs of Deflectors Used on Lift-Thrust and Lift Engines

Figure 7.5 presents a general view of the lift-thrust bypass Bristol-Siddeley BS-53 "Pegasus 5" engine (thrust 8,165 kg) produced for the Transsonic Hawker R-1127 Kestrel fighter-bomber (Great Britain) with vertical take-off and landing capability. The deflector was constructed under Scheme I[1]. Stand tests of the engine were begun in 1959, and in 1960 it underwent flight test. The engine has four tilting nozzles--two forward ones serve to angle the stream aft of the external pass compressor and the two rear serve to turn the stream of the inner engine pass aft of the turbine. Some of the air flow aft of the compressor of the outer pass is directed toward the inner main pass, and some--to a receiver that has two outlets with circular openings equipped with flanges on which the tilting nozzles are positioned. The gases of the inner pass aft of the turbine are directed to the exhaust pipe, terminating in two connecting pipes on which tilting nozzles have been installed. The nozzles are equipped with screens made of profiled vanes that ensure the required amount of stream turning.

Turning the nozzles by about 100° is done in stepless fashion, smoothly, with their fixation in a position, which governs the production of horizontal, vertical, or negative thrust or thrust at any intermediate angle. In Figure 7.6, we see a diagram of the control drive of the tilting nozzles[2]. Turning by an angle of 90° takes place in less than a second. /205

[1] *Interavia*, No. 4548, p. 4, 1960.
[2] *Flugwelt*, No. 3, p. 200, 1962.

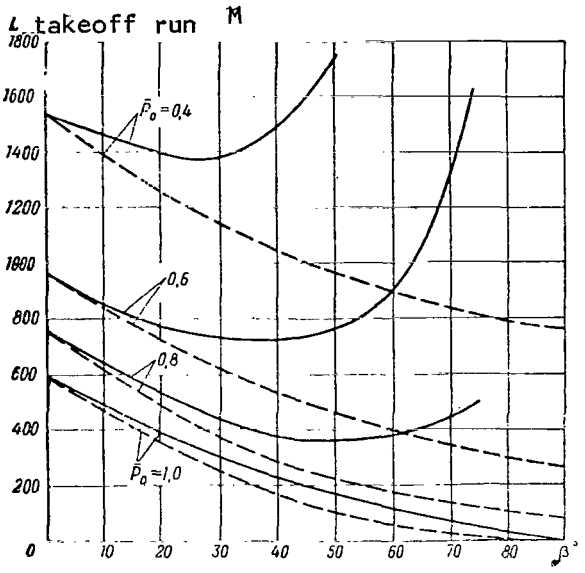

Figure 7.4. Takeoff Run Distance of an Aircraft as a Function of Angles by Which the Jet Stream is Deflected for Different Thrust-to-Weight Ratios $\bar{P}_0$: ———, Takeoff and Liftoff With Deflected Jet Stream; c_y = 1.0; - - - -, Takeoff With Undeflected Stream, Liftoff with Deflected Stream.

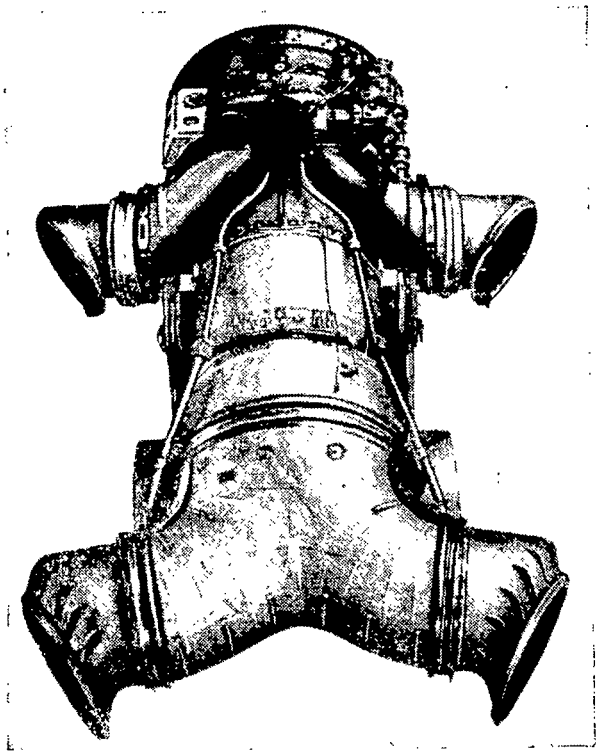

Figure 7.5. Bristol-Siddeley BS-53 Bypass Engine with Tilting Nozzles (Scheme I).

Figure 7.7. presents the experimental BS-100[1] lift-thrust bypass engine with afterburner chamber in the outer pass (thrust 17,000 kg), a modification of the Bristol-Siddeley BS-53 bypass engine. Use of a relatively low exit gas temperature in the afterburner (1,200°K) makes it possible to do without a special system for cooling the tilting nozzles. Sectioning of the nozzles is regulated by reflectors operating from the control mechanism. The BS-100 /206 engine is intended for the supersonic Hawker R-1154 fighter-bomber.

Figure 7.8 presents a general view of the experimental lift-thrust Rolls-Royce "Medueus" bypass engine (thrust 7,940 kg) equipped with a deflector constructed under Scheme II[2]. It consists of two tilting shutters and two connecting pipes (Figure 7.9) terminating in circular tilting nozzles equipped with deflecting screens [34]. In the nonworking position of the deflector, the shutters are positioned flush with the walls of the exhaust pipe, partition the side inlet windows of the connecting pipes, and do not block the

[1] *Flight*, Vol. 21/X, No. 2954, p. 693, 1965.
[2] *Aeroplane*, Vol. 5/III, No. 2733, p. 20, 1964.

direct exiting of the stream into the jet nozzle. When the deflector is in the operative position the shutters rotate backward, partition the gas duct and, opening simultaneously the inlet windows of the connecting pipes, direct the gases through the connecting pipes to the tilting nozzles. Depending on the nozzle position, set by the pilot, the jet stream can be deflected vertically downward (in vertical takeoff and landing of an aircraft), rearward (in acceleration), forward (in deceleration), or in any other intermediate direction. The Medueus engine was intended for the heavy military transport Hawker-Siddeley HS-681 with a short takeoff run. A similar deflector (Figure 7.10) has also been installed on the Rolls-Royce RB-163 "Spay" bypass engine (thrust 4,470 kg)[1]. /208

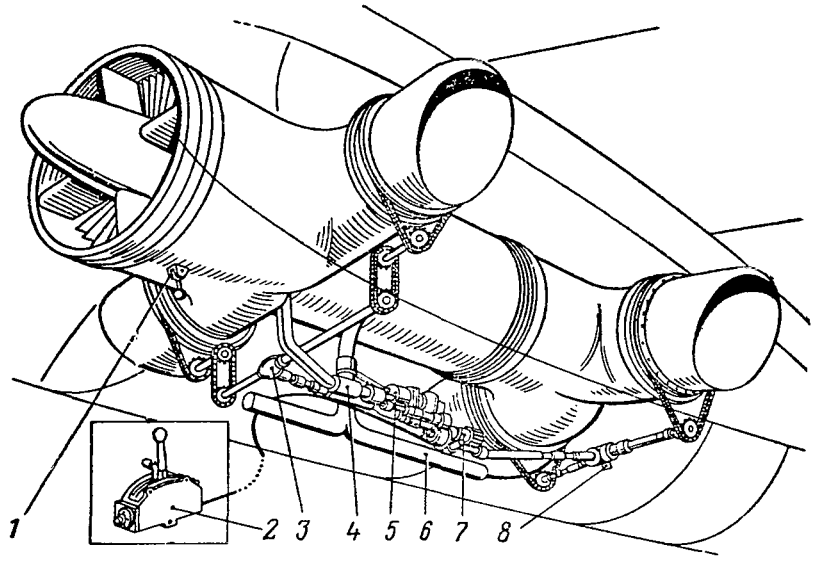

Figure 7.6. Diagram of Control Drives for Tilting Nozzles on the Bristol-Siddeley BS-53 Bypass Engine: 1, Engine Suspension; 2, Nozzle Control Lever in Pilot Cabin; 3, Forward Conical Transmission; 4, Air Bleed Valve; 5, Two Pneumatic Mechanisms with Rotating Pistons; 6, Air Conduit to Stabilizing Nozzle; 7, Reducer; 8, Rear Conical Transmission.

[1] *Aviation Week*, VI, Vol. 78, No. 25, p. 71, 1963.

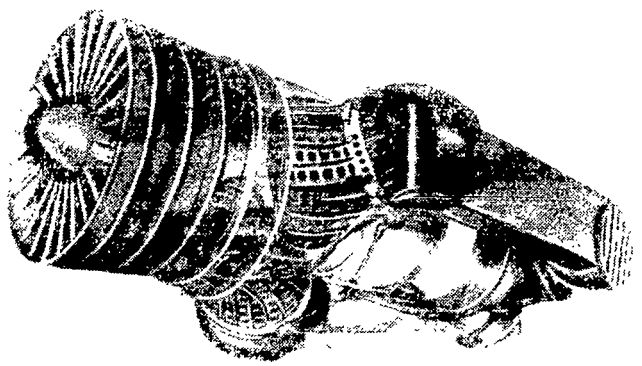

Figure 7.7. Bristol-Siddeley BS-100 Bypass Engine with Afterburner, Equipped with Tilting Nozzles with Afterburner in the Outer Pass.

The MAN Company, jointly with Rolls-Royce has produced the RB-153-61 bypass engine with afterburner (thrust without afterburner 3,107 kg, with afterburner 5,300 kg) which is equipped with a device for deflecting the jet stream that has been developed by the MAN Company (Figure 7.11). The deflector is located forward of the afterburner chamber. It has been proposed to install two engines on the vertical liftoff fighter VJ101D (FRG). Therefore, the deflector has been made with nonsymmetrical gas discharge[1]. /209

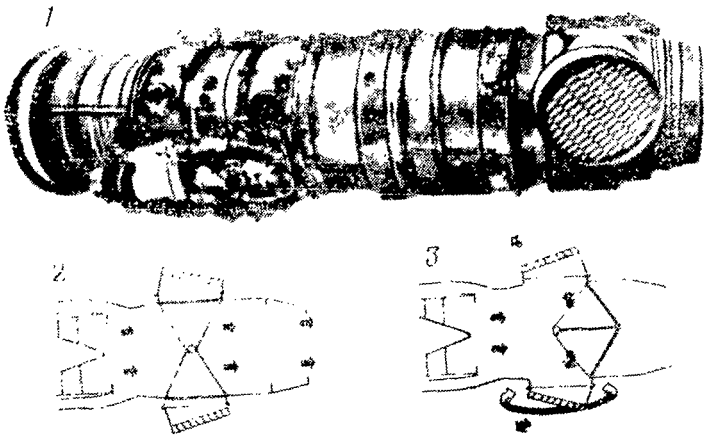

Figure 7.8. Rolls-Royce Bypass Engine Medueus with Deflector, and Its Operating Principle (Scheme II): 1, General View of Engine; 2, Position of Device for Deflecting Jet Stream in Flight; 3, In Takeoff, Landing, and Deceleration of the Aircraft.

Installation on an aircraft of the Scheme II deflector compared with Scheme I does afford certain advantages [4]. In Scheme I relatively high thrust losses due to turning of the stream in the bends of the connecting pipes and in the screens occur even in horizontal flight. Scheme II allows

[1] *Interavia*, Vol. 15/V, No. 5495, p. 6, 1964.

us to choose the thrust nozzle and the tilting (lift) nozzles in such a way that in takeoff maximum thrust is attained, but in horizontal flight the engine continues to operate in the minimum specific fuel consumption mode. In Scheme II thrust losses are caused, just as in the reversere of the similar scheme, only by gas leakage in the assembly of the throttling shutters. In the cruising mode Scheme II provides better economy compared to Scheme I. The engine nacelle for the power plant built under Scheme III can be designed with minimum lateral surface area. The Scheme II also exhibits operational advantages. In takeoff, in the initial acceleration of the aircraft the thrust nozzle is used. The tilting nozzles deflecting the jet stream downward precisely before liftoff of the aircraft (cf. §2 of this chapter) can be fixed at the required angle in advance and held in this position. This guarantees that the required direction of thrust in the critical section of liftoff will be provided. If the aircraft takes off in the usual way, then the tilting nozzle can be fixed in advance in the negative thrust position in the event that the liftoff has to be aborted. /210

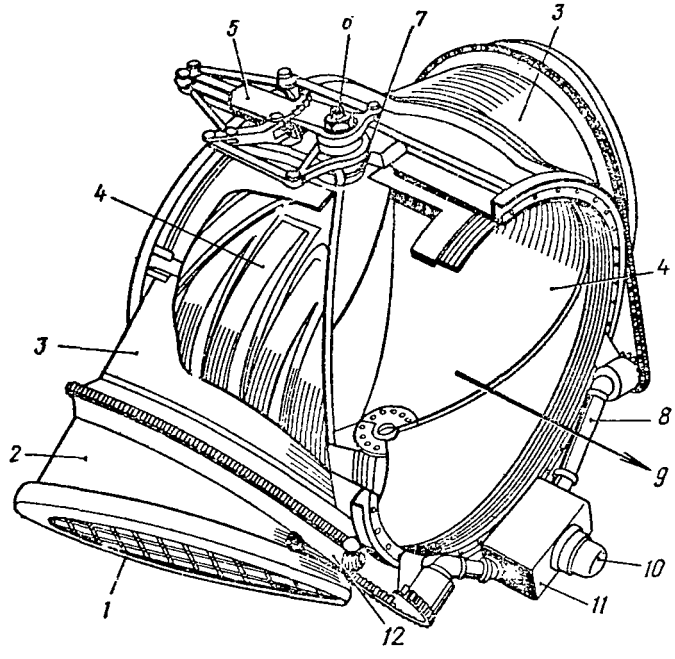

Figure 7.9. Assembly of Deflector Used in the Rolls-Royce Medueus Bypass Engine. Position of Shutters in Horizontal Flight: 1, Screen; 2, Tilting Nozzle; 3, Bend; 4, Shutters; 5, Hydrocylinder for Shutter Control; 6, Lift Lug; 7, Roller Bearings of Shutters; 8, Drive Shaft of Nozzle Tilting Mechanism; 9, Direction of Gas Flow to Jet Nozzle; 10, Hydraulic Motor of Nozzle Tilting Mechanism; 11, Reducer; 12, Tilting Nozzle Ball Bearing.

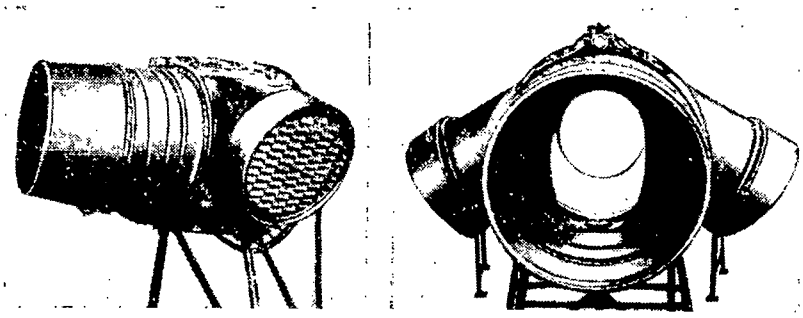

Figure 7.10. Deflector and Jet Nozzle of the Rolls-Royce "Spay" RB-163 Bypass Engine.

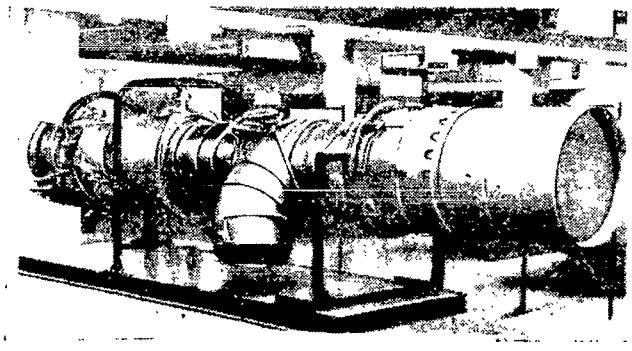

Figure 7.11. Rolls-Royce MAN RB-153-61 Bypass Engine with Deflector.

However, the problem of ingestion of exhaust gases at the engine inlet is more simply solved in the variant of Scheme I incorporating four tilting nozzles if the first nozzle pair is installed aft of the fan. The cold air streaming from these nozzles prevents incursion of exhaust gases from the rear pair of tilting nozzles into the engine inlet.

Figure 7.12 presents the tilted nozzle[1] of the Rolls-Royce RB-162 lift turbojet engine (thrust 2,000 kg), which can be deflected 15° to both sides relative to the engine axis. This lift engine is envisaged in 20 planned for vertical takeoff and landing aircraft now being developed in a number of foreign countries.

Noteworthy are deflectors used on lift engines of the experimental transsonic VTOL Dassault "Balzac" (France). A screen of tilting deflecting vanes, /211 which serve the following three functions, installed at the jet nozzle exit:

1. In flight, when the tilting angle is equal to zero, the vanes cover over the exit area of the engine nacelle of the lift engine and prevent bypassing of air between the lower and upper surfaces of the aircraft.

---

[1] *Luftfahrttechnik-Raumfahrttechnik*, No. 5, p. 135, 1964.

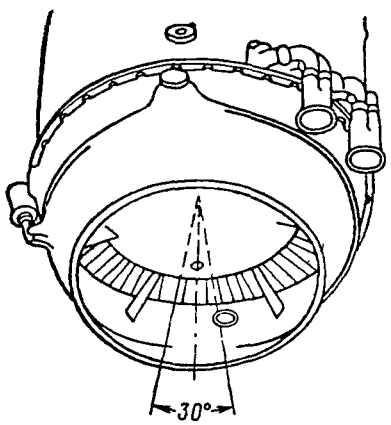

Figure 7.12. Tilted Nozzle of the Lift RB-162 Rolls-Royce Turbojet Engine.

2. In takeoff, the vanes are turned by 45° and deflect the jet stream downward. This prevents circulation of exhaust gases and simplifies the transition from takeoff to horizontal flight.

3. The gases do not strike the ground vertically, but are diverted rearward under the aircraft, which provides some interval of time between ignition of the engine and the lift required to check the engine and the control systems before they are switched over to full thrust.

The use of this deflecting screen makes it possible to solve the problem of takeoff from an unimproved area and to land in the same kind of runway. In flight, when the screen vanes are positioned at an angle of 90°, rarefaction is produced in the nozzle, affording start-up of engines before landing without use of a starter[1].

§5. Fundamentals of Gas Dynamic Calculation of Deflectors[2]

Under stand conditions the horizontal component of the thrust is equal to the sum of projections of the impulse of the deflected stream and the impulse of gas escaping from the nozzle in the straight-line direction:

$$R_{\text{horizontal}} = \frac{G_2}{g} v_2 \cos\beta + \frac{G_1}{g} v_1. \tag{7.10}$$

The horizontal thrust component will be as follows for stand conditions without bypassing of the gas to the jet nozzle

$$R_{\text{horizontal}} = \frac{G_2}{g} v_2 \cos\beta. \tag{7.11}$$

Vertical component of thrust

---

[1]*Interavia Review*, Vol. 19, No. 1, p. 48, 1964.
[2]Deflectors used with lift-thrust engines constructed under Scheme III are under consideration (cf. Figure 7.8).

$$R_{\text{vertical}} = \frac{G_2}{g} v_2 \sin\beta. \tag{7.12}$$

In these equations: /212

G_2 and v_2 = consumption through the deflector and the velocity at its exit;

G_1 and v_1 = consumption through the jet nozzle when the stream is deflected, and gas velocity at its exit;

β = angle between the direction of velocity v_2 and the horizon.

The equations (7.10, 7.11, and 7.12) have been written for the case of uniform pressure fields and the stream exit angle and complete expansion of gas in the exit area of the deflector and the jet nozzle.

Introducing the gas dynamic function f and the coefficients of total pressure recovery in the deflector σ_2 and in the nozzle σ_1 with the deflector cut-in, equations (7.10) and (7.12) can be transformed

$$R_{\text{hor}} = p_H F_2 \cos\beta [\pi^*_{\text{noz}} \sigma_2 f(\lambda_2) - 1] + p_H F_1 [\pi^*_{\text{noz}} \sigma_1 f(\lambda_1) - 1]; \tag{7.13}$$

$$R_{\text{ver}} = p_H F_2 \sin\beta [\pi^*_{\text{noz}} \sigma_2 f(\lambda_2) - 1], \tag{7.14}$$

where F_2 = minimum cross-sectional area of deflector;

F_1 = jet nozzle area when the stream is deflected.

The expression for the overall consumption is written in the following form:

$$G = m p_H \frac{\pi^*_{\text{nozzle}}}{\sqrt{T_0}} [F_2 q(\lambda_2) \sigma_2 + F_1 q(\lambda_1) \sigma_1)]. \tag{7.15}$$

For the combustion products of a turbojet engine, m = 0.389, for air m = = 0.3965.

The values of gas dynamic functions $f(\lambda)$ and $q(\lambda)$ are found from the known coefficients of total pressure recovery σ_2 and σ_1 from the tables listing the ratios

$$\Pi(\lambda_2) = \frac{1}{\pi^*_{\text{nozzle}} \sigma_2}, \quad \Pi(\lambda_1) = \frac{1}{\pi^*_{\text{nozzle}} \sigma_1}.$$

For the case of nonuniform pressure fields and angles in the exit area of the deflector and the jet nozzle, equations (7.13, 7.14, and 7.15) are expressed in integral form.

The thrust components of the engine are written as follows in terms of the coefficients of horizontal and vertical thrust components in the presence of an external flow /213

$$P_{\text{horizontal}} = \overline{R}_{\text{horizontal}} \left(P_{\text{ideal}} + \frac{G}{g} V\right) = \frac{G}{g} V, \tag{7.16}$$

$$P_{\text{vertical}} = \overline{R}_{\text{vertical}} \left(P_{\text{ideal}} + \frac{G}{g} V\right), \tag{7.17}$$

where P_{ideal} = ideal straight-line thrust of an engine, calculated for the condition of total expansion of gas in the nozzle.

CHAPTER VIII

EXPERIMENTAL RESEARCH ON DEFLECTORS IN MODEL FORM /214

§1. Deflectors Used to Lift-Thrust Engines

Deflectors With a Connecting Pipe and Throttling Shutters

The scheme of this deflector is shown in Figure 8.1. The deflector is placed between the turbine and the after chamber, as a consequence of which the parts of the unit are not subjected to high temperatures in the afterburner regime. The stream of gases after the turbine is emitted into the atmosphere through the deflecting connecting pipe formed by fixed lateral and tilting walls 1. A tilting guide vane 2 is installed in the connecting pipe. When the device has been cut-in, the throttling shutters 3 form a cone and direct the stream of gases into the connecting pipes. Some of the gases escape in a straight line through the gaps between the throttling shutters and the cowling (bypassing), into the jet nozzle 4. The area of the clearances is about 5% of the jet nozzle cross-sectional area.

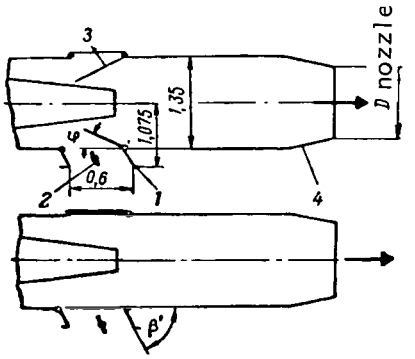

Figure 8.1. Deflector Equipped with a Connecting Pipe and With Throttling Shutters: 1, Tilting Walls; 2, Guide Vane; 3, Throttling Shutters; 4, Jet Nozzle.

The model has been studied for design angles of wall inclination β', equal to 78°, 60°, 45°, and 33°. For the values of the angle β' adopted, the exit areas of the deflector were chosen that ensured the same consumption with the device cut-in as when it was not operative. /215

Coefficients of vertical thrust component $\overline{R}_{ver}$ and horizontal thrust components $\overline{R}_{hor}$ as functions of the design angle β' are listed in Figure 8.2. The variation in the coefficient $\overline{R}_{ver}$ and $\overline{R}_{hor}$ with change in wall tilting angle ϕ in the working regime for $\pi^*_{nozzle} = 2.2$ is given in Figure 8.3.

The nature of the dependence of $\overline{R}_{hor}$ and $\overline{R}_{ver}$ on the stream exit angle (cf. Figure 8.2) is determined mainly by variation of the variables sin β and cos β (equations 7.10 and 7.12).

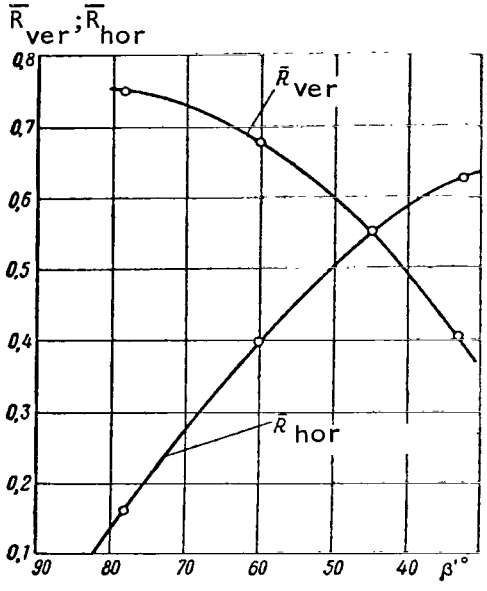

Figure 8.2. Coefficient $\bar{R}_{hor}$ and $\bar{R}_{ver}$ as Functions of the Angle β' of the Model in Figure 8.1 When π^*_{nozzle} = = 2.2.

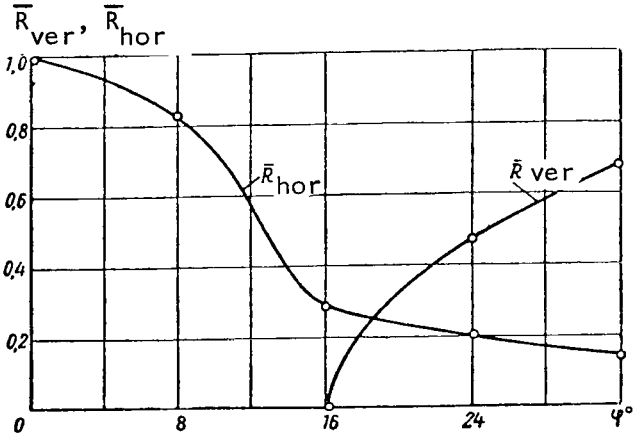

Figure 8.3. Coefficients $\bar{R}_{hor}$ and $\bar{R}_{ver}$ as Functions of the Angle φ By Which the Throttling Shutters of the Model in Fig. 8.1 are Tilted for π^*_{nozzle} = 2.2.

In the working regime, for the greatest design angle of inclination of deflector walls β' = 78° (Figure 8.4), the value $\bar{R}_{ver}$ = 0.75 and the coefficient of the resultant thrust $\bar{R}_{defl}$ = 0.77[1]. When the walls are positioned at an angle β' equal to 60°, 45°, and 33°, the value of $\bar{R}_{defl}$ lies within the limits 0.75-0.78.

The low $\bar{R}_{defl}$ values are explained by poor profiling of the throughput section of the deflector.

The consumption coefficient was retained at a constant value for all π^*_{nozzle} values in the investigated scheme of the deflector, just as in the similar scheme of the reverser. /216

Deflector Equipped with a Screen and Throttling Shutters

The deflector with throttling shutters and a deflecting screen (Figure 8.5) differs from that described above in that a screen of strips with a design angle β' = 90° is used in the deflector. The bypass area is about 5% of the jet nozzle area. Measurements showed that $\bar{R}_{hor} \approx 0$.

The maximum value $\bar{R}_{ver}$ = = $\bar{R}_{defl}$ when π^*_{nozzle} = 2.2 in this deflector was only 0.73, which is close to the values for deflectors described above

[1]Definitions of $\bar{R}_{ver}$, $\bar{R}_{hor}$, $\bar{R}_{defl}$, and $\bar{G}_{defl}$ have been presented above (§1, Chapter III).

In this way, installation of a screen of strips in the deflecting connecting pipes did not have any effect.

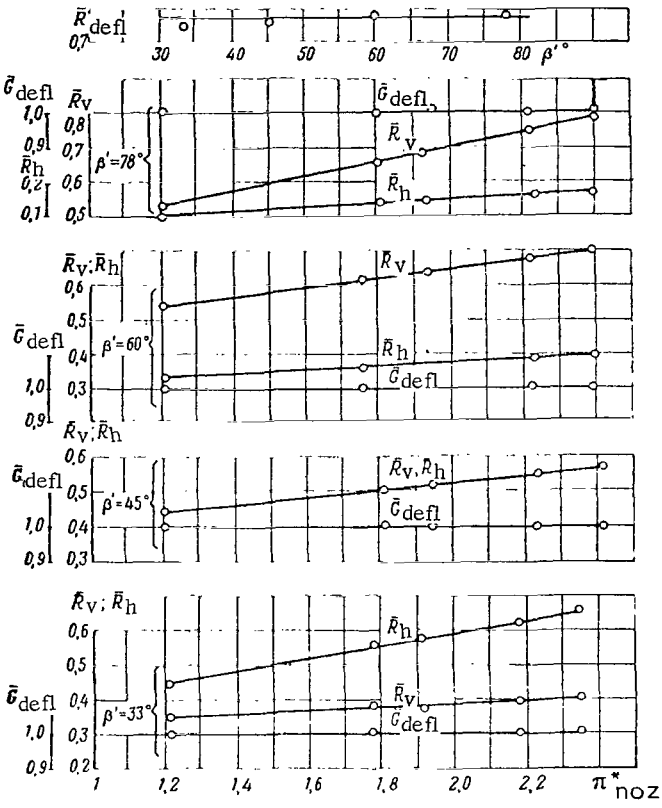

Figure 8.4. Coefficients $\bar{R}_{hor}$, $\bar{R}_{ver}$ and $\bar{G}_{defl}$ as Functions of π^*_{nozzle} for the Figure 8.1 Model for a Different β', and the Coefficient $\bar{R}_{defl}$ as a Function of the Angle β' when π^*_{nozzle} = 2.2.

Deflector Located Aft of the Jet Nozzle Exit Area

The scheme of the deflector shown in Figure 8.6 when the jet stream is deflected the shutters 1 and 2 rotating on pins 3 are fixed aft of the jet nozzle 4 and direct the stream downward. In the cut-out position the shutters are hinged in the horizontal position and extend beyond the limits of the nozzle, /218 not preventing direct stream exiting. The device can be used in non-afterburner and afterburner engine regimes. The afterburner regime provides higher thrust-to-weight ratio for the aircraft, and consequently, a higher vertical thrust component when the jet stream is deflected. In the model of the deflector cylindrical shutters for simplicity have been replaced by a connecting pipe which is secured to the jet pipe by means of a flange. The design of the model affords variation in the connecting pipe exit area by means of inserts. Studies have been conducted for a consumption coefficient equal to unity. When the entire flow is deflected the value $\bar{R}_{ver} \approx$ $\approx$0.9 is attained for π^*_{nozzle} = = 2.2.

Deflectors Incorporating Doubled Tilting Nozzles /219

The scheme of the deflector that series to deflect the jet stream by means of twinned tilting nozzles is shown in Figure 8.7. In the indicated position of the tilting nozzles 1 equipped with screen 2, direct exiting of the jet stream is provided. To deflect the stream downward in order to build up lift, the nozzles are rotated on flanges 3 by the angle β' = 90°. For

thrust reversal the nozzles are rotated by the angle $\beta' = 90°$. The deflector used on the Bristol-Siddeley BS-53 bypass engine (Great Britain) has been built according to this scheme.

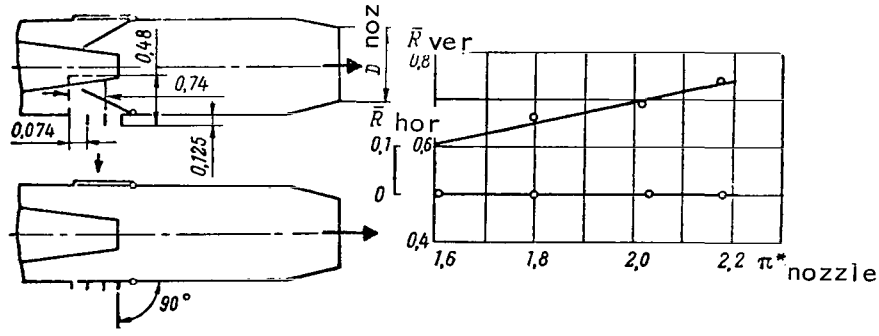

Figure 8.5. Deflector Incorporating a Screen and Throttling Shutters, and its Experimental Characteristics.

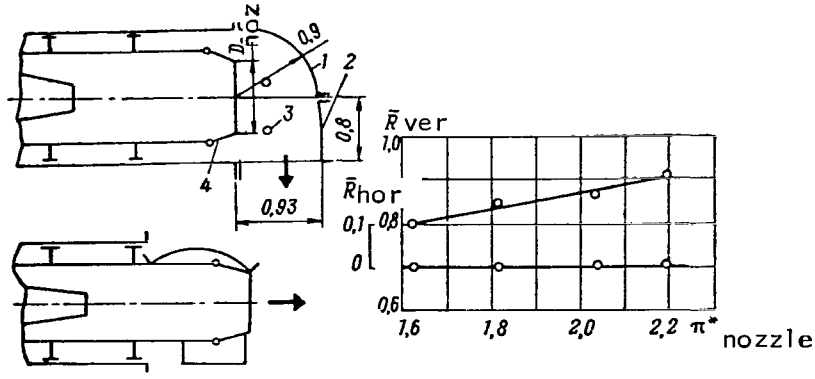

Figure 8.6. Deflector Positioned Aft of the Jet Nozzle Exit Area, and Its Experimental Characteristics.

The following variants of tilting nozzles were investigated:

1. Tilting nozzles that have leafwise vanes of screens with constant pitch (Figure 8.8):

a) Three-vane with relative screen pitch $t/c = 0.576$, where t is the screen pitch and c = vane chord;

b) Four-vane ($t/c = 0.461$);

c) Five-vane (t/c = 0.385).

2. Tilting nozzles that are equipped with leafwise vanes of screens with variable pitch (Figure 8.9):

a) Three-vane (t/c = 0.796; 0.64; 0.51; 0.359);

b) Four-vane (t/c = 0.575; 0.524; 0.473; 0.421; 0.312);

c) Five-vane (t/c = 0.46; 0.43; 0.40; 0.37; 0.337; 0.308).

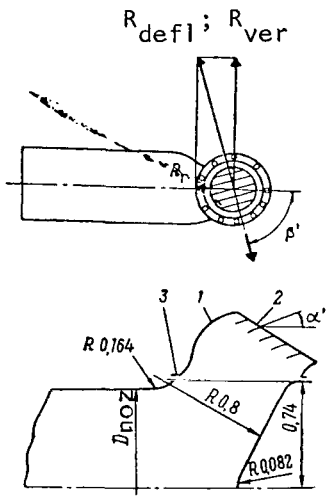

Figure 8.7. Deflector with Twinned Tilting Nozzles with Five-vanes with Constant Pitch: 1, Nozzle; 2, Screen; 3, Flanges.

A model of the device was built in accordance with the scheme. Only the thickness of the vanes was not modeled owing to its small value. The reduced velocity at the inlet to the model was about 0.65. Measurements were made of the vertical R'_{vert} thrust complement using a model with a single nozzle.

The nature of the curves of $\bar{R}_{hor}$, $\bar{R}_{vert}$ $\bar{R}'_{vert}$ as a function of π^*_{nozzle} for nozzles with three, four and five vanes at constant and variable pitch is approximately the same. In the range π^*_{nozzle} = 1.6-2.0, the values $\bar{R}_{hor} \approx \bar{R}_{ver} \approx 0.93$.

It follows from an examination of the data on $\bar{R}'_{ver}$ that the pattern of the curves $\bar{R}'_{ver}$ and $\bar{R}_{ver}$ is similar. The values of the $\bar{R}'_{ver}$ coefficients differ from those of $\bar{R}_{ver}$ mainly in absolute values. In the range π^*_{nozzle} = 1.6-2.4, the coefficient $\bar{R}^*_{ver} \approx 0.97$. Thus, a large part of the thrust losses in the device under study (about 4%) is associated with cleavage of the flow in the exhaust pipe and with its deflection in the bends of the tilting nozzles, and a smaller part (about 3%)--with deflection of the stream in the deflecting screens. From the data in the study [35], the coefficient of the thurst produced by individual tilting nozzles equipped with a screen is 0.97, but the coefficient the thrust of the entire deflector (considering losses in cleavage and turning of the stream in the jet pipe) is 0.9 based on the information given in the study [42].

/221

For all the investigated tilting nozzle models, the measured consumption levels for direct and deflected thrusts were the same.

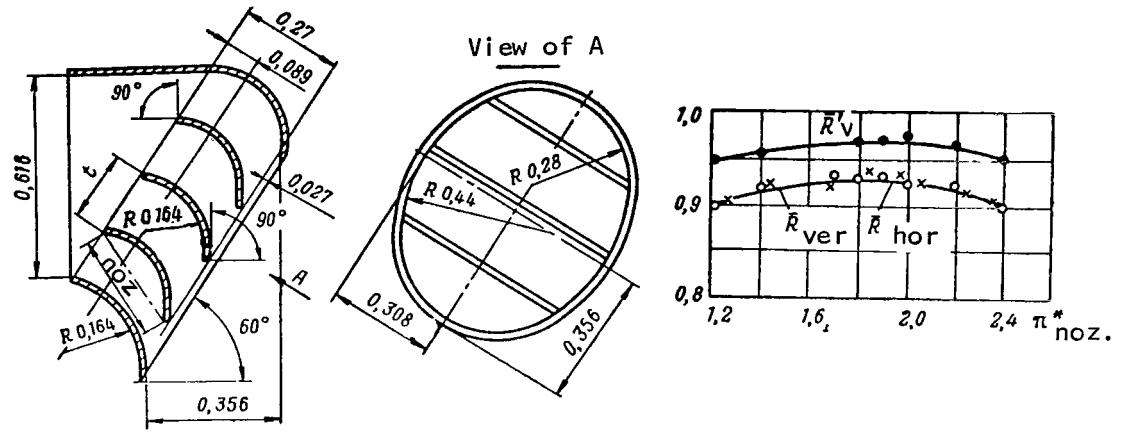

Figure 8.8. Tilting Nozzle With Constant Screen Pitch, and Experimental Characteristics for Four Vanes.

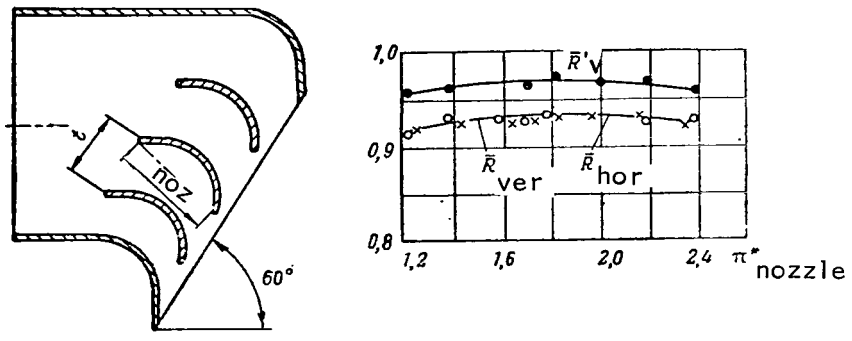

Figure 8.9. Tilting Nozzle With Variable Screen Pitch, and Experimental Characteristics for Use of Three Vanes.

The experiment established that as the angle of nozzle rotation β' is changed, the coefficients of horizontal and vertical thrust components are varied, respectively, in proportion to the variables cos β' and sin β'. The coefficient of the resulting thrust $\bar{R}_{defl}$ proved to be practically constant as the angle β' is changed when π^*_{nozzle} = const.

The actual stream exit angles were determined from the measured values of the horizontal $\bar{R}_{hor}$ and vertical $\bar{R}_{ver}$ thrust components. Measurements revealed that the geometrical angles β' and α', respectively, and the exit angles β and α agree.

Deflectors Incorporating a Single Tilting Nozzle[1] /222

A single tilting nozzle 1 (Figure 8.10) with a deflecting screen can be installed in a VTOL engine. In the position shown in the figure, the stream exits in the direction of the engine axis. The total lift is produced when the nozzle on the flange 2 is rotated by an angle equal to 120°. These tilting nozzles can be used in power plants that have two symmetrically arranged /223 engines, but they require synchronous control of the tilting nozzles.

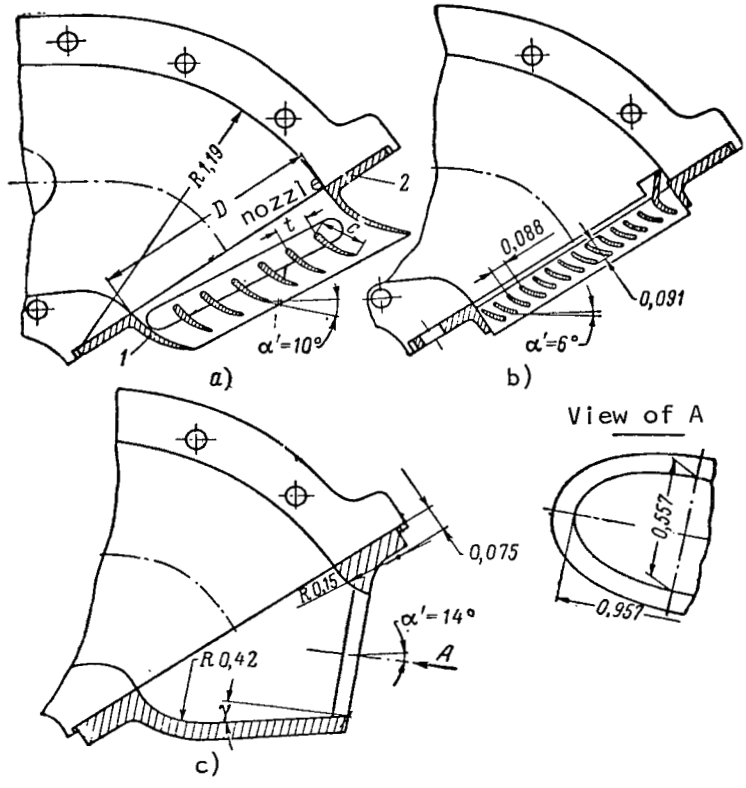

Figure 8.10. Single Tilting Nozzles: a, With Deflecting Screen Made up of Profiled Vanes: 1, Tilting Nozzle with Deflecting Screens; 2, Flange; b, With Screen Made of Leafwise Profiles: c, without Screens.

[1]The tilting nozzles were developed by V. N. Bazarov, A. P. Lev, etc. and were investigated by A. P. Lev and K. N. Popov.

The gas duct from aft of the turbine up to the tilting nozzle was constructed with a constant cross-sectional area. The possibility of increasing the coefficients of horizontal and vertical thrust components produced by the deflector via variation in the design of the throughput part of the tilting nozzle was explored. The following variants of the tilting nozzles were tested:

1. a nozzle with a deflecting screen made of profiled vanes. A deflecting screen with profiled vanes that had a relative pitch $t/c \simeq 0.7$ (cf. Fig. 8.10 a) was installed in its exit cross-section, elliptical in form.

2. nozzle with deflecting screen made of leafwise profiles. This was a variant of the nozzle differing from the foregoing in the fact that its exit section was circular in form and in it was installed a deflecting screen divided by twelve transverse stiffeners (cf. Figure 8.10 b). The screen was made of leafwise profiles with the aim of simplifying the design and reducing its manufacturing costs in production. The relative screen pitch $t/c \cong 0.78$.

3. nozzle without deflecting screen but with elliptical exit area. In contrast to the foregoing variants, the nozzle was built without a screen in the exit area in order to simplify cooling of the nozzle when operating an engine at high gas temperature (cf. Figure 8.10 c). Two variants of this nozzle were tested with angles γ of the nozzle wall inclination to its axis of 10 and 20°.

For the investigated nozzle variants, Figure 8.11 presents their experimental characteristics--the values of the coefficients $\bar{R}_{hor}$, $\bar{R}_{ver}$, $\bar{R}_{defl}$, the coefficient of total pressure recovery σ_{defl}, and the angle of stream exit α, determined from the values of R_{hor} and R_{ver}.

By comparing characteristics we can see that the thrust coefficients $\bar{R}_{hor}$ and $\bar{R}_{ver}$ of the four variants of the tilting nozzles in the working range of pressure reduction $\pi^*_{nozzle} = 2.0\text{-}2.5$ are approximately equal and amount to $\bar{R}_{hor} \approx \bar{R}_{ver} \approx 0.95$. The coefficient $\bar{R}_{defl} \approx 0.96$. As π^*_{nozzle} is decreased from 2.0 to 1.3, the thrust coefficients for these nozzle variants are reduced down to the values $\bar{R}_{hor} \approx \bar{R}_{ver} \approx 0.88$. The coefficients $\bar{G}^*_{hor}$ for all the pressure reduction levels investigated were maintained constant--$\bar{G}_{hor} = 1.0$.

The angle α of stream exit remains constant and is about 10° as π^*_{nozzle} is varied for the variant a. For the nozzle in variant b, the value of α is also kept constant, but is somewhat lower in value ($\alpha = 6°$). For the two /225

[1]The definition of $\bar{G}_{hor}$ has been given above (§1, Chapter III).

variants c, the angle α is reduced with increase in the extent of pressure reduction.

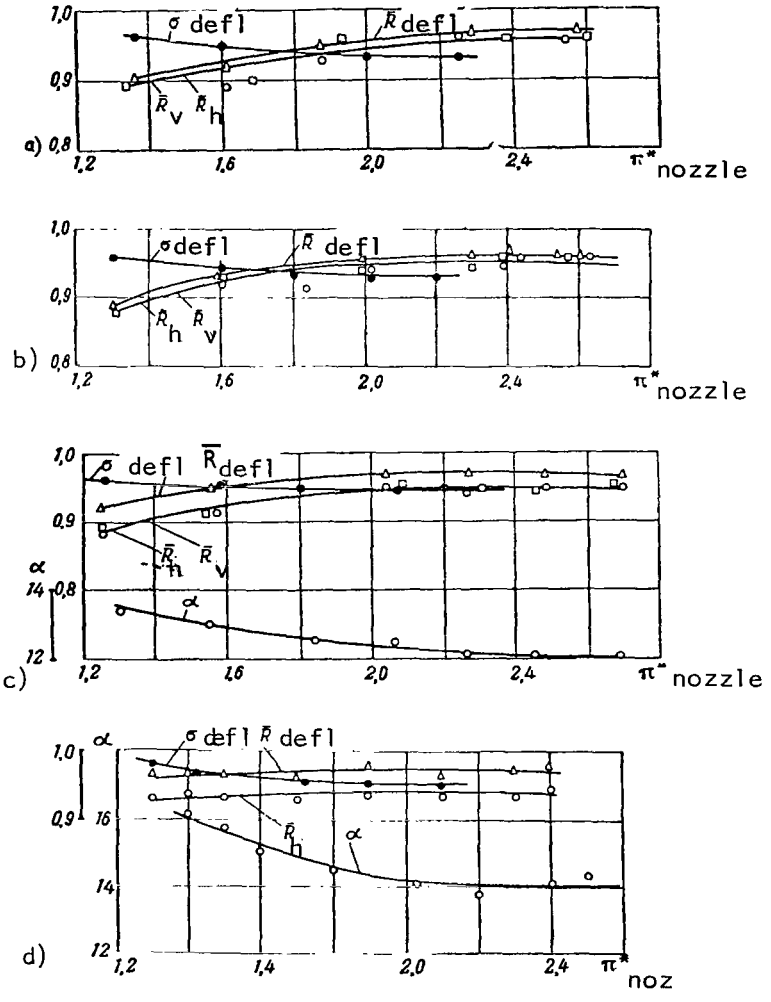

Figure 8.11. Coefficients $\overline{R}_{hor}$, $\overline{R}_{ver}$, and $\overline{R}_{defl}$, and the Angle α for the Tilted Nozzle as Functions of the Extent of Pressure Reduction: o, $\overline{R}_{hor}$; □, $\overline{R}_{ver}$; Δ, $\overline{R}_{defl}$; ●, σ_{defl}; a, With Screen Made of Profiled Vanes; b, With Screen Made of Leafwise Profiles; c, Without Screen When γ = 20°; d, Without Screen When γ = 10°.

The practical agreement of the thrust coefficients for the nozzle variants investigated is explained by the fact that part of the exhaust duct forward of their tilting nozzles is the same, but the different designs of the deflecting screens and the tilting nozzles are constructed with such a high degree of improvement that they ensure almost identical total pressure losses. The horizontal and vertical thrust components, as the angle of nozzle tilting β' is varied, as shown by tests, are varied, respectively, proportionally to the values of cos β' and sin β'.

Deflector Incorporating Tilting Nozzles and Throttling Shutters

The model of the deflector described here is given in Figure 8.12. It has a straight-line jet nozzle 1 and two connecting pipes 2 equipped with tilting nozzles 3 incorporating deflecting screens. The nozzles, tilting by means of a special mechanism, can deflect the stream downward to produce lift, deflected at an angle less than 90° when the aircraft is accelerating, and also deflect the stream at an angle greater than 90° (to as much as 180°) to produce negative horizontal thrust components when landing.

The device has two cylindrical throttling shutters 4, which, rotating on the pins 5, expose the inlet windows of the connecting pipes 2 and block direct exiting of the thrust through the jet nozzle.

The vanes in the deflecting screens were made of sheet 0.5 mm thick with an angle at the inlet equal to 90°, and at the outlet--30°. The relative pitch of the screen was equal to $t/c \approx 0.7$.

Figure 8.13 presents the values of the horizontal thrust coefficients $\overline{R}_{hor}$ in the case of direct (horizontal, $\beta' = 0$) exiting of the stream from the tilting nozzles, vertical thrust $\overline{R}_{ver}$ when the stream was deflected downward ($\beta' = 90°$), negative thrust $\overline{R}_{rev} = R_{rev}/R_{ideal}$ when the nozzles were in a position deflecting the thrust horizontally in the reverse direction ($\beta' = 180°$), resultant thrust $\overline{R}_{defl}$, consumption coefficient $\overline{G}_{defl}$[1], and the coefficient of total pressure recovery σ_{defl}. To prevent leakage of air in testing, the jet nozzle of the model was covered with an end cap 6 (cf. Figure 8.12).

From inspection of Figure 8.13 it follows that the coefficients $\overline{R}_{hor}$, $\overline{R}_{ver}$, and $\overline{R}_{rev}$ in the investigated range $\pi^*_{nozzle} = 1.3\text{-}2.0$ increase. Within the limits $\pi^*_{nozzle} = 2.0\text{-}2.5$, the values of the thrust composition are retained approximately constant $\overline{R}_{hor} \approx \overline{R}_{ver} \approx \overline{R}_{rev} \approx 0.9$. The consumption /227

[1]Definition of $\overline{G}_{defl}$ has been given above.

coefficient for all values of π^*_{nozzle} and nozzle tilting angles prove to be equal to unity. Consequently, tilting the nozzle when deflecting the jet stream does not have any effect on parameters of the turbocompressor groups of the engine. The coefficient of resultant thrust is equal to the coefficients of horizontal, vertical, and negative thrust $R_{defl} \approx R_{hor} \approx R_{ver} \approx R_{rev}$.

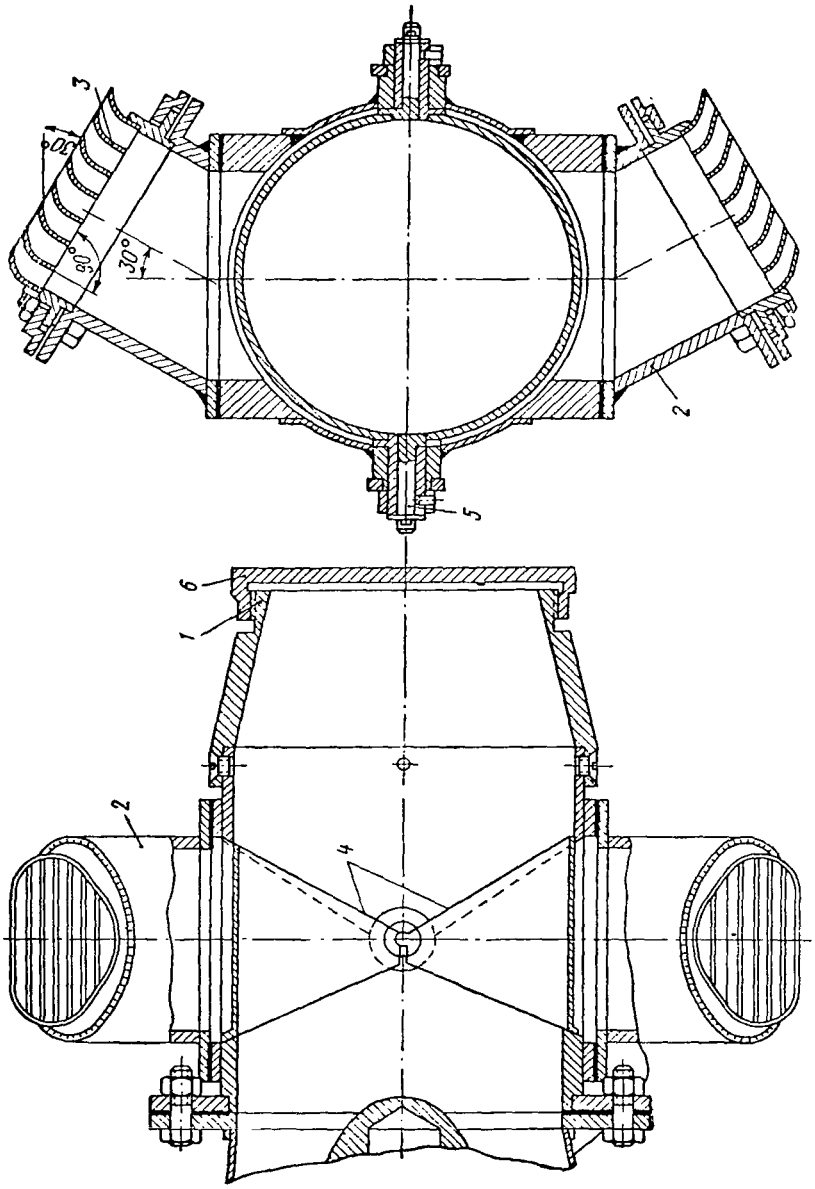

Figure 8.12. Model of a Deflector Incorporating Tilted Nozzles and Throttling Shutters.

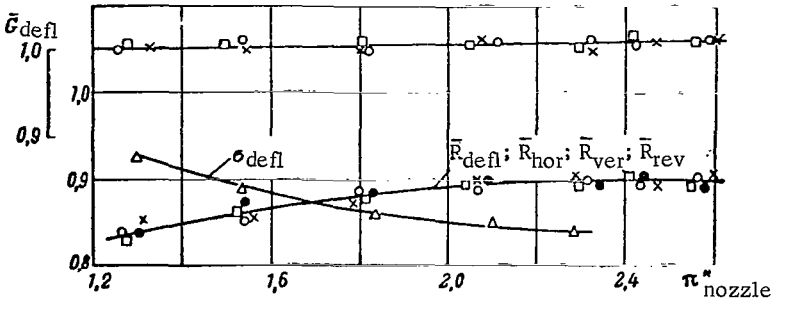

Figure 8.13. Coefficients of Thrust, Consumption Coefficient, and Coefficient of Total Pressure Recovery as Functions of the Extent of Pressure Reduction for a Model of a Deflector (cf. Figure 8.12): o, $\bar{R}_{hor}$; □ , $\bar{R}_{ver}$; ×, $\bar{R}_{rev}$; o, $\bar{R}_{defl}$.

Experiments established that as the nozzle tilting angle β' is varied, the horizontal and vertical thrust complements vary proportionally to the variables cos β' and sin β'. The value of the coefficient of the resultant thrust stays constant with variation in the nozzle tilting angle β' (Figure 8.14).

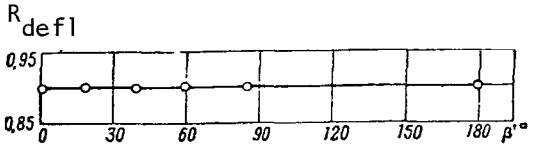

Figure 8.14. Resultant Thrust Coefficient as a Function of the Nozzle Tilting Angle in the Model (cf. Fig. 8.12) when $\pi^*_{nozzle} = 2.2$.

As results of studies made of a single nozzle equipped with a screen deflecting the stream by 90° have shown, thrust losses in this nozzle are about 3%. To the first approximation we can assume that in these tilted nozzles thrust losses will have the same value. The remaining thrust losses (approx. 7%) can be assigned to cleavage of the stream and its deflection by the shutters.

In the full-sized deflector it /228 is practically impossible to avoid leakage through the split between the shutters. Therefore thrust losses can prove to be somewhat higher than those obtained for this given model.

§2. Deflectors Installed in Lift Engines

Tilting Nozzle

The scheme of the tilting nozzle is shown in Figure 8.15. By means of two diametrically opposite pins 1, nozzle 2 can be tilted toward both sides

relative to the engine axis. Tilting of the nozzle will be executed also in conjunction with the cone-cowling 3 located aft of the engine turbine. /229

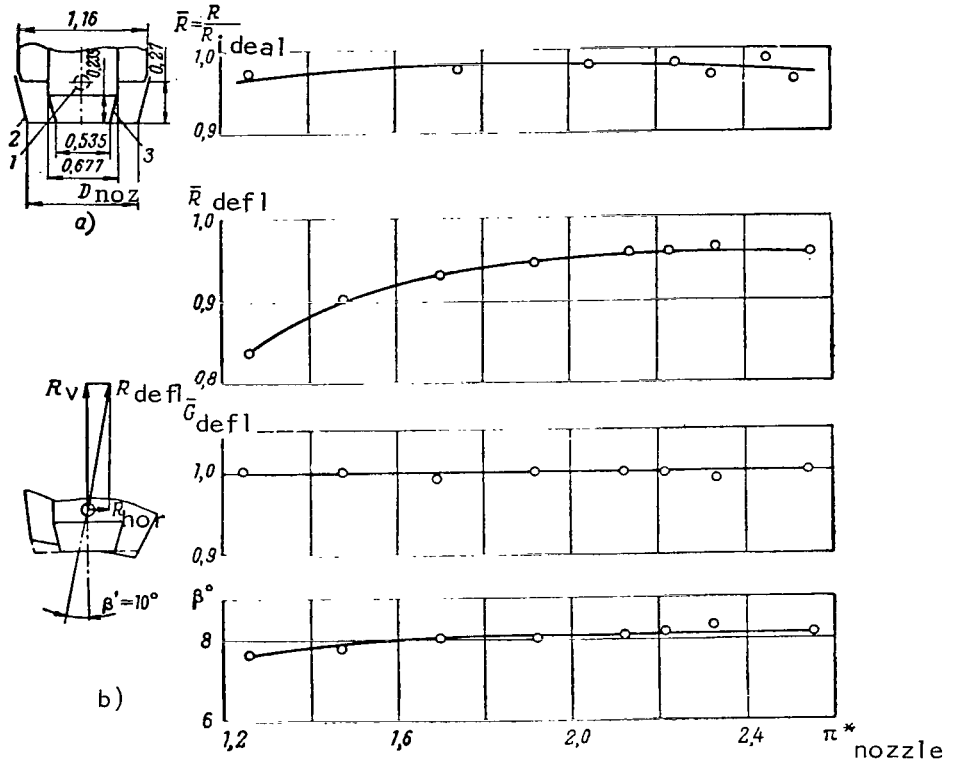

Figure 8.15. Scheme and Experimental Characteristics of a Tilting Nozzle Model Installed in a Lift Engine: a, Undeflected; 1, Pins; 2, Nozzle; 3, Cone-Cowling; 4, Deflected by 10°

Studies were made of the nozzle for nozzle tilting angles of 10° and 25°, for the nozzle tilted at an angle of 25° together with the conical cowling, and also for the untilted nozzle. The resulting experimental characteristics have been listed, respectively, in Figure 8.15 and 8.16.

When we compare the characteristics we can clearly see that in the working range of degrees of pressure reduction $\pi^*_{nozzle} \approx 2.0\text{-}2.5$, when the nozzle is tilted by the indicated angles, and also when the nozzle is tilted together with the cowling, the coefficient of the resultant thrust is retained approximately constant $\bar{R}_{defl} \approx 0.96$. This is accounted for by the fact that the aerodynamics of the throughput section remains essentially unchanged for these /230

relatively small angles of nozzle tilting. In nozzle tilting the consumption coefficient stays constant $\bar{G}_{defl} = 1.0$.

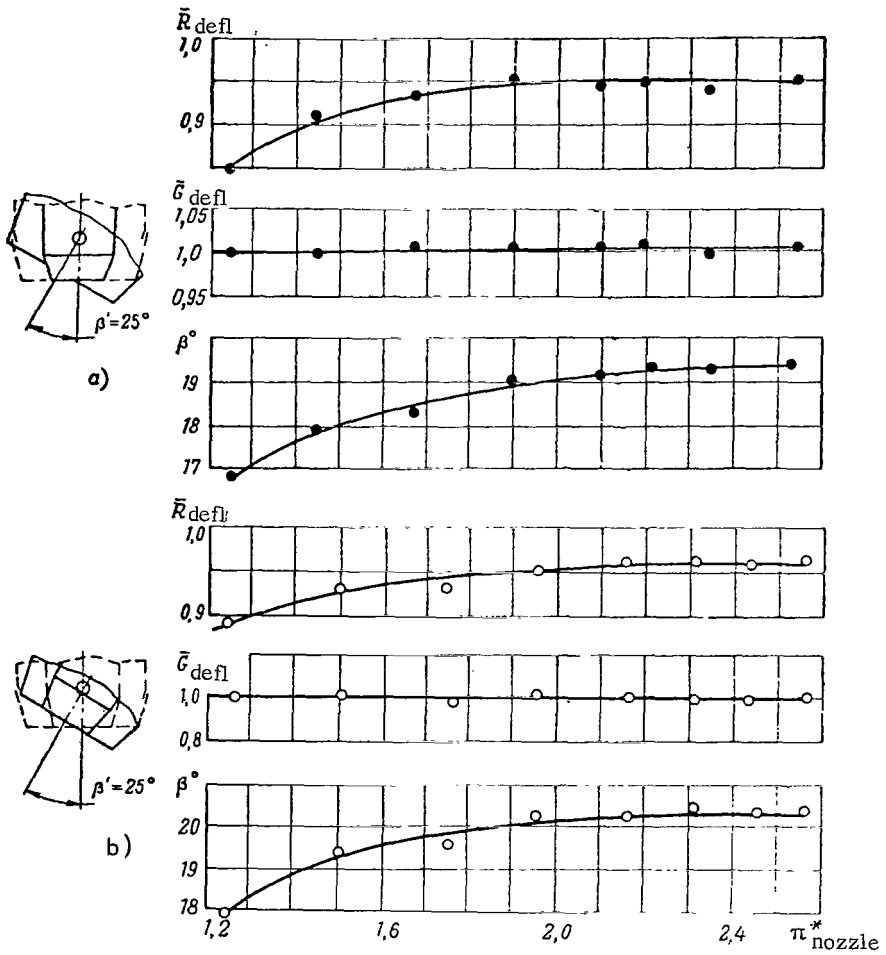

Figure 8.16. Experimental Characteristics of a Tilted Nozzle Model. a, Deflected by 25°; b, Deflected Together with a Cowling by 25°.

The stream exit angles were determined from the measured values of R_{hor} and R_{ver}.

Figure 8.17 presents the stream lagging angle $\nu = \beta' - \beta$ as a function of the nozzle tilting angle for $\pi^*_{nozzle} = 2.2$, where β is the actual stream exit angle and β' is nozzle tilting angle.

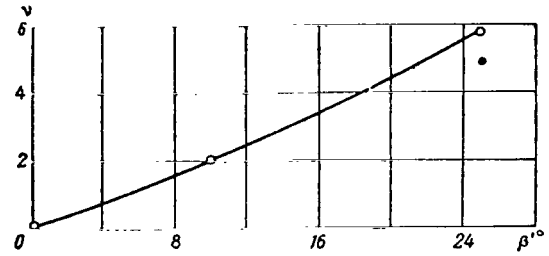

Figure 8.17. Angle of Stream Lag as a Function of Nozzle Tilting Angle (π^*_{nozzle} = 2.2): ●, Together with the Cowling.

Deflector Incorporating Box-type Shutter

This device (Figure 8.18) has a strut 1 secured to the engine 2 or the engine nacelle of the aircraft. Connected to the strut by means of a mechanism 3 is the box-type shutter 4, the sides of which 5 do not allow streaming of the gas beyond the limits of its lateral surface.

When the device is in the cut-in position, the shutter is placed at a desired angle relative to the nozzle axis that ensures the necessary values of horizontal R_{hor} and vertical R_{ver} thrust components. When the device is not cut-in, the shutters are folded together within the engine nacelle. The device can also be constructed in the form of a hinged part of the engine nacelle surface.

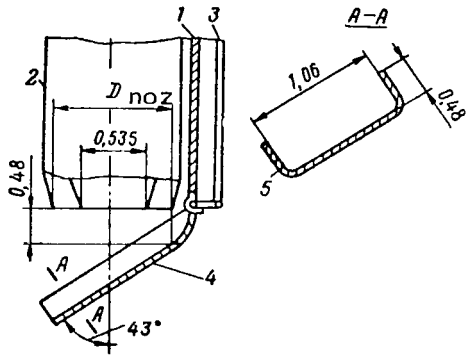

Figure 8.18. Scheme of Deflector Incorporated in a Lift Engine that Includes a Box-type Shutter: 1, Strut; 2, Engine; 3, Shutter Control Mechanism; 4, Shutter; 5, Sides of Shutter.

Experimental characteristics of the model of the device when the shutter is deflected by an angle of 43° are given in Figure 8.19. As the extent of pressure reduction is greater, /232 the coefficient of resultant thrust rises up to the value $\bar{R}_{defl} \approx 0.92$ for $\pi^*_{nozzle} = 2.2$. Further, as the extent of pressure reduction rises to $\pi^*_{nozzle} = 2.5$, the value of $\bar{R}_{defl}$ remains practically constant. Figure 8.19 also presents the characteristics of a model of the device incorporating a shutter without sides. Owing to the planar form of the shutter, much of the stream escapes toward the sides, which enduces sizeable thrust losses The maximum attained coefficient of the resulting thrust for the device incorporating this kind of shutter is $\bar{R}_{defl} \approx 0.7$.

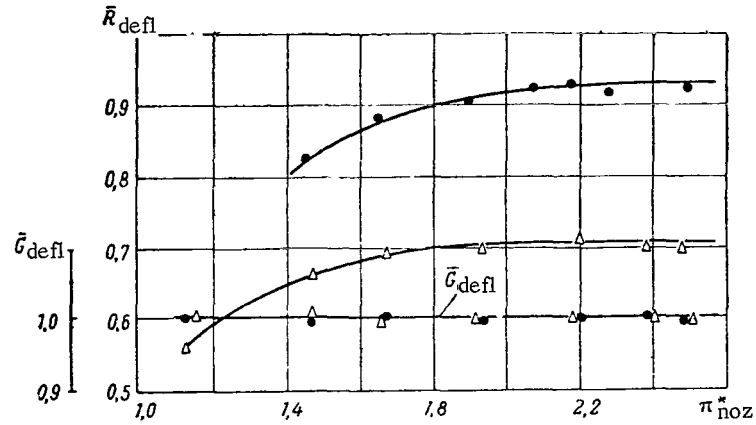

Figure 8.19. Experimental Characteristics of the Model of the Deflector Incorporating a Shutter: ●, Box-type Shutter; △ , Planar Shutter.

Deflector Incorporating Tilting Vanes

The scheme of the deflector is shown in Figure 8.20. It has guide vanes consisting of two parts: the upper 1 is fixed and the lower 2 tilts along hinges to both sides relative to the axis of the nozzle 3 of the engine by means of a mechanism. The vanes are restrained by the forks 4 secured to the engine or the engine nacelle of the aircraft.

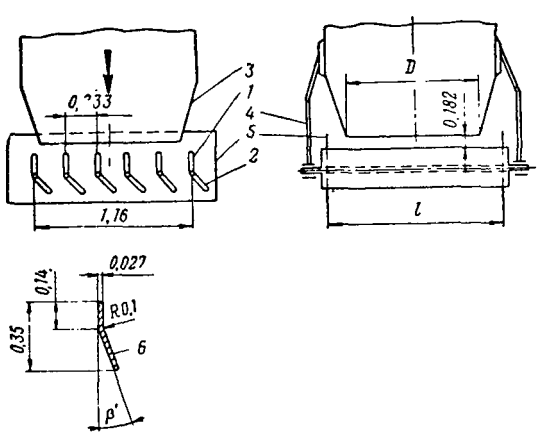

Figure 8.20. Scheme of Deflector Incorporated in a Lift Engine, Using Tilting Vanes: 1, Fixed Part of Vane; 2, Mobile Part of Vane; 3, Engine Nozzle; 4, Fork Restraining Vane; 5, Restrictive Strips; 6, Experimental Vane.

Owing to the reduction in the screen exit area when the vanes are tilted, the increase in the exit area is attained by shifting the restricting strips 5 (cf. Figure 8.20) toward the periphery. When the vanes are tilted by 19°, compensation for the reduction of the exit area is provided by the length of the vanes, equal to 1.14 D_{nozzle}, and when the vanes are rotated by 30°--by the length of the vanes equal to 1.33 D_{nozzle}. /233

Experimental characteristics of the model of the device are given in Figure 8.21. We can see that the consumption coefficient in both cases remains constant: $\overline{G}_{defl} = 1.0$. When the vanes are deflected by an angle of 19°, as π^*_{nozzle} is increased the coefficient of resultant thrust $\overline{R}_{defl}$ is reduced from ≈ 0.97 ($\pi^*_{nozzle} = 1.2$) down to 0.90 ($\pi^*_{nozzle} = 2.5$). For a 30° tilting of the vanes, this coefficient is reduced from ≈ 0.93 ($\pi^*_{nozzle} = 1.4$) down to ≈ 0.9 ($\pi^*_{nozzle} = 2,5$). The reduction in the resultant thrust coefficient with increase in the angle of vane tilting is accounted for by the rise in the losses of total pressure in the deflecting screen.

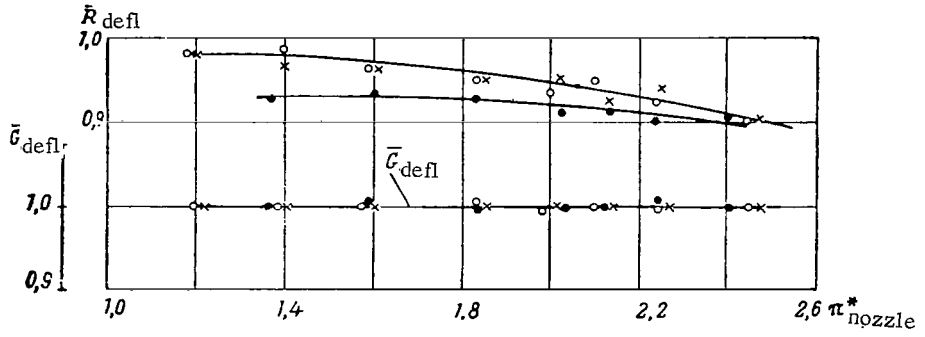

Figure 8.21. Experimental Characteristics of a Model of a Nozzle in a Lift Engine Incorporating Tilting Vanes (cf. Figure 8.20): $\beta' = 19°$: o, $l/D_{nozzle} = 1.14$; ×, $l/D_{nozzle} = 2.5$; when $\beta' = 30°$ ●, $l/D_{nozzle} = 1.33$.

Figure 8.22 presents the consumption coefficient $\overline{G}_{defl}$ as a function of the relative length of the screen vanes l/D_{nozzle}. We can clearly see from /234 the figure that the minimum vane length for which the screen with $\beta' = 30°$ does not affect consumption through the nozzle is $l \approx 1.33\ D_{nozzle}$. As l rises past $1.33\ D_{nozzle}$ the consumption coefficient stays constant.

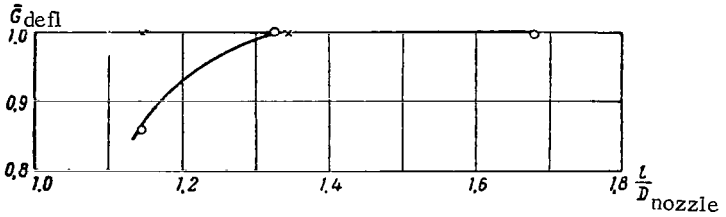

Figure 8.22. $\overline{G}_{defl}$ as a Function of the Ratio $l/D_{noz.}$ When $\pi^*_{nozzle} = 2.2$): ×, $\beta' = 19°$; o, $\beta' = 30°$.

The limited nature of the results of experimental studies on deflectors in turbojet engines does not yet allow us to make generalizations. However, the data given in this chapter can be used in new developments of deflectors.

REFERENCES

/235

1. Abramovich, G. N.: *"Turbu lentnyye Svobodnyye Strui Zhidkostey i Gazov"* (Turbulent Free Streams of Liquids and Gases), *Fizmatgiz*, 1960.
2. Andrenko, G. I.: "Aerodynamic Tests of Turbojet Engine Thrust Reversal," *Trudy Khar'kovskogo Aviatsionnogo Instituta*, No. 20, 1960.
3. Andrenko, G. I.: "Takeoff of Aircraft with Deflection of Jet Engine Gas Stream," *Izvestiya Vysshikh Uchebnykh Zavedeniy, Aviatsionnaya Tekhnika*, No. 3, pp. 8-15, 1958.
4. *"Aerodinamika Protochnoy Chasti Parovykh i Gazovykh Turbin,"* (Aerodynamics of the Throughput Part of Stream and Gas Turbines), Edited by I. I. Kirillov, *Mashgiz*, 1958.
5. Deych, M. Ye.: *"Tekhnicheskaya Gazodinamika,"* (Technical Gas Dynamics), *Gosenergoizdat*, 1961.
6. Inozemtsev, I. V.: *Aviatsionnyye Gazoturbinnyye Dvigateli,"* (Aviation Gas Turbine Engines), *Oborongiz*, 1955.
7. Kosterin, V. A. and Ye. V. Rzhevskiy: "Study of Correlations in the Interaction of Lateral Streams with the Entraining Flow," in: *Trudi KAI*, No. 86, pp. 38-49, Kazan, 1964.
8. Labazin, P. S.: "Analysis of the Thrust Efficiency of Turbojet Engines with Thrust Reversers for Pre-critical Pressure Drops in Nozzles," in: *Trudy Vysshego Aviatsionnogo Uchilishcha GVF*, No. 20, pp. 3-24, 1963.
9. Labazin, P. S. and N. S. Lobikov: "Investigation of the Effect of Major Factors on the Efficien y of Thrust Reversal in Ground Run of Aircraft," in: *Trudy Vysshego Aviatsionnogo Uchilishcha GVF*, No.13, pp. 53-96, 1962.
10. Lezhoyev, V. R.: "Analysis of Forces Acting on the Systems Controlling Thrust Reversers of Turbojet Engines," in: *Trudy Vysshego Aviatsionnogo Uchilishcha GVF*, No. 20, pp. 38-43, 1963.
11. Lezhoyev, V. R.: "Formulation of the Problem of the Stability of the Thrust Reverser Control System with Hydraulic Amplifier," in: *Trudy Vysshego Aviatsionnogo Uchilishcha GVF*, No. 20, pp. 25-27, 1963.
12. Pavlenko, V. F.: "Turbojet Engine Reversers," *Tekhnika Vozdushnogo Flota*, No. 3, 1957.
13. Pavlenko, V. F.: *"Samolety Vertikal'nogo Vzleta i Posadki,"* (Vertical Takeoff and Landing Aircraft), *Voyenizdat*, 1966.
14. Ruzhitskiy, Ye. I.: *"Bezaerodromnaya Aviatsiya,"* (Airport-less Aviation), *Oborongiz*, 1959.
15. *"Theoriya Reaktivnykh Dvigateley, Lopatochnyye Mashiny,"* (Theory of Jet Engines, Vane Machines), Edited by B. S. Stechkin, *Oborongiz*, 1956.
16. Tikhonov, A. S.: "Analysis of the Performance of Turbojet Engines Equipped with Thrust Reverser, Using the Method of Small Deviations," *Izvestiya Vysshikh Uchebnykh Zavedeniy, Aviatsionnaya Tekhnika*, No. 1, pp. 78-86, 1965.

17. Tikhonov, A. S.: "Calculation of Negative Thrust Produced by Turbojet Engines," *Trudy Kazanskogo Aviatsionnogo Instituta*, No. 55, 1960. /236
18. Tikhonov, A. S.: "Reversal of Turbojet Engine Thrust at Subsonic Flight Velocities," *Izvestiya Vysshikh Uchebnykh Zavedeniy, Aviatsionnaya Tekhnika*, No. 1, 1961.
19. Shandorov, G. I.: "Escape from a Channel in a Fixed and Moving Medium," *Zh. TF*, Vol. XXVII, No. 1, 1957.
20. Alford, J. S.: "Powerplants for Supersonic Transports," *J. RAS*, No. 598, pp. 617-628, 1960.
21. Ashwood, P. F. and D. Lean: "Flight Tests of a Meteor Aeroplane Fitted with Jet Deflection," *J. RAS*, No. 572, pp. 539-561, 29 Figs., 1958.
22. Barfoot, J. E.: "Design Development and Operational Experience of the Boeing 707 Thrust Reverser/Sound Suppressor," *SAE* preprint 57S, N.Y., 1959.
23. Barret, I. A.: "Recent Developments in Vectored-Thrust Turbofans," *Aircraft Engineering*, X, Vol. 37, No. 10, pp. 309-315, 1965.
24. Bradbury, L.J.S. and M. N. Wood: "The Static Pressure Distribution Around a Circular Jet Exhausting Normally from a Plane Wall Into a Airstream," *Lnd. H.M. Stat. off.*, p. 19, 18 Figs., 1965 (ARC c.p. No. 822).
25. Colley, R. H.: "Thrust Reversal for Jet Aircraft," *J. RAS*, X, Vol. 63, No. 586, pp. 563-571, 18 figs., 1959.
26. Datner, P. P.: "Thrust-Reverser Devices," *Aeronautical Engineering Review*, Vol. 16, No. 7, pp. 44-49, 1957.
27. Garnier, M.: "Problems of Motor Power for Supersonic Flight, Ejection System," *Technique et Science Aeronautiques et Spatiales*, III-IV, No. 2, pp. 96-100, 1964.
28. "G.E. Licks Noise, Thrust Reversal for 880," *Airlift*, Vol. 23, No. 4, pp. 65-68, 1959.
29. Glahn, U. H., and J. H. von Povolny: "Jet Deflection Devices," *SAE J.*, Vol. 66, No. 1, 1958.
30. Jackson, S. B.: "Advantages of a Brake Parachute Compared with Thrust Reversal for Landing Civil Aircraft," *J. RAS*, Vol. 69, No. 650, pp. 80-83, 1965.
31. Iserland, K.: "Braking the Landing Run of Jet Aircraft by Thrust Deviation," *Interavia Review*, Vol. VIII, No. 3, pp. 151-154, 1953.
32. Jordan, L. R. and C. M. Auble: "DC-8 Corrugated Nozzle, Retractable Ejector, Target Type Brake," *SAE J.*, No. 12, pp. 49-52, 1958.
33. Kohl, R. C. and J. S. Algranti: "Overheating Can Limit Performance of Jet Engine Thrust Reversers," *SAE J.*, Vol. 65, No. 11, pp. 38-40, 1957.
34. "The Deflector of the SNECMA Jet," *Aviation Magazine*, No. 96, pp. 16-19, 9 figs., 1954.
35. "Lift/Thrust Engines for VTOL Aircraft," *Research report on the work of Aero Division Bristol Siddley Engines Limited*, Fulton, Bristol. *Engineering*, No. 4961, pp. 710-711, 1961.
36. Lombard, A. A. and M. J.Day: "Jet Deflection," *Flight*, Vol. VI, No. 2833, 1963.
37. Pickerd, J. C.: "Thrust Reversers for Jet Aircraft (Selection and Design)," *Aerospace Engng*, I, Vol. 20, No. 1, pp. 30-31, 84-89, 16 figs., 1961.

38. Povolny, J. H.: F. W. Steffen and J. G. McArdle: "Summary of Scale Model Thrust-Reverser Investigation," *NASA*, Washington, Report No. 1314, p. 14, 33 figs., 1957. /237
39. Riemerschmid, F. and H. Prechter: "Aerodynamic and Design Problems of Thrust Vector Steering by Thrust Stream Deflection", *Aerodynamische und konstruktive Fragen der Schubvektorsteuerung mittels Schubstrahlumlenking, Luftfahrttechnik-Raumfahrttechnik*, No. 12, pp. 335-341, 1965.
40. "Rolls-Royce Reversers," *Flight*, Vol. 75, No. 2611, p. 187, 6/II, 5 figs, 1959.
41. Rotondi, G.: "The Liftoff Course of a Short Takeoff and Landing (STOL) With Directed Thrust", *Sulla corsa di distacco dei velivoli a breve distanza di decollo (STOL) contrazione orientabile. L'Aerotecnica*, X, Vol. 42, No. 5, pp. 201-212, 4 figs., 1962.
42. Saari, M. J.: "Turbojet Lift Engine Design for VTOL Transports," *Canadian Aeronautical Journal*, Vol. 5, No. 6, pp. 215-223, 1959.
43. Schairer G. S.: "Performance Characteristics of Jet Nozzles," *Third Anglo-American Aeronautical Conference*, Brighton, 1951, London, *RAS*, 1952.
44. Sweeney, R.: "Boeing 707 is "Honest" Airplane; Demands Planning Care," *Aviation Week*, Vol. 69, No. 14, p. 71, 1958.
45. "Thrust Reversal for the Comets," *Aeroplane*, Vol. 95, No. 2461, pp. 661-662, 4 figs., 1958.
46. Vincent, K. T. C.: "Thrust Reverser Ahead of Silencer Makes a Compact and Rugged Design," *SAE J.*, Vol. 67, No. 2, p. 47, 1959.
47. Wille, R. and H. Fernholz: "Report on the First European Mechanics Colloquim on the Coanda Effect," *J. Fluid Mech.*, Vol. 23, Part 4, p. 801, 1965.

Translated for the National Aeronautics and Space Administration under contract No. NASw-1695 by Techtran Corporation, P.O. Box 729, Glen Burnie, Maryland, 21061.

"The aeronautical and space activities of the United States shall be conducted so as to contribute . . . to the expansion of human knowledge of phenomena in the atmosphere and space. The Administration shall provide for the widest practicable and appropriate dissemination of information concerning its activities and the results thereof."

—NATIONAL AERONAUTICS AND SPACE ACT OF 1958

NASA SCIENTIFIC AND TECHNICAL PUBLICATIONS

TECHNICAL REPORTS: Scientific and technical information considered important, complete, and a lasting contribution to existing knowledge.

TECHNICAL NOTES: Information less broad in scope but nevertheless of importance as a contribution to existing knowledge.

TECHNICAL MEMORANDUMS: Information receiving limited distribution because of preliminary data, security classification, or other reasons.

CONTRACTOR REPORTS: Scientific and technical information generated under a NASA contract or grant and considered an important contribution to existing knowledge.

TECHNICAL TRANSLATIONS: Information published in a foreign language considered to merit NASA distribution in English.

SPECIAL PUBLICATIONS: Information derived from or of value to NASA activities. Publications include conference proceedings, monographs, data compilations, handbooks, sourcebooks, and special bibliographies.

TECHNOLOGY UTILIZATION PUBLICATIONS: Information on technology used by NASA that may be of particular interest in commercial and other non-aerospace applications. Publications include Tech Briefs, Technology Utilization Reports and Technology Surveys.

Details on the availability of these publications may be obtained from:

SCIENTIFIC AND TECHNICAL INFORMATION DIVISION

NATIONAL AERONAUTICS AND SPACE ADMINISTRATION

Washington, D.C. 20546